

MODERN DEVELOPMENT OF MAGNETIC RESONANCE

abstracts

2017

KAZAN * RUSSIA





MODERN DEVELOPMENT OF MAGNETIC RESONANCE

ABSTRACTS OF THE
INTERNATIONAL CONFERENCE

Editor:
KEV M. SALIKHOV

KAZAN, SEPTEMBER 25–29, 2017

This work is subject to copyright.

All rights are reserved, whether the whole or part of the material is concerned, specifically those of translation, reprinting, re-use of illustrations, broadcasting, reproduction by photocopying machines or similar means, and storage in data banks.

© 2017 Kazan E. K. Zavoisky Physical-Technical Institute, Kazan

© 2017 Igor A. Aksenov, graphic design

Printed in the Russian Federation

Published by Kazan E. K. Zavoisky Physical-Technical Institute, Kazan

www.kfti.knc.ru

CHAIRMEN

Alexey A. Kalachev

Kev M. Salikhov

PROGRAM COMMITTEE

Kev Salikhov, Chairman (Russia)

Albert Aganov (Russia)

Vadim Atsarkin (Russia)

Pavel Baranov (Russia)

Marina Bennati (Germany)

Bernhard Blümich (Germany)

Michael Bowman (USA)

Sabine Van Doorslaer (Belgium)

Rushana Eremina (Russia)

Jack Freed (USA)

Ilgiz Garifullin (Russia)

Alexey Kalachev (Russia)

Walter Kockenberger (Great Britain)

Wolfgang Lubitz (Germany)

Klaus Möbius (Germany)

Hitoshi Ohta (Japan)

Igor Ovchinnikov (Russia)

Vladimir Skirda (Russia)

Murat Tagirov (Russia)

Takeji Takui (Japan)

Valery Tarasov (Russia)

Yurii Tsvetkov (Russia)

Violeta Voronkova (Russia)

LOCAL ORGANIZING COMMITTEE

Kalachev A.A., Chairman	Latypov V.A.
Mamin R.F., Vice-Chairman	Mosina L.V.
Voronkova V.K., Scientific secretary	Oladoshkin Yu.V.
Akhmin S.M.	Salikhov K.M.
Falin M.L.	Siafetdinova A.Z.
Fazlizhanov I.I.	Tarasov V.F.
Galeev R.T.	Voronova L.V.
Goleneva V.M.	Yanduganova O.B.
Gubaidulina A.Z.	Yurtaeva S.V.
Guseva R.R.	Zaripov R.B.
Kupriyanova O.O.	Ziganshina S.A.
Kurkina N.G.	

SCIENTIFIC SECRETARIAT

Violeta K. Voronkova
Laila V. Mosina
Vlad A. Latypov
Sufia A. Ziganshina

The conference is organized under the auspices of the AMPERE Society

ORGANIZERS

Kazan E. K. Zavoisky Physical-Technical Institute
The Academy of Sciences of the Republic of Tatarstan
Kazan Federal University

SUPPORTED BY

The Government of the Republic of Tatarstan
The Russian Foundation for Basic Research, no. 17-02-20510-r
Bruker BioSpin

CONTENTS

ZAVOISKY AWARD LECTURE

- Topological High-Spin Organic Chemistry and Molecular Spin-Qubit
Quantum Technology Underlain by Electron Magnetic Resonance
T. Takui 2

PLENARY LECTURES

- Multi-Extreme THz ESR: Developments and Future Biological
Applications
H. Ohta, S. Okubo, E. Ohmichi, T. Sakurai, S. Hara, H. Takahashi 6
- Spinon Magnetic Resonance in a Quasi 1D $S = 1/2$ Antiferromagnet with
a Weak Exchange Interaction
A. I. Smirnov, T. A. Soldatov, K. Yu. Povarov, M. Hälg,
W. E. A. Lorenz, A. Zheludev 7
- A Pulse Dipole EPR-Based Distance Measurements at Ambient
Temperatures
E. Bagryanskaya 9
- EPR Methods to Determine Properties of Intrinsically Disordered
Proteins
M. Huber 10
- Soft Spins and Higgs Mode in Ruthenates
G. Khaliullin 11
- Insight into Protein Function by EPR
R. Bittl 12

SPECIAL SESSION DEVOTED TO THE 110 ANNIVERSARY OF E. K. ZAVOISKY

- E. Zavoisky and Kazan University
M. S. Tagirov 14
- About E. Zavoisky and His Discovery
K. M. Salikhov 15
- Dimer Self-Organization of Rare-Earth Impurity Ions in
Synthetic Forsterite
V. F. Tarasov 16

The Different Faces of Free Radical Spin Dynamics in Frozen Solution <i>M. K. Bowman, H. Chen, B. R. Fowler, A. G. Maryasov</i>	17
SECTION 1	
THEORY OF MAGNETIC RESONANCE	
Magnetic Resonance of Impurity Spin in Slow Normal Stochastic Local Field <i>F. S. Dzheparov, D. V. Lvov</i>	20
Manipulations of High Spin Kramers System States by Circularly Polarized MW Fields <i>A. G. Maryasov, S. L. Veber, M. V. Fedin</i>	21
Reversing Chaotic Dynamics of Nuclear Spins <i>B. V. Fine</i>	22
Probing of Fluorine Atom Electronic Shell by means of Topological Analysis of Helium Chemical Shift Surfaces <i>E. Yu. Tupikina, A. A. Efimova, G. S. Denisov, P. M. Tolstoy</i>	23
Theory of Chiral Systems and Molecular Machines <i>L. Khalilov</i>	24
SECTION 2	
LOW-DIMENSIONAL SYSTEMS AND NANO-SYSTEMS	
Magnetoresistive and Microwave Responses of Hybrid Josephson Structures with Ferromagnetic Layers <i>V. V. Ryazanov, I. A. Golovchanskiy, V. V. Bolginov, N. N. Abramov, V. I. Chichkov</i>	26
Dynamics of Majorana States in Nanowires and Josephson Junctions <i>A. S. Mel'nikov, I. M. Khaymovich, J. P. Pekola, A. Kopusov, I. A. Shereshevskii, N. Vdovicheva</i>	27
Spin Current and Second Harmonic Generation in Noncollinear Magnets <i>E. A. Karashtin, N. S. Gusev, K. D. Sladkov, I. A. Kolmychek, T. V. Murzina, A. A. Fraerman</i>	28
Electric Field Controlled ESR in Multiferroic CuCrO_2 <i>L. E. Svistov, S. K. Gotovko, T. A. Soldatov, H. D. Zhou</i>	30
Magnetic Properties of New Chiral 2D Magnet MnSnTeO_6 <i>E. A. Zvereva, G. V. Raganyan, V. B. Nalbandyan, M. A. Evstigneeva, S. V. Streltsov, A. I. Kurbakov, M. A. Kuchugura, A. N. Vasiliev</i>	32
The Influence of Adsorbate and Edge Covalent Bonds on Topological Zero Modes in Few-Layer Nanographenes <i>A. M. Ziatdinov</i>	34

Localized Ferromagnetic Resonance of Domain Wall in Curved Nanostripe <i>E. V. Skorohodov, A. P. Volodin, R. V. Gorev, V. L. Mironov</i>	36
ESR of a Doped Quasi-One-Dimensional $S = 1$ Antiferromagnet with Two Coupled Antiferromagnetic Sublattices <i>T. A. Soldatov, A. I. Smirnov, K. Yu. Povarov, E. Wulf, A. Mannig, A. Zheludev</i>	38
Nuclear Magnetic Resonance Studies of Nanodiamond Surface Modification <i>A. Panich</i>	40
^3He NMR in Nanostructures: Latest Progress <i>E. M. Alakshin, G. A. Dolgorukov, A. V. Klochkov, E. I. Kondratyeva, V. V. Kuzmin, D. S. Nuzhina, K. R. Safullin, A. A. Stanislavovas, M. S. Tagirov</i>	41
The Formation of Epsilon- $\text{Fe}_2\text{O}_3/\text{SiO}_2$ Nanoparticles: Spatial Stabilization and the Size Effect <i>S. S. Yakushkin, D. A. Balaev, G. A. Bukhtiyarova, O. N. Martyanov</i>	42

SECTION 3

SPIN-BASED INFORMATION PROCESSING

Exact Analytical and Genuine Zeeman Perturbation Approaches to the Eigen-Energies and -Functions of the ZFS and Electronic Zeeman Interaction Hamiltonian for the Spin Quantum Numbers up to $S = 7/2$: Applications to High Spin Metalloporphyrins and a Re(III, IV) Complex with Sizable ZFS Values and Quantum Chemical Calculations <i>T. Yamane, K. Sugisaki, T. Nakagawa, H. Matsuoka, T. Nishio, S. Kinjyo, N. Mori, S. Yokoyama, C. Kawashima, N. Yokokura, K. Sato, Y. Kanzaki, D. Shiomi, K. Toyota, D. H. Dolphin, W. C. Lin, the late C. A. McDowell, M. Tadokoro, T. Takui</i>	44
Molecular Spin Technology Based on Microwave Pulse with Arbitrary Waveform towards Spin Quantum Computing <i>K. Sato, S. Yamamoto, R. Hirao, K. Tanimoto, E. Hosseini, S. Nakazawa, K. Toyota, D. Shiomi, K. Ivanov, T. Takui</i>	46
Decoherence in Many-Qubit Clusters in Multiple Quantum NMR in One-Dimensional Systems <i>G. A. Bochkin, E. B. Fel'dman, S. G. Vasil'ev, V. I. Volkov</i>	47
Cross Relaxation Magnetometry with Diamond NV Centers <i>R. A. Akhmedzhanov, L. A. Gushchin, N. A. Nizov, V. A. Nizov, D. A. Sobgayda, I. V. Zelensky</i>	48
Electron-Electron and Electron-Nuclear Interactions in the Context of Spin-Based Quantum Computing <i>E. I. Baibekov</i>	49

SECTION 4 MOLECULAR MAGNETS AND LIQUID CRYSTALS

- Spin Magnetic Resonance Spectroscopy from Billions of Molecules to a Single Molecule
F. Shi 52
- Magnetic Properties, EPR and *ab initio* Investigation of a Series of Isostructural $\text{Fe}_2^{\text{III}}\text{Dy}_2^{\text{III}}$ Complexes
V. Vieru, L. Ungur, V. Cemortan, A. Sukhanov, A. Baniodeh, V. Mereacre, C. E. Anson, A. K. Powell, V. Voronkova, L. F. Chibotaru 53

SECTION 5 MODERN METHODS OF MAGNETIC RESONANCE

- Characterization of Liquid-Crystalline Materials by Separated Local Field Methods
S. V. Dvinskikh 56
- Novel Approaches in Magnetic Resonance & Microwave Detection of Energetic and Illicit Material
B. Rameev, G. Mozzhukhin 57

SECTION 6 STRONGLY CORRELATED ELECTRON SYSTEMS

- Signatures of Fractionalized Spin Excitations in the Proximate Quantum Spin Liquid $\alpha\text{-RuCl}_3$ from Sub-THz Spectroscopy in Strong Magnetic Fields
V. Kataev 60
- Electron Nematic Effect in CeB_6 : The ESR and Magnetoresistance Evidence
S. V. Demishev, V. N. Krasnorussky, V. V. Glushkov, A. V. Semeno, M. I. Gilmanov, A. V. Bogach, A. N. Samarin, N. A. Samarin, N. E. Sluchanko, N. Yu. Shitsevalova, V. B. Filipov 61
- Investigation of a Field Induced Magnetic Transition in the Low-Dimensional Magnet BiCoPO_5
M. Iakovleva, E. Vavilova, H.-J. Grafe, A. Alfonsov, B. Büchner, Y. Skourski, R. Nath, V. Kataev 62
- Magnetic Resonance in the Strongly Correlated Topological Insulator SmB_6
S. V. Demishev, M. I. Gilmanov, A. N. Samarin, A. V. Semeno, N. E. Sluchanko, N. Yu. Shitsevalova, V. B. Filipov, V. V. Glushkov 63
- ODMR and LAC Spectroscopy of Nitrogen-Vacancy Centers in Diamond
S. V. Anishchik, K. L. Ivanov, V. G. Vins, I. V. Zhukov, O. V. Chankina, Yu. N. Molin 64

SECTION 7

MAGNETIC RESONANCE IMAGING

MRI and Emotions

U. Eichhoff 68

Several Aspects of ^{19}F Gastrointestinal MRI

D. V. Volkov, M. V. Gulyaev, L. L. Gervits, D. N. Silachev,
N. V. Anisimov, A. P. Chernyaev, Yu. A. Pirogov 69

The Design of the Receiving Coils for Specialized MRI

A. A. Bayazitov, V. E. Khundiryakov, Ya. V. Fattakhov, I. R. Sitdikov,
A. R. Fakhrutdinov, V. A. Shagalov, R. Sh. Khabipov, A. N. Anikin 71

SECTION 8

MAGNETIC RESONANCE INSTRUMENTATION

Latest Developments in Pulsed Field Gradient and High Speed
Magic Angle Spinning NMR

K. Zick 74

SECTION 9

ELECTRON SPIN BASED METHODS FOR ELECTRONIC
AND SPATIAL STRUCTURE DETERMINATION IN
PHYSICS, CHEMISTRY AND BIOLOGY

Rapid Scan EPR

M. Tseytlin 78

Time-Resolved EPR and Theoretical Investigations of
Metal-Free Triplet Emitters for Organic Light Emitting Diodes

H. Matsuoka, M. Retegen, L. Schmitt, S. Höger, F. Neese,
O. Schiemann 79

Nanoclustering of Spin-Labeled Molecules in
Lipid Membranes as Revealed by “Instantaneous Diffusion”
Effects in Electron Spin Echo Decay

S. A. Dzuba, M. E. Kardash, V. N. Syryamina, E. F. Afanasyeva 80

EPR of Metal-Organic Stimuli-Responsive Materials

M. V. Fedin, A. M. Sheveleva, S. L. Veber 81

Defects Structure in Congruent Lithium Tantalite by NMR, ESR,
FTIR Spectroscopies and DFT Calculations

E. Vavilova, R. Zaripov, A. Vyalikh, M. Zschornak, T. Köhler,
M. Nentwich, T. Weige, S. Gemming, E. Brendler, D. C. Meyer 82

Stable Self-Organized Paramagnetic Complexes in the Asphaltenes’
Structures from the W-band EPR and ENDOR

S. B. Orlinskii, A. A. Rodionov, A. V. Galukhin, I. N. Gracheva,
G. V. Mamin, M. R. Gafurov 83

SECTION 10
CHEMICAL AND BIOLOGICAL SYSTEMS

- A Combined ESR – Fluorescence Approach for Investigation of Structure, Molecular Dynamics and Mechanism of Electron Transfer in Biological Systems: 50 Years of History
G. I. Likhtenshtein 86
- Structure and Properties of Mechanically Activated $\text{TiO}_2/\text{MoO}_3$, $\text{TiO}_2/\text{V}_2\text{O}_5$ and $\text{TiO}_2/\text{MoO}_3:\text{V}_2\text{O}_5$ Oxides Studied by EPR and XRD
A. I. Kokorin, I. V. Kolbanov, T. V. Sviridova, D. V. Sviridov 88
- NMR Methods to Study Protein-Ligand Interactions
V. I. Polshakov 90

SECTION 11
OTHER APPLICATIONS OF MAGNETIC RESONANCE

- Supermagnonics in YIG Film
Yu. M. Bunkov, T. R. Safin, A. R. Farhutdinov, M. S. Tagirov 94
- Ionic and Molecular Transport in Polymeric Electrolytes on Magnetic Resonance Data
V. I. Volkov 96
- Proton Dynamics in Strong Hydrogen Bonds: Solvent-Induced Distribution of NMR Chemical Shifts
P. M. Tolstoy, S. A. Pylaeva, E. Yu. Tupikina, G. S. Denisov, H. Elgabarty, D. Sebastiani 99
- ESR Study of $\text{Sc}_2\text{SiO}_5:\text{Nd}^{143}$ Isotopically Pure Crystals
R. Eremina, K. Konov, V. F. Tarasov, T. P. Gavrilova, A. V. Shestakov, Yu. D. Zavartsev, A. I. Zagumennyi, S. A. Kutovoi 100
- ESR Study of Intrinsic Magnetic Moments in Topological Insulators
V. Sakhin, E. Kukovitsky, N. Garifyanov, R. Khasanov, Yu. Talanov, G. Teitel'baum 102
- Investigation of Magnetic Anisotropy Field in Stressed Permalloy Microparticles by FMR
D. Bizyaev, A. Bukharaev, N. Nurgazizov, T. Khanipov 103
- Fullerene-Nitroxide Derivatives:
Polarizers with New Properties for DNP in Liquid State
N. Enkin, S.-H. Liou, T. Orlando, I. Tkach, M. Bennati 105

SECTION 12
PERSPECTIVE OF MAGNETIC RESONANCE IN
SCIENCE AND SPIN-TECHNOLOGY

Manifestations of the Collective Motion of Spins Induced by Stochastic Relaxation Processes <i>K. M. Salikhov</i>	108
Influence of Free Charge Carriers on EPR Parameters of Gd ³⁺ Centers in the Pb _{1-x} Ag _x S and Pb _{1-x} Cu _x S Semiconductors <i>V. A. Ulanov, A. M. Sinicin, R. R. Zainullin</i>	109
FMR Studies of Ultra-Thin Epitaxial Pd _{1-x} Fe _x Films <i>A. Esmaeili, I. R. Vakhitov, N. P. Nikitin, I. V. Yanilkin, A. I. Gumarov, B. M. Khaliulin, B. F. Gabbasov, M. N. Aliyev, R. V. Yusupov, L. R. Tagirov</i>	111
POSTERS	
EPR Investigation of Mechanoactivated Copper Gluconate <i>M. M. Akhmetov, G. G. Gumarov, V. Yu. Petukhov, G. N. Konygin, D. S. Rybin</i>	114
Cross-Correlation Effects in Spin-Lattice Relaxation and Symmetry Restricted Spin Diffusion in Single Crystals of Amino Acids <i>N. K. Andreev</i>	115
Application of the Multi-Pulse Protocols in Solid State ¹ H NMR in Cu(II)-Oxamidato Complex <i>E. Anisimova, R. Zaripov, I. Khairuzhdinov, K. Salikhov, T. Ruffer, E. Vavilova</i>	117
Routine of Determination of the Spin Exchange Rate Constants from EPR Line Shape Analysis of Nitroxyl Radicals in Liquids <i>M. M. Bakirov, R. T. Galeev, K. M. Salikhov</i>	118
FMR Investigation of Magnetic Anisotropy in Films were Synthesized by Co ⁺ Implantation into Si <i>V. V. Chirkov, G. G. Gumarov, V. Yu. Petukhov, M. M. Bakirov</i>	119
EMR Searching of Quantum Behavior of γ -Fe ₂ O ₃ Nanoparticles Encapsulated in Dendrimeric Matrix <i>N. E. Domracheva, V. E. Vorobeva, M. S. Gruzdev</i>	120
Action of Counterion on Spin-Crossover Behavior in Iron(III) Dendrimeric Complexes <i>N. E. Domracheva, V. E. Vorobeva, V. I. Ovcharenko, A. S. Bogomyakov, E. M. Zueva, M. S. Gruzdev, U. V. Chervonova, A. M. Kolker</i>	122
EPR of Er ³⁺ Ions in CsCaF ₃ Single Crystals <i>M. L. Falin, V. A. Latypov, S. L. Korableva</i>	123

Structural Models of the Yb ³⁺ Ion in the Hexagonal Perovskite RbMgF ₃ Single Crystal <i>M. L. Falin, V. A. Latypov, A. M. Leushin, G. M. Safullin</i>	124
Spin States of [Fe(Salten)Cl] Complexes in Acetonitrile <i>E. Frolova, T. Ivanova, O. Turanova, L. Mingalieva, E. Zueva, M. Petrova, I. Ovchinnikov</i>	125
EPR Spectroscopy of the Gd ³⁺ Ions in the SrY ₂ O ₄ Crystal <i>B. F. Gabbasov, D. G. Zverev, S. I. Nikitin, I. F. Gilmutdinov, R. G. Batulin, A. G. Kiiamov, R. V. Yusupov</i>	127
Studies of [Fe(Salten)L]BPh ₄ Complexes Solutions in Acetonitrile <i>L. Gafiyatullin, E. Frolova, E. Zueva, O. Turanova, E. Milordova, I. Ovchinnikov</i>	129
Dynamics of Nitric Oxide Production in Heart and Liver of Rats During Increasing 30-Days Restriction of Motor Activity and Subsequent Recovery <i>Kh. L. Gainutdinov, V. V. Andrianov, V. S. Iyudin, G. G. Yafarova, M. I. Sungatullina, I. I. Khabibrakhmanov, N. I. Ziatdinova, T. L. Zefirov</i>	130
EPR Investigation of the Conformation of the Irradiated Calcium Gluconate <i>I. A. Goenko, G. G. Gumarov, M. M. Bakirov, R. B. Zaripov, V. Yu. Petukhov, D. S. Rybin, G. N. Konygin</i>	132
Multiple Spin Echoes from ⁵⁷ Fe Nuclei in Ferrimagnetic Yttrium Iron Garnet Films <i>A. I. Gorbovanov, S. N. Polulyakh, V. N. Berzhansky, A. A. Gippius</i>	134
Topological Interactions of Magnetic Impurities in Topological Semimetal: ESR Data <i>Yu. V. Goryunov, A. N. Nateprov</i>	136
Temperature Dependence of Magnetic Anisotropy in Iron Silicide Films Ion-Synthesized in External Magnetic Field <i>G. G. Gumarov, O. N. Lis, A. V. Alekseev, M. M. Bakirov, V. Yu. Petukhov</i>	138
The Possibilities of EPR for the Connective Tissue Dysplasia Diagnosis <i>M. I. Ibragimova, D. K. Khaibullina, A. I. Chushnikov, I. V. Yatsyk, V. Yu. Petukhov, R. G. Esin</i>	139
Downhole Laboratory for Reservoir Fluid Real-Time Extended NMR, Optical and Dielectric Spectroscopy Analysis and Sampling <i>A. Imaev, A. Sayakhov, S. Gorshenin, M. Gorshenin, A. Sadikov, A. Bragin, V. Murzakaev, L. Gilyazov, A. Golubey, D. Zverev, I. Mumdzhi, S. Nikitin, D. Ivanov, D. Melnikova, A. Ivanov, O. Gnezdilov, R. Archipov, A. Aleksandrov, V. Skirda, Ya. Fattakhov, V. Shagalov, A. Fakhrutdinov, D. Kononov, R. Khabipov, A. Anikin</i>	140

Magnetic Interactions in the Chain Structure [Fe(salen)(2-Me-Him)] _n <i>T. Ivanova, I. Gilmutdinov, O. Turanova, L. Mingaliev, I. Ovchinnikov</i>	142
¹ H NMR Detection of Olive Oil <i>G. S. Kupriyanova, G. V. Mozzhukhin, A. Maraşlı, B. Z. Rameev</i>	144
Investigation of Fullerenes C ₆₀ and PCBM Triplet States Spin Dynamics in Ionic Liquids by Time-Resolved EPR Spectroscopy <i>I. Kurganskii, M. Ivanov, M. Fedin, S. Prikhod'ko, N. Adonin</i>	146
Protein Translational Diffusion under Crowding Conditions <i>A. M. Kusova, A. E. Sitnitsky, B. Z. Idiyatullin, D. R. Bakirova, Yu. F. Zuev</i>	148
Spin Probe EPR Study of CO ₂ /O ₂ /N ₂ Gas Sorption in ZIF-8 <i>D. Kuzmina, A. Sheveleva, A. Poryvaev, M. Fedin</i>	149
Spin Centers in Nanocrystalline Titania, Synthesized with Supercritical Flow Reactor Technique <i>N. T. Le, E. A. Konstantinova, B. B. Iversen</i>	150
The Coherence of the Exciting Radiation and Amplitude of Oscillations of Echo Intensity vs External dc Magnetic Field <i>V. N. Lisin, A. M. Shegeda, V. V. Samartsev</i>	152
ESR Study of CuEr Dilute Alloys <i>S. Lvov, E. Kukovitsky</i>	155
DFT Calculations of the ¹⁴ N NQR Spectra of Some Heterocycles <i>S. Mamadazizov, M. Shelyapina, G. Kupriyanova</i>	156
¹⁴ N NQR with Frank Sequence Excitation <i>I. Mershiev, B. Blümich</i>	158
EPR of {Dy ^{III} -Me ^{III} ₂ -Dy ^{III} } Clusters, Me ^{III} = Cr ^{III} , Mn ^{III} <i>L. V. Mingaliev, Y. Peng, V. K. Voronkova, A. K. Powell</i>	159
Investigation of Charge Accumulation Processes in TiO ₂ -Based Nanoheterostructures <i>A. A. Minnekhanov, E. V. Vakhrina, E. A. Konstantinova</i>	160
Nitrogen ¹⁴ N NMR Detection of Liquids <i>G. V. Mozzhukhin, G. S. Kupriyanova, A. Maraşlı, B. Z. Rameev</i>	162
Determination of Aggregation Stability and MRI Contrast Efficiency of Magnetic Nanoparticles by NMR-Relaxometry <i>A. V. Nikitina, Yu. V. Bogachev, A. A. Kostina, V. A. Sabitova, Ya. Yu. Marchenko, B. P. Nikolaev</i>	164
Towards Determination of Distances between Nanoparticles and Grafted Paramagnetic Ions by NMR Relaxation <i>A. M. Panich, N. A. Sergeev</i>	166
Multifunctional Properties of Ferromagnetics in Conditions of Photoexcitation <i>D. Pavlov, R. Mamin</i>	167

A Classical Vector Model for Magnetization of Two-Spin System with Dipole-Dipole Interaction <i>S. N. Polulyakh</i>	168
The First Decade After Zavoisky's Discovery: the EPR Technique in USSR <i>V. Ptushenko</i>	169
Field-Induced Long-Range Magnetic Order in A_2MnTeO_6 (A = Na, Li, Ag, Tl) <i>G. V. Raganyan, E. A. Zvereva, V. B. Nalbandyan, M. A. Evstigneeva, A. N. Vasiliev</i>	170
NMR Study a Fragmented Haldane Like Spin-Chains <i>T. Salikhov, V. Kataev, M. Gunter, H.-H. Klauss, E. Zvereva, V. Nalbandyan, E. Vavilova</i>	172
Magnetic Properties of Mixed-Valent System $LiMn_2TeO_6$ <i>T. Salikhov, E. Zvereva, V. Nalbandyan, R. Sarkar, H.-H. Klauss, E. Vavilova</i>	173
Magnetic Resonance Investigation in the Polycrystalline $Pr_{0.8}Sr_{0.2}MnO_3$ Films: Features of the Magnetic States above Curie Temperature <i>Yu. Samoshkina, M. Rautskii, D. Velikanov, M. Volochaev, A. Sokolov, N. Andreev, V. Chichkov</i>	174
NMR and Water Molecules Diffusion in Nanochannels of Natrolite <i>A. V. Sapiga, N. A. Sergeev</i>	176
Alignment of Anisotropic Particles by Magnetic Field as Seen by NMR <i>N. A. Sergeev, A. M. Panich, S. D. Goren</i>	177
Wide-Band EPR Spectroscopy of the Black Garnets <i>G. S. Shakurov, V. A. Vazhenin, A. P. Potapov, V. A. Isaev, A. V. Lebedev, S. A. Migachev</i>	178
The Study of the Receptor Properties of Decasubstituted Pillar[5]arenes to Fluorescein dye by Methods of the High Resolution NMR Spectroscopy <i>P. Skvortsova, D. Shurpik, I. Stoikov, Y. Zuev, B. Khairutdinov</i>	179
Photo-Induced States of Copper Complexes of Coproporphyrin I: from Monomer to Dimer Systems <i>A. A. Sukhanov, Y. E. Kandrashkin, L. I. Savostina, V. K. Voronkova, V. S. Tyurin</i>	180
Distance between Separated Charges in the Ion-Radical Pair $P_{700}^+A_1^-$ of the Photosystem I Reaction Center Complex Incorporated into Trehalose Matrix at Different Dehydration Levels Measured Using Out-of-Phase ESEEM <i>A. A. Sukhanov, M. D. Mamedov, A. Yu. Semenov, K. M. Salikhov</i>	182
EPR Study of Al_2Er_2 Molecular Cluster <i>A. A. Sukhanov, Y. Peng, V. K. Voronkova, A. K. Powell</i>	183

Triplet State Delocalization in Zincporphyrin Dimer Probed by TR EPR <i>A. A. Sukhanov, V. K. Voronkova, V. S. Tyurin</i>	184
EPR Study of Ribosomal Translational Complexes <i>I. Timofeev, O. Krumkacheva, A. Kuzhelev, A. Malygin, D. Graifer, M. Meschaninova, A. Ven'yaminova, M. Fedin, G. Karpova, E. Bagryanskaya</i>	185
EPR Study of Light-Induced Metastable States in Two-Spin Cu(hfac) ₂ L ^R Compounds <i>S. Tumanov, M. Fedin, S. Veber, S. Tolstikov, N. Artiukhova, V. Ovcharenko</i>	186
Electrically Detected FMR of Permalloy Microstrip via Spin Rectification Effect <i>M. Vafadar, B. Rameev</i>	187
Spin Properties of [Fe(Salten)Cl] Complex Solutions Studied by NMR and EPR <i>M. Volkov, O. Turanova, E. Milordova, E. Frolova, I. Ovchinnikov, A. Turanov</i>	189
Nanoscale Magnetic Resonance Imaging of Intracellular Proteins <i>P. Wang, S. Chen, M. Guo, S. Peng, M. Wang, F. Shi, X. Rong, J. Su, J. Du</i>	190
Diluted Iron Oxide in K ₂ O-Al ₂ O ₃ -B ₂ O ₃ Studied Method EPR <i>I. V. Yatsyk, R. M. Eremina, P. S. Shirshnev, F. G. Vagizov</i>	191
Temperature Dependence of Resonance Field of EMR Signals in Biological Tissues <i>S. Yurtaeva, V. Efimov</i>	194
³¹ P NMR Spectrum of Rat Blood in Conditions of Spinal Cord Injury <i>S. Yurtaeva, M. Volkov, G. Yafarova, D. Silantieva, E. Yamalitdinova</i>	196
Peculiarities of the Application of a Multi-Pulse Sequence for Spin Coherence Control <i>R. Zaripov, E. Vavilova, I. Khairuzhdinov, E. Anisimova, T. Salikhov, V. Voronkova, K. Salikhov, M. Abdulmalic, F. Meva, S. Weheabby, T. Ruffer, B. Büchner, V. Kataev</i>	198
Determination of HFI Constants of Cu Oxamato-Complex by ENDOR and ED NMR Techniques <i>R. Zaripov, E. Vavilova, I. Khairuzhdinov, K. Salikhov, V. Voronkova, M. A. Abdulmalic, F. E. Meva, S. Weheabby, T. Ruffer, B. Büchner, V. Kataev</i>	199
Topological Zero Modes in Few-Layer Nanographenes: EPR, CESR and Magnetic Susceptibility Studies <i>A. M. Ziatdinov</i>	200

ZAVOISKY AWARD LECTURE

Topological High-Spin Organic Chemistry and Molecular Spin-Qubit Quantum Technology Underlain by Electron Magnetic Resonance

T. Takui

Department of Chemistry and Molecular Materials Science, Graduate School of Science,
Osaka City University, Osaka 558-8585, Japan;

Research Support/URA Center, University Administration Department,
Osaka City University, 3-3-138 Sugimoto, Sumiyoshi-ku, Osaka 558-8585, Japan;
takui@sci.osaka-cu.ac.jp

The past decades since 1967, when the first genuinely organic spin-quintet aromatic hydrocarbon in its electronic ground state appeared [1, 2], have witnessed a continuous development of organic molecule-based magnetism as an interdisciplinary field between chemistry, physics and related areas [3–5]. This is due to the fact that this exotic magnetism is relevant to the topological symmetry of the electron spin networks in open-shell molecular frames and thus has made important conceptual advances in chemistry and physics, contrasting with putative magnetism originating in d-electrons, as predicted by Heisenberg.

The topological MO degeneracy can be extended to polyanionic organic open-shell molecules and their clusters [6], which are stable even in solution at ambient temperature. They afford models for genuinely organic ferromagnetic metals and testing grounds for charged high spin systems with non-vanishing ZFS tensors whose spin states can be controlled by both magnetic and electric dipole transitions. From the theoretical side, the charged high spins having non-Kramers doublets and their relevant quantum control technology require non-conventional formalism or realm of the ZFS/electronic Zeeman interaction spin Hamiltonians [7].

The latest trend in open-shell chemistry and materials science is any possible applications of stable molecular spins, single molecule or in-ensemble based, to spin-based quantum computing/quantum information processing [5]. The current progress in this emerging field is toward the molecular optimization of scalable spin qubits, AWG-based technological implementation, and reduction of quantum decoherence to which the spin qubits are subject in their assemblages. We also emphasize that it is immensely important to implement practical quantum algorithms enabling us to carry out quantum chemical calculations on quantum computers and they are emerging [8].

1. Itoh K.: *Chem. Phys. Lett.* **1**, 235 (1967)
2. Wasserman E., Murray R.W., Yager W.A., Trozzolo A.M., Smolinsky G.: *J. Am. Chem. Soc.* **89**, 5076 (1967)
3. Itoh K., Takui T.: *Proc. Japan Acad. Ser. B* **80**, 29 (2004)
4. Lahti P.M., ed.: *Magnetic Properties of Organic Materials*; Chapter 11, 197–236. New York: Marcel Dekker 1999; Itoh K., Kinoshita M., eds.: *Molecular Magnetism: New Magnetic Materials*. Tokyo and Amsterdam: Kodansha and Gordon & Breach 2000.

5. Sato K., Nakazawa S., Rahimi R.D., Ise T., Nishida S., Yoshino T., Mori N., Toyota K., Shiomi D., Yakiyama Y., Morita Y., Kitagawa M., Nakasuji K., Nakahara M., Hara H., Carl P., Hoefer P., Takui T., *J. Mat. Chem.* **19**, 3739 (2009)
6. Nakazawa S., Sato K., Shiomi D., Yano M., Kinoshita T., Franco M.L.T.M.B., Lazana M.C.R.L.R., Shohoji M.C.B.L., Itoh K., Takui T.: *Phys. Chem. Chem. Phys.* **13**, 1424 (2011)
7. Yamane T., Sugisaki K., Matsuoka H., Sato K., Takui T. *et al.*: *Phys. Chem. Chem. Phys.*, in press (2017): DOI: 10.1039/c7cp03850j
8. Sugisaki K., Yamamoto S., Nakazawa S., Toyota K., Sato K., Shiomi D., Takui T.: *J. Phys. Chem. A.*, **120**, 6459 (2016)

PLENARY LECTURES

Multi-Extreme THz ESR: Developments and Future Biological Applications

**H. Ohta¹, S. Okubo¹, E. Ohmichi², T. Sakurai³,
S. Hara³, and H. Takahashi⁴**

¹ Molecular Photoscience Research Center, Kobe University, Kobe 657-8501, Japan, hohta@kobe-u.ac.jp

² Graduate School of Science, Kobe University, Kobe 657-8501, Japan

³ Center for Support to Research and Education Activities, Kobe University, Kobe 657-8501, Japan

⁴ Organization of Advanced Science and Technology, Kobe University, Kobe 657-8501, Japan

Recent developments and applications of our multi-extreme THz ESR in Kobe will be shown. Our multi-extreme THz ESR can cover the frequency region between 0.03 and 7 THz [1], the temperature region between 1.8 and 300 K [1], the magnetic field region up to 55 T [1], and the pressure region up to 1.5 GPa [2] simultaneously. Recently we have developed the hybrid-type pressure cell, which consists of the NiCrAl alloy inner cell, the Cu-Be alloy outer cell and the ceramic piston parts, and achieved 2.7 GPa [3]. Developments of our micro-cantilever ESR [4], which reached 1.1 THz [5], will be also shown. Finally our THz ESR measurements of hemin [6], which is the model substance of Myoglobin, will be presented, and we will discuss the future applications of micro-cantilever ESR to the biological systems.

1. Ohta H. *et al.*: *J. Low Temp. Phys.* **170**, 511 (2013)
2. Sakurai T. *et al.*: *Rev. Sci. Instr.* **78**, 065107 (2007); Sakurai T.: *J. Phys.: Conf. Series* **215**, 012184 (2010)
3. Fujimoto K. *et al.*: *Appl. Mag. Res.* **44**, 893 (2013); Ohta H. *et al.*: *J. Phys. Chem. B* **119**, 13755 (2015); Sakurai T. *et al.*: *J. Mag. Res.* **259**, 108 (2015); *J. Mag. Res.* **280**, 3 (2017)
4. Ohta H. *et al.*: *AIP Conf. Proceedings* **850**, 1643 (2006); Ohmichi E. *et al.*: *Rev. Sci. Instrum.* **79**, 103903 (2008); Ohmichi E. *et al.*: *Rev. Sci. Instrum.* **80**, 013904 (2009); Ohta H., Ohmichi E.: *Appl. Mag. Res.* **37**, 881 (2010); Ohmichi E. *et al.*: *J. Mag. Res.* **227**, 9 (2013); Ohmichi E. *et al.*: *Rev. Sci. Instrum.* **87**, 073904 (2016)
5. Takahashi H., Ohmichi E., Ohta H.: *Appl. Phys. Lett.* **107**, 182405 (2015)
6. Okamoto T. *et al.*: *J. Infrared Milli THz Waves* **37**, 1173 (2016); Okamoto T. *et al.*: *Appl. Mag. Res.* **48**, 435 (2017)

Spinon Magnetic Resonance in a Quasi 1D $S = 1/2$ Antiferromagnet with a Weak Exchange Interaction

**A. I. Smirnov¹, T. A. Soldatov^{1,2}, K. Yu. Povarov³, M. Halg³,
W. E. A. Lorenz³, and A. Zheludev³**

¹ P. L. Kapitza Institute for Physical Problems RAS, Moscow 119334, Russian Federation, smirnov@kapitza.ras.ru

² Moscow Institute for Physics and Technology, Dolgoprudny 141701, Russian Federation

³ Neutron Scattering and Magnetism, Lab. for Solid State Physics, ETH Zurich, Switzerland

A quasi-one-dimensional $S = 1/2$ antiferromagnet $\text{K}_2\text{CuSO}_4\text{Cl}_2$ is a rare example of a model spin-chain compound with Dzyaloshinsky-Moriya (DM) interaction of the uniform type. This kind of the DM interaction creates a preference for the spiral mean-field spin configuration in contrast to well known ‘‘canted’’ spin configuration of antiferromagnets with a weak ferromagnetism. The last configuration is a result of a more conventional ‘‘staggered’’ DM interaction. For $S = 1/2$ Heisenberg antiferromagnetic spin chain, exhibiting a disordered ground state and a continuum of pairs of fractional excitations (so called ‘‘spinons’’), the uniform DM interaction results in a fine structure of ESR and in an unusual spin gap at the center of the Brillouin zone. The fine structure in the form of an ESR doublet occurs at a distinct orientation of magnetic field and at temperatures far below $T_J = J/k_B$, here J is the exchange integral [1]. The frequencies of the doublet components are at the boundaries of the modified continuum at $q = 0$, the splitting of the doublet is of the order of the DM energy D , see, *e.g.*, [1–3]. The spinon ESR in form of a doublet and with the

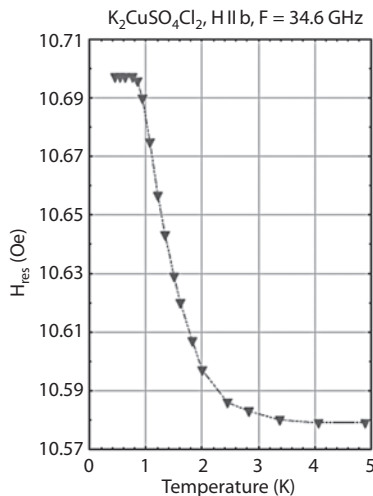


Fig. 1. Temperature dependence of the 34.6 GHz ESR magnetic field.

energy gap was indeed observed in antiferromagnetic compounds Cs_2CuCl_4 [e.g. 3, 4] and $\text{K}_2\text{CuSO}_4\text{Br}_2$ [5]. It was found experimentally, that the formation of a doublet and of the gap occurs below a temperature with empirically suggested value $T_{DJ} = (DJ)^{1/2}/k_B$, thus, the value of D should also affect conditions of the formation of the fine structure of the spinon continuum.

In this paper we check the formation of the spinon ESR in crystals of $\text{K}_2\text{CuSO}_4\text{Cl}_2$, which has much lower values of D (still unknown) and J (approximately 3 K), compared to the spin systems mentioned above. The measurements were done in the temperature range 0.4–10 K and in the frequency range 4–40 GHz. We observe a shift of the ESR line with cooling the sample down through the temperature $T = 1$ K (see Fig. 1). Besides, a small gap of ESR spectrum of about 0.3 GHz was found to open. The ESR spectrum, however, remains in a single-line form. At the same time, this single ESR line follows the position of the low-frequency component of the doublet, see the resonance field shift presented in Fig. 1. The observed shift of 118 Oe, directed to higher fields, corresponds to the value of $D \sim 0.015$ K, from this we estimate $T_{DJ} \sim 0.2$ K. We believe, that the higher component of the doublet is not visible because the temperature of the experiment 0.4 K is not lower than T_{DJ} . Note, that the previous compounds were also demonstrating the high-frequency doublet of much lower intensity, disappearing at heating well before the lower component disappears. Thus, the observed behavior of ESR in $\text{K}_2\text{CuSO}_4\text{Cl}_2$ is in a correspondence with the scenario of spinon ESR formation, despite we have failed to discover the pronounced doublet.

Work is supported by Russian Science Foundation grant No. 17-12-01505 and by the program of the Presidium of Russian Academy of Sciences.

1. Gangadharaiah S., Sun J., Starykh O.A.: Phys. Rev. B **78**, 054436 (2008)
2. Karimi H., Affleck I.: Phys. Rev. B **84**, 174420 (2011)
3. Povarov K.Yu. *et al.*: Phys. Rev. Lett. **107**, 037204 (2011)
4. Smirnov A.I. *et al.*: Phys. Rev. B **91**, 174412 (2015)
5. Smirnov A.I. *et al.*: Phys. Rev. B **92**, 134417 (2015)

A Pulse Dipole EPR-Based Distance Measurements at Ambient Temperatures

E. Bagryanskaya

N. N. Vorozhtsov Novosibirsk Institute of Organic Chemistry SB RAS,
Novosibirsk 630090, Russian Federation, egbagryanskaya@nioch.nsc.ru

Pulsed dipolar (PD) EPR spectroscopy is a powerful technique allowing for distance measurements between spin labels in the range of 2.5–10.0 nm. It was proposed more than 30 years ago, and nowadays is widely used in biophysics and materials science. Until recently, PD EPR experiments were limited to cryogenic temperatures ($T < 80$ K). Recently, application of spin labels with long electron spin dephasing time at room temperature such as triarylmethyl radicals and nitroxides with bulky substituents at a position close to radical centers enabled measurements at room temperature and even at physiologically relevant temperatures by PD EPR as well as other approaches based on EPR (e.g., relaxation enhancement; RE). In this presentation, the features of PD EPR and RE at ambient temperatures, in particular, requirements on electron spin phase memory time, ways of immobilization of biomolecules, the influence of a linker between the spin probe and biomolecule, and future opportunities are reviewed [1–8]. Distance measurements at room temperature can be useful in the cases when the dynamics of complexes of biomolecules and changes in distance at higher temperatures are expected. Thus, the development of new approaches to mild immobilization and spin labels with longer phase memory time and higher stability is still a highly relevant task for the future development of PDS distance measurements at ambient temperatures.

1. Bagryanskaya E.G., Krumkacheva O.A., Fedin M.V., Marque S.R.A.: *Methods in Enzymology* **563**, 365 (2015)
2. Krumkacheva O., Bagryanskaya E.: *J. Magn. Reson.* 2017, in press.
3. Krumkacheva O., Bagryanskaya E.: Trityl radicals as spin labels, Book EPR, From the book: *Electron Paramagnetic Resonance* **25**, 35–60 (2016)
4. Shevelev G. *et al.*: *J. Amer. Chem. Soc.* **136**, 9874–9877 (2014)
5. Kuzhelev A.A., Strizhakov R.K., Krumkacheva O.A., Polienko Y.F., Morozov D.A., Shevelev G.Yu., Pyshnyi D.V., Kirilyuk I.A., Fedin M.V., Bagryanskaya E.G.: *J. Magn. Reson.* **266**, 1 (2016)
6. Lomzov A.A., Sviridov E.A., Shernuykov A.V., Shevelev G.Yu., Pyshnyi D.V., Bagryanskaya E.G.: *J. Phys. Chem. B* **120**, no. 23, 5125 (2016)
7. Kuzhelev A.A., Tormyshev V.M., Rogozhnikova O.Yu., Trukhin D.V., Troitskaya T.I., Strizhakov R.K., Krumkacheva O.A., Fedin M.V., Bagryanskaya E.G.: *Zeitschrift für Physikalische Chemie*, 2017, doi: 10.1515/zpch-2016-0811
8. Kuzhelev A.A., Shevelev G.Yu., Krumkacheva O.A., Tormyshev V.M., Pyshnyi D.V., Fedin M.V., Bagryanskaya E.G.: *J. Phys. Chem. Lett.* **7**, 2544 (2016)

EPR Methods to Determine Properties of Intrinsically Disordered Proteins

M. Huber

Department of Physics, Huygens-Kammerlingh-Onnes Laboratory, Leiden University,
Leiden 2504RA, The Netherlands, huber@physics.leidenuniv.nl

Intrinsically Disordered Proteins (IDP's) gained notoriety by their involvement in neurodegenerative diseases. This class of proteins was discovered only two-and-a-half decades ago, which was when the term IDP was coined. Subsequent research showed that IDP's are relatively frequent in organisms (14% of expressed proteins in *E. coli*), have specific functions, and operate using special mechanisms, mechanisms that differ profoundly from regular protein function.

Understanding IDP's is a challenge. For example, weak interactions and perturbations can have large effects on the protein itself, and the flexibility enables these proteins to change conformation in response to changes in environment and available partners, be it proteins, DNA/RNA or biological membranes of different types. In general, traditional structural methods do not work well to study them, and EPR methods have to be adapted specifically [1].

We have developed a toolbox to characterize IDP's, based on liquid and frozen solution EPR. We will discuss how to apply double electron spin-electron spin resonance (DEER), use the continuous wave lineshape-derived mobility of the spin label to determine the interaction of IDP's with membranes [2] and detect distances of close approach [3]. Many experiments are based on spin-label EPR, however we recently explored methods to learn about metal-ions in Alzheimer's disease, focusing on iron [4].

1. Huber M. in: Specialist Periodic Reviews RSC: EPR, pp. 79–102 (2013)
2. Kumar P. *et al.*: PLOS One (2015) DOI: 10.1371/journal.pone.0142795
3. Hashemi Shabestari M. *et al.*: Peptide Science **102**, 244–251 (2014)
4. Kumar P. *et al.*: Scientific Reports Article number: 38916 (2016) doi:10.1038/srep38916

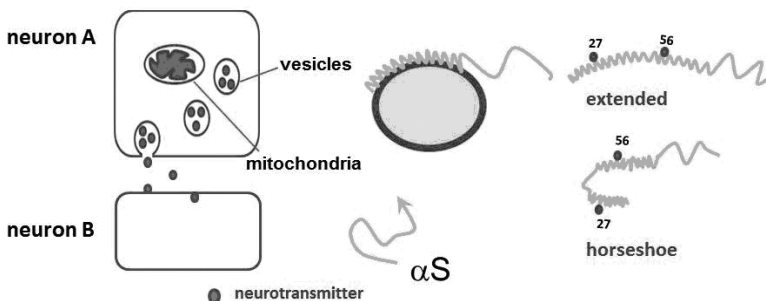


Fig. 1. Different interaction modes of alpha-synuclein, an IDP related to Parkinson's disease, with membranes.

Soft Spins and Higgs Mode in Ruthenates

G. Khaliullin

Max Planck Institute for Solid State Research, Stuttgart D-70569, Germany

I will discuss a special class of Mott insulators, where spin-orbit coupling dictates a nonmagnetic $J = 0$ ground state and the magnetic response is given by gapped singlet-triplet excitations. Exchange interactions as well as crystalline electric fields may close the spin gap, resulting in Bose-Einstein condensation of spin-orbit excitons. In addition to usual magnons, a Higgs amplitude mode, most prominent near quantum critical point, is expected. Upon electron doping, ferromagnetic correlations and triplet superconductivity may emerge. These predictions [1, 2] will be discussed in the context of recent neutron [3] and Raman light [4] scattering experiments in ruthenium oxides.

1. Khaliullin G.: Phys. Rev. Lett. **111**, 197201 (2013)
2. Chaloupka J., Khaliullin G.: Phys. Rev. Lett. **116**, 017203 (2016)
3. Jain A. *et al.*: Nature Phys., DOI:10.1038/nphys4077 (2017)
4. Souliou M. *et al.*: arXiv:1704.04991.

Insight into Protein Function by EPR

R. Bittl

Freie Universität Berlin, Berlin 14195, Germany, robert.bittl@fu-berlin.de

In my talk, I will be discuss the role of flavin reduction to the EPR-active semiquinone radical state in the signalling of blue-light photoreceptors with particular focus on cryptochromes (Cry). This photo-reduction is a long-standing matter of dispute for all three blue-light photo-receptor classes. A transient photo-reduction of the flavin has early been identified as key step for BLUF photoreceptors but later put in question. For LOV proteins a transient photo-reduction has been postulated as an intermediate for the flavin-Cys covalent bond formation but has not been unequivocally established. However, recently light-dependent signalling has been shown for LOV constructs lacking the reactive Cys, and thus lacking the photo-adduct usually identified as the signalling state. In these constructs a flavin radical serves as the photoproduct initiating the signalling cascade.

Even more disputed is the role of flavin reduction in Cry proteins. *In cell* EPR experiments have clearly shown the presence of a flavin semiquinone as a result of Cry photo-activation for wild type AtCry1, AtCry2 and DmCry. Nevertheless, its role as signalling state has been challenged on the basis of *in vitro* optical experiments on Cry constructs lacking one or more of the conserved Trp residues. The Trp residues form an essential Trp electron transfer cascade in the related photolyase protein family. However, electron transfer in Cry has been shown by EPR to be much more variable than in photolyases, and several alternative electron transfer pathways besides the Trp triad have been identified.

For AtCry2, we have resolved the apparent discrepancy between the wild type *in cell* EPR and the mutant *in vitro* EPR data by showing the influence of abundant small molecule metabolites, e.g. ATP, on the electron transfer in Trp triad mutants. Recently, we have extended these EPR studies to AtCry1, where we again find a promotion of electron transfer in the presence of ATP. Furthermore, we also have identified a flavin semiquinone upon photo-activation of robin Cry.

SPECIAL SESSION DEVOTED TO THE
110 ANNIVERSARY OF E. K. ZAVOISKY

E. Zavoisky and Kazan University

M. S. Tagirov

Kazan Federal University, Kazan 420008, Russian Federation, Murat.Tagirov@kpfu.ru

About E. Zavoisky and His Discovery

K. M. Salikhov

Zavoisky Physical-Technical Institute, Russian Academy of Sciences, Kazan 420029,
Russian Federation, salikhov@kfti.knc.ru

Dimer Self-Organization of Rare-Earth Impurity Ions in Synthetic Forsterite

V. F. Tarasov

Zavoisky Physical-Technical Institute, Russian Academy of Sciences, Kazan 420029,
Russian Federation, tarasov@kfti.knc.ru

EPR study of forsterite (Mg_2SiO_4) single crystals doped with rare earth (RE) ions showed that some impurity RE ions have a tendency to the formation of dimer associates. When the distribution of impurity ions over lattice sites is strictly statistical, the ratio of dimer C_{dim} and single-ions C_{singl} concentrations is determined by the equation [1] $C_{\text{dim}}/C_{\text{singl}} = 2c(1 - c^2)$, where c is the total mole fraction of impurity ions in the crystal with respect to the major host component substituted by the impurity ions. In this case, the probability of dimer formation at low RE concentrations ($c \ll 1$) also should be rather low. Despite this anomalously high concentration of the RE dimer associates was observed for Ho^{3+} [2], Tb^{3+} [3], Er^{3+} and Yb^{3+} ions in forsterite. The samples for investigation were grown by Czochralski technique in the Laser Materials and Technology Research Center at the General Physics Institute of the Russian Academy of Sciences. Measurements were performed at helium temperatures by the EMX plus and ELEXSES E-580 spectrometers in the X- and Q-bands and by the wide-band EPR spectrometer in the frequency band of 70–350 GHz. Dimer associates were identified by the hyper fine structure of the EPR spectra, by the fine structure of electron spin levels or by the properties of the spin dynamics. We assume that mechanism leading to the association of the trivalent impurity ions into the dimers is related with the necessity to conserve the total cation charge during the heterogeneous substitution. In this case three Mg^{2+} cations are replaced by a RE dimer associate with magnesium vacancy between them.

This work was supported in part by RFBR and the Government of the Republic of Tatarstan according to the research project No. 15-42-02324 a.

1. Motokawa M., Ohta H., Makita N., Ikeda H.: J. Phys. Soc. Jpn. **6**, 322 (1992)
2. Gaister A.V., Zharikov E.V., Kononov A.A., Subbotin K.A., Tarasov V.F.: JETP Letters **77**, 625 (2003)
3. Kononov A.A., Lis D.A., Subbotin K.A., Tarasov V.F., Zharikov E.V.: Appl. Magn. Reson. **45**, 193 (2014)

The Different Faces of Free Radical Spin Dynamics in Frozen Solution

M. K. Bowman¹, H. Chen¹, B. R. Fowler¹, and A. G. Maryasov²

¹ Chemistry Department, The University of Alabama, Tuscaloosa, Alabama 35487, USA, mkbowman@ua.edu

² V. V. Voevodsky Institute of Chemical Kinetics and Combustion, Siberian Branch of Russian Academy of Sciences, Novosibirsk, 630090, Russia, maryasov@kinetics.nsc.ru

The electron spin dynamics of solutions of triaryl methyl (TAM or trityl) radicals are important for applications ranging from EPR imaging and oximetry; through spin labeling for measurement of macromolecular distances; to dynamic nuclear polarization (DNP) for sensitivity enhancement of magnetic resonance spectroscopy and imaging (NMR and MRI). We report here on the electron spin dynamics of frozen TAM solutions over the range of concentrations used in DNP.

The electron spin dynamics appear in several forms, in addition to the relaxation of electron spin magnetization characterized by the classic Bloch T_1 and T_2 . These include the evolution of dipolar fields from the electron spins; the spatial diffusion of electron spin magnetization; changes in the resonance frequency of individual electron spins; and the interconversion of various coherences and magnetizations among the electron (and nuclear) spins.

At millimolar concentration and below, the relaxation of electron spin magnetization to the lattice is characterized by a single, uniform relaxation rate of $1/T_1$ having a temperature dependence characteristic of the well-known two-phonon Raman relaxation process. At concentrations of tens of millimolar, the relaxation below ~ 50 K is characterized by a distribution of relaxation rates skewed toward high rates and with a temperature dependence characteristic of Orbach-Aminov relaxation through an excited state a few wavenumbers (cm^{-1}) above the ground state. This is the result of cross relaxation to clusters of radicals that spontaneously assemble as the samples freeze. Contact between radicals in the cluster produces an electron exchange interaction and splittings of a few wavenumbers.

Measurements of the relaxation of the dipolar field were made with the pulse sequence suggested by Jeener and Broekaert for inhomogeneously broadened systems. The dipolar relaxation is highly non-exponential, with significant relaxation in less than 100 ns but with part of the dipolar field lasting tens of microseconds. The dipolar field relaxes completely before any noticeable relaxation of the electron spin magnetization and appears to be driven by electron spin diffusion processes more than by spin-lattice relaxation.

Measurements of the spectral diffusion kernel show changes in the EPR frequency of a single radical occurring on the nanosecond to millisecond timescale. The initial resonant frequency of a radical starts off at a single value and spreads out until it covers part or all of the EPR spectrum, Fig. 1. Several mechanisms can be identified in the spectral diffusion including: instantaneous diffusion described originally by Klauder and Anderson; nuclear modulation (ESEEM) and discrete saturation (solid effect); and nuclear spin flip-flops (T_{1n}).

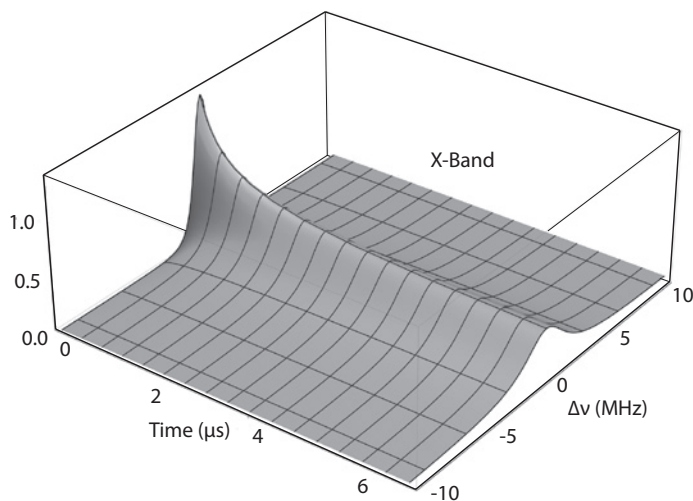


Fig. 1. The initial 7 μs of the evolution of the EPR frequency of a 50 mM frozen solution TAM radical at 50 K as the spin packet spreads out from nearly a δ -function to cover more than 10 MHz.

These occur in the first few microseconds and result in a limited change in a radical's resonant frequency. There is also a gradual broadening on the 1–100 μs timescale that becomes faster and ultimately broader as the radical concentration increases. This component of spectral diffusion seems to involve the relaxation of the dipolar field and spin diffusion from one radical to another. This measurement of the spectral diffusion kernel makes it possible to calculate the time dependence of the EPR frequency of radicals involved in cross-effect and thermal mixing interactions in DNP.

This work was supported by the Chemistry Division of the National Science Foundation, Award No. 1416238 and by Russian Foundation for Basic Research grant No. 14-03-93180.

SECTION 1

THEORY OF MAGNETIC RESONANCE

Magnetic Resonance of Impurity Spin in Slow Normal Stochastic Local Field

F. S. Dzheparov and D. V. Lvov

National Research Center “Kurchatov Institute”, ITEP, Moscow 117218, Russian Federation,
dzheparov@itep.ru

Spin system with the Hamiltonian (written in the rotating frame)

$$H = H_0(t) + H_1, \quad H_1 = \omega_1 I_x, \quad H_0(t) = (\Delta + \omega_f(t)) I_z,$$

is considered for slow time dependence of the local field $\omega_f(t)$, when spin evolution is quasi-adiabatic. Here I_α is spin operator, Δ is the detuning from the resonance, ω_1 represents magnitude of the rotating field, and $\omega_f(t)$ is considered as a normal stochastic process with the correlation function $\langle \omega_f(t) \omega_f(t_1) \rangle_n = M_2 \kappa(|t - t_1|)$, $M_2 = \langle \omega_f^2 \rangle_n$.

The longitudinal spin evolution was calculated in [1] with the result

$$F(t) = \langle I_z I_z(t) \rangle / \langle I_z^2 \rangle = (2/\pi) \arcsin \kappa(t),$$

valid for $\Delta = 0$ in zero order in small parameters $\varepsilon_1 = \omega_1^2 T_2^2 \ll 1$ and $\varepsilon_s = (\omega_1 \tau')^{-2} \ll 1$, where $\tau' = |\partial^2 \kappa(t=0) / \partial t^2|^{-1/2} \sim \tau_c = \int_0^\infty dt \kappa(t)$. We extended this analysis to obtain realistic approximation of slow evolving part of $F(t)$ in adiabatic conditions for arbitrary ε_1 and to calculate exponentially small in ε_s quasi-adiabatic losses at small ε_1 [2].

1. Dzheparov F.S., Lvov D.V.: Magn. Reson. Solids **18**, 16201 (2016)
2. Dzheparov F.S., Lvov D.V.: Nuclear magnetic resonance in Gaussian stochastic local field. Preprint ITEP 01-17, Moscow 2017.

Manipulations of High Spin Kramers System States by Circularly Polarized MW Fields

A. G. Maryasov¹, S. L. Veber², and M. V. Fedin²

¹ Voevodsky Institute of Chemical Kinetics and Combustion, SB RAS,
Novosibirsk 630090, Russian Federation, maryasov@kinetics.nsc.ru

² International Tomography Center, SB RAS, Novosibirsk 630090, Russian Federation,
sergey.veber@tomo.nsc.ru

High spin Kramers systems ($S \geq 3/2$) having large zero field splitting (ZFS) are promising objects to be used as, e.g., single molecular magnets (SMM) [1]. In weak external magnetic fields such systems behave as a set of Kramers doublets. Inside of each doublet the system state may be driven by mw fields which induce EPR transitions. Of interest are also transitions between Kramers doublets which resonance frequencies maybe up to terahertz range.

Analysis demonstrates that for axial ZFS the circularly polarized MW field (with magnetic component perpendicular to the molecular axial axis) induces transitions just between two particular components of two Kramers doublets, the system spin Hamiltonian (in angular frequency units) in the rotating frame (RF) is

$$\hat{H} = D(\hat{S}_Z^2 - S(S+1)/3) + (\omega_Z - \omega)\hat{S}_Z + \omega_1\hat{S}_X.$$

Here D is ZFS parameter, ω_Z is the secular part of Zeeman interaction, ω_1 is MW magnetic field strength in the RF which induces resonance transitions, ω is frequency of MW field. It is supposed that $\omega_1 \ll \omega_Z \ll |D| \approx |\omega|$. The energy levels in the RF are $\omega_m \approx D(m^2 - S(S+1)/3) + (\omega_Z - \omega)m$. The resonance condition in RF is $\omega_m - \omega_{m-1} = 0$, or $\omega = \omega_Z + D(2m - 1)$. This means that resonance frequencies for, e.g., transitions $3/2 \leftrightarrow 1/2$ and $-1/2 \leftrightarrow -3/2$ have nearly the same absolute values but opposite signs thus providing selectivity to the system excitation by circularly polarized MW fields.

Applications of this selectivity for high spin qubits and SMMs are considered. The work was supported by Russian Science Foundation (grant 17-13-01412).

1. Juan Bartolomé J., Luis F., Julio F. Fernández J. F., eds.: Molecular Magnets, Physics and Applications. Berlin: Springer 2014.

Reversing Chaotic Dynamics of Nuclear Spins

B. V. Fine

Skolkovo Institute of Science and Technology, Moscow, Russian Federation,
University of Heidelberg, Germany,
b.fine@skoltech.ru

The response of many-particle systems to imperfect time-reversal known in nuclear magnetic resonance (NMR) as “magic echo” and in the broader community as “Loschmidt echo” has recently come into a sharp focus of statistical physics research focused on the role and the manifestations of microscopic chaos. Although the notion of chaos is frequently invoked in the foundations of statistical physics, its definition for many-particle quantum systems is still not fully understood. We show that nonintegrable lattices of spins $1/2$, which are often considered to be chaotic, do not exhibit the basic property of classical chaotic systems, namely, exponential sensitivity to small perturbations [1]. We compare the Loschmidt echo responses of chaotic lattices of classical spins and nonintegrable lattices of spins $1/2$. In the classical case, Loschmidt echoes exhibit exponential sensitivity to small perturbations characterized by twice the value of the largest Lyapunov exponent of the system. In the case of spins $1/2$, Loschmidt echoes are only power-law sensitive to small perturbations. Our findings imply that it is impossible to define Lyapunov exponents for lattices of spins $1/2$ even in the macroscopic limit. At the same time, the above absence of exponential sensitivity to small perturbations is an encouraging news for the efforts to create quantum simulators. We further show that the classical chaotic behavior is gradually recovered once the value of lattice quantum spins is increased from $1/2$ to larger values. The power-law sensitivity of spin- $1/2$ lattices to small perturbations is predicted to be observable in NMR magic echo experiments.

1. Fine B.V., Elsayed T.A., Kropf C.M., de Wijn A.S.: Phys. Rev. E **89**, 012923 (2014) (eprint arXiv:1305.2817)
2. Elsayed T.A., Fine B.V.: Phys. Scr. 014011 (2015) (eprint arXiv:1409.4763)

Probing of Fluorine Atom Electronic Shell by means of Topological Analysis of Helium Chemical Shift Surfaces

E. Yu. Tupikina¹, A. A. Efimova¹, G. S. Denisov¹, and P. M. Tolstoy²

¹ Department of Physics, St. Petersburg State University, St. Petersburg 198504, Russian Federation, elenatupikina@gmail.com

² Center for Magnetic Resonance, St. Petersburg State University, St. Petersburg 198504, Russian Federation

Non-covalent interactions play crucial role in structure stabilization of molecules. The ability of a molecule to participate in non-covalent interactions is determined by the features of its electron shell. In recent years in study of non-covalent interactions (in particular hydrogen bonds) there have been a numerous attempts to find a parameter that could describe the features of the electron shell of isolated molecule and predict some characteristics of intermolecular interactions, such as the geometry and binding energy. Such parameters as calculated quantum mechanical functions of the molecular electrostatic potential [1], electron localization [2, 3], and electron density were proposed to use the. However, the problem of finding principally measurable parameter which will be capable to describe features of the electronic shells remains an issue. In this work we propose to use ³He atom as a probe particle. Our approach is to place the ³He atom sequentially in a set of points around investigated molecule and calculate interaction energy and NMR parameters such as chemical shift of the helium atom δ_{He} . It is shown that the chemical shift δ_{He} is sensitive even to weak changes in the electronic shell. At first step, we calculate the surfaces of chemical shift of the helium atom δ_{He} . Further, a topological analysis of this surface is carried out. Interestingly, features of δ_{He} surface turned out to be more informative markers for hydrogen bond properties than other electronic structure parameters. As a model molecule for this work we used such simple fluorine containing proton donors FH, (HFH)⁺ and acceptors F⁻, (FHF)⁻.

This work supported by RFBR grant 17-03-00497.

1. Clark T., Hennemann M., Murray J.S., Politzer P.: *J. Mol. Model.* **13**, 291–296 (2007)
2. Becke A.D., Edgecombe K.E.: *J. Chem. Phys.* **92**, 5397–5403 (1990)
3. Kavitha S., Deepa P., Karthika M., Kanakaraju R.: *Polyhedron* **115**, 193–203 (2016)

Theory of Chiral Systems and Molecular Machines

L. Khalilov

Institute of Petrochemistry and Catalysis of Russian Academy of Science, Ufa,
Russian Federation, khalilovlm@gmail.com

SECTION 2

LOW-DIMENSIONAL SYSTEMS AND NANO-SYSTEMS

Magneto-resistive and Microwave Responses of Hybrid Josephson Structures with Ferromagnetic Layers

**V. V. Ryazanov^{1,3}, I. A. Golovchanskiy^{2,3}, V. V. Bolginov^{1,2},
N. N. Abramov², and V. I. Chichkov²**

¹ Institute of Solid State Physics, Chernogolovka 142432, Russian Federation, ryazanov@issp.ac.ru

² National University of Science and Technology "MISIS", Moscow 119049, Russian Federation, chichkov.vladimir@gmail.com

³ Moscow Institute of Physics and Technology, State University, Dolgoprudny 141700, Russian Federation, golov4anskiy@gmail.com

In recent years weak ferromagnetic layers regain strong practical interest due to their integration in various superconductor-ferromagnet-superconductor (SFS) Josephson spintronic elements and ultra-fast electronic devices (see [1]). Pd-Fe alloys with a low Fe content exhibit in-plane magnetic anisotropy and small coercive field that makes them perfect candidates for novel Josephson cryogenic magnetic memory elements [1]. High-sensitive ferromagnetic-resonance (FMR) experiment on Pd_{0.99}Fe_{0.01} films [2] has enabled to estimate the saturation magnetization, anisotropy field, and Gilbert damping constant. A detailed analysis of FMR spectra has allowed to estimate characteristic time scale for magnetization dynamics in Pd-Fe based cryogenic memory elements as $(3-5) \cdot 10^{-9}$ s. Investigations [3] have shown that the rectangular magnetic Josephson junctions (Nb-PdFe-Nb) can be used as an effective Josephson memory element with the critical current defined by the orientation of magnetic moment at zero magnetic field. We have proposed also a hybrid device based on a long Josephson junction inductively coupled to an external ferromagnetic layer. The Josephson junction in the zero-field-step mode induces a localized AC magnetic field in the ferromagnetic layer and enables to create a synchronized magnetostatic standing wave, which in its turn induces additional dissipation for Josephson soliton propagation in the junction and also enables a phase locking (resonant soliton synchronization) at frequency of natural ferromagnetic resonance.

1. Larkin T.I., Bol'ginov V.V., Stolyarov V.S. *et al.*: Appl. Phys. Lett. **100**, 222601 (2012)
2. Golovchanskiy I.A. *et al.*: Journ. Appl. Phys. **120**, 163902 (2016)
3. Golovchanskiy I.A. *et al.*: Phys. Rev. B. **94**, 214514 (2016)
4. Golovchanskiy I.A. *et al.*: Supercond. Sci. Technol. **30**, (2017)

Dynamics of Majorana States in Nanowires and Josephson Junctions

**A. S. Mel'nikov¹, I. M. Khaymovich^{1,2}, J. P. Pekola^{3,4}, A. Kopasov¹,
I. A. Shereshevskii¹, and N. Vdovicheva¹**

¹Institute for Physics of Microstructures, Russian Academy of Sciences, Nizhny Novgorod 603950,
Russian Federation

²Laboratoire de Physique et Modélisation des Milieux Condensés, Université de Grenoble
Alpes and CNRS, Grenoble 38042, France

³Low Temperature Laboratory, Aalto University, Aalto FI-00076, Finland

⁴Chair of Excellence of the Nanosciences Foundation, Grenoble 38000, France

The goal of our work is to develop a theoretical description of the essentially nonequilibrium dynamics of Majorana states taking account of the beating of the quasiparticle wavefunction consisting of the contributions corresponding to both positive and negative energies of the Bogolubov-de Gennes Hamiltonian. We consider two examples of such beating phenomenon: (i) dynamic transport through a nanowire placed in contact with normal reservoirs, (ii) ac Josephson effect in a junction with Majorana states and the peculiarities of the related odd-even Shapiro phenomenon. Our study includes also the analysis of the self-consistency equation for the induced superconducting states and allows to take account of the gap function modulation near the positions of the Majorana states. We also analyze the Majorana state structure beyond the quasiclassical limit and consider the states localized both at the wire edges and the thermally induced phase slip centers. The results of this self-consistent analysis are compared with the case of singlet superconducting wire. We consider both the limits of weak and strong Coulomb effects and find that the beating phenomenon survives and is robust to the strong Coulomb blockade influence.

Spin Current and Second Harmonic Generation in Noncollinear Magnets

E. A. Karashtin¹, N. S. Gusev¹, K. D. Sladkov², I. A. Kolmychek²,
T. V. Murzina², and A. A. Fraerman¹

¹ Institute for Physics of Microstructures RAS, Nizhny Novgorod 603950, GSP-105,
Russian Federation

² Department of Physics, Moscow State University, Moscow 119991, Russian Federation,
andr@ipmras.ru

We report theoretical and experimental studies of the new mechanism of second harmonic generation (SHG) induced by spin current in a non-collinearly magnetized medium. Spin current is the flow of spin, which may be accompanied by the flow of electric charge. A special kind of spin current systems is a system where the pure spin current exists in equilibrium [1], when the charge flow is zero. Such a case can be realized in magnetic systems with non-collinear magnetization distribution. They attract attention due to new interesting properties induced by the simultaneous inversion and the time reversal symmetry broken in equilibrium in such systems. This leads to a number of new phenomena, such as the flexo-magnetoelectric effect predicted in non-collinearly magnetized media [2, 3] and the second harmonic generation induced by the spin current [4]. Due to its high symmetry sensitivity, the SHG effect is considered as a sensitive tool for the spin current diagnostics. The mechanism of the second-order non-linear optical effect due to the pure spin current in the non-collinear magnetic system has not been considered till now. In this work we study the microscopic mechanisms of the second harmonic generation in such system. The magnetic-field induced SHG is investigated experimentally in a multilayer magnetic system that consists of the two interacting subsystems with the perpendicular (out-of-plane) and with the in-plane magnetic anisotropy. Symmetry considerations show that in such a system there can be the SHG polarization $P(2\omega)$ contribution proportional to the equilibrium spin current described by the second-rank tensor $S_{\{jk\}}$ and to the wave electric field \mathbf{E} squared.

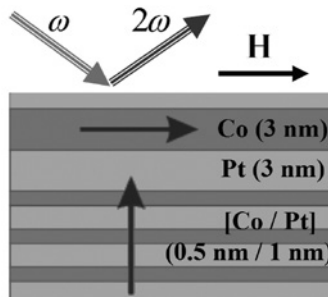


Fig. 1. Schematic view of the sample and the geometry of the experiment.

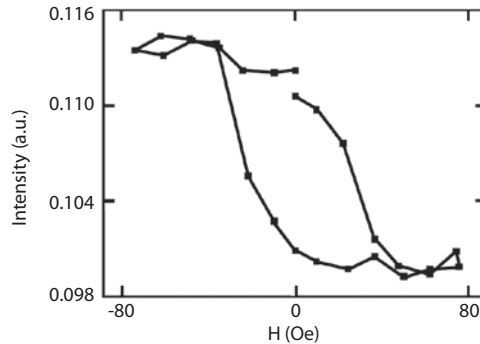


Fig. 2. Second harmonic intensity hysteresis for the -p-p combination of the pump and second harmonic signal polarizations.

The schematic view of the studied structure is shown in Fig. 1. We use a multilayer ferromagnetic sample [Co (0.5 nm) / Pt (1 nm)] \times 3 / Pt (3 nm) / Co (3 nm) grown by magnetron sputtering on silicon or fused quartz substrates. The sample consists of a subsystem with the perpendicular magnetic anisotropy (Co/Pt trilayer) and a subsystem with the in-plane anisotropy (3 nm – thick Co layer) separated by a 3 nm – thick Pt spacer. The subsystems weakly interact through such a spacer [5]. Therefore we may control the magnetization of each layer. If an external magnetic field is applied in the layers plane, the thick Co layer reverses its magnetization in a small field (tens of Oe), while the Co/Pt subsystem is splitted into domains in a higher field (hundreds of Oe) and is magnetized in the sample plane in a much greater field. In accordance with the symmetry analysis, the experiments are performed for the longitudinal magnetic field and for the p-in, p-out(SHG) combination of polarizations. In that case, the magnetization-induced SHG from individual layers is absent due to the symmetry restrictions. However we observe the SHG effect in such geometry in a weakly interacting system, which appears as a magnetic hysteresis in the SHG intensity as is shown in Figure 2. The width of the hysteresis loop corresponds to the magnetization reversal of the thick Co layer. Such effect is absent for a simple systems with a uniform Co (3 nm) film or for a [Co (0.5nm) / Pt (1 nm)] \times 3 multilayer. Thus the SHG dependencies attained for the structure with non-collinear magnetization is a manifestation of the spin-current induced SHG.

This work was supported by the Russian Science Foundation (Grant No. 16-12-10340)

1. Sonin E., *Advances in Physics* **59**, 181 (2010)
2. Bar'yakhtar V.G., L'vov V.A., Yablonskii D.A.: *Pis'ma Zh. Exp. Teor. Fiz.* **37**, 565 (1983)
3. Katsura H., Nagaosa N., Balatsky A.V., *Phys. Rev. Lett.* **95**, 057205 (2005)
4. Wang J., B.-F. Zhu, and R.-B. Liu, *Phys. Rev. Lett.* **104**, 256601 (2010)
5. E.S. Demidov, N.S. Gusev, L.I. Budarin et al., *J. Appl. Phys.* **120**, 173901 (2016)

Electric Field Controlled ESR in Multiferroic CuCrO_2

L. E. Svistov¹, S. K. Gotovko^{1,2}, T. A. Soldatov^{1,2}, and H. D. Zhou³

¹ P. L. Kapitza Institute for Physical Problems RAS, Moscow 119334, Russian Federation

² Moscow Institute of Physics and Technology, 117303 Moscow, Russian Federation

³ Department of Physics and Astronomy, University of Tennessee, Knoxville 37996, Tennessee, USA, svistov@kapitza.ras.ru

CuCrO_2 is an example of quasi-two-dimensional antiferromagnet ($S = 3/2$) with triangular lattice structure. The neutron scattering experiments detected a three dimensional coplanar magnetic order with incommensurate wave vector $q_{ic} = (0.329, 0.329, 0)$ that slightly differs from the wave vector of a commensurate 120° -structure. According to ESR and NMR investigations the orientation of the spin plane of magnetic structure is defined by strong easy axis anisotropy perpendicular to trigonal plane and weak anisotropy perpendicular to one side of the triangle. The magnetic ordering is accompanied by the appearance of an electric polarization [1]. The electric polarization is perpendicular to spin plane

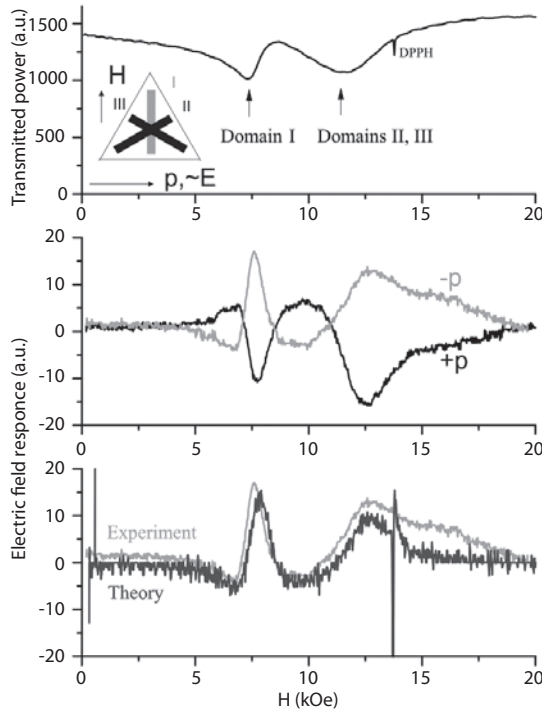


Fig. 1. Upper panel: ESR absorption lines for three domains. Middle panel: The responses of transmitted power on alternating electric field $\sim E = 100$ V/mm (gray and black lines correspond to different signs of domain polarization) Lower panel: Experimental and calculated responses on $\sim E = 200$ V/mm. $T = 4.2$ K, $\nu = 38.5$ GHz.

and is defined by their orientation in space. According to [2] the main magnetic and multiferroic properties of antiferromagnetic CuCrO_2 have explanation in frame of Dzyaloshinski-Landau theory of magnetic phase transitions. Particularly, the natural frequencies of uniform oscillations of spin plane were found. The oscillation frequencies depend not only on anisotropy constants and applied magnetic field, but on applied static electric field. We report the results of experimental study of ESR experiments on single crystals of CuCrO_2 at the applied electric field. The shift of ESR absorption lines was observed with use of modulation technique. The alternating low frequency electric field $\sim E$ was applied to the sample together with HF magnetic field. The orientations of applied fields H , $\sim E$, polarization P and orientation of spin plane in respect to crystallographic axes are shown in the inset to Fig. 1. The field dependency of transmitted through resonator HF power is shown on the upper panel. The response of transmitted power on the alternating electric field is shown on the middle panel. The response on the frequency of applied electric field $\sim E$ is proportional to derivative of absorption line. The change of electric polarization sign results in a change of the response sign (red and black lines). The blue line on the lower panel represents the real derivative of the absorption curve multiplied by a coefficient obtained within the theoretical model. This agrees with experimental response. The shift of the resonance field by electric field can be considered as the change of the gap in the ESR specter on the value: $\Delta\nu = 5 \cdot 10^{-7} \text{ GHz}/(\text{V/m}) \cdot E$.

1. Kimura K., Nakamura H., Kimura S., Hagiwara M., Kimura T.: Phys. Rev. Lett. **103**, 107201 (2009)
2. Marchenko V.I.: JETP **119**, 1084 (2014)

Magnetic Properties of New Chiral 2D Magnet MnSnTeO_6

**E. A. Zvereva¹, G. V. Raganyan¹, V. B. Nalbandyan²,
M. A. Evstigneeva², S. V. Streltsov³, A. I. Kurbakov^{4,5},
M. A. Kuchugura^{4,5}, and A. N. Vasiliev¹**

¹ Faculty of Physics, Moscow State University, Moscow 119991, Russian Federation, zvereva@mig.phys.msu.ru

² Faculty of Chemistry, Southern Federal University, Rostov-on-Don 344090, Russian Federation

³ Institute of Metal Physics, Ekaterinburg 620990, Russian Federation

⁴ Petersburg Nuclear Physics Institute – NRC Kurchatov Institute, Gatchina 188300, Russian Federation

⁵ Faculty of Physics, St. Petersburg State University, St. Petersburg 198504, Russian Federation

Static and dynamic magnetic properties of new trigonal layered compound MnSnTeO_6 were studied both experimentally (through magnetization, specific heat, neutron diffraction and ESR) and theoretically (through *ab initio* DFT calculations). In the crystal structure magnetic layers of Mn^{2+} and Te^{6+} ions alternate with non-magnetic layers of Sn^{2+} and Te^{6+} ions (Fig. 1a) Magnetic susceptibility and specific heat evidence an onset of antiferromagnetic order at $T_N \sim 10$ K (Fig.

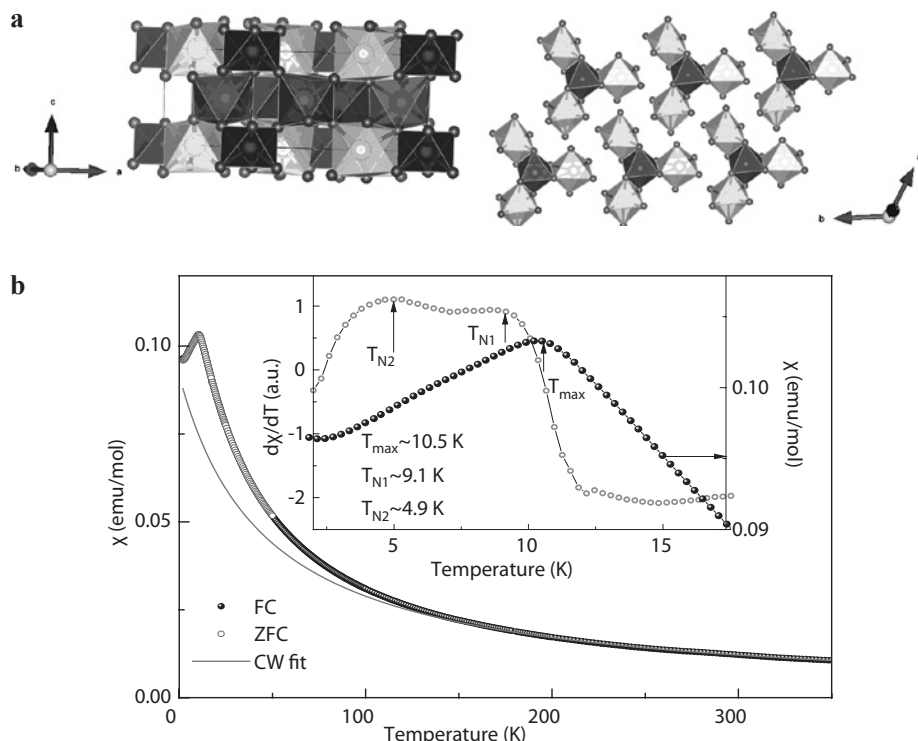


Fig. 1. Layered crystal structure (a, left), triangular network of Mn^{2+} ions (light grey octahedra) in magnetic layers (a, right) for MnSnTeO_6 and temperature dependence of the magnetic susceptibility at $B = 0.1$ T (b).

1b). However, there observes an additional anomaly at $T^* \sim 5$ K, which can't be related to structural transition as confirmed from the neutron data. To clear up the origin of this transition the local diagnostic by means of ESR technique and *ab initio* DFT calculations have been applied. The exchange parameters were determined and possible spin-configuration model was suggested. The spin dynamics was discussed in the terms of critical broadening and BKT scenario.

The Influence of Adsorbate and Edge Covalent Bonds on Topological Zero Modes in Few-Layer Nanographenes

A. M. Ziatdinov

Institute of Chemistry, Far-Eastern Branch of the Russian Academy of Sciences, Vladivostok 690022, Russian Federation, ziatdinov@ich.dvo.ru

According to the data of theoretical and experimental [1–5] studies, near zigzag edges of honeycomb carbon structures the π -electronic states with zero energy (topological zero modes) stabilize and the density of edge π -electronic states $D(E)$ at the Fermi level E_F dozens of times exceeds the value of corresponding parameter for macroscopic ordered graphite although the energy of the $D(E)$ maximum is ~ 30 meV less than the E_F [6]. Mentioned modes substantially change known properties of nanosized carbon structures [1–6], but also may initiate essentially new phenomena such as edge magnetism [7] and edge superconductivity [8]. The zigzag edges of single- or few-layer graphene are perfect one-dimensional conductors owing to a set of gapless states that are topologically protected against backscattering and demonstrate atomic limit edge-mode quantum electrical conduction via spin-polarized edge states [9]. Near armchair edges of honeycomb carbon structures similar electronic states do not exist [1–6].

In recent years a new field of research in the technology of nanoscale carbon structures has been developed, which is aimed at fine adjustment of their properties with changing chemical state of peripheral atoms. For instance, the emergence of topological zero modes has been established recently at etching graphenic *armchair* edges by hydrogen [10]. However, with appreciating the significance of those works, up to now the problem of influence of adsorbed molecules (adsorbate) on the edge π -electronic band and, thereby, on the properties of nanosized carbon structures, was not treated properly. At the same time, evidently, this information is important for establishing the reasons and mechanisms of changing the properties of carbon nanostructures under the influence of different reagents, for ranking the factors determining their structural organization, electronic structure and chemical reactivity, as well as for solving problems of practical application.

In this work the results of investigations by EPR, CESR and magnetic susceptibility methods of electronic and magnetic structure of few-layer nanographenes (nanographites) and their changes under the influence of adsorbed molecules and edge covalent bonds are presented. In electronically decoupled nanographenes the presence of specific edge π -electronic states with zero energy (topological zero modes) and reversible decrease of $D(E_F)$ at their interaction with adsorbed molecules of oxygen, chlorine and water have been established. The explanation of discovered effect has been proposed in the terms of model of spin splitting of edge π -electronic states, initiated by transferring small portion of electronic density from nanographites to adsorbed molecules. It has been shown that change in sign of the temperature coefficient of current carrier spin relaxation rate at

presence of adsorbate may be accounted for by their interactions with edge spin-split (magnetically ordered) states. Saturation of free (dangling) σ -orbitals of the edge carbon atoms with chlorine 3p-electrons neither eliminates edge π -electronic states with zero energy nor initiates their spin splitting. However, formation of such covalent bonds changes some characteristics of the current carriers.

This work was supported by the Russian Federal Agency for Scientific Organizations (project No. 0265-2015-0002) and Russian Academy of Sciences (project “Far East” No. 15-I-3-007).

1. Fujita M., Wakabayashi K., Nakada K., Kusakabe K.: *J. Phys. Soc. Jpn.* **65**, 1920 (1996)
2. Kobayashi Y., Fukui K., Enoki T., Kusakabe K.: *Phys. Rev. B* **71**, 193406 (2005)
3. Ziatdinov M., Fujii S., Kusakabe K., Mori T., Enoki T.: *Phys. Rev. B* **87**, 115427 (2013)
4. Enoki T., Ando T.: *Physics and chemistry of graphene: graphene to nanographene*. 476 pp. Singapore: Pan Stanford Publishing Pte Ltd. 2013.
5. Ziatdinov A.M.: *Russian Chemical Bulletin* **64**, 1 (2015)
6. Niimi Y., Matsui T., Tagami K., Tsukada M., Fukuyama H.: *Appl. Surf. Sci.* **241**, 43 (2005)
7. Son Y.-W., Cohen M.L., Louie S.G.: *Nature* **444**, 347 (2006)
8. Sasaki K., Jiang J., Saito R., Onari S., Tanaka Y.: *J. Phys. Soc. Jpn.* **76**, 033702 (2007)
9. Kinikar A., Sai T.P., Bhattacharyya S., Agarwala A., Biswas T., Sarker S.K., Krishnamurthy H. R., Jain M., Shenoy V.B., Ghosh A.: *Nature Nanotechnology*, doi:10.1038/nnano.2017.24. (2017)
10. Ziatdinov M., Lim H., Fujii S., Kusakabe K., Kiguchi M., Enoki T., Kim Y.: *Phys. Chem. Chem. Phys.* **19**, 5145 (2017)

Localized Ferromagnetic Resonance of Domain Wall in Curved Nanostripe

E. V. Skorohodov¹, A. P. Volodin², R. V. Gorev¹, and V. L. Mironov¹

¹ Institute for Physics of Microstructures RAS, GSP-105, Nizhny Novgorod 603950, Russian Federation

² KU Leuven, Afdeling Vaste-stoffysica en Magnetisme, Celestijnenlaan 200D, Leuven BE-3001, Belgium, mironov@ipmras.ru

We report on the magnetic resonance force microscopy (MRFM) measurements and micromagnetic modeling of the ferromagnetic resonance (FMR) of single domain wall (DW) in the bent planar Permalloy nanowire (NW).

The ferromagnetic resonance spectra and spatial distributions of the resonant oscillation amplitude were calculated by numerical solution of Landau-Lifshitz equation using the standard Object Oriented MicroMagnetic Framework (OOMMF) code [1]. As a model system we investigated the V-shaped 60°-bent planar Permalloy NW with two shoulders of 3000 nm long, 600 nm width and 30 nm thick. For the analysis of spectra and spatial structure of resonant modes we simulated the time dependences of steady-state oscillations induced by microwave magnetic field for all magnetization components [2].

The simulated spectrum of the magnetization oscillations in the NW with 60° transverse DW is shown in Fig. 1a. The intense peak corresponds to the oscillations localized in the DW area. Appropriate distribution of the FMR amplitude is shown in Fig. 1b.

Experimentally the localized mode of DW oscillations was explored by MRFM. The square grating array of Permalloy V-shaped NWs (element size is 3000×600×30 nm, period is 11 μm) was fabricated on the glass substrate by e-beam lithography and lift-off process. The MRFM measurements were

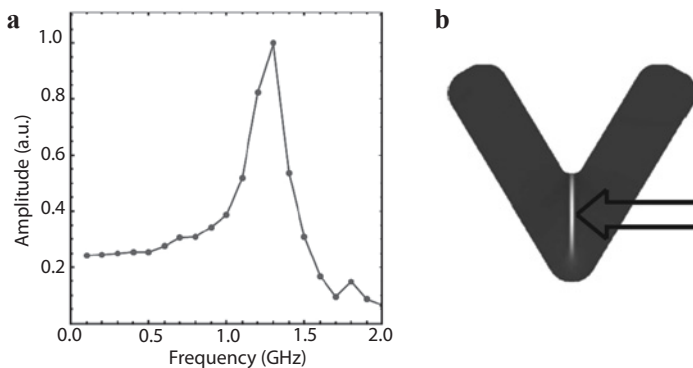


Fig. 1. **a** The simulated spectrum of DW magnetization oscillations. **b** Spatial distribution of magnetization oscillations amplitude for DW resonant mode at 1.3 GHz. DW resonance is indicated by arrow.

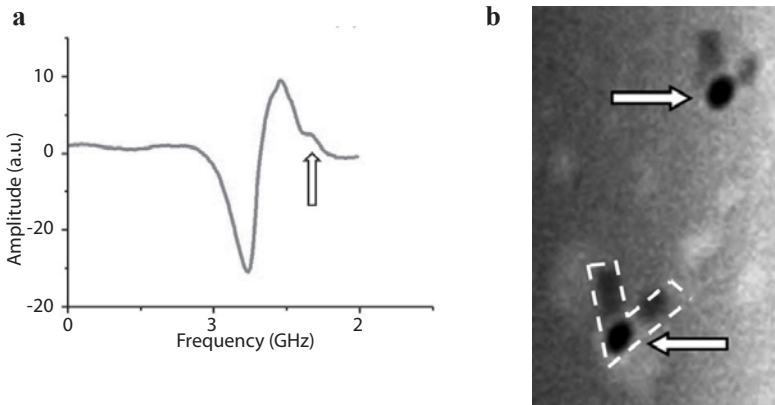


Fig. 2. **a** The MRFM spectrum obtained with the probe located over the DW region of NW. The arrow indicates FMR of DWs far away from the probe for which the probe magnetic field is negligible. **b** The MRFM image of NWs at resonant frequency 1.045 GHz. The resonant areas are indicated by white arrows.

performed using high vacuum scanning probe microscope equipped with strip line for the microwave excitation of the sample magnetization. A magnetic Co particle (about 10 μm in diameter) was mounted at the pyramid tip of standard cantilever to obtain the MRFM probe. The resonant MRFM spectrum and corresponding MRFM image of DW resonance are represented in Fig. 2.

The pronounced minimum on spectrum corresponds to DW FMR which is shifted toward smaller frequency by the probe magnetic field. The fact that the probe-induced FMR is minima is due to the reversed sign of the probe field gradient for DWs far away from the probe for which FMR corresponds to maxima (indicated by arrow in Fig. 2a). The measured MRFM spectra and spatial distribution of resonant signal agree with micromagnetic modeling.

The sample preparation and micromagnetic simulations were supported by Russian Scientific Foundation (project # 16-12-10254).

1. Donahue M.J., Porter D.G.: "OOMMF User's Guide", Interagency Report NISTIR 6376, NIST, Gaithersburg, <http://math.nist.gov/oommf>
2. Gorev R.V., Skorokhodov E.V., Mironov V.L.: *Physics of the Solid State* **58**, 2212 (2016)

ESR of a Doped Quasi-One-Dimensional $S = 1$ Antiferromagnet with Two Coupled Antiferromagnetic Sublattices

**T. A. Soldatov^{1,2}, A. I. Smirnov¹, K. Yu. Povarov³, E. Wulf³,
A. Mannig³, and A. Zheludev³**

¹ P. L. Kapitza Institute for Physical Problems RAS, Moscow 119334, Russian Federation, tim-sold@yandex.ru

² Moscow Institute for Physics and Technology, Dolgoprudny 141701, Russian Federation

³ Neutron Scattering and Magnetism, Lab. for Solid State Physics, ETH Zürich, Switzerland

Spin-gap quasi-one-dimensional $S = 1$ antiferromagnet with large single ion anisotropy $\text{NiCl}_2 \cdot 4\text{SC}(\text{NH}_2)_2$ (DTN) exhibits spin-liquid behavior in weak fields while in a high field, closing the spin gap, it demonstrates a field-induced transition to antiferromagnetic (AFM) phase. This transition depends both on the values of the external magnetic field and temperature. Maximum transition temperature corresponds to the magnetic field 8 T and reaches 1.2 K [1]. Intrachain exchange interaction $J_c = 2.2$ K significantly exceeds the interchain ones $J_{a,b} = 0.2$ K. In the present work we study the influence of doping on the spectrum of magnetic excitations in spin-liquid phase and in the field-induced AFM phase by the electron spin resonance (ESR) method. Influence of impurities on the triplet excitation spectrum at the boundary of the Brillouin zone has been recently detected in neutron scattering experiments [2], while we test the spectrum of excitation in the center of the Brillouin zone. Nonmagnetic doping was performed by substitution of Cl per Br. Crystals with different concentrations of Br (0, 13 and 40%) were studied.

The most pronounced influence of doping is a broadening of resonance modes. Besides, for the field-induced AFM phase of doped samples we observe the decrease of the antiferromagnetic resonance gap from 80 to 70 GHz. Moreover, weak resonances near the frequency of 30 GHz, which are interpreted [3, 4] as an optical mode of two nested AFM sublattices, disappear. We suppose that the disappearance of this mode may be presumably attributed to the change of the mutual orientation of spins from different interpenetrating sublattices. The interaction between the interpenetrating sublattices is frustrated, and their mutual orientation is controlled by a fluctuation mechanism (so-called order from disorder mechanism) [4]. As shown in [5], the presence of a weak random modulation of exchange bonds may compete with the order-by-disorder mechanism and may essentially change the ground state. This, naturally, should change the ESR frequency of the optical mode while other frequencies, originating from interactions within a sublattice, should be not affected. Besides, both in pure and doped samples, we observe a large (of the order of that of ESR modes) non-resonance dynamic susceptibility in the microwave frequency range in the whole field range of the AFM order. This susceptibility results in a shift of the resonator frequency, presented in Fig. 1, left panel, and arises at the boundaries of AFM phase. At heating above the maximum temperature of the antiferromagnetic transition only

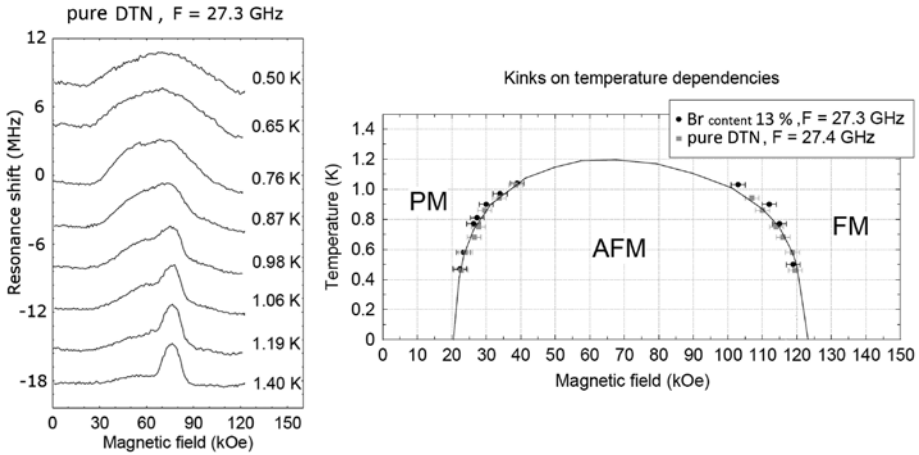


Fig. 1. Left panel: field-dependencies of the shift of the 27.3 GHz microwave resonator frequency for a pure DTN sample inside at different temperatures. Right panel: solid line – phase boundary measured in [1], symbols represent the boundaries of the field range of the non-resonance dynamic susceptibility for a pure and 13%-doped samples.

the ESR susceptibility remains. This effect is not yet explained but allows one to reconstruct the phase diagram, see right panel of Fig. 1.

Thus, our experiments detect a diminishing of the spin wave energy gap of the field-induced antiferromagnetic phase, and a change of the mutual orientation of the interpenetrating sublattices caused by nonmagnetic doping. Besides, we observe a large dynamic susceptibility of the unknown nature in the exotic field-induced antiferromagnetic phase.

Work is supported by Russian Science Foundation grant No. 17-12-01505 and by the program of the Presidium of Russian Academy of Sciences.

1. Paduan-Filho A. *et al.*: J. Appl. Phys. **95**, 7537 (2004)
2. Povarov Yu K. *et al.*: Phys. Rev. B **92**, 024429 (2015)
3. Zvyagin S. *et al.*: Phys. Rev. B **77**, 092413 (2008)
4. Sizanov A.V., Syromyatnikov A.V.: J. Phys.: Condens. Matter **23**, 146002 (2011)
5. Maryasin V., Zhitomirsky M.: Phys. Rev. Lett. **111**, 247201 (2013)

Nuclear Magnetic Resonance Studies of Nanodiamond Surface Modification

A. Panich

Department of Physics, Ben-Gurion University of the Negev, Be'er Sheva 8410501, Israel,
pan@bgu.ac.il

We report on NMR studies of surface modification of detonation nanodiamonds (DNDs). The spectra of chemically functionalized – fluorinated, chlorinated, hydroxylated and carboxylated DNDs show formation of C-F, C-Cl, C-OH and C-COOH covalent bonds with the surface carbon atoms. These bonds reveal different chemical shifts that allow distinguishing between different atomic groups in the NMR spectra. The aforementioned findings are well supported by our XPS measurements.

DND particles grafted by paramagnetic gadolinium ions [1] were prepared by mixing of aqueous nanodiamond suspension with aqueous solution of gadolinium nitrate hexahydrate. Dissociated cations in this solution undergo ion exchange with hydrogen atoms of the surface carboxyl groups. Attachment of ions to the DND surface was proved by ^{13}C and ^1H NMR relaxation measurements, which show noticeable acceleration of ^{13}C and ^1H nuclear spin-lattice relaxation on grafting. Herewith the relaxation rate is proportional to the Gd^{3+} ion concentration and thus results from the interaction between nuclear spins and paramagnetic ions, which creates an additional nuclear relaxation channel. This finding clearly shows that Gd^{3+} ions are chemically bound to the nanodiamond surface. Similar results were obtained for the copper- and cobalt-grafted DNDs. A model of positioning of the transition metal ions on the nanodiamond surface is presented. The distance between the ions and surface is calculated from the relaxation data. Our NMR data are well supported by the EPR measurements, which show increase in the electron spin-lattice relaxation rate of the paramagnetic defects in the diamond core with increasing gadolinium content. Biomedical applications of the studied nanomaterials are discussed.

1. Panich A.M., Shames A.I., Sergeev N.A., Osipov V.Yu., Alexenskiy A.E., Vul' A.Ya.: *J. Phys. Chem. C* **120**, 19804 (2016)

^3He NMR in Nanostructures: Latest Progress

**E. M. Alakshin¹, G. A. Dolgorukov¹, A. V. Klochkov¹,
E. I. Kondratyeva¹, V. V. Kuzmin¹, D. S. Nuzhina¹, K. R. Safiullin¹,
A. A. Stanislavovas¹, and M. S. Tagirov^{1,2}**

¹ Kazan Federal University, Kazan 420008, Russian Federation,
alakshin@gmail.com

² Institute of Perspective Research, Academy of Sciences of the Republic of Tatarstan, Kazan 420111,
Russian Federation, murat.tagirov@gmail.com

The study of the spin kinetics of ^3He in contact with aerogels, nanodiamonds and trifluoride nanoparticles by the pulsed nuclear magnetic resonance (NMR) methods will be presented.

Nanodiamonds. In recent years nanodiamonds have become a widely investigated material for quantum engineering, biological and electronic applications. The spin-lattice (T_1) and spin-spin (T_2) relaxation times of ^3He were measured in adsorbed, gas and liquid phases in a detonation nanodiamond sample at the frequency range of 5–18 MHz and at $T = 1.6$ K temperature. The observed T_1 and T_2 are much shorter in comparison with ^3He in similar experiments for samples with restricted geometry, thus we assume a strong impact of paramagnetic centers on nuclear magnetic relaxation. Experiments with nanodiamond surface preplated with N_2 or ^4He layers will be presented. The model of ^3He relaxation in contact with detonation nanodiamonds that describes our experimental results will be proposed.

Aerogels. Earlier, we systematically studied the nuclear magnetic relaxation of ^3He in contact with silicate aerogels. The determining role of the adsorbed layer in relaxation processes of gaseous and liquid ^3He was confirmed. It is known that aerogel acts as an impurity and affects phases of superfluid ^3He . Nowadays, it is of interest to study superfluid ^3He in contact with anisotropic aerogels. An additional mechanism of the ^3He relaxation in aerogels is found and it is shown that this relaxation mechanism is not associated with the adsorbed layer. A hypothesis about the influence of intrinsic paramagnetic centers on the relaxation of gaseous ^3He is proposed.

Trifluoride nanoparticles. The spin kinetics data of ^3He in contact with various trifluoride nanosized powders will be presented. For example, the influence of phase transition to ferromagnetic state on ^3He relaxation will be shown.

The work was supported by the RFBR (Project No. 16-32-60155 mol_a_dk).

The Formation of Epsilon-Fe₂O₃/SiO₂ Nanoparticles: Spatial Stabilization and the Size Effect

**S. S. Yakushkin, D. A. Balaev, G. A. Bukhtiyarova,
and O. N. Martyanov**

Boreskov Institute of Catalysis SB RAS, Novosibirsk 630090, Russian Federation,
stas-yk@catalysis.ru;

Kirensky Institute of Physics, Federal Research Center KSC SB RAS,
Krasnoyarsk, Russian Federation,

The systems based on ϵ -Fe₂O₃ nanoparticles attract particular and growing attention during the last decades, mostly because of its unique magnetic properties (high coercivity ~ 20 kOe at room temperature). The ϵ -Fe₂O₃ phase, intermediate between α - and γ -Fe₂O₃, was characterized in 1998 [1]. Thanks to the low surface energy ϵ -Fe₂O₃ can be synthesized in nanoparticle form only, and tends to transform to the α -Fe₂O₃ with the increase of nanoparticles size. When creating nanostructured functionalized catalyst, based on ϵ -Fe₂O₃ nanoparticles, the admixture of other iron oxide polymorphs may be the main limitation for practice.

In the Boreskov Institute of Catalysis the ϵ -Fe₂O₃/SiO₂ nanoparticle system having narrow size distribution was created for the first time with no other detectable iron-oxide polymorphs [2]. It turns out the system displays unique catalytical properties, e.g. elevated stability to sulphurizing [3].

It was shown that the system displays superparamagnetic behavior at room temperature [4]. FMR method *in situ* in comparison with HR TEM, XRD, Mossbauer spectroscopy, and magnetization measurements data [5] were applied to investigate the initial stages of the ϵ -Fe₂O₃/SiO₂ nanoparticles formation. It was shown that the stabilization of the nanoparticles precursor on the silica support is the key factor to obtain the system free of admixture of other iron oxide polymorphs.

Support by Russian Science Foundation (Grant No. 17-12-01111).

1. Tronc E., Chaneac C., Jolivet J.P.: J. Sol. Stat. Chem. **139**, 93 (1998)
2. Bukhtiyarova G.A., Shuvaeva M.A., Bujukov O.A., Yakishkin S.S., Martyanov O.N.: J. Nanoparticle Res. **13**, 5527 (2011)
3. Shuvaeva M.A., Delii I.V., Mart'yanov O.N., Bayukov O.A., Osetrov E.I., Saraev A.A., Kaichev V.V., Sakaeva N.S., Bukhtiyarova G.A.: Kinet. Catal. **52**, 898 (2011)
4. Yakushkin S.S., Dubrovskiy A.A., Balaev D.A., Shaykhutdinov K.A., Bukhtiyarova G.A., Martyanov O.N.: J. Appl. Phys. **111**, 044312 (2012)
5. Dubrovskiy A.A., Balaev D.A., Shaykhutdinov K.A., Bayukov O.A., Pletnev O.N., Bukhtiyarova G.A.: J. Appl. Phys. **118**, 213901 (2015)

SECTION 3

SPIN-BASED INFORMATION PROCESSING

Exact Analytical and Genuine Zeeman Perturbation Approaches to the Eigen-Energies and g -Functions of the ZFS and Electronic Zeeman Interaction Hamiltonian for the Spin Quantum Numbers up to $S = 7/2$: Applications to High Spin Metalloporphyrins and a Re(III, IV) Complex with Sizable ZFS Values and Quantum Chemical Calculations

T. Yamane¹, K. Sugisaki¹, T. Nakagawa¹, H. Matsuoka¹, T. Nishio¹, S. Kinjyo¹, N. Mori¹, S. Yokoyama¹, C. Kawashima¹, N. Yokokura¹, K. Sato¹, Y. Kanzaki¹, D. Shiomi¹, K. Toyota¹, D. H. Dolphin², W. C. Lin², C. A. McDowell², M. Tadokoro³, and T. Takui^{1,4}

¹ Department of Chemistry and Molecular Materials Science, Graduate School of Science, Osaka City University, Osaka 558-8585, Japan

² Department of Chemistry, The University of British Columbia, Vancouver, British Columbia, V6T 1Z1 Canada

³ Department of Chemistry, Faculty of Science, Tokyo University of Science, Tokyo 162-0825, Japan

⁴ Research Support/URA Center, University Administration Department, Osaka City University, 3-3-138 Sugimoto, Sumiyoshi-ku, Osaka 558-8585, Japantakui@sci.osaka-cu.ac.jp

The effective (fictitious spin-1/2) Hamiltonian approach is the putative method to treat the fine-structure/hyperfine ESR spectra of high spin metallocomplexes with sizable zero-field splitting (ZFS). The approach gives salient principal g -values far from around $g = 2$ without explicitly providing their ZFS parameters in most cases. The significant departure of the g -values from $g = 2$ indicates the occurrence of their high spin state, but naturally they never agree with true g -values acquired by quantum chemical calculations such as sophisticated DFT or *ab initio* MO calculations.

In this work [1], we propose facile approaches to determine the magnetic tensors of high spin metallocomplexes having sizable ZFS, instead of performing advanced high-field/high-frequency ESR spectroscopy. We have revisited analytical expressions for the relationship between effective g -values and true principal g -values for high spins. The useful exact analytical formulas for the $g^{\text{eff}}-g^{\text{true}}$ relationships are given for S 's up to $7/2$. The exact analytical expressions for the eigen-energies and g -functions of the spin Hamiltonian, which is composed of the rank-2 ZFS tensors and electronic Zeeman interaction terms, are given for S 's up to $7/2$ in the principal-axis coordinate system, for the first time. The genuine Zeeman perturbation formalism gives the exact solutions for $S = 3/2$, and for higher S 's it is much more accurate than the pseudo Zeeman perturbation approach documented so far [2–5], in which the $E(S_x^2 - S_y^2)$ term is putatively treated as the second order. To show the usefulness of the present approach, we analyzed the magnetic tensors for Fe^{III}(Cl)OEP ($S = 5/2$) (OEP: 2,3,7,8,12,13,17,18-octaethylporphyrin) and Co^{II}OEP ($S = 3/2$) well magnetically diluted in the diamagnetic host crystal lattice of Ni^{II}OEP. A Re^{III,IV} dinuclear

complex with sizable ZFS in the mixed valence state was also treated. In this work, we carried out the DFT-based/*ab initio* MO calculations of the magnetic tensors for all the high spin entities, comparing the theoretical tensors with the experimental ones.

1. Yamane T., Sugisaki K., Matsuoka H., Sato K., Takui T. *et al.*: Physical Chemistry Chemical Physics, in press (2017): DOI: 10.1039/c7cp03885j
2. Abragam A., Bleaney B.: Electron Paramagnetic Resonance of Transition Metal Ions, 1970.
3. Pilbrow J.R.: J. Magn. Reson. **31**, 479 (1978)
4. Trandafir F. *et al.*: Appl. Magn. Reson. **31**, 553 (2007)
5. Fittipaldi M. *et al.*: J. Phys. Chem. B **112**, 3859 (2008)

Molecular Spin Technology Based on Microwave Pulse with Arbitrary Waveform towards Spin Quantum Computing

K. Sato¹, S. Yamamoto¹, R. Hirao¹, K. Tanimoto¹, E. Hosseini¹, S. Nakazawa¹, K. Toyota¹, D. Shiomi¹, K. Ivanov², and T. Takui¹

¹ Graduate School of Science, Osaka City University, Osaka 558-8585, Japan
sato@sci.osaka-cu.ac.jp

² International Tomography Center SB RAS, Novosibirsk, Russian Federation

Realization of practical quantum computing and quantum information processing (QC/QIP) has been one of the current challenging topics in advanced scientific fields. Electron and nuclear spins are typical candidates of qubits for molecular spin quantum computers. It is essential to precisely control quantum states of molecular spins in QC/QIP. We have been studying electronic structures of molecular spin qubit systems for QC/QIP and manipulating both electron and nuclear spins in the molecular spin systems by pulse-based ESR/ENDOR/ELDOR spectroscopy [1–4].

We have recently implemented AWG (Arbitrary Wave Generator)-based electron spin technology for precise manipulation of molecular spins. The AWG-based spectrometer developed enables us to manipulate molecular spins with coherent multi-microwave pulses. In this work, the advanced pulse-ESR technology based on AWG was applied to stable molecular spin systems for manipulating electron spins. We present pulsed ESR experiments with X-band arbitrary shape pulses, indicating that the electron spin state is controlled on the Bloch sphere. It illustrates the establishment of NMR-paradigm ESR spectroscopy. It is known that a quantum adiabatic process has a high tolerance for environmental disturbances compared to standard quantum gate operations for quantum information science. We have applied the AWG-based ESR technique in order to implement electron spin manipulation under the adiabatic quantum process. We will also show GRAPE (GRAdient Ascent Pulse Engineering) and adiabatic quantum spin manipulation approaches in molecular spin systems.

1. Sato K., Nakazawa S., Morita Y., Takui T. *et al.*: *J. Mater. Chem.* **19**, 3739 (2009)
2. Nakazawa S., Sato K., Morita Y., Takui T. *et al.*: *Angew. Chem. Int. Ed.* **51**, 9860 (2012)
3. Park D., Shibata T., Sato K., Takui T. *et al.*: *Quantum Inf. Process.* **14**, 2435 (2015)
4. Yamamoto S., Sato K., Takui T. *et al.*: *Phys. Chem. Chem. Phys.* **17**, 2742 (2015)

Decoherence in Many-Qubit Clusters in Multiple Quantum NMR in One-Dimensional Systems

G. A. Bochkin¹, E. B. Fel'dman¹, S. G. Vasil'ev¹, and V. I. Volkov¹

¹ Institute of Problems of Chemical Physics of Russian Academy of Sciences, Chernogolovka 142432, Russian Federation, efeldman@icp.ac.ru

A theory of dipolar relaxation of multiple quantum (MQ) NMR coherences in one-dimensional chains with various numbers of spins is developed [1, 2] on the basis of the exact theory of MQ NMR dynamics [3]. The theory is in good agreement with the experimental data obtained on ¹⁹F nuclei in a single crystal of calcium fluorapatite.

Dipolar relaxation of the MQ NMR coherence of the second order is considered as a model of decoherence of quantum states in many-qubit clusters. The growth of correlated many-spin clusters on the preparation period of the MQ NMR experiment [4] is studied. The relationship between the number of the correlated spins, the duration of the preparation period of the MQ NMR experiment [4], and the space dimension is obtained.

We have also found a connection between the dipolar relaxation time of the MQ NMR coherence of the second order and the number of the correlated spins in the many-spin cluster, responsible for that MQ coherence. As a result, we obtain the dependence of the relaxation (decoherence) time on the number of the correlated spins. The theoretical predictions are in good agreement with experimental data for clusters with small numbers of spins. We show that the decoherence time decreases slowly with the growth of the number of the spins in correlated clusters. This implies that the problem of decoherence can be overcome in scalable quantum computations in the considered model.

Our work is supported by the Russian Foundation for Basic Research (Grants No. 16-03-00056, 16-33-00867) and the Program of the Presidium of RAS No. 1.26 "Electron spin resonance, spin-dependent electron effects and spin technologies" (Grant No. 0089-2015-0191).

1. Bochkin G.A., Fel'dman E.B., Vasil'ev S.G.: *Zeitschrift fur Phys. Chem. – Int. J. Res. Phys. Chem. Chem. Phys.* **231**, 513 (2017)
2. Bochkin G.A., Fel'dman E.B., Vasil'ev S.G., Volkov V.I.: *Chem. Phys. Lett.* **680**, 56 (2017)
3. Fel'dman E.B.: *Appl. Magn. Reson.* **45**, 797 (2014)
4. Baum J., Munowitz M., Garrowsay A.N., Pines A.: *J. Chem. Phys.* **83**, 2015 (1985)

Cross Relaxation Magnetometry with Diamond NV Centers

**R. A. Akhmedzhanov, L. A. Gushchin, N. A. Nizov, V. A. Nizov,
D. A. Sobgayda, and I. V. Zelensky**

Institute of Applied Physics of the RAS, Nizhny Novgorod 603950, Russian Federation,
zelensky@appl.sci-nnov.ru

NV centers in diamond have been studied extensively over the last few years for multiple applications including magnetic sensing and imaging [1]. Magnetic sensing with NV centers is commonly done using the optically detected magnetic resonance (ODMR) technique. This technique involves probing the ground state transitions with tunable microwave (MW) radiation and observing changes in optically induced fluorescence. The most important limitation of such approach is that MW radiation cannot be applied in some situations. To work around this limitation other approaches are investigated including one exploiting the properties of the ground state level anticrossing [2]. Though it doesn't require MW radiation, strong magnetic field necessary also limits potential applications.

We investigate interaction between groups of NV centers differently oriented with respect to diamond lattice. We observe cross relaxation resonances on fluorescence profile in scanning magnetic field that appear when the transitions between ground state sublevels of different NV groups overlap. We show that the number and positions of resonances depend on the value and orientation of additional magnetic field that is applied to the sample.

We suggest a new magnetometry protocol that is based on measuring the positions of cross relaxation resonances on the fluorescence scan. This protocol does not require MW radiation and can be used to find all components of the unknown magnetic field vector. An important feature of the protocol is that, unlike conventional ODMR, it does not rely on measuring the exact value of the ground state splitting so it is not dependent on temperature.

The work was supported by Russian Foundation for Basic Research (grant 14-29-07152), (grant 16-07-01012).

1. Rondin L., Tetienne J.-P., Hingant T., Roch J.-F., Maletinsky P., Jacques V.: Rep. Prog. Phys. **77**, 056503 (2014)
2. Wickenbrock A., Zheng H., Bougas L., Leefer N., Afach S., Jarmola A., Acosta V.M., Budker D.: Appl. Phys. Lett. **109**, 053505 (2016)

Electron-Electron and Electron-Nuclear Interactions in the Context of Spin-Based Quantum Computing

E. I. Baibekov¹

¹ Kazan Federal University, Kazan 420008, Russian Federation, edbaibek@gmail.com

I discuss the decoherence processes accompanying the manipulations of an electron spin interacting with either nuclear or electron spin bath. In particular, I present the calculation schemes allowing one to compute the decay of Rabi oscillations (nutations of the electron spin excited by a long pulse of the microwave field of resonant frequency). The nutation frequency Ω_R (Rabi frequency) is usually proportional to the microwave field amplitude.

Three specific cases leading to well-pronounced effects are considered:

(i) An ensemble of electron spins diluted in a solid diamagnetic host and weakly coupled by magnetic dipolar interactions. The decay rate of Rabi oscillations at certain conditions is found to depend linearly on Ω_R .

(ii) An electron spin coupled to the nuclear spin bath. When Ω_R is close to the Larmor frequency of the nuclear spins ω_N (Hartmann-Hahn condition [1]), the electronic decoherence is drastically enhanced due to the presence of the electron-nuclear cross-relaxation processes.

(iii) In the case of strong coupling of the electron spin with the nuclear spin bath, forced regime of oscillations is realized. After a short initial period of oscillations with Ω_R , the electronic nutation frequency switches to ω_N .

The theoretical models leading to the above effects are corroborated by recent experimental data [2–8]. This work was supported by the Russian Scientific Fund (Grant No. 17-72-20053) and by the Russian President's Stipend for Young Scientists.

1. Hartmann C.R., Hahn E.L.: Phys. Rev. **128**, 2042 (1962)
2. Boscaino R., Gelardi F.M., Korb J. P.: Phys. Rev. B **48**, 7077 (1993)
3. Bertaina S. *et al.*: Nature Nanotechnol. **2**, 39 (2007)
4. Baibekov E.I.: JETP Lett. **93**, 292 (2011)
5. Shim J.H. *et al.*: Phys. Rev. Lett. **109**, 050401 (2012)
6. Baibekov E.I. *et al.*: Phys. Rev. B **90**, 174402 (2014)
7. Baibekov E.I. *et al.*: Phys. Rev. B **95**, 064427 (2017)
8. Kveder M. *et al.*: to be published.

SECTION 4

MOLECULAR MAGNETS AND LIQUID CRYSTALS

Spin Magnetic Resonance Spectroscopy from Billions of Molecules to a Single Molecule

F. Shi

CAS Key Laboratory of Microscale Magnetic Resonance and Department of Modern Physics,
University of Science and Technology of China, Hefei 230026, China, fzshi@ustc.edu.cn

Magnetic resonance (MR) is one of the most important techniques for characterizing compositions, structure and dynamics of molecules. However, current methods need billions of uniform units on centimeter-scale to accumulate large enough signal-to-noise ratio. High sensitivity MR techniques are urgently needed for new applications on nanoscale. A sensor to accomplish nanoscale targets detection is the recently developed atomic sized magnetic field sensor based on the nitrogen-vacancy (NV) defect center in diamond. By combining the quantum controls and long coherence time of NV, we have experimentally realized nanoscale nuclear MR and electron spin resonance. We and co-workers have successfully obtained the first single-protein spin resonance spectroscopy under ambient conditions [1], realized atomic-scale structure analysis of single nuclear-spin clusters in diamond [3], and succeeded in detection of $(5 \text{ nm})^3$ hydrogen nuclear spin magnetic resonance spectroscopy [4]. These results, together with the relation works in the field, open a door to nanoscale/single molecule MR and will be potentially used as a new tool on a broad range of scientific areas from life science to physics and chemistry.

1. Shi F., Zhang Q., Wang P., Sun H., Wang J., Rong X., Chen M., Ju C., Reinhard F., Chen H., Wrachtrup J., Wang J., Du J.: *Science* **347**, 1135 (2015)
2. Wang P., Yuan Z., Huang P., Rong X., Wang M., Xu X., Duan C., Ju C., Shi F., Du J.: *Nature Communication* **6**, 6631 (2015)
3. Shi F., Kong X., Wang P., Kong F., Zhao N., Liu R., Du J.: *Nature Physics* **10**, 21 (2014)
4. Staudacher T., Shi F., Pezzagna S., Meijer J., Du J., Meriles C.A., Reinhard F., Wrachtrup J.: *Science*, **339**, 561 (2013)
5. Shi F., Zhang Q., Naydenov B., Jelezko F., Du J., Reinhard F., Wrachtrup J.: *Phys. Rev. B* **87**, 195414 (2013)

Magnetic Properties, EPR and *ab initio* Investigation of a Series of Isostructural Fe₂^{III}Dy₂^{III} Complexes

V. Vieru¹, L. Ungur¹, V. Cemortan¹, A. Sukhanov², A. Baniodeh^{3,4},
V. Mereacre³, C. E. Anson³, A. K. Powell^{3,4},
V. Voronkova², and L. F. Chibotaru¹

¹ Theory of Nanomaterials Group, Katholieke Universiteit Leuven, Leuven 3001, Belgium,
veaceslav.vieru@kuleuven.be

² Zavoisky Physical-Technical Institute, Russian Academy of Sciences, Kazan 420029,
Russian Federation

³ Institute of Inorganic Chemistry, Karlsruhe Institute of Technology, Karlsruhe D-76131, Germany

⁴ Institute of Nanotechnology, Karlsruhe Institute of Technology, Postfach 3640,
Karlsruhe D-76021, Germany

High anisotropy of lanthanide ions, such as Tb^{III}, Dy^{III}, Ho^{III}, Er^{III}, makes them good candidates for synthesis of single-molecule magnets (SMM). However, their presence does not always guarantee SMM behavior. It has been established that the high axially of the ground doublet, which is quantified by the axially of its *g*-tensor in the case of Kramers lanthanide ions, is required for suppression of quantum tunneling of magnetization [1].

Usually, the *g*-tensors are determined routinely by means of *ab initio* calculations [2], which proved to be highly successful in the prediction of SMM behavior of strongly anisotropic complexes.

In this presentation we report EPR measurements and *ab initio* calculations on a series of [Fe₂Dy₂(OH)₂(teaH)₂(RC₆H₄COO)₆] complexes, where teaH₃ = triethanolamine and R = meta-CN (**1**), para-CN (**2**), meta-CH₃ (**3**), para-NO₂ (**4**) and para-CH₃ (**5**). Poor SMM behavior was corroborated by relatively large transversal components of the *g*-tensor of Dy^{III} ions. Furthermore, the experimental EPR spectra are described satisfactorily from the *ab initio* results. The low-temperature EPR spectra can be modelled by considering only the lowest four exchange states originating from the Ising-type exchange interaction between Dy ions.

1. Guo Y.N. *et al.*: J. Am. Chem. Soc. **133**, 11948 (2011)
2. Chibotaru L.F.: Structure and Bonding **164**, 185 (2015)

SECTION 5

MODERN METHODS OF MAGNETIC RESONANCE

Characterization of Liquid-Crystalline Materials by Separated Local Field Methods

S. V. Dvinskikh^{1,2}

¹ Royal Institute of Technology, Department of Chemistry, Stockholm SE-10044, Sweden, sergeid@kth.se

² St. Petersburg State University, Laboratory of Biomolecular NMR, St. Petersburg 199034, Russian Federation, sdvinskikh@mail.ru

Liquid crystals (LC) or mesophases represent substances that exist, under certain conditions, in a particular state that is intermediate between the solid and liquid states. The unique feature of a material in the mesophasic state is that a high degree of molecular mobility, which results in fluidity or plasticity, is combined with partial orientational and positional order. The presence of order in fluid material leads to new dynamic properties, exploited in modern technological applications. Whereas most of the research has been done on low-molecular-weight LC, also macromolecules, supramolecular aggregates, and nanoparticles can act as building blocks of LC. Solid-State NMR contributes to fundamental understanding of diverse molecular organization and complex dynamic processes in these exiting materials [1]. Focus of this talk is on development and application of advanced Solid-State NMR methodologies for liquid crystals studies with the emphasis on the techniques for measurements of static anisotropic spin couplings. The discussion is centered on applications of separated dipolar local field NMR spectroscopy.

Anisotropic spin interactions in liquid crystals are not averaged to zero, and usually dominate the NMR-spectra of spin-1/2 nuclei. The progress in methods for spin decoupling/recoupling, sensitivity enhancement, polarization transfer, has considerably increased the potential of NMR in mesophases. Separation of spin interactions in multidimensional experiments facilitates analysis and enables determination of the direct dipolar couplings. General protocols for local field spectroscopy developed in static aligned samples, are also applied to MAS samples, with important difference that suitable dipolar recoupling sequences must be used during dipolar evolution period.

1. Dvinskikh S.V. in: Modern Methods in Solid-State NMR. A Practitioner's Guide. Royal Society of Chemistry 2017.

Novel Approaches in Magnetic Resonance & Microwave Detection of Energetic and Illicit Material

B. Rameev^{1,2} and G. Mozhukhin²

¹ Zavoiisky Physical-Technical Institute, Kazan 420029, Russian Federation

² Gebze Technical University, Gebze/Kocaeli 41400, Turkey,
rameev@gyte.edu.tr

Detection of explosive and illicit substances is a problem of vital importance for our civilization [1–4]. Especially, so-called improvised explosive devices (IEDs) or home-made explosives (HME), made from commercially available chemical materials, became used more frequently in terrorist attacks over world. The techniques, which provide a possibility of the chemical-specific identification of explosive, looks prospective for various security applications. Among the explored techniques, the time-domain nuclear magnetic resonance (TD-NMR) is considered as very promising bulk detection method for liquid energetic (explosive), flammable, dangerous and poisoning materials [5–11]. TD NMR looks very attractive because of its high selectivity as well as relatively low price and maintenance expenses. However, the classical NMR relaxometry cannot provide reliable discrimination in a *large number* of various substances. Apparently, there is a need to use the methods, which provide additional parameters for discriminations (e.g., the real and imaginary permittivities by dielectric spectroscopy, the ¹⁴N NMR signal or diffusion constant). Another issue is unacceptably long time of T_1 relaxation parameter measurements by classical sequences. In this work, we review possible approaches to probe additional information about liquid content as well as to make the procedure of liquid scanning faster. These are novel NMR methods as well as dielectric spectroscopy in MW range.

Firstly, we analyze the sequences prospective to apply in ¹H TD NMR measurements for detection of some flammable liquids or explosive precursors. Another NMR approach, studied in this work for realization of a fast liquid scanning protocol as well as obtaining an additional parameter for discrimination between various liquids, is based on the detection of ¹⁴N NMR signal. ¹⁴N NMR signal of various liquids has been successfully detected and the relaxation parameters of various nitrogen-based liquids, including dangerous and energetic materials, have been obtained. Secondly, the methods of MW dielectric spectroscopy for detection of explosive and illicit substances are reviewed. Various possible sensors for bottle scanning applications (e.g. microstripes, a partially shielded dielectric resonators, ring resonators, semi-circular dielectric waveguides, etc.) are discussed.

The work was supported by NATO Science for Peace and Security Programme (NATO SPS grant No. 985005 [G5005]). Authors also acknowledge a partial support by East Marmara Development Agency (MARKA, project No. TR42/16/ÜRETİM/0013) and by Research Fund of Gebze Technical University (grants Nos. BAP 2015-A-19 and BAP 2017-A-105-44).

1. Miller J.B., Barrall G.A.: Explosives Detection with Nuclear Quadrupole Resonance. *American scientist* **93**, no. 1, 50–57 (2005)
2. Fraissard J., Lapina O., eds.: *Explosives Detection using Magnetic and Nuclear Resonance Techniques*, NATO Science for Peace and Security Series B: Physics and Biophysics. Dordrecht, Netherlands: Springer, 2009.
3. Rameev B.Z., Mozzhukhin G.V., Aktas B., eds.: *Magnetic Resonance Detection of Explosives and Illicit Materials*. *Appl. Magn. Reson.* **43**, no. 4, 463–467 (2012)
4. Apih T., Rameev B., Mozzhukhin G., Barras J., eds.: *Explosives Detection using Magnetic and Nuclear Resonance Techniques*, NATO Science for Peace and Security Series B: Physics and Biophysics, Dordrecht, Netherlands: Springer, 2014.
5. Burnett L.J.: Liquid Explosives Detection. *Proc. SPIE* **2092**, 208–217 (1994)
6. Kumar S., McMichael W.C., Kim Y.-W., Sheldon A.G., Magnuson E.E., Ficke L., Chhoa T.K.-L., Moeller C.R., Barrall G.A., Burnett L.J., Czipott P.V., Pence J.S., Skvoretz D.C.: Screening sealed bottles for liquid explosives. *Proc. SPIE* **2934**, 126–137 (1997)
7. Kumar S.: Liquid-content verification for explosives, other hazards, and contrabands by magnetic resonance. *Appl. Magn. Reson.* **25**, 585–597 (2004)
8. Mauler J., Danieli E., Casanova F., Blumich B., Identification of liquids encountered in carry-on-luggage by mobile NMR, in NATO book: “Explosives Detection using Magnetic and Nuclear Resonance Techniques”, NATO Science for Peace and Security Series B: Physics and Biophysics (J. Fraissard, O. Lapina, eds.), pp. 193-203. Dordrecht, Netherlands: Springer, 2009.
9. Kumar S., Prado P.J.: Detection of concealed liquid explosives and illicit drugs in un-opened bottles, in NATO book: “Explosives Detection using Magnetic and Nuclear Resonance Techniques”, NATO Science for Peace and Security Series B: Physics and Biophysics (J. Fraissard, O. Lapina, eds.), pp. 73–79. Springer, Dordrecht, Netherlands: Springer, 2009.
10. Prado P.J., Mastikhin I., Karlsson M.T.: Rapid Method to Screen Unopened Bottles to Detect Concealed Drugs. *Appl. Magn. Reson.* **43**, 531–540 (2012)
11. Balcı E., Rameev B., Acar H., Mozzhukhin G.V., Aktaş B., Çolak B., Kupriyanov P.A., Ievlev A.V., Chernyshev Y.S., Chizhik V.I.: Development of Earth’s Field Nuclear Magnetic Resonance (EFNMR) Technique for Applications in Security Scanning Devices. *Appl. Magn. Reson.* **47**, no. 1, 87–99 (2016)

SECTION 6

STRONGLY CORRELATED ELECTRON SYSTEMS

Signatures of Fractionalized Spin Excitations in the Proximate Quantum Spin Liquid α -RuCl₃ from Sub-THz Spectroscopy in Strong Magnetic Fields

V. Kataev¹

¹ Leibniz Institute for Solid State and Materials Research IFW Dresden, Dresden D-01171, Germany, v.kataev@ifw-dresden.de

Topologically ordered states of matter are generically characterized by excitations with quantum number fractionalization. A prime example is the spin liquid realized in the so-called Kitaev's honeycomb-lattice compass model where spin-flip excitations fractionalize into Majorana fermions and Ising gauge fluxes [1]. Recently, the quasi-two-dimensional ruthenium-based magnetic insulator α -RuCl₃ with Ru³⁺ (4d⁵) effective spins-1/2 anisotropically coupled on a honeycomb lattice has been proposed as a proximate material to host such exotic excitations [2]. In particular, inelastic neutron scattering (INS) experiments reveal, besides conventional magnon excitations associated with residual magnetic order, a broad excitation continuum consistent with the scattering of neutrons by Majorana excitations inherent in the Kitaev quantum spin liquid [2, 3].

In our work, we have focused on the low-energy part of magnetic excitations below 2 meV (< 500 GHz) inaccessible in the INS studies. For that we have employed a sub-THz ESR setup operational in magnetic fields up to 16 T. With this approach we could disentangle the response from conventional magnon modes from the conjectured Majorana continuum and study its magnetic field dependent properties. In the talk, our recent experimental findings will be overviewed and their possible connection to the Kitaev's physics will be discussed.

This work has been done in collaboration with A. Alfonsov, J. van den Brink, B. Büchner, C. Wellm, A.U.B. Wolter, J. Zeisner (IFW Dresden), T. Doert, A. Isaeva, M. Vojta (Technical University Dresden).

1. Kitaev A.: *Annals of Physics* **321**, 2 (2006)
2. Banerjee A. *et al.*: *Nature Materials* **15**, 733 (2016)
3. Banerjee A. *et al.*: *Science* **356**, 1055 (2017)

Electron Nematic Effect in CeB₆: The ESR and Magnetoresistance Evidence

**S. V. Demishev^{1,2,3}, V. N. Krasnorussky¹, V. V. Glushkov^{1,2,3},
A. V. Semeno^{1,2}, M. I. Gilmanov², A. V. Bogach¹,
A. N. Samarin², N. A. Samarin¹, N. E. Sluchanko^{1,2},
N. Yu. Shitsevalova⁴, and V. B. Filipov⁴**

¹ Prokhorov General Physics Institute of RAS, Moscow 119991, Russian Federation,
demis@lt.gpi.ru

² Moscow Institute of Physics and Technology, Dolgoprudny 141700, Russian Federation

³ National Research University Higher School of Economics, Moscow 101000, Russian Federation

⁴ Institute for Problems of Materials Science of NASU, Kiev 03680, Ukraine

Investigating of spontaneously generated spatial anisotropy in the translationally invariant metallic phase, i.e. electron nematic effect, addresses a great challenge for both experimentalists and theoreticians. So far, these effects were discovered in experimental objects like ultra clean quantum Hall systems, ruthenates, high- T_c superconductors and iron-based superconductors. An interesting new option for the realization of an electron nematic phase is provided by the system with orbital ordering, as long as both orbitally ordered states and electron nematic phases possess broken spatial symmetry. Here we report the detailed study of the angular dependences of the electron spin resonance (ESR) and magnetoresistance in the orbitally ordered antiferroquadrupole (AFQ) phase of dense Kondo system CeB₆. Experiments were carried out with the help of the installation, which allows combining high accuracy measurements with precise temperature stabilization (for the details concerning experimental technique see Sci. Rep. **6**, 22101, 2016 and Sci. Rep. **6**, 39196, 2016). Our data allowed revealing the electron nematic effect, which develops when the magnetic field exceeds a critical value of 0.3–0.5 T. As a result, new phase boundary inside the AFQ phase corresponding to the change of the symmetry of magnetic scattering in CeB₆ is discovered. To our best knowledge, this is first time for studying of electron nematic effect, when full information about angular distribution function is obtained, which provides an opportunity for obtaining an order parameter in analogy with liquid crystals theory. The data obtained shed new light on the genesis of ESR in AFQ phase of CeB₆.

This work was supported by RSF grant 17-12-01426.

Investigation of a Field Induced Magnetic Transition in the Low-Dimensional Magnet BiCoPO_5

**M. Iakovleva^{1,2}, E. Vavilova², H.-J. Grafe¹, A. Alfonsov¹, B. Büchner¹,
Y. Skourski³, R. Nath⁴, and V. Kataev¹**

¹ Leibniz Institute for Solid State and Materials Research (IFW Dresden), Dresden 10069, Germany

² Zavoisky Physical-Technical Institute, Russian Academy of Sciences, Kazan 420029, Russian Federation

³ Dresden High Magnetic Field Laboratory (HLD-EMFL), HZDR, Dresden 01328, Germany

⁴ Indian Institute of Science Education and Research-Thiruvananthapuram (IISER), Kerala 695016, India

Frustrated dimeric chain compound BiCoPO_5 is a potential quantum phase transition (QPT) material. BiCoPO_5 orders antiferromagnetically at $T_N = 11$ K. Application of an external magnetic field reduces the transition temperature down to $T = 0$ K at a field of 15.3 T and pushes the system to the quantum critical point (QCP) [1]. In this work we present an investigation of the title compound by means of magnetometry, high-field/frequency electron spin resonance (HF-ESR) and nuclear magnetic resonance (NMR) techniques. The high-field magnetization measurements show no saturation of the magnetic moment up to the highest magnetic field of 60 T. The magnetic isotherm (M vs. H) measured at $T = 2$ K exhibits a feature associated with the field induced spin-flop transition at 4.5 T [1]. In the HF-ESR measurements at paramagnetic state we observe a broad line from Co^{2+} ions with a typical for the distorted octahedral ligand coordination g -factor value of $g = 3.58$. At low temperatures the broad line splits into several narrow lines that indicates a formation of magnetic order. The ^{31}P NMR spectrum consists of two lines, which probably indicates the presence of two magnetically nonequivalent ^{31}P positions in BiCoPO_5 . The temperature dependence of the ^{31}P NMR relaxation rates measured at 9 T at both sites shows a maximum at $T = 8$ K corresponding to the AFM order. At a magnetic field of 15 T the T -dependence of the relaxation rates shows gapped behavior at both sites with $\Delta_1 = 6$ K for the 1st and $\Delta_2 = 16$ K for 2nd position of phosphorus that might be associated with the approaching of QCP. All these remarkable results are summarized in field-temperature phase diagram of BiCoPO_5 and will be discussed in the talk.

1. Mathews E., Ranjith K.M., Baenitz M., Nath R.: Solid State Comm. **154**, 56 (2013)

Magnetic Resonance in the Strongly Correlated Topological Insulator SmB_6

S. V. Demishev^{1,2,3}, M. I. Gilmanov², A. N. Samarin¹,
A. V. Semeno^{1,2}, N. E. Sluchanko^{1,2}, N. Yu. Shitsevalova⁴,
V. B. Filipov⁴, and V. V. Glushkov^{1,2,3}

¹ Prokhorov General Physics Institute of RAS, Moscow 119991,
Russian Federation, wlesavo@gmail.com

² Moscow Institute of Physics and Technology, Dolgoprudny 141700, Russian Federation

³ National Research University Higher School of Economics, Moscow 101000, Russian Federation

⁴ Institute for Problems of Materials Science of NASU, Kiev 03680, Ukraine

Mixed valence compound SmB_6 with the hybridization gap ~ 20 meV demonstrate unusual low temperature properties, which initially were attributed to the formation of exciton-polaron complexes for $T < 6\text{--}7$ K leading to strongly correlated ground state in the sample bulk [1, 2]. Recently it was shown that the surface of SmB_6 satisfies the conditions allowing topologically protected Z_2 invariant, and therefore this material can be attributed to the class of strongly correlated topological insulators [3, 4] and low temperature state is due to surface effects. In the present work, we report results of magnetic resonance probing of undoped single crystals of SmB_6 in 60 GHz cavity experiments. Resonant magnetoabsorption can be detected only for $T < 6$ K and observed spectra consists of several lines, which include the doublet A, B accompanied by satellites A_1 , B_1 and extra line C (Fig. 1). The interpretation, attributing the A, B lines with defects in the surface layer and line C with the contribution of electrons in the surface layer, is purposed. This work was supported by programmes of Russian Academy of Sciences “Electron spin resonance, spin-dependent electronic effects and spin technologies”, “Electron correlations in strongly interacting systems” and by RFBR grant 17-02-00127 A.

1. Kikoin K.A., Mishchenko A.S.: J. Phys.: Condens. Matt. 7, 307 (1995)
2. Gorshunov B. *et al.*: Phys. Rev. B **59**, 1808 (1999)
3. Takimoto T.: J. Phys. Soc. Japan **80**, 123710 (2011)
4. Kim D.J. *et al.*: Nature Mater **10**, 1038 (2014)

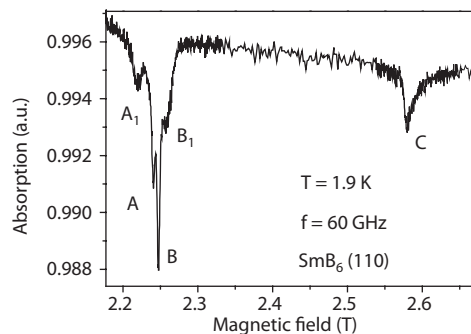


Fig. 1. Magnetic resonance spectrum of SmB_6 for the case when the magnetic field is perpendicular to (110) surface.

ODMR and LAC Spectroscopy of Nitrogen-Vacancy Centers in Diamond

**S. V. Anishchik¹, K. L. Ivanov², V. G. Vins³, I. V. Zhukov⁴,
O. V. Chankina¹, and Yu. N. Molin¹**

¹ Voevodsky Institute of Chemical Kinetics and Combustion SB RAS,
Novosibirsk 630090, Russian Federation, svan@kinetics.nsc.ru

² International Tomography Center SB RAS, Novosibirsk 630090, Russian Federation

³ VinsDiam Ltd., Novosibirsk 630058, Russian Federation

⁴ Novosibirsk State University, Novosibirsk 630090, Russian Federation

The NV center in diamond is a widely known defect of a diamond lattice with consisting of a nitrogen atom and a vacancy located in adjacent lattice sites. The NV center has a C_{3v} symmetry with the symmetry axis of an individual center coinciding with one of the four equivalent [111] crystallographic axes of the diamond. The negatively charged nitrogen-vacancy center (NV^- center) in diamond is of great interest due to its unique properties [1]. The NV^- center has triplet ground and excited states 3A_2 and 3E with a zero-field splitting of 2.87 and 1.42 GHz, respectively. A spin projection-selective intersystem crossing from the excited triplet state to the excited singlet one as well as from the ground singlet state to the ground triplet state leads to, firstly, a much higher quantum yield of luminescence when excited from the state with zero spin projection on the symmetry axis rather than from the states with projections +1 or -1. Secondly, it leads to a non-equilibrium state of the NV^- center after multiple absorption and emission of light, with a population of the zero spin projection state much higher than those of the states with spin projections +1 or -1. The latter effect is usually referred to as optically-induced spin polarization.

Optically Detected Magnetic Resonance (ODMR) is based on the idea to transfer the detection of a microwave absorption or emission to the optical domain and to take advantage of the concomitant increase in photon energy to enhance the sensitivity of the experiment. We discuss the results of a study of the NV^- center by the technique of ODMR taking advantage of its high sensitivity to simultaneously register the EPR lines of both the ground and the excited states. In order to measure the ODMR spectrum of the excited state 3E of the NV^- center with a lifetime of about 10 ns we used an elevated power of the MW pumping. This approach turned out to be able to successfully register all the other weak ODMR lines as well, including the line of the forbidden low-field transition.

NV^- centers are promising systems for numerous applications, especially for quantum information processing and nanoscale magnetometry. Magnetic dipole-dipole interactions between NV^- centers and other paramagnetic defects are of relevance for many applications. An efficient tool for probing such interactions is the Level Anti-Crossing (LAC) spectroscopy. It is well known that in the magnetic field dependence of the photo-luminescence intensity of precisely oriented NV^-

centers sharp lines are observed. The most prominent line is observed at 1024 G, which comes from a level anti-crossing of the triplet levels in the NV⁻ center (LAC line). Other lines are termed, perhaps, misleadingly, cross-relaxation lines [2]. In reality, all lines are due to the coherent spin dynamics and are caused by LACs of the entire spin system of the interacting defect centers. Thus, it is reasonable to term the observed dependences “LAC spectra”.

For sensitive detection of such LAC-lines we use lock-in detection to measure the photoluminescence intensity [3]. This experimental technique allows us to obtain new LAC lines [3, 4]. Additionally, a remarkably strong dependence of the LAC-lines on the modulation frequency is found. Specifically, upon decrease of the modulation frequency from 12 kHz to 17 Hz the amplitude of the LAC-lines increases by approximately two orders of magnitude [5].

Theoretical modeling of such LAC-spectra enables characterization of paramagnetic defect centers and determination of their magnetic resonance parameters, such as zero-field splitting and hyperfine coupling constants. The outlined method thus enables sensitive detection of paramagnetic impurities in diamond crystals.

The work was supported by Foundation for Basic Research (grant 16-03-00672).

1. Doherty M.W., Manson N.B., Delaney P., Jelezko F., Wrachtrup J., Hollenberg C.L.: *Physics Reports* **528**, 1–45 (2013)
2. van Oort E., Glasbeek M.: *Phys. Rev. B* **40**, 6509–6517 (1989)
3. Anishchik S.V., Vins V.G., Yelisseyev A.P., Lukzen N.N., Lavrik N.L., Bagryansky V.A.: *New J. Phys.* **17**, 023040 (2015)
4. Anishchik S.V., Vins V.G., Ivanov K.L.: *ArXiv e-prints*, 1609.07957 (2016)
5. Anishchik S.V., Ivanov K.L.: *ArXiv e-prints*, 1703.07101 (2017)

SECTION 7

MAGNETIC RESONANCE IMAGING

MRI and Emotions

U. Eichhoff

Bruker BioSpin GmbH (retired); barbara.uwe@t-online.de

Four Nobel Prizes for NMR and MRI are a good reason for positive emotions for all of us working in this field. But NMR cannot only create emotions, MRI can be used for their location in the brain and for investigation of the underlying neuronal processes including emotional dysregulation.

Today the most accepted hypothesis of the origin of mental diseases is an impaired connectivity between various brain areas. Diffusion Tensor Imaging and MR-tractography reveal structural connectivities through neuronal fibers between brain areas.

Functional Imaging in the Resting State (rs-fMRI) allows to visualize functional connectivities analyzing the time course of rapidly repeated MRI for changes in the Blood Oxygen Level Dependent (BOLD). Even in complete rest the brain is active and oxygen is extracted from blood and fresh blood is supplied. The detection of the small signal changes needs highest sensitivity and the MRI scans must be repeated as fast as possible. Statistical evaluation and cross-correlation of the signals in all voxels show synchrony of signal level fluctuations even in remote brain areas. This allows to establish networks in the brain.

The most important networks are the Default Mode Network (DMN), the Salience Network (SN) and the Central Executive Network (CEN). Anatomical locations within the brain sharing two or three of these networks determine our relation to external stimuli, our emotional reaction and activities.

The manifestation of emotional dysregulation in PostTraumatic Stress Disorder will be discussed in some clinical examples. Experiments in transgenic animals may help to understand the development of Autism Spectrum Disorder.

Deep Brain Stimulation (DBS) is a still controversive method for therapy of mental diseases. It is now accepted for Parkinson disease and under evaluation for major depressive disorders. MR-tractography and rs-fMRI allow to select the most favourable location for the excitation electrodes and to evaluate the therapeutic results.

Several Aspects of ^{19}F Gastrointestinal MRI

**D. V. Volkov¹, M. V. Gulyaev¹, L. L. Gervits², D. N. Silachev¹,
N. V. Anisimov¹, A. P. Chernyaev¹, and Yu. A. Pirogov¹**

¹Lomonosov Moscow State University, Moscow 119991, Russian Federation,
mdanf1@gmail.com

²Nesmeyanov Institute of Organoelement Compounds of RAS, Moscow 119334, Russian Federation

For present the ability to visualize the organs of the gastrointestinal tract (GIT) is a key to the complex study of its physiological state, as a unified system. The conventional proton magnetic resonance imaging (^1H MRI) is scarcely suitable for this task, since a strong background ^1H NMR signal, created by the surrounding organs of the intraperitoneal space, makes the differentiation of the GI tract on ^1H MR images quite complex.

To solve this problem, it is proposed, for example, to use contrast agents based on gadolinium chelates (Magnevist®, Gadovist®, etc.). However, in practice, the use of contrast agents does not always allow achieving the desired result [1].

Recently quite a lot of works have been dedicated to the multi-nuclear MRI studies, in particular, on fluorine-19 nuclei (^{19}F MRI). Due to its physical properties these nuclei are favorable for use in MRI. Since fluorine-19 nuclei are almost absent in living organisms, the location of injected fluorine-containing compounds (e.g. perfluorocarbons) could be unequivocally interpreted. Besides, perfluorocarbons (PFCs) are chemically and biologically inert, and in an undiluted form give a strong ^{19}F NMR signal [2].

In this report several aspects of ^{19}F GI MRI on laboratory animals are described. Among the fluorocarbon compounds, Perftoran® and its main fluorine-containing compound perfluorodecalin (PFD) were chosen for this study [3]. Perftoran® is a fluorocarbon emulsion system with a particle size about 100 nm. Such particles can be used as biocontainers for targeted therapy. Therefore, from the point of clinical practice, the use of Perftoran® seems much promising.

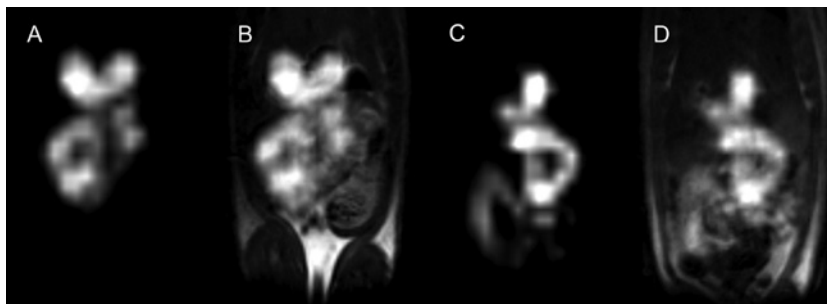


Fig. 1. MR images of the rat gastrointestinal tract. After 4 ml injection: A: ^{19}F -, B: $^{19}\text{F}+^1\text{H}$ fused MRI. After 2+2 injection: C: ^{19}F -, D: $^{19}\text{F}+^1\text{H}$ fused MRI.

MRI experiments were performed at 7 T MR scanner Bruker BioSpec 70/30 USR. A firm birdcage coil was modified for work on two frequencies – of proton and fluorine. Parameters for scanning pulse sequence – 3D spin-echo pulse sequence, RARE factor = 8, TR/TE = 500/5.9 ms – were optimized in the previous work [4]. The reference ^1H MR images were obtained in the same geometry. Then ^1H and ^{19}F MR images were fused in the ImageJ software.

In the experiments with rats, various amounts of PFD and Perftoran® were orally administered via special catheter. The analysis of images has shown that 2 ml of PFD or 5 ml of Perftoranum® is enough to obtain informative ^{19}F MR images of different parts of GIT. In order to visualize gastrointestinal tract as a separate system, either the volume of injected agent should be increased (single time administration) or the contrast agent should be administrated sequentially at some intervals (fractionated administration). According to our data, with the same total amount of the introduced PFC, the procedure of fractionated administration allows to visualize a larger volume of the gastrointestinal tract. Most likely, this is due to the fact that, with fractionated administration, the first fractions are moving along the digestive system during the time between administrations further than with a single administration of the PFC, which results in the filling of a larger number of GIT parts.

Thus, it was shown that fluorocarbon compounds (in particular PFD and Perftoran®) can be successfully used for ^{19}F gastrointestinal MRI. For the purpose of selective GIT organs visualization, it is preferable to use the method of single administration (e.g. 2 ml of PFD or 5 ml of Perftoran®). Fractionated administration allows examining the GI tract as a unified system, with compromise amounts of injected agent. It should be noted that there were no any harmful effects of the introduced substances on laboratory animals. Such data are promising for transferring to the clinical practice.

The work was carried out in the MSU Collective Using Center “Biospectromotography” with the financial support by the RFFI grant No. 17.02.00465A.

1. Thornton E., Morrin M., Yee J.: *Radiograph*. **30**, 1 (2010)
2. Jacoby C. *et al.*: *NMR in Biomed.* **27**, 3 (2014)
3. Ivanitskiy G., Vorobyov S.: *Vestnik RAS* **67**, 11 (1997)
4. Volkov D. *et al.*: *Tekhn. zh. sistem* **13**, 7 (2016)

The Design of the Receiving Coils for Specialized MRI

**A. A. Bayazitov¹, V. E. Khundiryakov², Ya. V. Fattakhov¹,
I. R. Sitdikov¹, A. R. Fakhrutdinov¹, V. A. Shagalov¹,
R. Sh. Khabipov¹, and A. N. Anikin¹**

¹ Zavoisky Physical-Technical Institute, Russian Academy of Sciences, Kazan 420029,
Russian Federation, bayazitov.alfis@kfti.knc.ru

² Kazan Federal University, Kazan 420008, Russian Federation

The work describes the results of research and development of a receiving coil for a magnetic resonance imaging system with induction of magnetic field of 0.4 T. This coil is the oval-shape with semi-axes of the oval R_z and R_y . We consider the problem of inevitable decreasing of the field homogeneity during the transition from a circular cylindrical coil to an oval coil and an optimal solution of the problem is proposed.

The advantage of the oval-shape coil is to reduce the coil size in one direction, i.e. the filling factor increases, hence the amplitude of the received signal increases too. Since when the shape of the coil changes, the uniformity also changes. It is necessary to select the optimum parameters of the coil for obtaining the best homogeneity. To improve homogeneity, we used additional turns located at the edges of the coil as well as the selection of the appropriate parameters X_1 , X_2 , R_z , R_y , where X_1 and X_2 are the distance between the turns Fig. 1. The homogeneity of the field was estimated by calculating the root-mean-square deviation from the mean value of the field, referred to its average value

The calculation of the field distribution along the longitudinal axis of the coil (X -axis) passing through the center of the coils for a region of ± 75 mm from the center was carried out in the work. And also the distribution of the field along the Y and Z axes was calculated, both at the center and at the edges of the region of interest. When modeling the sensor, parameters such as X_1 , X_2 , R_z , R_y , and the number of turns were changed. It was assumed that the maximum deviation of the field from the mean value should be less than 10%. Taking into account the simulation results, the model was created and its characteristics were measured.

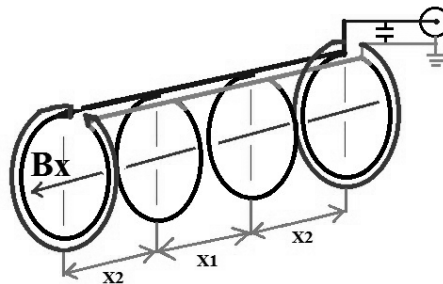


Fig. 1. Scheme receiving coils.

SECTION 8

MAGNETIC RESONANCE INSTRUMENTATION

Latest Developments in Pulsed Field Gradient and High Speed Magic Angle Spinning NMR

K. Zick

Bruker BioSpin GmbH, Rheinstetten 76287, Germany, klaus.zick@bruker.com

In the talk our new 111 kHz, 0.7 mm, CPMAS probe is briefly introduced. Its main feature is obviously the high spinning speed of up to 111 kHz allowing mainly extending the application range of ^1H detected experiments. This allows running so-called inverse experiments like in solution NMR making use of the much higher sensitivity of ^1H for structure determination of biological molecules. On the other hand the high spinning speed also allows investigating paramagnetic materials or materials in highly disordered environments, e.g. battery electrodes.

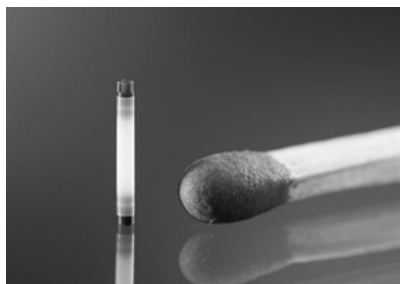


Fig. 1. 0.7 mm rotor.

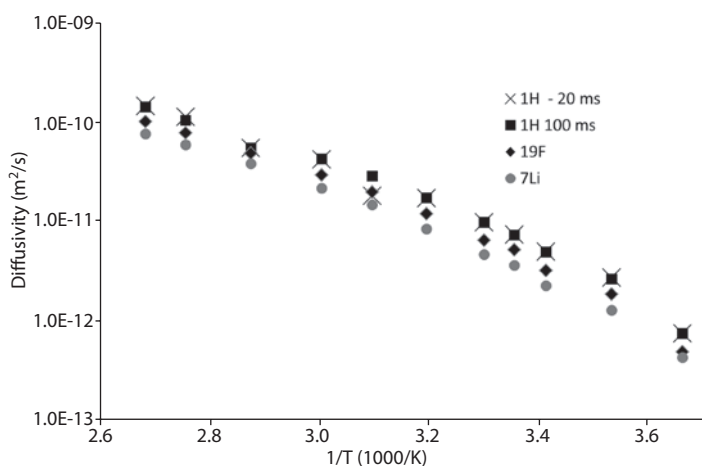


Fig. 2. Arrhenius plot of the diffusion coefficients obtained from ^1H , ^{19}F , and ^7Li over the temperature range of 0 to 100 °C. The activation energy is approximately the same for all ions (0.43 eV).

The second topic addressed in this talk is our new multinuclear diffusion probe having a gradient strength >17 T/m and covering a temperature range of currently -40 °C to $+150$ °C. The probe has also the capability of automatic tune and match being particularly useful in automatic temperature runs, where the tuning changes with temperature. A typical application of this probe is the investigation of ionic liquids used e.g. in batteries. These liquids typically have different ions with different NMR active nuclei, e.g. ^1H , ^{19}F , ^7Li , and ^{23}Na , which can be investigated in the same experiment. The mobility of the individual ions is crucial for the function of battery. Fig. 2 shows the results such of a series of diffusion experiments in the temperature range of 0 to 100 °C.

SECTION 9

ELECTRON SPIN BASED METHODS FOR ELECTRONIC AND SPATIAL STRUCTURE DETERMINATION IN PHYSICS, CHEMISTRY AND BIOLOGY

Rapid Scan EPR

M. Tseytlin

Department of Biochemistry, West Virginia University, Morgantown, USA

Time-Resolved EPR and Theoretical Investigations of Metal-Free Triplet Emitters for Organic Light Emitting Diodes

H. Matsuoka^{1,2}, M. Retegen³, L. Schmitt⁴, S. Höger⁴, F. Neese³, and O. Schiemann¹

¹ Graduate School of Science, Osaka City University, Osaka 558-8585, Japan, matsuoka@sci.osaka-cu.ac.jp

² Institute for Physical and Theoretical Chemistry, University of Bonn, Bonn 53115, Germany

³ Max Planck Institute for Chemical Energy Conversion, 45470, Germany

⁴ Kekulé Institute of Organic Chemistry and Biochemistry, University of Bonn, Bonn 53115, Germany

Organic light-emitting diodes (OLEDs) have attracted significant attention for the application in next generation display technologies. Utilization of triplets is important for preparing organic light-emitting diodes with high efficiency. Very recently, both electrophosphorescence and electrofluorescence could be observed at room temperature for thienyl-substituted phenazines without any heavy metals [1]. It was found that the phosphorescence efficiency depends on the orientation of fused thiophenes. In this work, the excited triplet states of the thienyl-substituted phenazines were investigated in more detail. To understand how the luminescence process is tuned by the orientation of the fused thiophene and the number of thiophene rings, the EPR parameters and spin density distributions of the thienyl-substituted phenazines were calculated using the DFT and CASSCF methods. In addition, TD-DFT calculations and symmetry consideration were performed in order to provide a schematic view of the phosphorescence mechanism. The theoretical calculations clearly show that the electron spin density distributions within the triplet states as well as the singlet-triplet energy gaps are strongly affected by the molecular geometry, thus resulting in the enhancement or suppression of phosphorescence.

1. Ratzke W., Schmitt L., Matsuoka H., Bannwarth C., Retegan M., Bange S., Klemm P., Neese F., Grimme S., Schiemann O., Lupton J.M., Höger S.: *J. Phys. Chem. Lett.* **7**, 4802–4808 (2016)

Nanoclustering of Spin-Labeled Molecules in Lipid Membranes as Revealed by “Instantaneous Diffusion” Effects in Electron Spin Echo Decay

S. A. Dzuba, M. E. Kardash, V. N. Syryamina, and E. F. Afanasyeva

Institute of Chemical Kinetics and Combustion, Russian Academy of Sciences,
Department of Physics, Novosibirsk State University, Novosibirsk 630090, Russian Federation,
dzuba@kinetics.nsc.ru

Nanoclustering is an important feature of plasma membrane organization. Developing the methods for quantifying membrane heterogeneities is a challenging task, because of their transient nature and small size. It is suggested that membrane heterogeneities can be frozen at cryogenic temperatures. Except of capturing the transient structures, the freezing allows to benefit from employing the appropriate solid-state experimental techniques. Here, pulsed version of electron paramagnetic resonance (EPR) spectroscopy – the electron spin echo (ESE) technique – is employed for spin labeled guest molecules in lipid bilayers. The multilamellar bilayers studied here were prepared from saturated and unsaturated lipids and from cholesterol (Chol), with small amount added of spin-labeled substances 5-doxy1-stearic-acid (5-DSA) or 3 β -doxy1-5 α -cholestane (DChlstn). ESE decays were refined for the pure contribution of nanoscale magnetic dipole-dipolar interaction between spin labels using a so-called “instantaneous diffusion effect” in ESE decays. The results obtained show high local concentration of these guest molecules which evidences formation of lipid-mediated nanoclusters. For 5-DSA molecules, two-dimensional clusters were found while flat DChlstn molecules were found to cluster into stacked one-dimensional structures [1]. In presence of Chol, these clusters were found to be destroyed, for the compositions known at room temperatures for lipid rafts formation. Antimicrobial peptides, such as alamethicin and trichogin, captures these clusters serving as nucleation cores [2].

This work was supported by Russian Science Foundation, grant No. 15-15-00021 and by Russian Foundation for Basic Research, grant No. 15-03-02186.

1. Kardash M.E., Dzuba S.A.: *J. Phys. Chem. B* **121**, 5209–5217 (2017)
2. Afanasyeva E.F., Syryamina V.N., Dzuba S.A.: *J. Chem. Phys.* **146**, 011103 (2017)

EPR of Metal-Organic Stimuli-Responsive Materials

M. V. Fedin, A. M. Sheveleva, and S. L. Veber

International Tomography Center SB RAS, Novosibirsk 630090, Russian Federation,
mfedin@tomo.nsc.ru

Metal-organic stimuli-responsive materials are actively investigated in view of their numerous potential applications in materials science. Among other techniques, EPR plays an important role in this research. This report overviews our recent studies of two types of stimuli-responsive metal-organic materials.

The first one, copper-nitroxide based molecular magnets $\text{Cu}(\text{hfac})_2\text{L}^{\text{R}}$, represents an interesting type of thermo- and photo-switchable materials which exhibit reversible magneto-structural rearrangements. We overview experimental EPR-based approaches developed for these systems, discuss general trends and characteristics of thermally/light-induced spin state switching and relaxation in this family of compounds [1].

The second type of studied materials refers to metal-organic frameworks (MOFs) sensitive to various external stimuli such as temperature, light, or adsorption of guest molecules in these highly porous systems. Since most of the MOFs are EPR-silent, we have proposed and demonstrated the application of nitroxide spin probes to study naturally-diamagnetic MOFs by EPR [2]. Such approach allows studying temperature-induced structural rearrangements in MOFs, as was exemplified using MIL-53(Al) having reversible transitions between large-pore and narrow-pore crystalline states with a significant hysteresis. Moreover, the mobility of nitroxides allows investigation of gas adsorption processes, where nitroxide acts as multifunctional agent competing with gas molecules for the adsorption sites. Finally, EPR studies of some photosensitive MOFs relevant for photocatalysis are reported [3]. Overall, high potential of EPR for the emerging applications of metal-organic stimuli-responsive materials is emphasized.

This work was supported by Russian Science Foundation (No. 14-13-00826).

1. Fedin M.V. *et al.*: *Coord. Chem. Rev.* **289–290**, 341 (2015)
2. Sheveleva A.M. *et al.*: *J. Phys. Chem. Lett.* **5**, 20 (2014); *J. Phys. Chem. C* **120**, 10698 (2016)
3. Nasalevich M.A. *et al.*: *Energy Environ. Sci.* **8**, 364 (2015); *Sci. Rep.* **6**, 23676 (2016)

Defects Structure in Congruent Lithium Tantalite by NMR, ESR, FTIR Spectroscopies and DFT Calculations

**E. Vavilova¹, R. Zaripov¹, A. Vyalikh²,
M. Zschornak^{2,3}, T. Köhler², M. Nentwich², T. Weige^{1,2},
S. Gemming^{3,4}, E. Brendler⁵, and D. C. Meyer²**

¹ Zavoiisky Physical-Technical Institute, Russian Academy of Sciences, Kazan 420029, Russian Federation

² Institut für Experimentelle Physik, Technische Universität Bergakademie Freiberg Freiberg 09596, Germany

³ Institute of Ion Beam Physics and Materials Research, Helmholtz-Zentrum Dresden-Rossendorf, Dresden 01314, Germany

⁴ Institute of Physics, TU Chemnitz, Chemnitz 09111, Germany

⁵ Institut für Analytische Chemie, Technische Universität Bergakademie Freiberg, Freiberg 09596, Germany

Single crystals of $(\text{Li, Na})\text{MO}_3$, ($M = \text{V, Nb, Ta}$) have a wide range of technological applications due to the multiplicity of their physical properties. LiMO_3 -based compounds exhibit such unusual properties as ferroelectricity, piezoelectricity and pyroelectricity, ionic conductivity; they are used as nonlinear optical media and so on. These complex perovskites are particularly sensitive to structural distortions, defects, and methods of preparation. Here we report a combinational approach based on DFT calculations of electric field gradients and solid-state nuclear magnetic resonance (NMR), electron spin resonance (ESR) and Fourier transform infrared (FTIR) spectroscopies in order to reveal the defect structure in congruent lithium tantalate. We show that two congruent samples of LiTaO_3 provided by commercial companies and grown by the same Czochralski method demonstrate different defect structure and properties that can be changed by heat treatment.

Stable Self-Organized Paramagnetic Complexes in the Asphaltenes' Structures from the W-band EPR and ENDOR

S. B. Orlinskii, A. A. Rodionov, A. V. Galukhin, I. N. Gracheva,
G. V. Mamin, and M. R. Gafurov

Kazan Federal University, Kazan 420008, Russian Federation,
Sergei.Orlinskii@kpfu.ru

Structural characterization of asphaltenes and their aggregates in native hydrocarbons (oil, bitumen, coal, oil-containing cores, etc.) as well as in their fractions are in the focus of scientific and industrial interests since many years. However, after decades of intensive studies, the association and aggregation of asphaltenes are still not well characterized and are subjects of debates [1, 2]. The content of the high-molecular asphaltene components could reach the values of 45 wt% in native oils and up to 73 wt% in natural asphalts and bitumen. Asphaltene impact all aspects of crude oil production and utilization. Undesirable asphaltene precipitation is a serious concern to the petroleum industry because asphaltenes can plug up well bores and stop oil production, in addition to blocking pipelines [3].

Commercial availability of the pulsed high field EPR/ENDOR spectrometers [4–7] open new ways for the hydrocarbon analysis and the asphaltenes' structural investigation using intrinsic paramagnetic centers (PC) as sensitive probes. Asphaltenes can contain up to 10^{22} PC per 1 gram of substance which are essentially due to “free” carbon radicals (FR) mainly localized within the

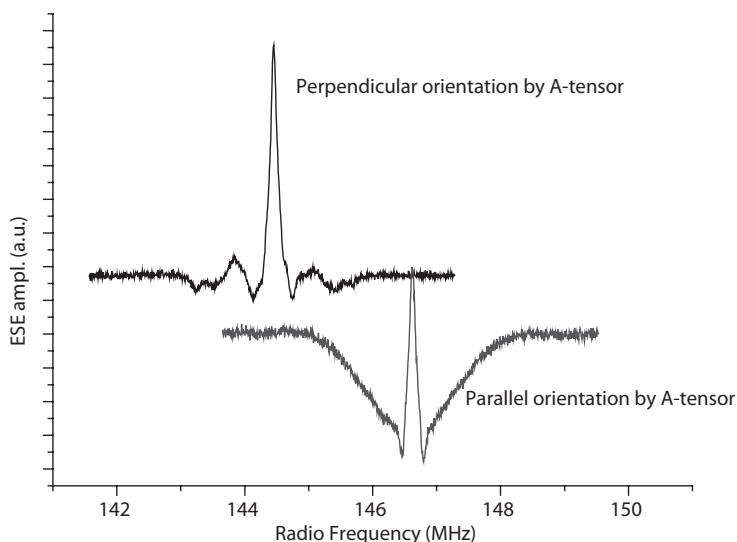


Fig. 1. Difference (for initial asphaltene sample and those deposited and on the surface of Al_2O_3) ENDOR spectra of protons involved in the network of the self-organized asphaltene complexes. $T = 20$ K, W-band.

polyaromatic condensed nuclei of the asphaltene molecules and/or vanadyl (VO^{2+}) complexes which also revealed in another constituent of hydrocarbons – resins.

We present pulsed EPR and ENDOR approaches and some preliminary results to study paramagnetic VO^{2+} complexes of initial asphaltenes and those deposited on surface of aluminum oxide (Al_2O_3) [8, 9] in the magnetic field of about 3.4 T (W-band). Application of high magnetic field allows to separate FR and VO^{2+} signals due to the difference in their g -factors, choose “pure” parallel and perpendicular orientations for VO^{2+} complexes. The anisotropy of the self-organized asphaltene complexes is demonstrated by ENDOR (Fig. 1).

The work was supported by the Program of the competitive growth of Kazan Federal University (“5-100”).

1. Ganeeva Yu.M., Yusupova T.N., Romanov G.V.: Russ. Chem. Rev. **80**, 993 (2011)
2. Evdokimov I.N., Fesan A.A., Losev A.P.: Energy Fuels **30**, 4494 (2016)
3. Speight J.G.: Handbook of Petroleum Product Analysis, 2nd edition, 368 p. Hoboken: Wiley&Sons, 2015.
4. Ramachandran V., van Tol J., McKenna A. *et al.*: Anal. Chem. **87**, 2306 (2015)
5. Mamin G.V., Gafurov M.R., Yusupov R.V. *et al.*: Energy Fuels **30**, 6942 (2016)
6. Biktagirov T., Gafurov M., Mamin G. *et al.*: Energy Fuels **31**, 1243 (2017)
7. Gracheva I., Gafurov M., Mamin G. *et al.*: Magn. Reson. Solids **18**, 16102 (2016)
8. Mukhambetov I.N., Lamberov A.A., Yavkin B.V. *et al.*: J. Phys. Chem. C **118**, 14998 (2014)
9. Mamin G.V., Orlinskii S.B., Rodionov A.A., Tagirov M.S.: JETP Lett. **102**, 628 (2015)

SECTION 10

CHEMICAL AND BIOLOGICAL SYSTEMS

A Combined ESR – Fluorescence Approach for Investigation of Structure, Molecular Dynamics and Mechanism of Electron Transfer in Biological Systems: 50 Years of History

G. I. Likhtenshtein

Department of Chemistry, Ben-Gurion University of the Negev, Beer-Sheva 8410501, Israel,
gertz@bgu.ac.il

Institute of Problems of Chemical Physics, Russian Academy of Science, Chernogolovka, Russian Federation

Since 1968 [1] the basic idea underlying our approach to solving a number of tasks in chemical biophysics and biomedicine is combining the classic ESR, as a basic method, with luminescence and Mössbauer techniques and the chemical kinetics [2–10]. Such an approach allowed us to markedly expand the potential of investigation in comparison with the each individual methods. The following combine methods were developed. **The combine physical labeling approach** employs radical pairs, nitroxide, fluorescence, dual nitroxide -phosphorescence and Mössbauer labels for investigation of molecule dynamics of proteins and enzymes in a range of correlation times from minutes to subnano seconds in the temperature interval of 50–320 K. **Nitroxide spin probe (NSP) and stilbene fluorescence-photochrome probe (SFPP) method** for study of molecular dynamics of membranes allowed to expand values of the correlation times of the probes motion and to establish detail mechanism of their dynamics. For quantitative investigation of lateral translational diffusion in membranes in a range characteristic time (10^3 – 10^{-9} s⁻¹), **the spin cascade method (SCM)** was invented and developed. A spin cascade system consists with the triplet sensitizer, SFPP and NSP quenching the excited triplet state of the sensitizer, which in turn effects on the SFPP photoisomerization. In the frame of **dual fluorophore-nitroxide probes (FNPs) method**, FNPs keeping all properties of spin and fluorescent probes, possess an important new advantage: the nitroxide fragment is a strong intramolecular quencher of the fluorescence of the chromophore fragment. Then, chemical or photo-reduction of this fragment would result in a decrease of ESR signal and a strong increase in fluorescence (up to 2000) which is very sensitive technique (up to picomolar concentration). The ESR and fluorescence properties of the dual probes was intensively exploited as the basis of several methodologies which include a real time analysis of antioxidants, nitric oxide, superoxide and the establishment of antioxidant status of blood. In addition, FNPs, being incorporated in proteins, can serve as a suitable training area for experimental investigation factors affected on electron transfer, namely, molecular dynamics and micropolarity in the vicinity of the dual probe donor and acceptor fragments and chemical nature of bridge between them. **The suggested spin exchange approach** is based on a connection between superexchange in electron transfer (ET) and such electron exchange processes as triplet-triplet energy transfer (TTET) and spin-exchange (SE). Using experimental data on long distance TTET and SE

in bridged nitroxide biradicals, this approach allows to estimate values of spin exchange attenuation factor for individual bridge groups, the exchange integral (I_{SE}) and rate constant of electron transfer (k_{ET}) donor-acceptor pairs.

1. Likhtenshtein G.I.: *Biofisika* **13**, 396 (1968)
2. Likhtenshtein G.I.: *Spin Labeling Method in Molecular Biology*. N.Y.: Wiley Interscience 1976.
3. Likhtenshtein G.I.: *Chemical Physics of Redox Metalloenzymes*. Heidelberg: Springer-Verlag 1998.
4. Likhtenshtein G.I.: *Biophysical Labeling Methods in Molecular Biology*. Cambridge, N.Y.: Cambridge University Press 1993.
5. Likhtenshtein G.I.: *New Trends in Enzyme Catalysis and Mimicking Chemical Reactions*. N.Y.: Kluwer Academic/ Plenum Publishers 2003.
6. Denisov E.T., Sarkisov O.M., Likhtenshtein G.I.: *Chemical Kinetics. Fundamentals and Recent Developments*. Elsevier Science 2003.
7. Likhtenshtein G.I., Yamauchi J., Nakatsuji S., Smirnov A., Tamura R.: *Nitroxides: Application in Chemistry, Biomedicine, and Materials Science*. Weinheim: WILEY-VCH 2008.
8. Likhtenshtein G.I.: *Stilbenes: Application in Chemistry, Life Science and Material Science* WILEY-VCH, Weinheim 2009.
9. Likhtenshtein G.I.: *Solar Energy Conversion. Chemical Aspects*. Weinheim: WILEY-VCH 2012.
10. Likhtenshtein G.I.: *Electron Spin in Chemistry and Biology: Fundamentals, Methods, Reactions Mechanisms, Magnetic Phenomena, Structure Investigation*. Springer 2016.

Structure and Properties of Mechanically Activated $\text{TiO}_2/\text{MoO}_3$, $\text{TiO}_2/\text{V}_2\text{O}_5$ and $\text{TiO}_2/\text{MoO}_3:\text{V}_2\text{O}_5$ Oxides Studied by EPR and XRD

A. I. Kokorin¹, I. V. Kolbanev¹, T. V. Sviridova², and D. V. Sviridov²

¹ N. Semenov Institute of Chemical Physics RAS, Moscow 119991,
Russian Federation, alex-kokorin@yandex.ru

² Department of Chemistry, Belarus State University, Minsk, Belarus, sviridov@bsu.by

The binary mixed oxides such as $\text{MoO}_3:\text{V}_2\text{O}_5$ prepared by different chemical methods are very effective and rather stable heterogeneous catalysts and photocatalysts for many oxidation reactions [1–3]. It was recently shown that nanoparticles of $\text{MoO}_3:\text{V}_2\text{O}_5$ oxides can be prepared also using the method of mechanochemical activation (MCA) in mills of various types [4]. Also, the thin-film mixed oxide photocatalysts $\text{TiO}_2/\text{MoO}_3$ and $\text{TiO}_2/\text{MoO}_3:\text{V}_2\text{O}_5$ obtained through the combination of sol-gel and sintering techniques were investigated employing reactions of photooxidation of probing dyes, EPR spectroscopy with *in situ* UV irradiation, scanning electron microscopy, X-ray diffraction analysis and photoluminescent detection of peroxo species [5]. It has been shown that due to accumulation of charges produced under UV illumination these photocatalysts retain oxidation activity in the dark for a long time after illumination.

In this report, we describe our recent results of structural properties of photoactive oxides $\text{TiO}_2/\text{MoO}_3$, $\text{TiO}_2/\text{V}_2\text{O}_5$, and $\text{TiO}_2/\text{V}_2\text{O}_5:\text{MoO}_3$ prepared by the MCA technique and studied using CW X-band EPR and XRD analysis. Fig. 1 shows typical EPR spectra of such mixed oxide system which was treated in Spex mill at room temperature in air for different times. It is seen from these spectra that (a) the amount of paramagnetic vanadium V(IV) ions exhibits

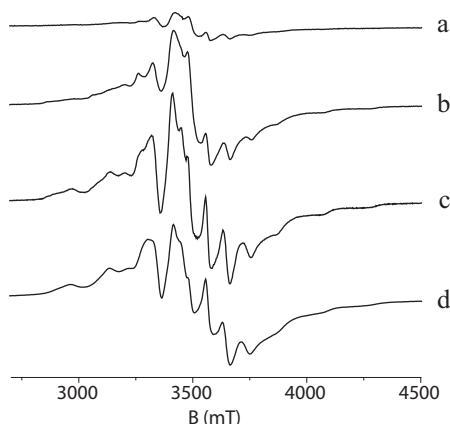


Fig. 1. EPR spectra at 77 K of the sample $\text{TiO}_2/\text{MoO}_3:\text{V}_2\text{O}_5 = 5:0.5:0.5$ (molar ratio) before (a) and after 10 (b), 60 (c), and 180 min (d) treatment in Spex mill in air.

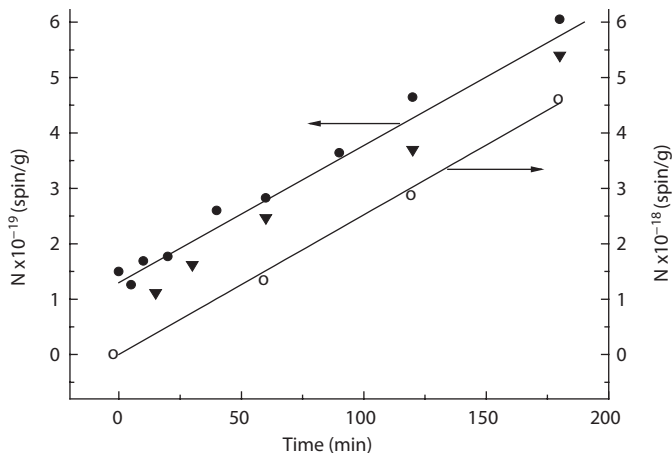


Fig. 2. Content of V(IV) and Mo(V) ions in $\text{TiO}_2/\text{V}_2\text{O}_5:\text{MoO}_3 = 5:0.5:0.5$ (●), $\text{TiO}_2/\text{V}_2\text{O}_5 = 5:1$ (▼) and $\text{TiO}_2/\text{MoO}_3 = 5:1$ (○) mixed oxides as a function of time of treatment in Spex mill.

an increase with the milling time (Fig. 2), and (b) the system becomes more dispersed under milling, that manifests itself as the enhanced signal from the isolated V(IV) centers (Fig. 1c, d).

Our investigations have evidenced that in the case of thin-film $\text{TiO}_2/\text{MoO}_3:\text{V}_2\text{O}_5$ oxide the system of photoelectron-trapping centers, which are characterized by different life time in contact with molecular oxygen, is formed. The peroxy species generated as the result of this interaction impart oxidation activity to the photocatalyst surface, this activity being retained for a long time after UV-light exposition. Several types of paramagnetic centers (PCs) were detected and characterized by EPR, and peculiarities of changes of PCs concentration under the UV-light illumination time and in the post-illumination period allowed us to describe the most probable detailed mechanism of the photocatalytic processes and those occurring under the “dark” conditions. Better understanding of these processes should drive us to the creation of new optimized and effective photocatalytic systems.

This work was supported by Russian Foundation for Basic Research (Grant No. 16-53-00136-Bel-a) and by the Basic Research Foundation of Belarus (project No. X16P-074).

1. Tomskii I.S., Vishnetskaya M.V., Kokorin A.I.: Russ. J. Phys. Chem. B **2**, 562 (2008)
2. Sviridova T.V., Kokorin A.I., Sviridov D.V.: Russ. J. Phys. Chem. B **7**, 734 (2013)
3. Baraboshina A.A., Sviridova T.V. *et al.*: Russ. J. Phys. Chem. B **10**, 28 (2016)
4. Kolbanev I.V., Degtyarev E.N., Streletskii A.N., Kokorin A.I.: Appl. Magn. Reson. **47**, 575 (2016)
5. Sviridova T.V., Sadovskaya L.Yu., Kokorin A.I. *et al.*: Russ. J. Phys. Chem. B **11**, 348 (2017)

NMR Methods to Study Protein-Ligand Interactions

V. I. Polshakov

Center for Magnetic Tomography and Spectroscopy, Faculty of Fundamental Medicine,
M. V. Lomonosov Moscow State University, Moscow 119991, Russian Federation, vpolsha@mail.ru

The processes that determine the nature of life are stages of an endless chain of intermolecular interactions involving biomacromolecules. The study of the molecular basics of the interaction of biomacromolecules with each other, with low molecular weight ligands, with metal ions, etc. lies at the heart of biochemistry, molecular biology and other life science disciplines. NMR spectroscopy is one of the most important tools for studying protein-ligand interactions. NMR provides a wide variety of techniques for determining the structure of protein-ligand complexes, detecting ligand binding sites, determining the stoichiometry of the protein-ligand interaction, measuring ligand binding constants. NMR screening techniques have been developed for design of compounds build from small molecular fragments and capable to bind specifically to the desired center of the target protein.

Several examples of the use of modern NMR spectroscopy tools for the studies of protein-ligand interactions will be presented. Thus, structure and dynamics of several complexes of the pharmacologically important enzyme dihydrofolate reductase with the antibacterial drug trimethoprim have been investigated in order to reveal the nature of the cooperative effects of ligand binding (Fig. 1a) [1, 2]. Interaction interface of the human translation termination factor eRF1 with the eukaryotic ribosome has been determined using the heteronuclear NMR methods

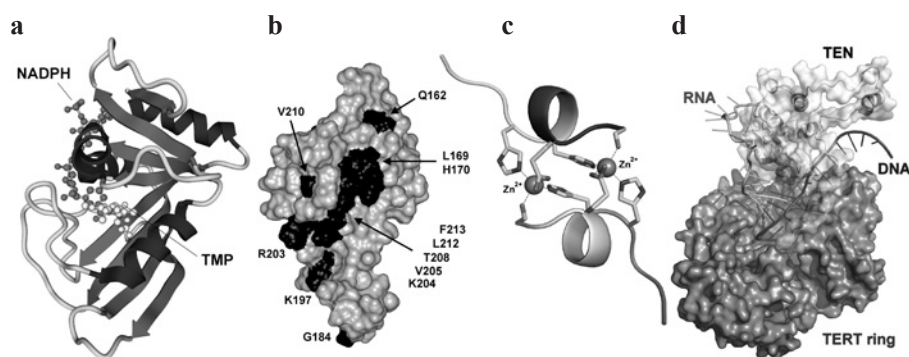


Fig. 1. Structure of protein-ligand complexes studied by NMR methods. **a** Ternary complex of *Lactobacillus casei* dihydrofolate reductase with co-factor NADPH and antibacterial drug trimethoprim. **b** Results of NMR detection of protein-ribosome interaction. Shown if molecular surface for the middle domain of human eRF1. Residues interacting with the 60S ribosome subunit are colored black. **c** Novel binuclear zinc interaction fold discovered in homodimer of Alzheimer's amyloid- β fragment with Taiwanese mutation D7H. **d** 3D model of the thermotolerant yeast *Hansenula polymorpha* build on the basis of NMR studies of interactions of its N-terminal domain with DNA fragments and the telomerase RNA.

(Fig. 1b) [3]. NMR screening techniques have been successfully applied for the design of inhibitors of the methionine γ -lyase, compounds with potential antibacterial properties [4]. NMR methods have been used to study interactions of the fragments of β -amyloid peptide isoforms with zinc ions in order to understand the molecular mechanism of the initial stages of β -amyloid aggregation linked to the Alzheimer's disease (Fig. 1c) [5–7]. More recently, NMR techniques have been applied to study interaction of the N-terminal domain of the main reverse transcriptase subunit of yeast telomerase with its potential partners in the catalytic cycle of the process of chromosome elongation catalyzed by telomerase (Fig. 1d). The above examples illustrate the high capabilities of NMR spectroscopy in the studies of protein-ligand interactions.

The work was supported by the Russian Science Foundation (grant 14-14-00598).

1. Polshakov V.I., Birdsall B., Feeney J.: *J. Mol. Biol.* **356**, 886–903 (2006)
2. Feeney J., Birdsall B., Kovalevskaya N.V., Smurnyy Y.D., Navarro-Peran E.M., Polshakov V.I.: *Biochemistry* **50**, 3609–3620 (2011)
3. Ivanova E.V., Alkalaeva E.Z., Birdsall B., Kolosov P.M., Polshakov V.I., Kiselev L.L.: *Mol. Biol.* **42**, 939–948 (2008)
4. Batuev E.A., Lisunov A.Y., Morozova E.A., Klochkov V.V., Anufrieva N.V., Demidkina T.V., Polshakov V.I.: *Mol. Biol.* **48**, 896–905 (2014)
5. Kozin S.A., Kulikova A.A., Istrate A.N., Tsvetkov P.O., Zhokhov S.S., Mezentsev Y.V., Ivanov A.S., Polshakov V. I., Makarov A.A.: *Metallomics* **7**, 422–425 (2015)
6. Istrate A.N., Kozin S.A., Zhokhov S.S., Mantsyzov A.B., Kechko O.I., Pastore A., Makarov A.A., Polshakov V.I.: *Sci. Rep.* **6**, 21734 (2016)
7. Polshakov V.I., Mantsyzov A.B., Kozin S.A., Adzhubei A.A., Zhokhov S.S., van Beek W., Kulikova A.A., Indeykina M.I., Mitkevich V.A., Makarov A.A.: *Angew. Chem. Int. Ed.*, **56**, doi: 10.1002/anie.201704615 (2017)

SECTION 11

OTHER APPLICATIONS OF MAGNETIC
RESONANCE

Supermagnonics in YIG Film

Yu. M. Bunkov, T. R. Safin, A. R. Farhutdinov, and M. S. Tagirov

Kazan Federal University, Kazan 420008, Russian Federation

It is well known that deviations of spins from the magnetic order in magnetic materials (ferromagnets, antiferromagnets and ferrites) have a collective character and are described in terms of spin waves and their quanta, magnons. Since magnons have a magnetic moment, one can create extra magnons by the external pumping, alternating magnetic field, and increase disorder in the magnetic system. However, in certain conditions, increase the density of magnons can lead to entirely new states be called magnon condensates, macroscopic number of magnons in coherent quantum states (see [1]). These macroscopic quantum states significantly alter the properties of the magnetic system, its dynamics and transport. For example, a single-particle long-range coherency occurs in a quasi-equilibrium as the phenomenon of Bose-Einstein condensation of magnons on the bottom of their spectrum. And it leads to the phenomenon of spin superfluidity. The spin superfluidity is an extremely interesting and promising phenomenon both for fundamental and applied studies. The superfluidity means a long distance correlation of a non-diagonal terms of the matrix of density, which does not, in general, take place in magnetically ordered materials.

For the first time the magnons Bose condensation was demonstrated in 1984 [2] in the antiferromagnetic liquid crystal of superfluid ^3He where the magnetic part of energy does not directly related to mass superfluidity. The BEC state described by a single wave function $S \exp(i\omega t + \varphi)$. The phase of precession appears spontaneously after a condensation of non-coherent magnons and radiates a coherent signal of induction even in a very inhomogeneous magnetic field. This spontaneously emerging steady state preserves the phase coherence across the whole sample and exhibits all the superfluid properties which follow from the off-diagonal long-range order for magnons. The BEC state can radiate the signal in 10^3 – 10^5 longer than the one follows from the inhomogeneity of magnetic field. In other words, the BEC state very effectively suppresses the local field inhomogeneity.

Since magnons have a finite lifetime and the total number of magnons decreases with decreasing of temperature (and reaches zero at $T = 0$), there is no phenomenon of magnon BEC at thermodynamic equilibrium. However, one can consider an analog of Bose-Einstein condensation of magnons as instability in the quasiequilibrium magnetic system pumped by the external sources. Magnon-magnon scattering conserves the total number of quasiparticles and hold the distribution function with the effective temperature T . The condition of this quasiequilibrium BEC and the critical density N of magnons will contain both the density of thermal magnons $N(0; T)$ at a given temperature and the effec-

tive density of pumped magnons N_p . The quasiequilibrium BEC will be entirely determined by pumping if the density of

$$N_p/V_s \simeq (k_B T_{\text{BEC}}/4\pi\hbar a^3)(\omega_0^{1/2}/\omega_{\text{ex}}^{3/2}), \quad T_{\text{BEC}} \simeq 4\pi(\hbar\omega_{\text{ex}}/k_B)(\omega_{\text{ex}}/\omega_0)^{1/2}[a^3(N_p/V_s)],$$

An estimate for YIG, where $\omega_{\text{ex}} a^2 = 0.092 \text{ cm}^{-2}\text{s}^{-1}$ for $\omega_0 = 2\pi \cdot 2.5 \text{ GHz}$ gives $T_{\text{BEC}} \simeq 2,14 \cdot 10^{-17}(N_p/V_s) \text{ cm}^3\text{K}$. Thus we obtain a room-temperature BEC $T_{\text{BEC}} \simeq 300 \text{ K}$ at the pumped magnon density $N_p/V_s = 1.41 \cdot 10^{19} \text{ cm}^{-3}$.

Let us now estimate the critical angle of the magnetic moment deviation from the equilibrium, which is assumed to correspond to a critical number of excited magnons. This angle is defined by the ratio of perpendicular spin component to its longitudinal component. For the room temperature $T = 300 \text{ K}$, YIG film thickness $6 \mu\text{m}$, $\omega_0 = 2\pi \cdot 2.5 \text{ GHz}$, $\Delta\omega = 2\pi \cdot 1 \text{ Hz}$ we have $\theta_{\text{film}} \approx 0.018$. In the experiments with YIG film we have reached the angle of deflection in 10 times bigger, then the critical angle of magnon BEC [3] and observed the coherent spin precession by pulse and CW FMR. Furthermore, we have made a YIG film in form of two electrodes, connected by a bridge. We have seen the spin supercurrent between the electrodes. The experimental results will be observed in the presentation.

1. Bunkov Yu.M., Volovik G.E.: Spin superuidity and magnon BEC, Chapter IV of the book "Novel Superuids" (Bennemann K.H., Ketterson J.B., eds.). Oxford: Oxford University Press 2013.
2. Borovik-Romanov A.S., Bunkov Yu.M., Dmitriev V.V., Mukharskiy Yu.M.: JETP Lett. **40**, 1033 (1984)
3. Bunkov Yu.M., Vetoshko P.M., Motygullin I.G., Safin T.R., Tagirov M.S., Tukmakova N.A.: Magnetic Resonance in Solids **17**, 15205 (2015)

Ionic and Molecular Transport in Polymeric Electrolytes on Magnetic Resonance Data

V. I. Volkov

Institute of Problems of Chemical Physics RAS, Science Center in Chernogolovka RAS,
Chernogolovka 1142432, Russian Federation, vitwolf@mail.ru

Ion-exchange membranes and polymer electrolytes for lithium cells attract keen attention of scientists in view of the development of modern environmentally clean and energy efficient technologies. The conventional technologies are based on the methods of mixture separation that employ ion-exchange membranes (chlorine electrolysis, electrodialysis, extraction of metal ions from solutions, separation of water-organic mixtures, etc.). The interest in ion-exchange membranes has increased due to the development of alternative energy sources based on fuel cells. Lithium cells are used for autonomous power supply in various devices such as laptops, cellular phones, digital video cameras, etc. and, lately, in automobile, space, aviation and ship-building industries. The development of highly efficient materials requires fundamental scientific knowledge of the mechanisms of ion and molecular transport. The studies performed in this field so far mainly concerned the macroscopic processes of electro and mass transfer; however, elucidation of the mechanism of selective ion and molecular transport requires investigation of diffusion at the microscopic level. Of most interest is the relationship between the following fundamentally important characteristics that determine the ion and molecular transport.

1. The nanoscale structure of ion transport channels. The structure and dynamics of polymer matrix at the submicrolevel, i.e., from several tenths of nanometer (sizes of solvated ions and molecules) to several nanometers or several tens of nanometers (characteristic lateral dimensions and lengths of ionic channels), determine the selective ion transport because these structural units form transport path for ion transfer by macroscopic distances. Studying the nanostructure opens up the prospects for targeted synthesis of polymer electrolytes, insofar as their preparation is accompanied by the formation of the nanostructure.

2. The type of interaction of mobile ions with functional groups and solvating molecules (water, organic compounds) and the state of solvent molecules in the polymer electrolyte. Data on the structure of ionic complexes and also on the mechanisms of interaction of ions and molecules with the polymer matrix are necessary for understanding the nature of selectivity of ion-exchange membranes and elementary steps of the diffusion transport of ions in polymer electrolytes.

3. The elementary steps of diffusion of ions and molecules, which can be characterized by the lifetime of a species the time of translational displacement, the partial diffusion coefficient on various spatial scales (if diffusion occurs in a heterogeneous medium or the diffusant consists of different species). The problem of elementary diffusion jumps logically follows from the aforesaid. Evidently, the time of elementary jump and the height of the potential barrier overcome by

a moving species are largely determined by the geometry of diffusion channels and the structure of solvate ionic complexes. This information is necessary for both the elaboration of adequate transport models and the targeted synthesis of high-performance polymer electrolytes.

Highly attractive methods that allow the mentioned information to be acquired are the magnetic resonance methods, particularly, NMR. The main advantage of these methods is the possibility of studying the structural and dynamic properties over a wide spatial scale and in wide ranges of molecular motion frequencies in systems under real conditions.

The following possibilities of the most popular magnetic resonance techniques are:

Electron paramagnetic resonance (EPR) provides information on the composition and structure of the first coordination sphere of paramagnetic ions, their mobility and local concentrations [1].

The method of electron-nuclear double resonance (ENDOR) makes it possible to selectively study the structure and dynamics of the environment of a paramagnetic centre in the range from 0.3 ± 0.5 to 1.5 nm [1, 2]. The EPR and ENDOR methods substantially supplement the traditional research technique such as small-angle X-ray scattering, the resolving power of which usually does not exceed 2–2.5 nm.

The main methods used in studying the state and mobility of ions in polymer electrolytes are NMR spectroscopy and pulsed NMR techniques, in particular, the NMR relaxation and pulsed field gradient NMR.

NMR spectroscopy. The most popular method is ^1H NMR, which was used to study sulfonate cation exchanger and the corresponding membranes and also perfluorinated cation-exchange membranes. To date, techniques have been developed for recording high-resolution NMR spectra and the main factors that determine the chemical shift of water protons and cation hydration numbers calculation. The required information can also be obtained from the solid-state high-resolution NMR spectroscopy. Information on hydration of ionic channels in membranes is of fundamental importance for understanding the mechanism of migration of cations and water molecules. NMR studies of cations in membranes and in gel and solid electrolytes of lithium cells reported [1]. The possibility of recording ^7Li , ^{23}Na and ^{133}Cs

NMR spectra for these systems have been demonstrated. The analysis of concentration dependences of chemical shifts and the shapes of NMR lines for these nuclei provided information on the mechanisms of interaction of alkali metal ions with ionogenic groups and on the cation mobility.

NMR relaxation. The NMR relaxation methods provide unique information on the mobility of ions and molecules [3]. Unfortunately, the quantitative treatment of experimental data was difficult due to the wide distribution of the correlation times of the ionic and molecular and the presence of paramagnetic impurities in these systems.

The pulsed field gradient NMR method, which makes it possible to directly measure the ionic and molecular self-diffusion is free from these drawbacks.

The NMR methods are especially attractive for acquiring detailed information on the ion and molecular transport in polymer electrolytes. The proposal

presentation is demonstrating the potential of NMR methods in studying the formation of transport channels, the mechanisms of ion-polymer matrix interaction, the mobility and diffusion of ions and molecules in polymer electrolytes are analyzed and generalized. Ion-exchange membranes with polymer matrices of various chemical types and polymeric electrolytes for lithium batteries are considered. The translational mobilities of ions measured by pulsed field gradient NMR are compared with the data on ionic conductivity acquired by impedance spectroscopy methods [4]. Attention is focused on the possibilities of NMR methods in studying the state of ions and molecules in electrolytes and also their diffusion mobility on different spatial scales. Based on the NMR data, the mechanisms of ion transport in ion-exchange perfluorinated membranes are proposed.

1. Volkov V.I., Marinin A.A.: *Russ. Chem. Rev.* **82**, no. 3, 248–272 (2013)
2. Volkov V.I., Pukhov K.K., Choh S.H., Park I.-W., Volkov E.V.: *Appl. Magn. Res.* **24** 177 (2003)
3. Volkov V.I., Vasilyak S.L., Park I.-W., Kim H.J., Ju H., Volkov E.V., Choh S.H.: *Appl. Magn. Res.* **25** 43 (2003)
4. Volkov V.I., Dobrovolsky Yu.A., Nurmiev M.S., Sanginov E.A., Volkov E.V., Pisareva A.V.: *Solid State Ionics* **179**, 148 (2008)

Proton Dynamics in Strong Hydrogen Bonds: Solvent-Induced Distribution of NMR Chemical Shifts

**P. M. Tolstoy¹, S. A. Pylaeva², E. Yu. Tupikina³, G. S. Denisov³,
H. Elgabarty², and D. Sebastiani²**

¹ Center for Magnetic Resonance, St.Petersburg State University, St. Petersburg, Russian Federation, peter.tolstoy@spbu.ru

² Institute of Chemistry, Martin-Luther Universität, Halle-Wittenberg, Germany

³ Department of Physics, St. Petersburg State University, St. Petersburg, Russian Federation

Strong XH...Y hydrogen bonds display striking NMR features, such as extreme values of $\delta^1\text{H}$ chemical shifts (and significant changes in $\delta^{13}\text{C}$, $\delta^{15}\text{N}$, $\delta^{19}\text{F}$, $\delta^{31}\text{P}$ etc.), maximal values of $^1\text{h}J_{\text{HY}}$ and $^2\text{h}J_{\text{XY}}$ couplings etc. In condensed phase, strong H-bonds are quite sensitive to the minute changes in their surroundings. Fluctuations in the solvation shell induce significant geometry changes (including full proton transfer), while transient asymmetric solvation breaks the symmetry of the complex. In the NMR time scale these dynamic processes are usually fast and can be detected as the changes in the time-averaged NMR observables. In this work we combine low-temperature NMR, UV-Vis, IR spectroscopy and *ab initio* MD simulations in order to analyze the intrinsic distributions of $\delta^1\text{H}$ for several strongly H-bonded model complexes in polar aprotic medium. We consider examples of (OHO)⁻ [1], OHN [2] and (FHF)⁻ [3] bonds. We discuss how instant values of $\delta^1\text{H}$ reflect the H-bond geometry and how H/D isotope effects on chemical shifts can be used to elucidate the average symmetry of the bond. We speculate how the NMR parameters of the medium can be used to probe the properties of the solute.

This work was supported by the RFBR grant 17-03-00497. The calculations were partially performed in the Computing Center of St. Petersburg State University Research Park.

1. Pylaeva S., Allolio C., Koeppel B., Denisov G.S., Limbach H.H., Sebastiani D., Tolstoy P.M.: *Phys. Chem. Chem. Phys.* **17**, 4634 (2015)
2. Koeppel B., Pylaeva S.A., Allolio C., Sebastiani D., Nibbering E.T.J., Denisov G.S., Limbach H.H., Tolstoy P.M.: *Phys. Chem. Chem. Phys.* **19**, 1010 (2017)
3. Pylaeva S.A., Elgabarty H., Sebastiani D., Tolstoy P.M.: *Phys. Chem. Chem. Phys.* (2017), *submitted*

ESR Study of $\text{Sc}_2\text{SiO}_5:\text{Nd}^{143}$ Isotopically Pure Crystals

**R. Eremina^{1,2}, K. Konov¹, V. F. Tarasov¹, T. P. Gavrilo^{1,2},
A. V. Shestakov¹, Yu. D. Zavartsev^{1,3}, A. I. Zagumennyi^{1,3},
and S. A. Kutovoi^{1,3}**

¹ Zavoisky Physical-Technical Institute, Russian Academy of Sciences, Kazan 420029, Russian Federation, REremina@yandex.ru

² Kazan Federal University, Kazan 420008, Russian Federation

³ Prokhorov General Physics Institute, Moscow 119991 Russian Federation

Sc_2SiO_5 (SSO) crystals were grown by the Czochralski method in Ir crucibles in the 99 vol.% Ar + 1 vol.% O_2 atmosphere. The purity of primary components, i.e., Sc_2O_3 , Nd_2O_3 and SiO_2 was no worse than 99.99%. This structure SSO is X_2 -polymorph and was indexed in a monoclinic unit cell with space group $I2/c$; the resulting unit cell parameters were $a = 9.9674(2)$ Å, $b = 6.4264(9)$ Å, $c = 12.0636(2)$ Å, and $\beta = 103.938(1)^\circ$ [1].

We studied SSO single crystals doped with 0.005% $^{143}\text{Nd}^{3+}$. The continuous wave (CW) EPR spectra of $\text{Sc}_2\text{SiO}_5:^{143}\text{Nd}^{3+}$ single crystals were recorded on a Bruker EMX+ spectrometer at the frequency of 9.4 GHz. The measurements of the spin-spin and spin-lattice relaxation times were carried out on an Elexsys E580 EPR spectrometer (Bruker) in the X-band (9.7 GHz). Both spectrometers were equipped with a flow helium cryostat (Oxford Instruments) for measurements in the temperature region from 4 to 10 K.

We measured the angular dependencies of EPR CW spectra in three crystallographic (ab), (bc) and (ac) planes at 10K in X-band. The view ESR spectra are presented in Fig 1a. The ^{143}Nd isotope has the nuclear spin $I = 7/2$. Two groups of resonance lines belonging to two magnetically non-equivalent $^{143}\text{Nd}^{3+}$ substituting Sc^{3+} ions in one of the two distinct crystallographic sites were observed in the CW and EPR spectra. The g -tensor parameters were obtained from angular

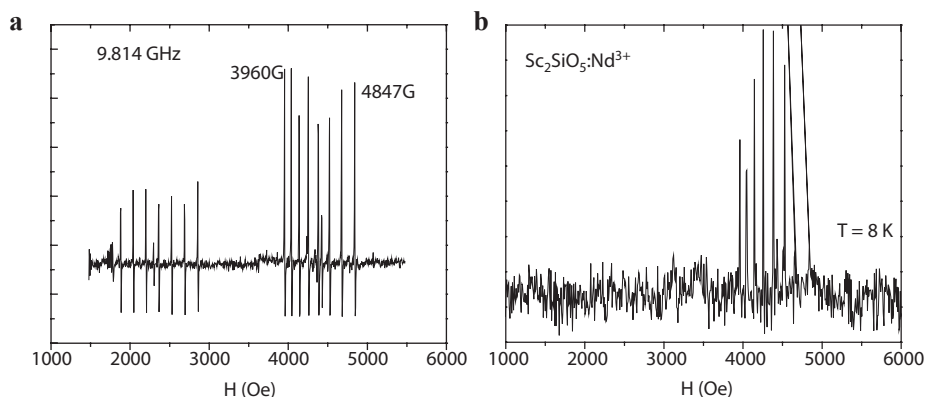


Fig. 1. The EPR spectra Nd^{3+} in Sc_2SiO_5 (a) echo-detected, (b) CW-registrations at 10 K.

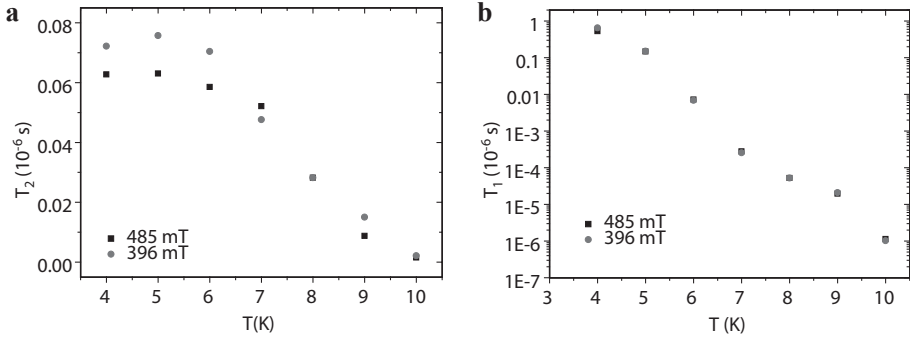


Fig. 2. The spin-spin (a) and spin-lattice (b) relaxation times Nd^{3+} in Sc_2SiO_5 monocrystal.

dependencies resonance lines in three planes. The results are similar with data which published in [2]. But only one group of resonance lines was observed in echo-detected EPR spectra (see Fig. 1b). We measured the temperature dependencies of the spin-spin and spin-lattice relaxation times (see Fig. 2). The spin-spin relaxation times are 3 order smaller for Nd^{3+} in Sc_2SiO_5 than in Y_2SiO_5 [3], but the times of spin-lattice relaxation practically are similar for two crystals. We believe that it is connected with fact that nuclear spin of Sc $I = 7/2$ but for Y nuclear spin equal $I = 1/2$.

This work was supported by the Russian Science Foundation (project No. 16-12-00041).

1. Alba M.D., Chain P., Iez-Carrascosa T.G.: J. Am. Ceram. Soc. **92**, no. 2, 487 (2009)
2. Kurkin I.N., Chernov K.P.: Sov. Phys. J. **25**, no. 7, 610 (1982)
3. Sukhanov A.A., Tarasov V.F., Eremina R.M., Yatsyk I.V., Likerov R.F., Shestakov A.V., Zavartsev Yu.D., Zagumennyii A.I., Kutovoi S.A.: Appl. Mag. Res. **48**, 589 (2017)

ESR Study of Intrinsic Magnetic Moments in Topological Insulators

**V. Sakhin¹, E. Kukovitsky¹, N. Garifyanov¹, R. Khasanov²,
Yu. Talanov¹, and G. Teitel'baum¹**

¹ Zavoiisky Physical-Technical Institute, Russian Academy of Sciences, Kazan 420029,
Russian Federation, sahin@kfti.knc.ru

² Paul Scherrer Institute, Villigen 5232, Switzerland

Topological insulators (TI) represent a novel class of quantum materials [1] having insulating bulk and dissipationless conducting surface, protected by time-reversal symmetry (TRS). Introducing local magnetic moments in TI can lead to breaking TRS due to appearance of the spontaneous magnetization. This gives rise to the new type of quantum behavior of a conducting surface layer. It manifests itself, for example, with anomalous quantum Hall effect [2]. Commonly emergence of magnetism in TI is associated with doping TI compound with external magnetic ions. However, it was discovered that local magnetic moments in topological insulators can originate not solely from doped magnetic ions but also from structural imperfections of undoped compound [3, 4]. In case of Bi_2Te_3 and Bi_2Se_3 these local moments appear due to the anti-site defects in Se (Te) layer of typical quintuple structure: some of Se (Te) atoms are replaced by Bi atoms. In our work, we concentrate on investigation of the intrinsic magnetism of TI on the example of bismuthates' family.

We studied single crystals of undoped compounds $\text{Bi}_2\text{Te}_2\text{Se}$ and $\text{Bi}_{1.08}\text{Sb}_{0.9}\text{Sn}_{0.02}\text{Te}_2\text{S}$ by EPR and SQUID magnetometry methods. In case of $\text{Bi}_2\text{Te}_2\text{Se}$ SQUID data reveal the dependence of magnetization on the cooling history for the fields smaller than 1000 Oe at temperatures below 80–90 K. Furthermore, we observed the magnetic resonance signal of the local magnetic moments in $\text{Bi}_{1.08}\text{Sb}_{0.9}\text{Sn}_{0.02}\text{Te}_2\text{S}$ that could originate from anti-site defects. Upon cooling down the signal shifts to the lower fields presumably due to the slowing down of magnetic fluctuations in the vicinity of the magnetic ordering of microscopic clusters formed by anti-sites defects. Such behavior could be associated with disordered spin-glass phase.

The work was supported by RFBR through the grant No. 15-42-02477.

1. Hasan M.Z. *et al.*: Rev. Mod. Phys. **82**, 3045 (2010)
2. Chekelsky J.G. *et al.*: Nature Physics **8**, 729 (2012)
3. Xiao G. *et al.*: Angew. Chem. Int. Ed. **53**, 729 (2014)
4. Li-Xian Wang *et al.*: Nanoscale **7**, 16687 (2015)

Investigation of Magnetic Anisotropy Field in Stressed Permalloy Microparticles by FMR

D. Bizyaev¹, A. Bukharaev^{1,2}, N. Nurgazizov¹, and T. Khanipov¹

¹ Zavoisky Physical-Technical Institute, Russian Academy of Sciences, Kazan 420029, Russian Federation, timurkhanipov@gmail.com

² Kazan Federal University, Kazan 420008, Russian Federation

Influence of mechanical stress on magnetic properties of ferromagnetics is in great interest nowadays. It is well known that creating of magnetic data storages and logical elements for micro- and nanoelectronics is available using stress induced magnetic effect and extremely low energy consumption is the special feature of these devices [1].

In this article permalloy (75% Ni, 25% Fe) microparticle arrays with different thicknesses were studied using the ferromagnetic resonance (FMR). Size of each particle was $25 \times 25 \mu\text{m}^2$. All samples were fabricated the same way. Glass substrate was bended by fixing on a special holder with constant curvature radius. On the next step, permalloy was deposited through the grid with $25 \times 25 \mu\text{m}^2$ hole sizes by electron beam evaporation in ultrahigh vacuum on Multiprobe P (Omicron). After that, sample was extracted from the holder, so that compressed permalloy particle array was created on the glass substrate.

Values of induced by compression magnetic anisotropy H_k were calculated from the angular dependence of ferromagnetic resonance field [2]. Samples with different permalloy layer thicknesses were studied. All samples were bended the same way during permalloy deposition. Dependence of H_k from permalloy layer thickness was studied (Fig. 1).

As we can see from Fig. 1, induced magnetic anisotropy in permalloy particles linearly grows with increasing of permalloy layer thickness.

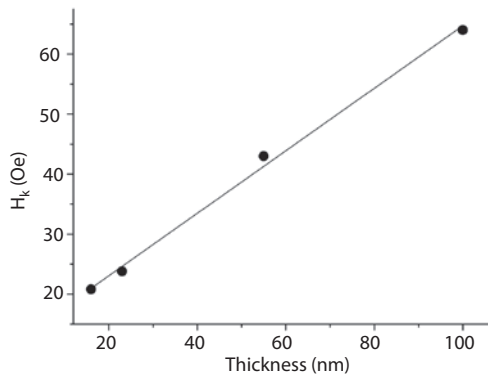


Fig. 1. Dependence of H_k from permalloy layer thickness.

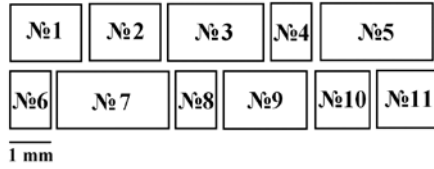


Fig. 2. Sample divided on pieces for FMR measurements.

Table 1. Dependence of anisotropy field from piece number.

Piece №	1	2	3	4	5	6	7	8	9	10	11
H_k (Oe)	11.7	11.8	17.8	19.2	20.5	No signal	15.0	15.7	24.8	19.1	25.7

Also, a sample with glass substrate sizes of 10×3 mm² that was fabricated the same way was studied. Permalloy layer thickness was 15 nm. Sample was cut as it shown on Fig. 2. Each piece was studied by ferromagnetic resonance and anisotropy field distribution was built, that is shown on Table 1.

As it seen from Table 1, in spite of uniform substrate bending while permalloy deposition, anisotropy field grows from one sample side to another. It could be cause of non-simultaneous substrate squeezing to the holder.

Thus, it is shown that FMR could be used for investigation of strain distribution in substrates.

1. Roy K.: Appl. Phys. Lett. **103**, 173110 (2013)
2. Belyaev B.A., Izotov A.V.: Physics of Solid State **49**, 1731 (2007)

Fullerene-Nitroxide Derivatives: Polarizers with New Properties for DNP in Liquid State

N. Enkin¹, S.-H. Liou¹, T. Orlando¹, I. Tkach¹, and M. Bennati^{1,2}

¹ RG EPR spectroscopy, Max-Planck Institute for Biophysical Chemistry,
Göttingen 37077, Germany, nikolay.enkin@mpibpc.mpg.de

² Department of Chemistry, University of Göttingen, Göttingen 37077, Germany

Dynamic nuclear polarization (DNP) is a rapidly developing method to enhance the sensitivity of nuclear-magnetic resonance (NMR) techniques. The method relies on polarization transfer from paramagnetic centres to coupled magnetic nuclei. DNP in liquids is governed by the Overhauser mechanism due to the cross-relaxations which are driven by time-dependent interactions (dipolar and scalar). In a conventional DNP experiment, a polarizer molecule, such as

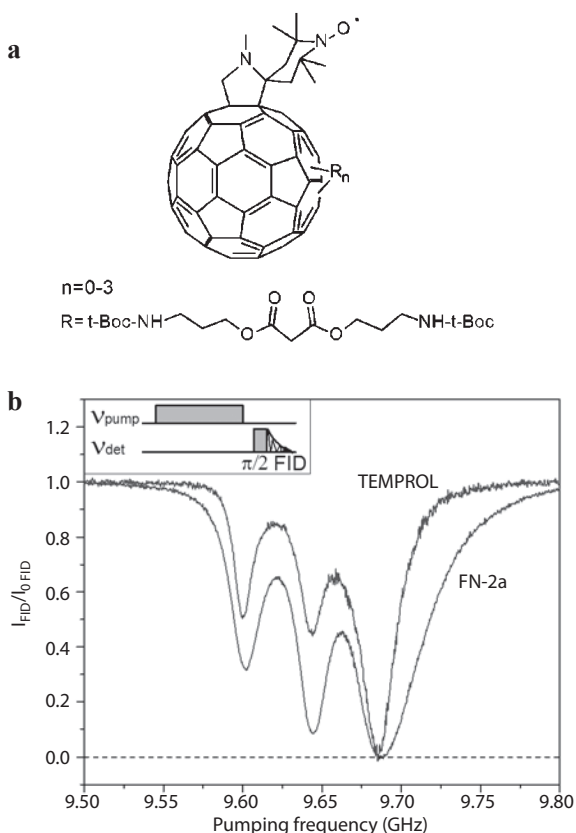


Fig. 1. a Structure of the investigated fullerene-nitroxide derivatives. **b** Normalized FID intensity of one FN derivative and TEMPOL as a function of the pumping ELDOR frequency. Here the signal reductions (y axis) give the saturation factor values of the low field EPR transition (adapted from [1]).

nitroxide radical, is mixed to the target molecule and pumped by microwave irradiation. The NMR signal enhancement depends on the efficiency of such pumping (saturation factor) and the cross relaxation (coupling factor). Here we present fullerene-nitroxide (FN) derivatives (Fig. 1a) as polarizers with several interesting properties, which can help to optimize the DNP performance of standard nitroxides in liquids.

The efficiency of conventional liquid DNP with nitroxide radicals is limited by two factors. The first one is the difficulty of reaching a high saturation factor because of the presence of several EPR transitions (as result of the hyperfine interaction between the unpaired electron and the ^{14}N nitrogen nucleus). The second one is the volume restriction caused by strong microwave absorption in liquids. We have recently demonstrated that ^{14}N nuclear spin relaxation of the nitroxide can increase the saturation transfer between different EPR transitions. Pulse ELDOR experiments permit to directly compare the saturation factor of TEMPO with FN (Fig. 1b) [1]. Secondly, in FN the fullerene moiety covalently linked to the TEMPO allows to polarize the radical by light irradiation [2]. This phenomenon can lead to DNP without MW but using instead light excitation.

Finally, we have also observed that FN can lead to high scalar DNP enhancement of ^{13}C nuclei. Our most recent experiments and results will be discussed.

1. Enkin N., Liu G., Gimenez-Lopez M., Porfyrakis K., Tkach I., Bennati M.: *Phys. Chem. Chem. Phys.* **17**, 11144 (2015)
2. Rozenshtein V., Berg A., Stavitski I., Levanon H., Franco L., Corvaja C.: *J. Phys. Chem. A* **109**, 11144 (2005)

SECTION 12

PERSPECTIVE OF MAGNETIC RESONANCE IN SCIENCE AND SPIN-TECHNOLOGY

Manifestations of the Collective Motion of Spins Induced by Stochastic Relaxation Processes

K. M. Salikhov

Zavoisky Physical-Technical Institute, Kazan 420029, Russian Federation, salikhov@kfti.knc.ru

In the recent work [1] for two simple model systems I have demonstrated that the coherence transfer between spin probes induced by the exchange interaction between spin probes in a course of their random binary collisions leads to formation of the collective motion modes of the quantum spin coherences of all spin probes. This is one more interesting example of arising of some kind the ordered motion pushed by a random molecular motion. Here I developed further the subject and considered a few new model systems.

The formation of the collective modes for the spin s coherences allows to formulate new interpretation, new vision, of the well known phenomenon of the exchange narrowing of spectra. As known, this spectra narrowing effect arises when the spin coherence transfer rate exceeds the critical value. In terms of collective motion modes the exchange narrowing effect happens due to the specific microwave field excitation pattern of spins. It appears that all collective modes except one of them are not excited by the MW field when detecting spectra, they behave as “dark states”.

Speculations will be presented concerning possible designs of experiments to manipulate with the collective modes of the spin coherence motion.

This work is supported by the Grant for the fundamental research of the Presidium of the Russian Academy of Sciences 1.26 II.

1. Salikhov K.M.: Appl. Magn. Reson. **47**, 1207–1227 (2016)

Influence of Free Charge Carriers on EPR Parameters of Gd^{3+} Centers in the $Pb_{1-x}Ag_xS$ and $Pb_{1-x}Cu_xS$ Semiconductors

V. A. Ulanov^{1,2}, A. M. Sinicin², and R. R. Zainullin^{1,2}

¹ Zavoisky Physical-Technical Institute, Kazan 420029, Russian Federation,
ulvlad@inbox.ru

² Kazan State Power Engineering University, Kazan 420066, Russian Federation

PbS (galena) has the rock salt structure and belongs to family of the lead chalcogenide narrow gap semiconductors (PbS, PbTe, and PbSe). Due to unusual physical properties these materials have important applications in thermoelectric and infrared devices. To modify the physical properties of the lead chalcogenides, usually they prepare solid solutions, mixing the PbS, PbTe, and PbSe in various proportions. For such purpose the various impurity and native defects in volumes of the lead chalcogenides are created too. Prevalent native defects in PbS crystal are sulfur vacancies. Each of them provides two free electrons. So, the sulfur vacancies in galena can be considered as donors of free electrons. Doping PbS by an acceptor impurity one can get a semiconductor with hole type conductivity.

The goal of the present work was to study, using the EPR method, the effects that may be realized by doping the galena with Cu and Ag, transition group elements. As in various compounds these elements frequently are found in monovalent states, in galena they can be considered as acceptor impurities. A few Gd^{3+} paramagnetic centers were created in volumes of the $Pb_{1-x}Cu_xS$ and $Pb_{1-x}Ag_xS$ crystals to get some information about lattice deformations and characteristics of free charge carriers (electrons or holes) present in the crystals with concentration depending on quantities of Cu and Ag. The crystals under study were all grown using the Bridgeman method. Copper, silver, and gadolinium

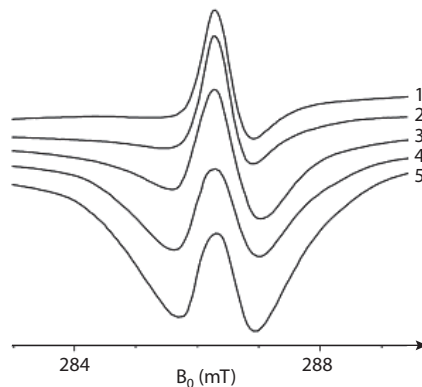


Fig. 1. Dependence of EPR line shape of the low field fine structure component of the EPR spectrum of Gd^{3+} on microwave power observed at $T = 4.2$ K ($B_0 \parallel \langle 001 \rangle$)

were introduced into the galena in stoichiometric proportions. In the crystals thus grown free carrier concentrations were measured by Hall method using the formula $c = 1/eR$ ($c = n, p$). In these measurements it was found that type of conductivity of $\text{Pb}_{1-x}\text{Ag}_x\text{S}$ crystals was inverted from n to p at Ag concentration about $x = 0.0045$. But, no inversion of the type of conductivity was found for $\text{Pb}_{1-x}\text{Cu}_x\text{S}$ in the range $0 \leq x \leq 0.015$. As it was found, Gd^{3+} formed in the $\text{Pb}_{1-x}\text{Cu}_x\text{S}$ and $\text{Pb}_{1-x}\text{Ag}_x\text{S}$ crystals the paramagnetic centers with cubic symmetry. The X-band EPR spectra of these centers could be described by well-known spin-Hamiltonian

$$H_s = \beta_e g H \cdot S + (1/60)b_4(O_4^0 + 5O_4^4) + (1/1260)b_6(O_6^0 - 21O_6^4).$$

It was found too that the g , b_4 , and b_6 parameters of the spin-Hamiltonian are dependent on temperature and free carrier concentration. Comparing g -factors for $\text{PbS}:\text{Gd}^{3+}$ and $\text{PbTe}:\text{Gd}^{3+}$ one could find that g -factor of Gd^{3+} was not sensitive to lattice distortions induced by Ag and Cu impurities, while sensitivity of the crystal field parameters b_4 and b_6 to distortions could be observable. In the $\text{PbS}:\text{Gd}^{3+}$ crystal the parameters determined at 4.2 K were following: $g = 1.9901 \pm 0.0002$; $b_4 = 59.37 \pm 0.05$; $b_6 = -0.18 \pm 0.05$ (b_4 and b_6 in MHz). For $T = 77$ K these parameters were: $g = 1.9922 \pm 0.0002$; $b_4 = 57.92 \pm 0.05$; $b_6 = -0.32 \pm 0.05$. Results of g -factor dependences on the concentration and type of conductivity of the $\text{Pb}_{1-x}\text{Cu}_x\text{S}$ and $\text{Pb}_{1-x}\text{Ag}_x\text{S}$ samples studied in this work show that these ones are qualitatively the same as for Mn^{2+} centers in PbTe [1], but much less pronounced. Main result of the present work is an unusual dependence of the EPR line shapes of Gd^{3+} centers on microwave power P_r acting in the resonator of the spectrometer (Fig. 1). In this figure the fragment 1 corresponds to $P_r = 0.02$ mW, and fragment 5 to $P_r = 25$ mW. The same result was observed for other six EPR lines at $T = 4.2$ K.

From Fig. 1 one can see that at low microwave powers the shapes of the EPR lines have a Dysonian form, but, at higher powers these lines acquire a new form which cannot be described by Dyson's theory.

1. Story T., Swuste C.H.W., Egenkamp P.J.T, Swagten H.J.M., de Jonge W.J.M.: Phys. Rev. Lett. 77, 2802 (1996)

FMR Studies of Ultra-Thin Epitaxial Pd_{1-x}Fe_x Films

**A. Esmaili¹, I. R. Vakhitov¹, N. P. Nikitin¹, I. V. Yanilkin¹,
A. I. Gumarov¹, B. M. Khaliulin¹, B. F. Gabbasov¹, M. N. Aliyev³,
R. V. Yusupov¹, and L. R. Tagirov^{1,2,4}**

¹ Kazan Federal University, Kazan 420008, Russian Federation, yanilkin-igor@yandex.ru

² Zavoisky Physical-Technical Institute, Russian Academy of Sciences, Kazan 420029,
Russian Federation

³ Baku State University, AZ-1148 Baku, Azerbaijan

⁴ Institute for Advanced Studies ASRT, Kazan 420111, Russian Federation

Palladium-iron alloy, Pd_{1-x}Fe_x, represents a unique class of ferromagnetic materials. A small, even less than 1 at.%, amount of iron atoms in palladium matrix induces ferromagnetism (FM) [1] at low temperatures. Iron atoms, substituting for palladium in the crystal lattice, create strong polarization around, and long-range ferromagnetism occurs when these localized magnetic polaron clouds of 4d-electrons overlap. Concentration of iron in the alloy controls principal ferromagnetic properties of these materials. Thin films of Pd_{1-x}Fe_x are attractive materials for cryogenic memory elements [2, 3].

Ultrathin Pd_{1-x}Fe_x films with $x = 0.01-0.08$ were deposited by molecular beam epitaxy (MBE system by SPECS) technique under ultra-high, $3 \cdot 10^{-10}$ mbar, vacuum conditions onto the (001)-oriented MgO substrates. Magnetic properties were studied by the vibrating sample magnetometry technique using Quantum Design PPMS-9 system. Commercial X-band Bruker ESP300 electron spin resonance spectrometer was used for ferromagnetic resonance (FMR) measurements.

FMR spectra were recorded at the in-plane and out-of-plane geometries. The film normal was kept parallel to the magnetic microwave field component during the in-plane measurement, whereas the external DC magnetic field was rotated in the film plane (angle φ_H is varied, see Fig. 1). For the out-of-plane measurements, the magnetic field component of the microwave field was in the film plane, whereas the external DC magnetic field was rotated from the film plane ($\theta_H = 90^\circ$) toward the film normal ($\theta_H = 0^\circ$).

FMR experimental data were described assuming the cubic magnetic anisotropy with the tetragonal distortion:

$$F_{\text{anis}} = (2\pi M_0^2 - K_p)\cos^2\theta - (1/2)K_1(\sin^4\theta(\cos^4\varphi + \sin^4\varphi)) - (1/2)K_2\cos^4\theta,$$

where M_0 is the saturated magnetization, θ and φ are the polar and azimuthal (measured from the [110] direction) angles of the magnetization vector \mathbf{M} with respect to the reference axes, K_p , K_1 , K_2 – magnetic anisotropy constants.

FMR measurements of samples have shown the four-fold in-plane anisotropy. It was found that the magnetization and Curie temperature of the films grew monotonically while increasing the iron concentration. Magnetic measurements at low temperatures ($T = 5$ K) revealed low coercive field values (from 7 to 23 Oe) for the epitaxial films of Pd_{1-x}Fe_x with $x = 0.01-0.08$.

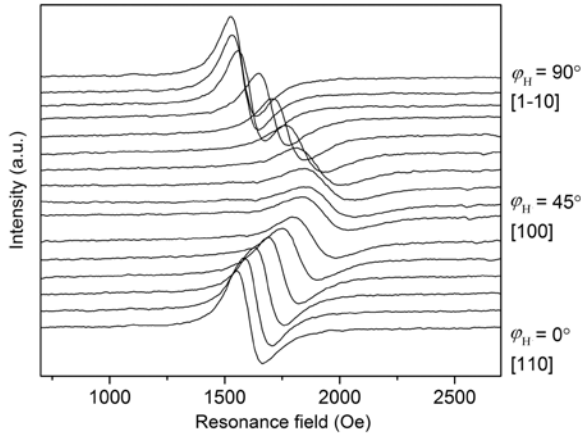


Fig. 1. In-plane angular dependence of the FMR spectra for $\text{Pd}_{0.92}\text{Fe}_{0.08}$ film.

The Program of Competitive Growth of Kazan Federal University supported by the Russian Government is gratefully acknowledged, as well as partial support from RFBR projects No. 14-02-00793_a and 16-02-01171-a. Synthesis and analysis of the films were carried out at the PCR Federal Center of Shared Facilities of KFU.

1. Nieuwenhuys G.J.: *Adv. Phys.* **24**, 515 (1975)
2. Larkin T.I. *et al.*: *Appl. Phys. Lett.* **100**, 222601 (2012)
3. Golovchanskiy I.A. *et al.*: *Journ. Appl. Phys.* **120**, 163902 (2016)

POSTERS

EPR Investigation of Mechanoactivated Copper Gluconate

**M. M. Akhmetov¹, G. G. Gumarov¹, V. Yu. Petukhov¹,
G. N. Konygin², and D. S. Rybin²**

¹Zavoisky Physical-Technical Institute, Russian Academy of Sciences, Kazan 420029,
Russian Federation, mansik86@mail.ru

²Physical-Technical Institute Ural Branch of RAS, Izhevsk, Russian Federation, dsrybin@mail.ru

The study of the complexation of copper(II) with biologically active ligands has been the subject of research over the past few decades, a number of aspects being still unclear. Copper plays an important role in pharmacology, as it is necessary for the normal operation of the mechanism of muscle contraction. Copper sulfate, chloride and copper gluconate are used to treat copper deficiency. It was previously shown that mechanoactivation leads to a sharp increase in the biological activity of calcium gluconate [1]. The aim of this work is to study the influence of mechanochemical treatment on the change in the magnetic and structural properties of copper gluconate using EPR methods in the X and L bands, and to identify some regularities occurring in gluconic acid salts during mechanoactivation.

For copper gluconate (X-band), a set of lines with parameters $g_{\parallel} \approx 2.31$ and $g_{\perp} \approx 2.07$ is observed in the initial state. In the case of mechanical grinding in a planetary-ball mill, the intensity of the EPR line decreases. The drop in the EPR intensity of the copper(II) lines in the spectra for the L and X bands can be attributed to the fact that the copper ion passes into a nonparamagnetic state. Donor centers of Cu in the states Cu^0 ($3d^{10}4s^1$) and Cu^{2+} ($3d^9$) are paramagnetic and should appear in the EPR spectra, therefore, it is most probable that the copper ion is in the state Cu^+ ($3d^{10}$). Also, the drop can be explained by fast spin relaxation, as a result of which the levels are blurred so much that the EPR spectrum can not be detected because of the large line width. It can be assumed that the mechanism of acceleration of spin relaxation is associated with the magnetic interaction of Cu^{2+} ions with other rapidly relaxing centers (oxygen admixture) present in significant quantities in copper gluconate [2]. It is assumed that the configuration of the Cu(II) ion in the octahedral field of the ligands is a tetragonally elongated octahedron.

1. Konygin G.N. *et al.*: Materials of conference "Topical issues of Pediatric Surgery", 56 (2003)
2. Bondar V.D., Grudzinski A.S., Zaritzki I.M. *et al.*: Solid state physics 37, 1 (1995)

Cross-Correlation Effects in Spin-Lattice Relaxation and Symmetry Restricted Spin Diffusion in Single Crystals of Amino Acids

N. K. Andreev

Kazan State Power Engineering University, Kazan 420066, Russian Federation,
ngeikandreev@gmail.com

The aim of the report is to represent the results of the investigations nuclear magnetic relaxation processes in the single crystals of the amino acids: sulfamic acid $\text{NH}_3^+\text{SO}_3^-$, glycine $\text{NH}_3^+\text{CH}_2\text{COO}^-$, L-alanine $\text{NH}_3^+\text{CH}_2\text{CH}_3\text{COO}^-$, partly deuterated L-alanine $\text{ND}_3^+\text{CH}_2\text{CH}_3\text{COO}^-$ and L-valine $\text{NH}_3^+\text{CHCH}(\text{CH}_3)_2\text{COO}^- \cdot \text{H}_2\text{O} \cdot \text{HCl}$. The molecules of amino acids are the fragments of large protein molecules which itself represent biopolymers. Therefore the aminoacids can be the subject of interest from the point of view of studying structure and molecular motion of proteins. To date, many investigations [1–3] were devoted to study the structure and molecular motions in solid amino acids by the pulse NMR technique. For the aim of our investigation, the amino acids are the objects that contain three-spin amino $-\text{NH}_3^+$ and methyl $-\text{CH}_3$ groups with proton nuclear spins $I = 1/2$ undergoing stochastic hindered rotation around the fixed axes of the third order C_3 .

The single crystals were grown from aqueous and weak hydrochloric solutions. The measurements of spin-lattice relaxation processes in the laboratory and rotating reference frames (LRF and RRF), M_z , M_{zp} were performed by using $180^\circ-\tau-90^\circ$ and $90_0-\tau_{90}$ pulse sequences at the main resonance frequency 27.5 MHz. The temperature was regulated in the range $(-180 - +200 \pm 0.5)^\circ\text{C}$ by the slow evaporation of liquid nitrogen.

The program of the report included the study of the dependence of the magnetization recovery on the orientation of the crystal in the external magnetic field and temperature. The nonexponential character of relaxation of magnetizations, M_z , M_{zp} , in the laboratory and rotating reference frames has been revealed. At the same conditions the relaxation of magnetizations for the powder sample of NH_4Cl was exponential. The initial slope of the relaxation curves gave us values of spin-lattice relaxation times T_1 and T_{1p} . The relaxation is dependent on the orientation of a crystal in an external constant magnetic field, i.e. is highly anisotropic. The crystal structures of the amino acids studied have been determined by the X-ray and neutron diffraction methods. The measured angular dependencies of the relaxation times were compared by the calculated values. As the molecules of the investigated amino acids contain one amino group and one or two methyl groups the temperature dependencies of relaxation times have low temperature minima stipulated by the rotation of methyl groups and high temperature minima stipulated by the rotation of amino groups. Therefore the angular dependence of the relaxation time changes its form with the change of a temperature. The relaxation anisotropy and nonexponentiality decrease with a number of protons in a molecule.

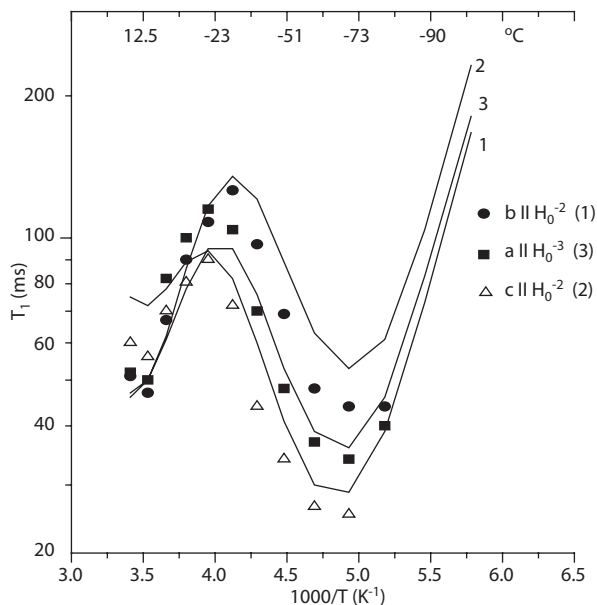


Fig. 1. Temperature dependence of the relaxation time T_1 for the three orientations of the single crystal of hydrochloride monohydrate of L-valine.

The results were discussed from the point of view of symmetry restricted spin diffusion processes. The relaxation is stipulated by the two processes: the relaxation of the longitudinal nuclear magnetization and rotary polarization. The conclusion was performed that the rotary polarization also inserts its own contribution into the angular dependence of a relaxation rate.

1. Zaripov M.R.: Protonnaya magnitnaya relaxatiya i molekulyarnye dvizheniya v polycrystallakh aminokislot (in russian) in: Radiospectroscopia, p. 193–229. Moscow: Nauka Edition 1973.
2. Andreev N.K.: Metody i priory nizkochastotnoy relaxacionnoy YaMR-introscopii (in russian). Kazan: Kazan State Power Engineering Univ. Edition 2003.

Application of the Multi-Pulse Protocols in Solid State ^1H NMR in Cu(II)-Oxamidato Complex

**E. Anisimova^{1,2}, R. Zaripov¹, I. Khairuzhdinov¹, K. Salikhov¹,
T. Ruffer³, and E. Vavilova¹**

¹ Zavoisky Physical-Technical Institute, Russian Academy of Sciences, Kazan 420029, Russian Federation

² Kazan Federal University, Kazan 420008, Russian Federation

³ Technische Universität Chemnitz, Fakultät für Naturwissenschaften, Institut für Chemie, Chemnitz D-09111, Germany

The materials under study that can be used for spintronics and quantum computing. Increasing the coherence time in presence of spectral diffusion can be achieved with the CPMG pulse protocol [1]. The ESR investigations of Cu(II)-oxamidato complexes have shown that under different conditions the behavior of the echo intensity is not exponential because of the contribution of a parasitic component originating from the stimulated echo [2]. In this work, the same effect was studied by proton NMR in the same compound. It was found that when using a CPMG sequence, the echo signal of the protons contains a contribution of the stimulated echo, but due to the inhomogeneity of the magnetic field on different hydrogen positions in the molecule the situation is more complicated than for Cu(II) ESR.

1. Zaripov R., Vavilova E., Miluykov V., Bezkishko I., Sinyashin O., Salikhov K., Kataev V., Büchner B.: *Phys Rev B*. **88**, 094418 (2013)
2. Zaripov R., Vavilova E., Khairuzhdinov I., Salikhov K., Voronkova V., Abdulmalic M.A., Meva F.E., Weheabby S., Ruffer T., Büchner B., Kataev V.: *Beilstein J. Nanotechnol.* **8**, 943–955 (2017)

Routine of Determination of the Spin Exchange Rate Constants from EPR Line Shape Analysis of Nitroxyl Radicals in Liquids

M. M. Bakirov, R. T. Galeev, and K. M. Salikhov

Zavoisky Physical-Technical Institute, Russian Academy of Sciences, Kazan 420029,
Russian Federation, pinas1@yandex.ru

The shape of the EPR spectra of the spin probes depends on the spin decoherence and spin coherence transfer rates between probes. These parameters depend on the different interactions: spin exchange interaction, dipole-dipole interaction and the hyperfine interaction (HFS) of the unpaired electrons with magnetic nuclei. In papers [1, 2] different algorithms of separating dipole-dipole and Heisenberg spin exchange interactions are proposed.

In our recent work [3] proposed algorithm [1] was examined in detail on the model EPR spectra of paramagnetic probes. Numerical calculations showed that nitrogen hyperfine components of the EPR spectrum contain contributions of absorption and of dispersion in the limit of slow spin exchange. In a case, when each nitrogen hyperfine component of the EPR spectrum has unresolved hyperfine structure caused by the hyperfine interaction with protons/deutons which can be approximated by the Gaussian distribution of resonance frequencies, it was found that the dispersion contribution does not practically depend on the hyperfine interaction of the unpaired electron with magnetic nuclei of the methyl groups of the radical, H and D atoms.

In this work algorithms developed in [1, 2] were applied for interpretation of the experimental EPR spectra of several nitroxyl radicals solutions. EPR measurements of 4-Hydroxy-2,2,6,6-tetramethylpiperidine 1-oxyl (TEMPO), 4-Hydroxy-2,2,6,6-tetramethylpiperidine-1-¹⁵N-oxyl, (TEMPO-¹⁵N) and 4-Hydroxy-2,2,6,6-tetramethylpiperidine-d₁₇-1-¹⁵N-oxyl, (TEMPO-¹⁵N-d₁₇) in 60% water glycerol solution were carried out. Experiment was performed at temperature range from 273 to 340 K and concentrations from 10⁻⁴ to about 50 · 10⁻² mole/l.

This work was done in cooperation with Dr. I. A. Kirilyuk (Novosibirsk organic chemistry institute of SB RAS, Russia), Prof. B. Bales (Western Institute of Nanoelectronics, University of California, Los Angeles, USA), Prof. A. I. Kokorin (Institute of chemical physics of RAS, Moscow, Russia).

This work was financially supported by the budget of Kazan physical-technical institute of RAS and by the Program of fundamental researches of the Russian academy of sciences Presidium (program 1.26II).

1. Salikhov K.M.: Appl. Magn. Reson. **38**, 237–256 (2010)
2. Peric M., Bales B., Peric M.: J. Phys. Chem. A **116**, 2855–2866 (2012)
3. Salikhov K.M., Bakirov M.M., Galeev R.T.: Appl. Magn. Reson. **47** (2016)

FMR Investigation of Magnetic Anisotropy in Films were Synthesized by Co^+ Implantation into Si

V. V. Chirkov¹, G. G. Gumarov¹, V. Yu. Petukhov¹, and M. M. Bakirov¹

¹ Zavoisky Physical-Technical Institute, Russian Academy of Sciences, Kazan 420029, Russian Federation, chirkov672@gmail.com

Thin ferromagnetic films were synthesized by Co^+ implantation into monocrystalline silicon in a magnetic field. The results of scanning magnetopolarimetry (MOKE) [1] showed the appearance of uniaxial magnetic anisotropy in samples synthesized with implantation dose more $2.4 \cdot 10^{17} \text{ cm}^{-2}$. Anisotropy field of these films increases with implantation dose. Presumably, the formation of induced magnetic anisotropy is due by directional atomic pair ordering (Neel-Taniguchi model). Repeated low-dose implantation into the synthesized films in a magnetic field switches the direction of the easy magnetization axis (EMA), which is a confirmation of the applicability of Neel-Taniguchi model.

From the results of FMR investigation, the anisotropy constant was determined in the temperature range from 40 to 300 K for a samples synthesized with a dose of $2.6 \cdot 10^{17} \text{ cm}^{-2}$ and $3 \cdot 10^{17} \text{ cm}^{-2}$. As can be seen from Fig. 1, the dependence of the anisotropy constant on temperature is linear. The exponent of the power law of reduced magnetization $K_u(T) \sim M_s(T)^n$ is 6. This temperature dependence does not agree with the Callen and Callen's theory. The linear temperature dependence of the uniaxial anisotropy constant can be caused by the reduced surface anisotropy related with a low thickness of ferromagnetic films [2].

The work was supported by the Fundamental Research Program of ONIT RAS No. 2.3.

1. Chirkov V.V., Gumarov G.G., Petukhov V.Yu., Denisov A.E.: J. Surf. Invest.: X-Ray, Synchrotron Neutron Tech. (2017) in print
2. Yong-Sheng Zhang *et al.*: Physica B. **512**, 32–36 (2017)

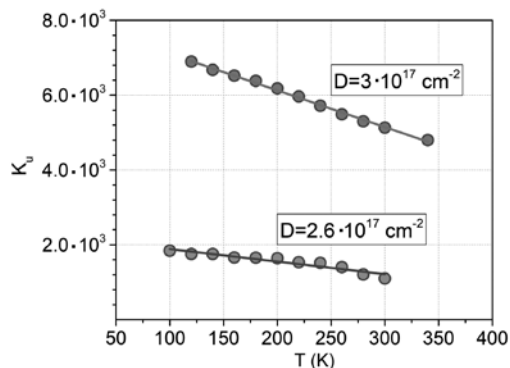


Fig. 1. Temperature dependence of the anisotropy constant.

EMR Searching of Quantum Behavior of $\gamma\text{-Fe}_2\text{O}_3$ Nanoparticles Encapsulated in Dendrimeric Matrix

N. E. Domracheva¹, V. E. Vorobeva¹, and M. S. Gruzdev²

¹ Zavoisky Physical-Technical Institute, Russian Academy of Sciences, Kazan 420029, Russian Federation, vvalerika@gmail.com

² G. A. Krestov Institute of Solution Chemistry, Ivanovo 153045, Russian Federation

In recent years, the study of magnetic nanoparticles (MNPs) has attracted considerable attention driven by both fundamental scientific interest and potential technological applications. Electron Magnetic Resonance (EMR) is one of the key tools for studying MNPs. We have investigated earlier [1] the EMR behavior of $\gamma\text{-Fe}_2\text{O}_3$ nanoparticles fabricated in the second-generation poly(propylene imine) dendrimer using the classical theoretical approach [2] based on parameters derived from bulk materials. However, we observed a signal at half-field in the EMR spectra of our NPs (of approximately 2.5 nm). This feature is interpreted in the literature [3, 4] as an evidence of the discrete structure of the energy levels and, therefore, of the quantum nature of the system (where the whole energy spectrum of a NP considered as a giant exchange cluster).

In the present work we have tried to find new arguments in favor of the quantum nature of our $\gamma\text{-Fe}_2\text{O}_3$ -MNPs. For this purpose the EMR spectra were recorded in both parallel and perpendicular configuration, i.e. with the H_1 field of the microwave radiation parallel and perpendicular to the external H_0 field. These alternative measurement configurations have different selection rules for

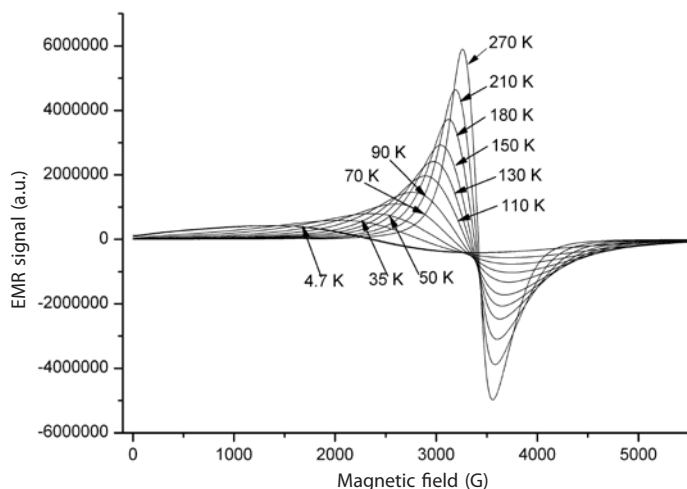


Fig. 1. EMR spectra of $\gamma\text{-Fe}_2\text{O}_3$ NPs in dendrimer recorded at X-band in perpendicular configuration at various temperatures ($\nu = 9.64$ GHz).

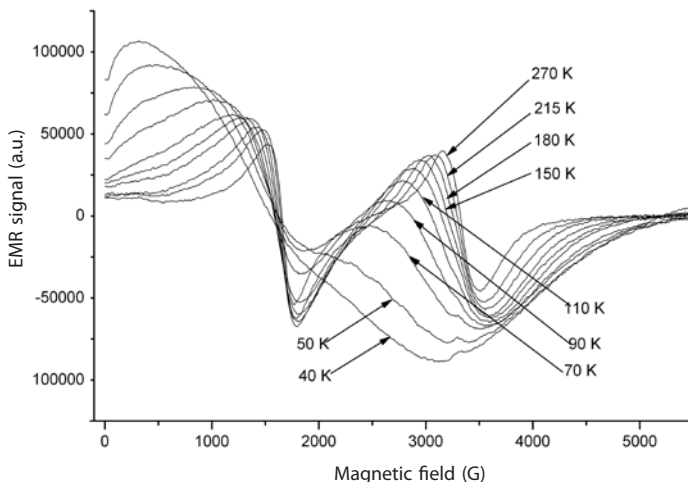


Fig. 2. EMR spectra of $\gamma\text{-Fe}_2\text{O}_3$ NPs in dendrimer recorded at X-band in parallel configuration at various temperatures. The microwave frequency was $\nu = 9.39$ GHz.

the allowed transitions between the total spin projections; therefore, this provides a means to perceive the quantum nature of the system.

EMR spectra of $\gamma\text{-Fe}_2\text{O}_3$ NPs in dendrimer were measured at the X-band both in perpendicular and parallel configurations at various temperatures (Fig. 1 and 2). As seen, the behavior of the EMR spectra recorded in the perpendicular configuration with cooling of the sample is typical for superparamagnetic materials [1, 2, 4], and it was described in detail in our previous work [1]. A small signal at $H_0/2$ (around 1500 G) is also observed, which is attributed to “forbidden” transitions between states with $\Delta M = \pm 2$, where M is the expectation value of and S the total spin of the MNP. If the model based on the giant spin is correct for the interpretation of the experimental results, then the intensity of the $H_0/2$ signal must increase when the EMR spectra is recorded in the parallel configuration. As seen from Fig. 2, the EMR experiments performed in this configuration confirm this prediction. An increase in the intensity of the transitions at half field is clearly observed. Thus, this experiment opens the possibility to analyze the properties of MNPs by using a simple model based on the giant spin, in which the spin is associated with the whole MNP and, consequently, the system must be treated as a quantum object. The best agreement between the experimental and theoretical spectra ($T = 180$ K) was obtained for the total spin $S = 30$ and zero-field splitting parameter $D = 40$ MHz.

1. Domracheva N.E., Pyataev A.V., Manapov R.A., Gruzdev M.S.: *ChemPhysChem* **12**, 3009 (2011)
2. Raikher Yu.L., Stepanov V.I.: *JMMM* **316**, 417 (2007)
3. Fittipaldi M., Gatteschi D. *et al.*: *Phys. Rev. B* **83**, 104409 (2011)
4. Noginova N., Weaver T., Atsarkin V.A. *et al.*: *Phys. Rev. B* **77**, 014403 (2008)

Action of Counterion on Spin-Crossover Behavior in Iron(III) Dendrimeric Complexes

**N. E. Domracheva¹, V. E. Vorobeva¹, V. I. Ovcharenko²,
A. S. Bogomyakov², E. M. Zueva³, M. S. Gruzdev⁴,
U. V. Chervonova⁴, and A. M. Kolker⁴**

¹ Zavoiisky Physical-Technical Institute, Russian Academy of Sciences, Kazan 420029, Russian Federation

² International Tomography Center, Novosibirsk 630090, Russian Federation

³ Kazan State Technological Institute, Kazan 420015, Russian Federation

⁴ G. A. Krestov Institute of Solution Chemistry, Ivanovo 153045, Russian Federation

The magnetic properties and the influence of counterions on the spin crossover properties of two novel Fe(III) dendrimeric complexes of the second generation, namely $[\text{Fe}(\text{L})_2]^+\text{X}^-$, where L = 3,5-di(3,4,5-tris(tetradecyloxy)benzoyloxy)benzoyl-4-oxy-salicylidene-N'-ethyl-N-ethylenediamine, X = Cl⁻ (**1**), ClO₄⁻ (**2**) have been studied for the first time by magnetic susceptibility and EPR in the wide (4.2–300 K) temperature range. EPR results showed that compound **1** contains about 94% of high-spin (HS, $S = 5/2$) and ~6% of low-spin (LS, $S = 1/2$) Fe(III) centers, and undergoes the antiferromagnetic ordering below 7 K, but the spin-crossover effect completely disappears in it. When the temperature is lowered from 300 to 30 K, the EPR integrated intensity of a broad line ($g \approx 2$), which corresponds to the HS iron(III) centers, passes through a broad maximum at $T_{\text{max}} \approx 100$ K, which indicates the formation of the short-range correlation effects. The anomalous broadening of this EPR line at low temperatures with the critical exponent $\beta = 1.5$ upon approaching the long-range ordering transition from above indicates the quasi-two-dimensional antiferromagnetic nature of magnetism in complex **1**. The obtained results and DFT calculations allow us to conclude that FeN₄O₂ octahedra in compound **1** are packed in the chains which form ionic bilayers. The compound **2** with ClO₄⁻ counterion demonstrates another magnetic behavior. EPR data show that compound **2** contains about 77% of LS and ~23% of HS Fe(III) centers. Complex **2** displays partial spin crossover ($S = 5/2 \leftrightarrow 1/2$) of ~23% of the Fe(III) molecules above 150 K and undergoes the antiferromagnetic ordering below 10.2 K. HS and LS iron(III) centers are linked together and form a dimeric structure. Thus, the replacing of a counterion dramatically alters the magnetic structure of the compound. The large ClO₄ anion leads to the formation of the dimer structure, while the small Cl anion promotes the formation of chain-like structures of Fe(III) centers in ionic bilayers.

EPR of Er³⁺ Ions in CsCaF₃ Single Crystals

M. L. Falin¹, V. A. Latypov¹, and S. L. Korableva²

¹ Zavoisky Physical-Technical Institute, Russian Academy of Sciences, Kazan 420029,
Russian Federation, vlad@kfti.knc.ru

² Kazan Federal University, Kazan 420008, Russian Federation

The Zeeman effect of a Γ_8 quartet state as the ground state is analyzed in the EPR spectrum of the Er³⁺ ion in the CsCaF₃ single crystal.

CsCaF₃ single crystals activated with Er³⁺ ions were grown by the Bridgman method in graphite crucibles in the argon atmosphere from the stoichiometric composition. The crystal growth rate was 2 mm/h. The erbium impurity was introduced in the form of ErF₃ in the amount of 0.1 at.%.

The parameters of the corresponding spin Hamiltonian were determined. The experimental results were analyzed in comparison with those for the same paramagnetic ion in other hosts [2–6].

This work was supported by the Grant of the Presidium of the Russian Academy of Sciences No. 5.

1. Bleaney B.: Proc. Phys. Soc. **73**, 937 (1959)
2. Abraham M.M., Finch C.B., Kolopus J.L., Lewis J.T.: Phys. Rev. B **3**, 2855 (1971)
3. Antipin A.A., Klimachev A.F., Korableva S.L., Livanova L.D., Fedii A.A.: Fiz. Tverd. Tela **17**, 1042 (1975)
4. Korableva S.L.: Fiz. Tverd. Tela **20**, 3701 (1978)
5. Falin M.L., Zaripov M.M., Leushin A.M., Ibragimov I.R.: Fiz. Tverd. Tela **29**, 2814 (1987)
6. Falin M.L., Eremin M.V., Zaripov M.M., Ibragimov I.R., Leushin A.M., Abdulsabirov R. Yu., Korableva S.L.: J. Phys.: Condens. Matter **1**, 2331 (1989)

Structural Models of the Yb³⁺ Ion in the Hexagonal Perovskite RbMgF₃ Single Crystal

M. L. Falin¹, V. A. Latypov¹, A. M. Leushin², and G. M. Safiullin¹

¹ Zavoisky Physical-Technical Institute of the RAS, Kazan 420029, Russian Federation
falin@kfti.knc.ru

² Kazan Federal University, Kazan 420008, Russian Federation

Fluorine perovskites RbMgF₃ activated with transition metal ions attract attention due to their application for optically stimulated luminescence and usage as radiation detectors [1]. Only crystals activated with iron group ions were studied by electron paramagnetic resonance (EPR) and to the best of our knowledge, the studies of rare-earth ions in this crystal are absent. RbMgF₃ has the hexagonal structure and the space group P63/*mmc* [2]. This report is concerned with the study of the impurity paramagnetic centers formed by Yb³⁺ ions in the RbMgF₃ single crystal.

EPR and optical spectroscopy of trigonal Yb³⁺ centers in RbMgF₃ are reported. The results of these experiments make it possible to conclude that Yb³⁺ ions replace two different host cation sites Mg²⁺ for three different types of paramagnetic centers. The Yb³⁺(I) center can be ascribed to the Yb³⁺ ion simply substituting at the Mg_I site without any charge compensators in its immediate neighborhood, while the Yb³⁺(II) center the compensation of the excess charge for the Mg_I site is implemented by the nearest Rb⁺ vacancy. The Yb³⁺(III) center is formed by the Yb³⁺ ion substituting at the other Mg²⁺ site in the Mg₂F₉ unit composed of two face-sharing fluorine octahedra (Mg_{II} site).

For the all three types of centers positions of lines in optical spectra were specified and schemes of energy levels were proposed. The values of *g*-factors of the ground Kramers doublets were determined from EPR spectra. The crystal field parameters of all centers were found from schemes of energy levels and *g*-factors of the ground Kramers doublets.

This work was supported by the Grant of the Presidium of the Russian Academy of Sciences No. 5. AML was funded by the subsidy allocated to the Kazan Federal University for the state assignment in the sphere of scientific activities (ND 02 VD 0211, Theme No. 021110102 “Budget 17-102”).

1. Dotzler C., Williams G.V.M., Rieser U., Robinson J.: Appl. Phys. **105**, 023107 (2009)
2. Dance J.M., Kerkouri N., Tressaud A.: Mat. Res. Bull., **14**, 869 (1979)

Spin States of [Fe(Salten)Cl] Complexes in Acetonitrile

**E. Frolova¹, T. Ivanova¹, O. Turanova¹, L. Mingalieva¹, E. Zueva^{2,3},
M. Petrova², and I. Ovchinnikov¹**

¹ Zavoisky Physical-Technical Institute, Russian Academy of Sciences, Kazan 420029,
Russian Federation, fro-e@yandex.ru

² Kazan National Investigation Technological University, Kazan 420015, Russian Federation

³ A. E. Arбузов Institute of Organic and Physical Chemistry, Kazan 420088,
Russian Federation

An iron(III) complex of pentadentate Schiff base [Fe(Salten)Cl] ($H_2\text{Salten} = 4\text{-azaheptamethylene-1,7-bis(salicylideneimine)}$) is a precursor of the [Fe(Salten) L]Y compounds in which spin crossover properties are quite sensitive to both nature of monodentate ligand L and outer-sphere anion Y [1]. Unfortunately, precursor properties were still not investigated. The aim of this paper is to find out structural features and spin properties of precursor in the phase of vitrified diluted solutions in polar solvent (acetonitrile). The relevance of these investigations is determined by the observation of unusual spin polarization of complexes under photo-irradiation processes [2].

EPR study of vitrified samples of acetonitrile solutions shows that [Fe(Salten) Cl] complexes demonstrates the coexistence of low-spin (LS, $S = 1/2$) and high-spin (HS, $S = 5/2$) fractions at $T = 5\text{--}200$ K. The EPR spectra components are broadened by dipole-dipole interactions between metal centers in the concentrations range 5–0.6 mmol/l, so one can conclude that precursor molecules intend to group in associates in the solutions.

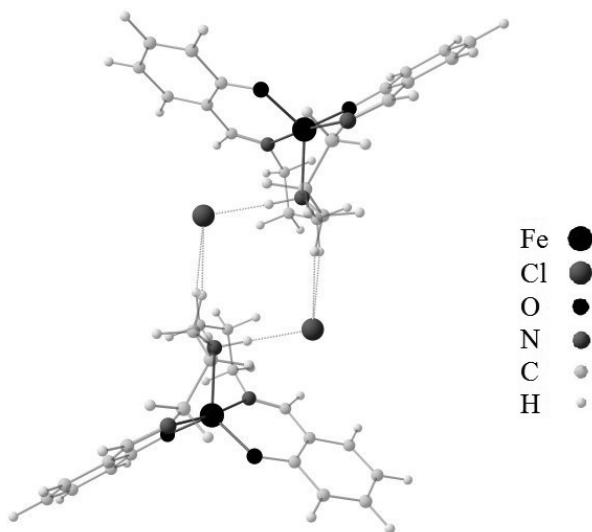


Fig. 1. Supramolecular dimer.

Spectra simulations (by computational package EasySpin) shows that HS fraction consists of six-coordinated Fe(III) centers with $D \gg h\nu$ and $E \sim 0.33D$ – about 2–7% and complexes which shows the EPR-line at $g_{\text{eff}} \approx 6$ – dominating amount. The line at $g_{\text{eff}} \approx 6$ corresponds to both six-coordinated Fe(III) complexes with $D \gg h\nu$ and $E \sim 0–0.09D$ and five-coordinated ones with square pyramid or trigonal bipyramid coordination polyhedron.

The EPR spectra of LS fraction consists of two types of subspectra of rhombic symmetry at least. Parameters and relative proportion of subspectra were estimated, the values of covalency parameters were calculated.

DFT screening of the structural forms of precursor molecules in solution in continual approximation shows that three conformers are energetically preferable (two six- and one five-coordinated) and of all of them have HS ground state. The most stable six-coordinated form (*a*) has the low symmetry of coordination polyhedron and can contribute to the EPR spectra lines with $D \gg h\nu$ and $E \sim 0.33D$. The (*b*) form characterized by higher energy of the ground state ($\Delta E_{\text{gs}} = 1.1$ kJ/mol) and demonstrate pseudo-octahedral symmetry. The five-coordinate form (*c*) has the highest energy of the ground state ($\Delta E_{\text{gs}} = 1.5$ kJ/mol) and the trigonal bipyramid configuration of the coordination unit: Cl^- decoordinates from central Fe-ion of (*a*) form and bounds with HN- (or H_2C -) groups of cation complex $[\text{Fe}(\text{Salten})]^+$ by specific interactions. Further, the energy gain of formation of outer-sphere coordinated complexes (*c*) compare of existence of two free ions in solution is equivalent to 21.1 (or 4.6) kJ/mol, respectively. DFT calculation shows that supramolecular dimers of two (*c*) complexes are formed profitably (Fig. 1), so Fe(III) complexes with five-coordinated trigonal bipyramid coordination are amassed in solution. Both types of complexes (*b*) and (*c*) can produce the EPR-line at $g_{\text{eff}} \approx 6$, but the last structure seems to be preferable in accordance with the fact that the intensity of the line arises significantly with the increase of the concentration of precursor in solutions.

The appearance of LS complexes in solutions we can explain with the help of supramolecular structures only.

Authors gratefully acknowledge the financial supports of the Grant of Pre-sidium of RAS-1.24II and the base part of the state assignment of the Ministry of Education and Science of the Russian Federation No. 4.5382.2017.

1. Ovchinnikov I., Ivanova T. *et al.*: Rus. Journ. Coord. Chem. **39**, no. 8, 598 (2013)
2. Ovchinnikov I., Ivanova T. *et al.*: Abstracts “MDMR 2015”, p. 125. Kazan, September 22–26, 2015.

EPR Spectroscopy of the Gd^{3+} Ions in the SrY_2O_4 Crystal

**B. F. Gabbasov, D. G. Zverev, S. I. Nikitin, I. F. Gilmutdinov,
R. G. Batulin, A. G. Kiiamov, and R. V. Yusupov**

Kazan Federal University, Kazan 420008, Russian Federation,
bulgabbasov@gmail.com

Compounds of a SrR_2O_4 family, where R is a rare-earth ion, due to the quasi-one-dimensional structure, geometric frustration and specific energy level patterns reveal various unusual magnetic states at the temperatures of ~ 1 K. Among the specific properties of these compounds, one can mention a coexistence of the long-range antiferromagnetic and short-range incommensurate magnetic order in $SrEr_2O_4$ and in $SrHo_2O_4$, noncollinear magnetic structure in $SrYb_2O_4$ and an absence of the long-range magnetic correlations in $SrDy_2O_4$ down to the lowest achievable temperatures.

Crystal structure of SrR_2O_4 (Fig. 1) contains the 1D-ladders with a triangular motif composed of R-ions at two crystallographically non-equivalent sites, R1 and R2. Macroscopic approaches like magnetization measurements, heat capacity or inelastic neutron scattering do not allow to separate the effects related to magnetic correlations in different sublattices. In this case, studies of the isostructural diamagnetic crystals doped with rare-earth ions at low concentration may provide a researcher with the information about the spectral and magnetic single-ion properties for two distinct sites.

Due to zero orbital angular momentum and purely spin nature of magnetism, Gd^{3+} ions (electronic configuration $4f^7$) are characterized by slow spin-lattice relaxation and therefore are the only trivalent rare-earth ions whose EPR spectra can be studied in a wide temperature range. Moreover, high spin value $S = 7/2$ allows to study the crystal field – spin-orbit effects which are responsible for the zero-field splitting pattern of the ground state.

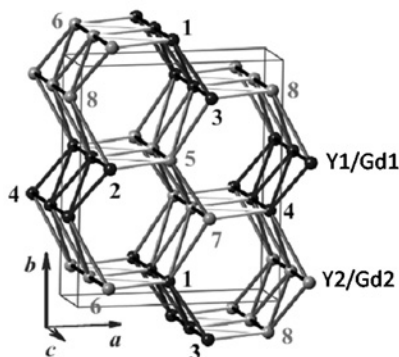


Fig. 1. Crystal structure of $SrY_2O_4 \cdot Gd^{3+}$.

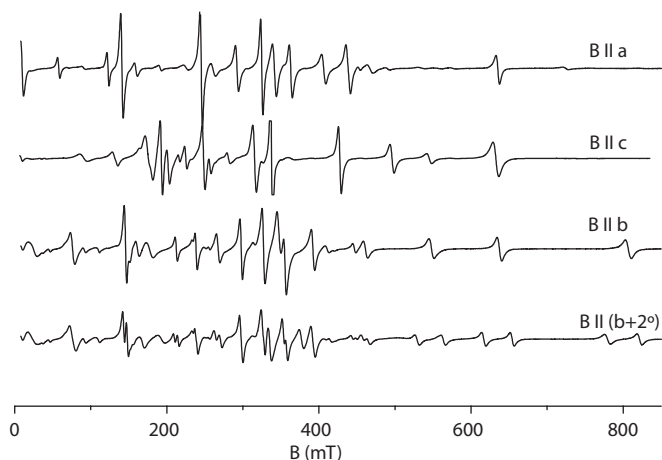


Fig. 2. Room temperature EPR spectra of the $\text{SrY}_2\text{O}_4:\text{Gd}^{3+}$ crystal for different sample orientations.

We report the results of the EPR study of a single crystal. The sample was grown by floating melted zone technique with optical heating. Concentration of Gd-ions was 0.5 at.%. Spectra and their angular dependencies were studied with the commercial X-band Bruker ESP300 EPR spectrometer at room temperature.

SrY_2O_4 crystal has an orthorhombic symmetry, space group Pnam (Fig. 1) [1]. Gd^{3+} ions substitute for the yttrium ions in Y1 and Y2 sites. Both Y1 and Y2 are found in the six-fold oxygen octahedral coordination. One of the sites is found in a weakly-distorted octahedron, another – in a strongly-distorted one. Substitution of Gd^{3+} ions for Y results in an occurrence of two magnetically-inequivalent centers for each of the Y1 and Y2 sites.

EPR spectra of $\text{SrY}_2\text{O}_4:\text{Gd}^{3+}$ crystal with the magnetic field applied along a , b and c crystallographic axes are presented in Fig. 2. Departure of the magnetic field from collinear to the b -axis direction reveals the presence of four magnetically-inequivalent centers via each line splitting (lowest spectrum in Fig. 2).

Orientation dependencies of the resonance fields have been analyzed using the spin-Hamiltonian

$$H = g\beta\bar{B} \cdot \hat{S} + \sum B_k^g \hat{O}_k^g.$$

Orientation dependencies have been nicely described within the model assuming the isotropic g -factor ($g = 1.990$) and a set of B_k^g parameters. It has been found that while the dependencies for the weakly-distorted site can be well described taking into account $B_k^g \hat{O}_k^g$ terms with $k \leq 4$, for the strongly-distorted site the terms with $k = 6$ are to be considered.

Studies of [Fe(Salten)L]BPh₄ Complexes Solutions in Acetonitrile

**L. Gafiyatullin¹, E. Frolova¹, E. Zueva², O. Turanova¹, E. Milordova¹,
and I. Ovchinnikov¹**

¹ Zavoiisky Physical-Technical Institute, Russian Academy of Sciences, Kazan 420029,
Russian Federation, lingafury@gmail.com

² Kazan National Research Technological University, Kazan 420015, Russian Federation

The [Fe(Salten)L]BPh₄ complexes (Salten – N,N'-bis(1-hydroxy-2-benzylidene)-1,7-diamino-4-azaheptane, L = Imidazole, Picoline) have been synthesized. Their composition and structure have been confirmed by elemental analysis, IR-, UV/Vis- spectroscopy and DFT calculations. Interest to this class of compounds is due to the fact that they are perspective for creating light sensitive switches for quantum computers.

The absorption bands in optical spectra of studied complexes at $\lambda \sim 250\text{--}400$ nm have been referred to ligands, and at $\lambda \sim 450\text{--}600$ nm to charge transfer (CT) state. Photoirradiation and heating leads to changes in absorption of CT band. It showed the existence of spin-crossover in studied compounds. Indeed both high-spin [HS] ($S = 5/2$, term 6A_1) and low-spin [LS] ($S = 1/2$, term 2T_2) Fe(III) ions signals have been registered in EPR spectra of frozen solutions of [Fe(Salten)L]BPh₄ complexes in CH₃CN. The temperature dependence of the integral intensity of HS and LS fractions in EPR spectra indicated the realization of an incomplete spin transition of Fe(III) in range 5–200 K.

DFT calculations (B3LYP/def2-TZVP) allowed to conclude that studied complexes exist in the form of [Fe(Salten)L]⁺ and BPh₄⁻ ions. In all cases, the LS state is the ground state. However, LS and HS states are energetically close to each other. It was shown that LMCT type transitions (CT from ligand to metal) have been observed in visible range only. The calculated wavelengths of absorption spectra are in good agreement with the experimental data in UV/Vis spectroscopy.

Dynamics of Nitric Oxide Production in Heart and Liver of Rats During Increasing 30-Days Restriction of Motor Activity and Subsequent Recovery

**Kh. L. Gainutdinov^{1,2}, V. V. Andrianov^{1,2}, V. S. Iyudin¹,
G. G. Yafarova^{1,2}, M. I. Sungatullina², I. I. Khabibrakhmanov²,
N. I. Ziatdinova², and T. L. Zefirov²**

¹ Zavoiisky Physical-Technical Institute, Russian Academy of Sciences, Kazan 420029, Russian Federation

² Kazan Federal University, Kazan 420008, Russian Federation, kh_gainutdinov@mail.ru

Nitric oxide (NO) is known to be a paramount signaling molecule modulating the physiological functions of the organism and the cell metabolism [1, 2]. Its role is documented for the central and autonomous nervous systems, for cardiovascular function and blood supply to the brain and the heart, where deviations in NO level may incur risks of stroke and infarction [3, 4]. The NO system is also essential in adaptation to environmental changes and external conditions such as physical load [5]. It has been found that NO impairs the progress of myocardial infarction, and this impairment lies in the reduced heart rate, reduced blood pressure, stroke volume and cardiac output [6]. There is also an opposite point of view, according to which an excess of NO is a compensatory factor that helps to maintain tissue perfusion and provides antiarrhythmic effect during reperfusion [7]. The described literature data indicate two opposite effects of NO: a stimulating, positive, as well as toxic, and damaging effect that can lead to cell death. There are clear contradictions in the assessment of the effects of the NO donors and the NOS blockers, when it is considered that these impacts or stimuli provide unambiguous effect, although the exact quantification of NO in the tissues has not been conducted under these conditions.

The restriction of motor activity (MA) is one of the most important medical and social problems caused by lifestyle, professional activity, prolonged bed rest, etc [2]. The destructive effect it has on virtually all organs and systems of the body is evidenced by extensive convincing experimental and clinical material. Reducing the load on the muscular apparatus leads to changes in functional and morphological properties of tissues down to pathological conditions, oxygen consumption by tissues and activity of oxidative processes are significantly reduced. Problems associated with the restriction of MA, in modern society are increasing, and this is due to lifestyle changes, with an increase in the number of patients who require bed rest. Molecular processes, which underlie the changes in physiological functions: the parameters of cellular respiration, skeletal muscle proteins and the system of NO, have attracted increasing attention lately. Therefore, the objective of the study was to investigate the role of NO in the consequences resulting from the recovery after restriction of MA by analyzing the NO-containing paramagnetic complexes in various tissues of rats growing under restricted physical activity.

Our team has studied the content of NO in tissues of rats by EPR spectroscopy using the method of spin traps. As spin trap were applied the complex of Fe^{2+} with diethyldithiocarbamate $\text{DETC})_2\text{-Fe}^{2+}\text{-NO}$. The records were carried out on EPR spectrometer X-band firm “Bruker” EMX/plus and ER 200E SRC. We have found that the amount of NO produced in the tissues of the ventricles and atria of the heart increases after 30-day restriction of MA in 2–3 times. It was found that after 2 weeks of recovery of MA the level of NO production in the tissues of the heart is reduced even more. Thus, the obtained results allow to conclude about the presence of close relations between the level of NO in the body with a regime of physical activity. Because the review of literature data shows that the restriction of MA causes significant changes in the cardiovascular system, blood flow and supply of oxygen to the body, it can be assumed that some of these changes caused a fixed increase of NO production in the key activities of the body tissues.

1. Terpolilli N.A., Moskowitz M.A., Plesnila N.: *J. Cereb. Blood Flow Metab.* **32**, no. 7, 1332–1346 (2012)
2. Gainutdinov Kh.L., Andrianov V.V., Iyudin V.S. *et al.*: *Biophysics* **58**, no. 2, 203–205 (2013)
3. Mikoyan V.D., Kubrina L.N., Serezhenkov V.A. *et al.*: *Biochim. Biophys. Acta* **1336**, no. 2, 225–234 (1997)
4. Gainutdinov Kh.L., Gavrilova S.A., Iyudin V.S. *et al.*: *Appl. Magn. Reson.* **40**, no. 3, 267–278 (2011)
5. Malyshev I.Yu., Manukhina E.B.: *Biokhimiya* **63**, no. 992 (1998)
6. Reutov V.P., Okhotin V.E., Shuklin A.V. *et al.*: *Uspekhi Physiol. Nauk* **38**, no. 4, 39–58 (2011)
7. Malyshev I.Yu., Zenina T.A., Golubeva L.Y.: *Nitric Oxide* **3**, no. 2 (1999)

EPR Investigation of the Conformation of the Irradiated Calcium Gluconate

**I. A. Goenko¹, G. G. Gumarov¹, M. M. Bakirov¹, R. B. Zaripov¹,
V. Yu. Petukhov¹, D. S. Rybin², and G. N. Konygin²**

¹ Zavoijsky Physical-Technical Institute, Russian Academy of Sciences, Kazan 420029, Russian Federation

² Physical-Technical Institute of the Ural Branch of the RAS, Izhevsk 426000, Russian Federation, ilya.goenko@mail.ru

The chemical and biological properties of substances strongly depend on their spatial structure, in particular on conformational isomerism and internal rotation of molecules. Previously, it was reported on conformations of calcium gluconate in aqueous solution, a widely known drug used in medicine for hypocalcemia [1]. In this work, conformation is studied in the crystalline state of calcium gluconate subjected to irradiation with Co^{60} gamma rays at a dose of 600 Gy, using the EPR method.

Irradiation of calcium gluconate leads to the formation of paramagnetic centers that are stable at room temperature. EPR spectra of irradiated calcium gluconate are multicomponent, with a pronounced hyperfine structure (Fig. 1). The overall width of the spectra measured in the X and Q ranges is approximately the same, indicating that there is no anisotropy of the g -factors for the components making up the spectra. The results of measurements at different microwave power levels indicate a multicomponent character of the spectrum.

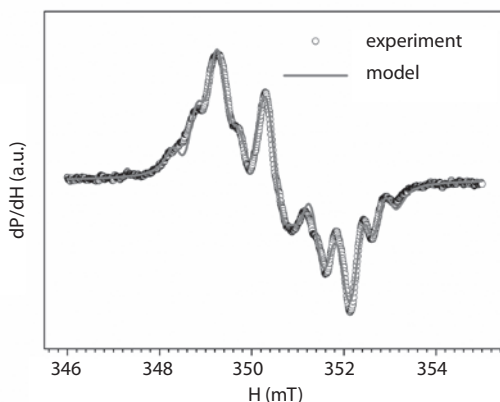


Fig. 1. EPR spectra of irradiated calcium gluconate.

The obtained spectra were decomposed into four components with $g \sim 2.0035$ and different values of the hyperfine interaction constants. Assuming that the paramagnetic centers obtained are π -radicals, the torsion angles for the C-C bonds were determined using the McConnell relation. A comparison of the obtained torsion angles with the structural formula of calcium gluconate made it possible to identify the positions of the radicals, and also to suggest the presence of two conformations of calcium gluconate in the solid state.

1. Akhmetov M.M. *et al.*: Abstracts "MDMR 2016", p. 114. Kazan, October 31–November 4, 2016.

Multiple Spin Echoes from ^{57}Fe Nuclei in Ferrimagnetic Yttrium Iron Garnet Films

**A. I. Gorbovanov¹, S. N. Polulyakh¹, V. N. Berzhansky¹,
and A. A. Gippius²**

¹ Physical-Technical Institute of CFU, Simferopol 295007, Russian Federation,
a.i.gorbovanov@cfuv.ru

² Faculty of Physics, Lomonosov Moscow State University, Moscow 119991, Russian Federation

The enrichment of ferromagnetic yttrium-iron garnet (YIG) with ^{57}Fe magnetic nuclei provides a possibility to observe spin echo at room and lower temperatures in thin-film samples. At $T = 77$ K the enhancement of nuclear interactions due to hyperfine interactions (HFI) results in the increase of spin echo decay with magnetic nuclei enrichment in ferromagnetic YIG films. The electron-nuclear interactions also yield anisotropy of transverse relation rate for nuclei that belong to iron ions in the octahedral lattice positions [1]. Here we are reporting about experimental study of spin echo signals from ^{57}Fe (spin $I = 1/2$) in YIG films at liquid helium temperature.

The sample is the YIG film on gadolinium-gallium garnet substrate in (111) plane. The enrichment with magnetic isotope ^{57}Fe is about 98%. Two-pulse Hahn spin echo has been registered with coherent technique (Fig. 1). Data in Fig. 1 correspond to ^{57}Fe nuclei of iron ions in tetrahedral lattice positions.

Along with the Hahn echo appeared at the time τ after second pulse (τ is a delay between pulses), additional spin echo at the time 2τ has been observed experimentally (Fig. 1). We have noticed that the registration of additional two-

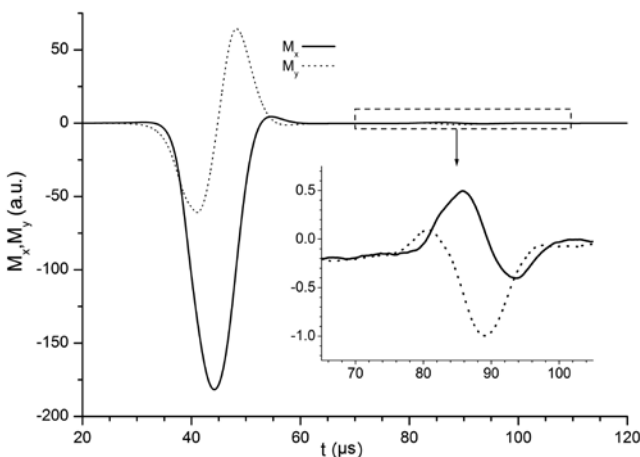


Fig. 1. Two-pulse spin echoes from ^{57}Fe nuclei ($\nu = 65$ MHz, $T = 4.2$ K). First pulse duration $t_1 = 2$ μs , second pulse duration $t_2 = 4$ μs . Delay between pulses $\tau = 40$ μs . Registration time starts after second pulse.

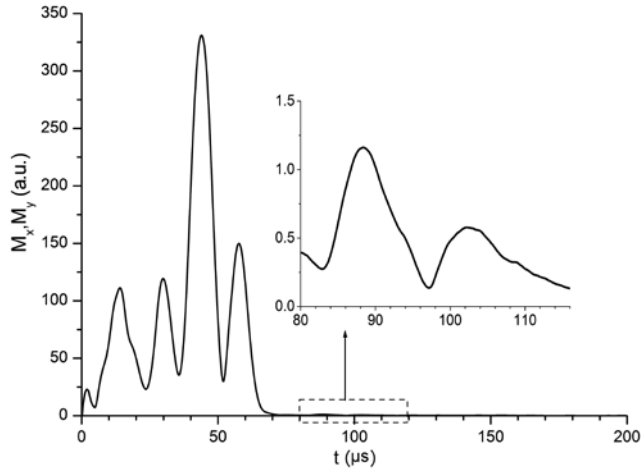


Fig. 2. Three-pulse nuclear echoes from ^{57}Fe nuclei ($\nu = 65$ MHz, $T = 4.2$ K). Pulses duration: $t_1 = 3$ μs , $t_2 = 2$ μs , $t_3 = 4$ μs . Delay between pulses: $\tau_{12} = 20$ μs , $\tau_{23} = 40$ μs . Registration time starts after third pulse.

pulse echo at $T = 77$ K has been not successful. We assume that the additional echo is caused by a phenomenon known as dynamical frequency shift in magnetic materials [2]. Nuclear magnetization during first echo induces ac magnetization due to the magnetic HFI. Induced electron magnetization produces additional ac magnetic fields at nuclei so that the first echo can be considered as an effective pulse which provides the formation of additional nuclear echo.

We also observed three-pulse nuclear echoes from non-quadrupole ^{57}Fe nuclei of iron ions in tetrahedral lattice positions of YIG (Fig. 2). In general, four echo signals at the times $t = \tau_{12}$, τ_{23} , $(\tau_{12} + \tau_{23})$ and $(\pm\tau_{12} \mp \tau_{23})$ are possible to be observed in the inhomogeneously broadened spin system. Here time t starts after third pulse, τ_{12} and τ_{23} give the delay between pulses. Besides the known echo signals we have experimentally found additional echo at the time $t \approx (\tau_{23} + \tau_{12})$. As a common idea, the discovered additional echo can be considered as an echo in four-pulse sequence where three-pulse echo acts as effective fourth pulse due magnetic HFI. Other possible reasons for additional three-pulse echoes are discussed.

1. Abelyashev G., Berzhansky V., Polulyakh S., Sergeev N.: JMMM **147**, 305 (1995)
2. De Gennes P.G. *et al.*: Phys. Rev. **129**, 1105 (1963)

Topological Interactions of Magnetic Impurities in Topological Semimetal: ESR Data

Yu. V. Goryunov¹ and A. N. Nateprov²

¹ Zavoisky Physical-Technical Institute, Russian Academy of Sciences, Kazan 420029, Russian Federation, goryunov@kfti.knc.ru

² Institute of Applied Physics of the ASM, Kishenu 2028, Moldova

Until recently, full picture of interactions in condensed matter was reduced to several types of interactions, based on the Coulomb interaction, modified by the prohibitions imposed by the laws of quantum statistics and, in particular, related to the existence of spin from the interacting particles. These are an ordinary Coulomb interaction, a direct exchange interaction, an isotropic indirect exchange interactions (such as the RKKY interaction and the Kramers-Anderson super-exchange), an anisotropic exchange interactions, symmetric and antisymmetric (the Dzyaloshinsky-Moriya interaction). The class of indirect exchange interactions implies the existence of an agent through which this interaction is provided. In general case, each of the interacting objects affects the agent through which the interaction is provided, and thus the object distinguishes the disturbed or unperturbed state of the agent. In the above examples, these perturbations are changes in the charge or spin density of the electrons in the medium. In the case of topological materials, just as the appearance of a property

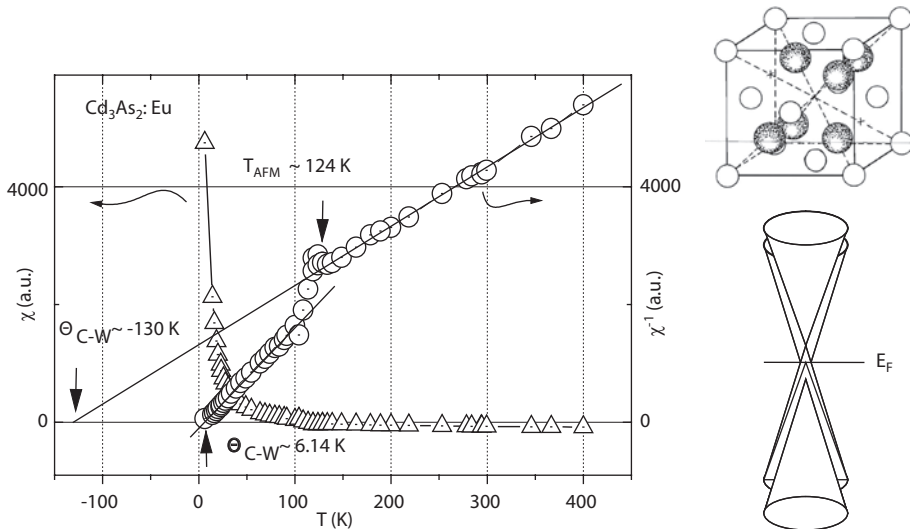


Fig. 1. The temperature dependence of a magnetic susceptibility χ of α - Cd_3As_2 doped by europium. At the high temperatures, the diamagnetic contribution of the matrix prevails. Right upper insert is main fragment of the α - Cd_3As_2 crystal cell. Right down insert is schema of the splitting of twice degenerated Dirac node on two Weyl nodes.

such as spin has indicated the necessity of using Bose or Fermi statistics, the appearance of such an attribute as chirality means that it is necessary to take into account the perturbations of substance symmetry, which introduce by the interacting objects. Specifically in our work, such objects are magnetic impurities of an Eu^{2+} ions in the 3D topological semimetal $\alpha\text{-Cd}_3\text{As}_2$, a 3D analog of graphene. The conduction band and the valence band of the $\alpha\text{-Cd}_3\text{As}_2$ have linear a dispersion law and touch each other in the 3D Brillouin zone in Dirac nodes. In the presence of time reversibility and inversion symmetry, the Dirac nodes are twice degenerate. The break of any symmetry leads to the splitting of the Dirac node into two Weyl nodes, separated either by the energy interval (see the right down insert in Fig. 1) or separated in momentum space. Thus, the presence of a magnetic field or magnetic impurities in the Dirac semimetal (DSM) transforms it into a Weyl semimetal (WSM) and leads to a number of unusual phenomena. Data on the magnetic susceptibility (see Fig. 1) and ESR showed the presence of an Eu^{2+} ions additional phase magnetized oppositely to the external field and ordered at $T_{\text{AFM}} \sim 124$ K. Measurements of the ESR allow us to conclude that this phase (g -factor near 4.4) consists of Eu^{2+} ions located in interstices positions – tetrahedral vacancies in fluorite type cell (see right upper insert in Fig. 1). Whereas the main phase ($g \sim 2.2$) consists of the Eu^{2+} ions in the positions substituting of the Cd^{2+} ions. These positions differ in the degree of chemical compression of the Eu^{2+} ions. Taking in attention, in normal cases $g \sim 2.0$, the ESR data show anomalous large values of the g -factor of the Eu^{2+} ions, which in its turn indicates very large values of the g -factor of the conduction electrons ($g \sim 16\text{--}18$). Analysis of the role of the RKKY interaction [1, 2] in this situation leads to the conclusion that the RKKY interaction in the classical view can not lead to change of a sign of interaction selectively in dependence on position types in the crystal lattice. Consequently, we are dealing with a new type of indirect interaction [3], whose agents are the local symmetry breakings of the crystal by magnetic ions. This interaction leads to the splitting of twice degenerate Dirac nodes on two Weyl nodes with different energies, on an analogical with splitting of electronic states with different spin directions.

1. Sun J.-H., Xu D.-H., Zhang F.-C., Zhou Y.: Phys. Rev. B **92**, 195124 (2015)
2. Chang H.-R., Zhou J. *et al.*: Phys. Rev. B **92**, 241103(R) (2015)
3. Kurdgelaidze D.: GESJ: Physics **2**(8), 10 (2012)

Temperature Dependence of Magnetic Anisotropy in Iron Silicide Films Ion-Synthesized in External Magnetic Field

**G. G. Gumarov¹, O. N. Lis², A. V. Alekseev¹, M. M. Bakirov¹,
and V. Yu. Petukhov^{1,2}**

¹ Zavoiisky Physical-Technical Institute, Russian Academy of Sciences, Kazan 420029,
Russian Federation

² Kazan Federal University, Kazan 420008, Russian Federation,
ifoggg@gmail.com

The induced magnetic anisotropy in thin ferromagnetic films is of great importance for most applications, including spin electronics. There is also a method for creating uniaxial anisotropy in a magnetic film by ion implantation in an external magnetic field [1]. To clarify the mechanism of the appearance of anisotropy in the implantation process, in the present study, the temperature dependence of the uniaxial anisotropy constant was studied by the ferromagnetic resonance (FMR) method.

For magnetically soft materials to determine the anisotropy constants, it is sufficient to measure the resonance values of the magnetic field strength in the directions of the easy magnetization axis and the axis of difficult magnetization. Approximation of the experimental dependence the anisotropy constant on temperature by a function of the form $y = ax^n$ yields the value $n = -0.94$, which is quite close to the inversely proportional temperature dependence assumed by the Neel-Taniguchi model [2]. Within the framework of this model, the uniaxial anisotropy constant also depends on the energy of the dipole-dipole interaction of neighboring atoms. This energy, calculated according to the formula describing the temperature dependence, was $0.96 \cdot 10^{-23}$ J. A direct estimate of this energy for a pair of iron atoms with magnetic moments of $2.2 \mu_B$ and a lattice constant in the Fe_3Si phase give a close value of $\sim 0.89 \cdot 10^{-23}$ J, that are a good agreement with the Néel-Taniguchi model.

The work is partially supported by the Fundamental Research Program of ONIT RAS “Element base of microelectronics, nanoelectronics and quantum computers, materials for micro- and nanoelectronics, microsystem technology”.

1. Alekseev A.V. *et al.*: Journal of Surface Investigation: X-Ray, Synchrotron and Neutron Techniques **10**, no. 3, 608–611 (2016)
2. Chikazumi S.: Physics of Ferromagnetism, 682 p. Oxford: Oxford University Press 1997.

The Possibilities of EPR for the Connective Tissue Dysplasia Diagnosis

**M. I. Ibragimova¹, D. K. Khaibullina², A. I. Chushnikov¹, I. V. Yatsyk¹,
V. Yu. Petukhov¹, and R. G. Esin²**

¹ Zavoiisky Physical-Technical Institute, Russian Academy of Sciences, Kazan 420029,
Russian Federation, ibragimova@kfti.knc.ru

² Kazan State Medical Academy, Kazan 420029, Russian Federation, dina.khaibullina@mail.ru

Connective tissue dysplasia is a multi-organ and multi-system pathology with progressive clinical course. The prevalence of this pathology in the population according to various authors varies from 26 to 80%. Despite the considerable progress of clinical medicine in the diagnosis and treatment of this disease, its pathogenesis is still not fully installed. According to modern concepts the trace elements play an important role in the development and implementation of clinical manifestations of connective tissue dysplasia. In particular, the special role is given to magnesium ions. This fact comes from a physiological point of view that the main part of Mg^{2+} is concentrated in bone, tooth enamel and in tissues with high metabolic activity (brain, heart *et al.*). At the same time, there are no practically any data on the impact of other trace elements to the pathogenesis of connective tissue dysplasia inside the human organism.

At present work X-band EPR study of blood serum samples collected from patients with back pain related to connective tissue dysplasia ($n = 17$) and controls (volunteers of adult outpatient department, $n = 3$) was carried out in the temperature range 5–80 K using the spectrometer “Bruker EMX-300”. EPR spectra gives the possibility for obtaining the quantitative information about such ions as Cu^{2+} in ceruloplasmin (Cp) and Fe^{3+} in transferrin.

In all patients EPR serum blood spectra the high level of Cu^{2+} -Cp was revealed. It must be emphasize that all patient's blood parameters such as the rate of blood sedimentation, C-reactive protein, rheumatoid factor (all of them are the characteristics of inflammatory process in the body) were in the normal range. At the same time, it is now established that the concentration of Cp in the serum increased in acute and chronic inflammatory processes. The increased level of the Cp indicates tissue damage and infections as well.

It should also be noted that in some cases were registered the changes in Cu^{2+} -Cp shape line. For such patients the changes in the ligand field of Cu^{2+} ions in Cp were correlated with biochemical parameters as elevated levels of the type I collagen (b-cross-laps) in the serum and secretions of deoxyypyridinoline in urine.

We think that in the pathogenesis of connective tissue dysplasia, the role of copper is underestimated. The data obtained will certainly be of interest and require further research.

Downhole Laboratory for Reservoir Fluid Real-Time Extended NMR, Optical and Dielectric Spectroscopy Analysis and Sampling

**A. Imaev¹, A. Sayakhov¹, S. Gorshenin¹, M. Gorshenin¹, A. Sadikov¹,
A. Bragin¹, V. Murzakaev¹, L. Gilyazov², A. Golubev², D. Zverev²,
I. Mumdzhi², S. Nikitin², D. Ivanov², D. Melnikova², A. Ivanov²,
O. Gnezdilov², R. Archipov², A. Aleksandrov², V. Skirda²,
Ya. Fattakhov³, V. Shagalov³, A. Fakhrutdinov³, D. Konovalov³,
R. Khabipov³, and A. Anikin³**

¹ TNG Group Ltd, Bugul'ma 423236, Russian Federation, vmurzakaev@rambler.ru

² Kazan Federal University, Kazan 420008, Russian Federation, kasanvs@mail.ru

³ Zavoisky Physical-Technical Institute, Russian Academy of Sciences, Kazan 420029, Russian Federation, fattakhov@kfti.knc.ru

Well logging techniques in most deposits give whole information necessary for well production. Nevertheless, in some complicated cases more precise formation evaluation is required to enhance reservoir productivity. To achieve this goal were developed downhole tools – so called formation testers [1]. They could provide real-time pressure and permeability measurements and obtain reservoir fluids samples. However, in most applications purity and quality of the samples is controlled only by optical spectroscopy.

TNG Group in cooperation with Kazan Federal University and Zavoisky Physical Technical Institute is developing downhole laboratory for reservoir fluid real-time extended NMR, optical and dielectric spectroscopy analysis and sampling. The main idea is to extend measurement complex with such informative techniques as nuclear magnetic resonance (NMR) and dielectric spectroscopy. These methods together with optical spectroscopy could provide more complete fluid characterization directly in the well and improve purity and quality of the fluid samples. Tool being developed consists of modular reservoir probe (MRP) and three measurement units – optical unit, NMR unit and dielectric unit.

The MRP provides a possibility of fast, precise and multiple real-time measurements of reservoir pressure and is used for multifold representative sampling of deep fluid exemplars from several stratums in order to control fluid composition along the well. The MRP includes the following blocks: storage chambers, hydraulic packers, metering detectors, temperature and pressure detectors, resistivity meter, detector of natural radioactivity, block of pumps.

The optical unit is intended for measuring partial chemical composition of a fluid and assessing the amount of a free gas in it. Therefore, the block consists of two main parts: a) optical spectrometer and b) gas detector. The optical spectrometer consists of the optical cell and the system of lightening and light detection. It provides the concentration of CO₂, H₂O, C₁H₄, C₂H₆-C₅H₁₂, C₆H₁₄. The design of gas detector is based on dependence the intensity of reflected

light on polarization and refractive index. This detector is used for qualitative measuring the presence of a free gas inside a fluid.

The dielectric unit is intended for to determine dielectric permeability and resistivity of the formation fluid. The measurements are provided in a wide frequency range from 1 MHz to 50 MHz. The method is based on varying of the capacitance of cylinder capacitor with lumped parameters in presence of fluids with different dielectric constant.

The NMR unit implements all methods, widely used in NMR-logging, including 2D T_1 - T_2 and D_s - T_2 distribution, which enables an ability to correspond data with NMR log. Along with this, it could provide data, which is unavailable for NMR logging tools, for example, information of solid component of the fluid due to implementation of solid-echo technique, and much wider range of diffusion coefficient spectrum, due to implementation of pulsed field gradient (PFG) technique. Measurements are carried out in a compact Halbach cylinder magnet with 12 MHz resonance frequency at ^1H nuclei.

Each unit has an independent power supply and control, and could provide: a) measurement; b) processing; c) transferring data to the memory block and to the surface interface. Therefore one could include/exclude any unit of the tool assembly, depending on the task. Tool was designed to operate at temperatures up to 85 °C and pressure up to 600 bar.

1. MDT Modular Formation Dynamics Tester // www.slb.com URL: http://www.slb.com/services/characterization/reservoir/wireline/modular_formation_dynamics_tester.aspx (дата обращения: 01.07.2017)

Magnetic Interactions in the Chain Structure [Fe(salen)(2-Me-Him)]_n

**T. Ivanova¹, I. Gilmutdinov², O. Turanova¹, L. Mingalieva¹,
and I. Ovchinnikov¹**

¹ Zavoiisky Physical-Technical Institute, Russian Academy of Sciences, Kazan 420029,
Russian Federation, alex@kfti.knc.ru

² Kazan Federal University, Kazan 420008, Russian Federation

Interest in the study of Fe(III) coordination compounds containing the tetradentate ligand salen is due on the one hand, to the possibility of obtaining spin-variable compounds, on the other hand, to their ability to form linear and zigzag chains. The cooperative interactions of Fe(III) ions in such structures are largely responsible for their specific physical and biological properties. Compounds [Fe(salen)(HL)]_n, where the bridged ligands HL are heterocyclic ligands based on N-donors, were synthesized in [1]. The formation of one-dimensional chains in these compounds was confirmed by X-ray diffraction analysis. The dependence of the magnetic properties of (salen)-containing chains on the type of the bridged ligand was discovered.

The purpose of our work was to study the magnetic properties (salen)-containing chains by using the substituents in the bridge ligand HL. The new compound [Fe(salen)(2-Me-Him)]_n was synthesized by the method analogous to

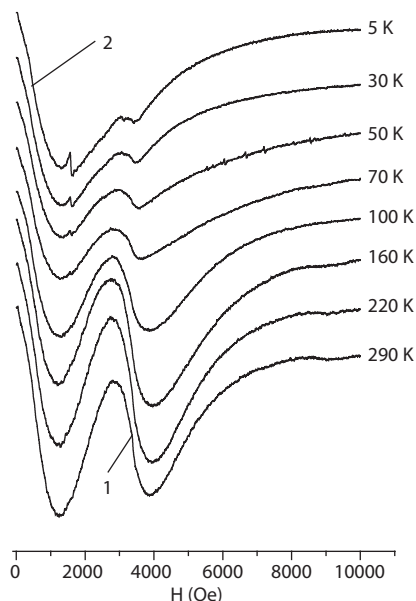


Fig. 1. MR spectra [Fe(salen)(2-Me-Him)]_n.

that described in [1] and was investigated by the methods of MR spectroscopy and magnetic susceptibility in the temperature range 5–300 K.

The MR spectra are a complex line, which can be represented as the sum of two overlapping spectra **1** and **2** (Fig. 1). Spectrum **1** has the standard form of the first derivative with effective parameters $g_{\text{eff}} \approx 2.0$, $\Delta H_{\text{eff}} \approx 1100$ Oe and the temperature dependence of the integrated intensity with a wide maximum at a temperature of ~ 100 K. It is interpreted as an exchange line from the Fe(III) centers, antiferromagnetically linked in a chains. Spectrum **2** is characterized by a nonzero absorption value in a zero magnetic field, negative sign of the detected signal over the entire range of the magnetic field (up to 10000 Oe) with a minimum at ~ 1400 Oe. It can be represented as an absorption line in the form of the first derivative, shifted toward weak fields by an amount of the order of 2–3 thousand Oe with respect to signal **1** due to the internal magnetic field produced by the ferromagnetic exchange interactions between the chains. This interpretation is confirmed by measurements of the spectrum in the Q-band and the absence of signal **2** in the spectrum of the frozen solution of the complexes in chloroform. The most probable reason of the occurrence of an internal magnetic field are the hydrogen C-H... π bonds between the methyl group of the bridging ligand and the π -system of the benzene ring of the complex of the neighboring chain.

In measurements of the field dependence of the magnetization, a hysteresis of the magnetic properties was detected. In the temperature range 30–300 K, the hysteresis loop is observed together with the general increase in magnetization with increasing magnetic field. Its parameters are practically independent of temperature. This indicates the presence of regions with weak ferromagnetic correlations. As the temperature is lowered, the residual magnetization and the coercive force of the hysteresis loop increase sharply and reach at 5 K ~ 0.0023 emu and ~ 540 Oe, respectively. This is connected, probably with the appearance at a low temperature of an additional ferromagnetic magnetization. The ferromagnetic magnetization at low temperatures also manifests itself in the difference in the temperature dependence of the static magnetization $M_{\text{dc}}(T)$ observed in the sample when it is cooled in a magnetic field of 1000 Oe (FC) and in a zero magnetic field (ZFC). Taking into account the tendency of such structures to form zigzag chains, the dependence of $M_{\text{dc}}(T)$ on the magnetic pre-history of the sample can be explained by the occurrence of ferromagnetic magnetization due to the Dzyaloshinsky-Moriya interaction, which is characteristic for antiferromagnets with a canted spin structure [2]. At the same time, experiments on the measurement of dynamic magnetization have shown that the maximum of the dependence of $M_{\text{ac}}(T)$ shifts toward higher temperatures with increasing frequency, which is usually associated with the transition to the spin-glass state [3]. Probably, the random distribution of fragments of canted antiferromagnetic chains (oligomers) in the bulk of the sample promotes the realization of the spin glass state.

The work was supported by the Grant of Presidium of RAS-1.26II.

1. Herchel R., Sindelar Z., Travnicek Z., Zboril R., Vanco J.: Dalton Trans. 9870 (2009)
2. Manna K., Sarkar R., Fuchs S. *et al.*: Phys. Rev. B **94**, 144437 (2016)
3. Petrakovskii G.A., Aleksandrov K.S., Bezmaternikh L.N., Aplestin S.S.: Phys. Rev. B **63**, 184425 (2001)

^1H NMR Detection of Olive Oil

**G. S. Kupriyanova^{1,2}, G. V. Mozzhukhin¹, A. Maraşlı¹,
and B. Z. Rameev^{1,3}**

¹ Gebze Technical University, Gebze/Kocaeli 41400, Turkey, mgeorge@yandex.ru

² Baltic Federal University by Immanuel Kant, Kaliningrad 236041, Russian Federation

³ Zavoisky Physical-Technical Institute, Russian Academy of Sciences, Kazan 420029, Russian Federation

The study of natural compounds, as well as food products made from these compounds, is a complex and important task. One of the most interesting objects of research are olives and olive oil, to the quality of which high demands are made in accordance with the standard developed in the countries of the European Union (European Commission Regulation No 432/2012 of 16 May 2012). ^1H NMR spectroscopy is a powerful method for rapid quantification of fatty acids in olive as well as minor components without the need for any sample treatment. ^1H NMR methods have been used to characterize and classify olive oils according to the variety [1] and geographical origin of olives [2, 3]. In recent years, NMR relaxation methods have been intensively developing, using fast Laplace transform algorithms that make it possible to extract data on the relaxation times T_1 , T_2 and T_1 - T_2 , T_2 - T_2 correlations. The main goal of this paper is to propose the fast method based on NMR relaxometry to identify olive oils.

This paper presents the results of ^1H NMR spectroscopy and NMR relaxometry studies of several varieties of oils: bone, flaxseed, canola, sunflower and various branches of olive oils (Komili Riviera and Sızma, Tariş Sızma and a commercial Greek extra-virgin). Besides the mixtures of sunflower and olive oils in various proportions have been studied. NMR spectra of Turkish oils were registered by 400 MHz Varian NMR spectrometer. NMR relaxation measurements have been carried out with Magritek Kea-2 NMR console (1–100 MHz) equipped by home-made permanent magnetic system with 34 mm air gap, magnetic field of 0.374 T (the proton frequency of 15.9 MHz) and closed-circle magnet temperature stabilization system. Although seven different basic measurement macros have been tested the most informative results have been obtained with CPMG (Carr-Purcell-Meiboom-Gill) and T_1 -IR-Echo (T_1 -Inversion Recovery-Echo) measurements. The comparison of the experimental data for various oils have been done using both bi-exponential and inverse Laplace transform fits.

Analysis of the ^1H NMR spectra at 400 MHz of the samples studied showed that it is possible to identify areas of non-overlapping signals that are specific for each sample. For example, NMR peaks of triglyceryl protons at 4.048, 4.062 and 0.529 ppm were only observed for extra-virgin olive oil, but these peaks are absent for bone and flaxseed oil.

The TD NMR relaxation measurements have shown that different types of oils have different T_1 and T_2 relaxation times and specific relaxation map (Fig. 1). The correlation dependence between the relaxation times T_2 of the sunflower-olive oil mixture as a function of the olive oil concentration has been found.

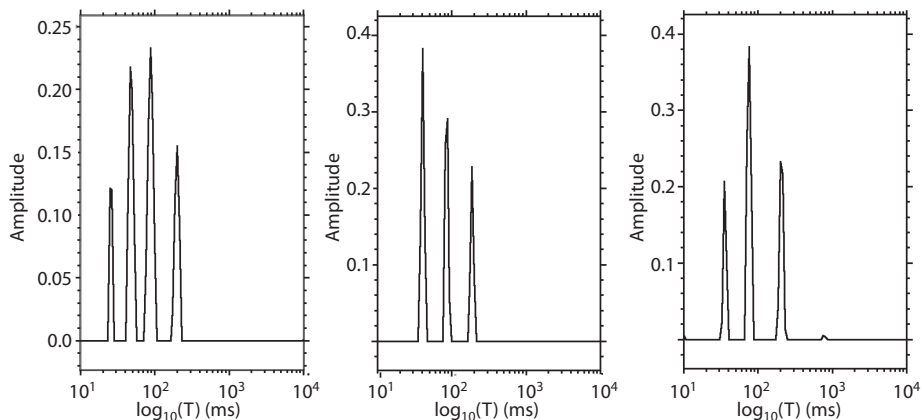


Fig. 1. Relaxation spectra after inverse Laplace transform of **a** Komili Sızma olive oil, **b** Tariş Sızma olive and **c** 20% Tariş olive oil and 80% Yüdümlü sunflower oil.

Thus, it is shown that in addition to high-resolution NMR spectroscopy the TD NMR technique is also useful method of identification or quantification of olive oils and the presence of impurities of oils of other origin.

The work was supported by NATO Science for Peace and Security Programme (NATO SPS project No. 985005 [G5005]), TUBITAK grant under the Programme 2221 for Visiting Scientist (G. S. Kupriyanova), and East Marmara Development Agency (MARKA), project No. TR42/16/ÜRETİM/0013. Authors also acknowledge a partial support by Research Fund of Gebze Technical University (grants Nos. BAP 2015-A-19 and BAP 2017-A-105-44).

1. Sacchi R., Addeo F., Paolillo L.: ^1H and ^{13}C NMR of virgin olive oil. An overview, *Magnetic Resonance in Chemistry* **35**, 133–145 (1997)
2. Ruiz-Aracama A., Goicoechea E., Guillén M.D.: Direct study of minor extra-virgin olive oil components without any sample modification. ^1H NMR multisuppression experiment: A powerful tool. *Food Chemistry* **228**, 301–314 (2017)
3. Merchak N., Bacha E.E., Khouzam R.B., Rizk T., Akoka S., Bejjani J.: Geoclimatic, morphological, and temporal effects on Lebanese olive oils composition and classification: A ^1H NMR metabolomic study. *Food Chemistry* **217**, 379–388 (2017)

Investigation of Fullerenes C_{60} and PCBM Triplet States Spin Dynamics in Ionic Liquids by Time-Resolved EPR Spectroscopy

I. Kurganskii¹, M. Ivanov², M. Fedin², S. Prikhod'ko³, and N. Adonin³

¹ Novosibirsk State University, Novosibirsk 630090, Russian Federation, kurganskiy.ivan@gmail.com

² International Tomography Center SB RAS, Novosibirsk 630090, Russian Federation

³ Borekov Institute of Catalysis SB RAS, Novosibirsk 630090, Russian Federation

Ionic liquids are interesting solvents for “green” chemistry due to their specific properties. However most of their properties depend on their microscopic structure. It makes investigation of ionic liquid’s microscopic structure very important matter. For this goal one can use the method of EPR spectroscopy of spin probes due to their good sensibility on molecular scale.

The goal of the present work is the investigation of the dynamics of PCBM and C_{60} chemically induced electron spin polarization (CIDEP) in different ionic liquids and other solvents. The results of this work would be useful for future use of these fullerenes as spin probes on microstructuring of ILs. Experiments were performed on an X-band time-resolved EPR spectrometer.

In experiments we received TR EPR spectra of fullerenes C_{60} and PCBM dissolved in ionic liquids $[C_{10}mim][BF_4]$, $[bmmim][PF_6]$, $[bmim][BF_4]$ and toluene,

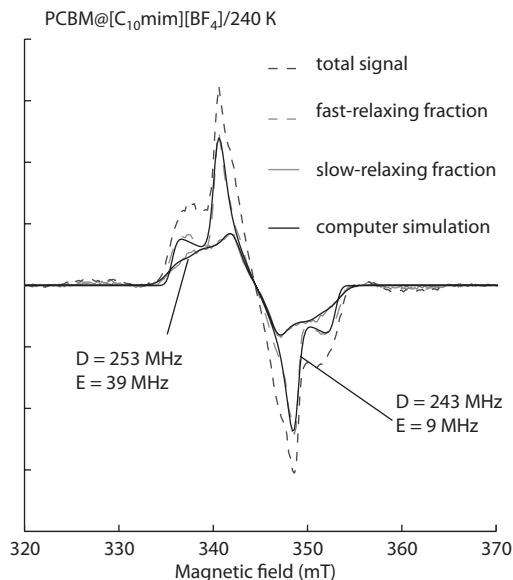


Fig. 1. Decomposition of an EPR spectrum of PCBM at $[C_{10}mim][BF_4]$.

ortho-terphenyl, THF at 100 K. The influence of used solvent on the EPR spectrum line shape was noticed. The analysis of EPR spectra and CIDEP relaxation kinetics of PCBM at $[\text{C}_{10}\text{mim}][\text{BF}_4]$ at 90 K up to 240 K was performed. The existence of two PCBM fractions in ionic liquids with different CIDEP relaxation time at 140 K up to 240 K was supposed. The decomposition procedure of EPR spectra lines into two components corresponding to each subensemble was applied (Fig. 1) and specific parameters of EPR spectra line shapes were calculated. Probable mechanism of two fractions formation was proposed.

This work was supported by the Russian Science Foundation (No. 14-13-00826).

Protein Translational Diffusion under Crowding Conditions

**A. M. Kusova^{1,2}, A. E. Sitnitsky¹, B. Z. Idiyatullin¹, D. R. Bakirova¹,
and Yu. F. Zuev^{1,2}**

¹ Kazan Institute of Biochemistry and Biophysics, Russian Academy of Sciences, Kazan,
Russian Federation, alexakusova@mail.ru

² Kazan Federal University, Kazan 420008, Russian Federation

All biochemical processes in the cells occur in a medium with a high concentration of macromolecules. Proteins, nucleic acids and other macromolecules occupy more than 30% of the cytoplasm volume [1, 2]. This condition, when the distances between neighboring macromolecules are comparable with their linear dimensions, named macromolecule crowding. The effect of the excluded volume is realized in this case. Macromolecule crowding effects on the thermodynamics and kinetics of processes in the cytoplasm, the association and aggregation of macromolecules, the aggregation of proteins, the kinetics of enzymatic and signaling processes [3, 4].

The behavior of proteins in solutions is of the great importance for biological systems. Translational diffusion is one of the fundamental physical phenomena that describes the mobility of molecules. A detailed understanding of the diffusion of proteins in solutions containing high concentrations of soluble macromolecules is presently lacking. Up to the present, much attention had been paid to dilute solutions of globular proteins. However, in cellular environment diffusion of macromolecules can be different from the conditions of dilute solutions.

We have studied the diffusion of proteins in highly concentrated globular and irregular shape protein solutions imitating the crowded conditions encountered in cellular environments.

Diffusion experiments were performed using the NMR spectrometer Bruker AVANCE III, operating at 600.13 MHz equipped with a standard z -gradient inverse probe head (TXI, 5 mm tube). We used a stimulated-echo sequence incorporating bipolar gradient pulses and a longitudinal eddy current delay (BPP-LED).

Our experimental data are interpreted within the framework of two theoretical approaches: hydrodynamic model of rigid spheres [5] and phenomenological approach based on the frictional formalism of non-equilibrium thermodynamics [6]. Our results testify that the Vink's approach is quite universal and provides a satisfactory description of experimental data for all types of proteins while the model of Tokuyama and Oppenheim is applicable only to globular proteins. The results allow the prediction of protein translational diffusion in conditions close to that of living cell.

The work was supported by the Russian Foundation for Basic Research grants: No. 15-44-02230-r_Volga_region_a, No. 15-29-01239-ofi_m.

1. Lavalett D. *et al.*: *Eur. Biophys. J.* **35**(6), 517 (2006)
2. Martinez M.C.L. *et al.*: *Int. J. Biol. Macromol.* **6**, 261 (1984)
3. Nsemelova I.V., Skirda V.D., Fedotov V.D.: *Biopolymers* **63**, 132 (2002)
4. Roos M. *et al.*: *Biophys. J.* **108**, 98 (2015)
5. Tokuyama M., Oppenheim I.: *Phys Rev.* **50**, 16 (1994)
6. Vink H.: *J. Chem. Soc. Faraday Trans.* **81**, 1725 (1985)

Spin Probe EPR Study of CO₂/O₂/N₂ Gas Sorption in ZIF-8

D. Kuzmina^{1,2}, A. Sheveleva^{1,2}, A. Poryvaev^{1,2}, and M. Fedin^{1,2}

¹ Department of Physics, Novosibirsk State University, Novosibirsk 630090, Russian Federation, dl.kuzmina@ya.ru

² Laboratory of Magnetic Resonance, International Tomography Center SB RAS, Novosibirsk 630090, Russian Federation

Metal organic frameworks (MOFs) are recently developed materials with astonishing adsorption characteristics. MOFs are simple for the synthesis, so the variety of forms has been created, and now physical properties of this material have to be studied by modern methods. One of the promising applications for MOFs is a gas storage. So gas adsorption at MOFs is the topic of the actual research.

Due to the exceptional thermal (till 500 °C) and chemical stability, the zeolitic imidazolate frameworks (ZIFs) subgroup of MOFs was chosen for the research of gas adsorption. One of the most popular and chemically studied ZIFs is ZIF-8. It has a cubic lattice structure and sodalite (SOD) topology with 11.6 Å and 3.4 Å diameter cavities. Small pore apertures of ZIF-8 are expected to separate branched alkanes from linear. Recently ZIF-8 membranes were shown to be able to split up gas mixtures, such as H₂/CH₄, CO₂/CH₄, C₂/C₃, ethylene/ethane, propylene/propane, H₂/propane.

Electronic paramagnetic resonance (EPR) method is well used for MOFs research. As metal organic frameworks have no EPR signal, TEMPO probe molecules are used to scan the structure of the frame by a continuous wave (CW) and pulsed EPR methods through molecular mobility inside the frame.

In this work we conducted EPR experiments with TEMPO probe. CW EPR technique was applied for TEMPO@ZIF-8 system filled with different gases (CO₂/O₂/N₂). Line shape analysis was made to demonstrate that the high quantity of adsorbed gas inside the frame tends to increase the rotational correlation time of the system. Molecular dynamic (MD) and TGA were made as supporting methods.

Diana Kuzmina thanks RSF grant No. 14-13-00826; Alena Sheveleva thanks the Presidential Grant (No. MK.3272.2017.3).

Spin Centers in Nanocrystalline Titania, Synthesized with Supercritical Flow Reactor Technique

N. T. Le¹, E. A. Konstantinova^{1,2}, and B. B. Iversen³

¹ Faculty of Physics, Lomonosov Moscow State University, Moscow 119991, Russian Federation, lenickola@physics.msu.ru

² National Research Center Kurchatov Institute, Moscow 123182, Russian Federation

³ Department of Chemistry, Aarhus University, Aarhus C, 312 8000, Denmark

Titanium dioxide (TiO_2) is the most important semiconductor photocatalyst because of its non-toxicity and high catalytic activity in various photooxidation reactions [1, 2]. The most important role in photocatalytic reactions on the surface of nanocrystalline titania plays O_2^- radicals and other defects. Traditionally these defects are paramagnetic, so it is perspective to use the EPR spectroscopy for their investigation. The size of nanoparticles also plays an important role in practical usage: the higher is the surface area – the higher is the amount of adsorbed molecules, which can take part in photocatalytic reactions.

The aim of this work is the study of influence of specific surface area on the concentration of spin centers and their nature in nanocrystalline titania, which were synthesized with supercritical flow reactor technique. A solvent (propanol-2: H_2O 19:1) was added into the reactor in supercritical state ($T = 235.6$ °C, $P = 53.7$ bar) with a 0.1 M solution of titanium isopropoxide (ACROS 98%) in propanol-2 [3]. After typical supercritical flow reactions the product was titania nanoparticles. The sizes of nanoparticles were 7–28 nm. EPR spectra were detected by the standard Bruker EPR spectrometer ELEXSYS-500 (X-band,

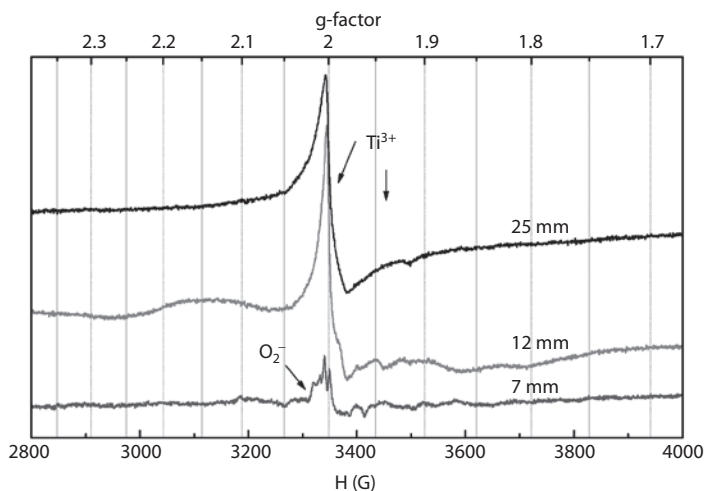


Fig. 1. Spin centers in various series of TiO_2 nanoparticles, synthesized with supercritical flow reactor.

sensitivity is around $\sim 10^{10}$ spin/G). The measurements were made at 300 K and 20 K. The samples were illuminated “in situ” with a 50 W tungsten lamp.

The EPR signal from Ti^{3+} centers (in volume: $g_{\perp} = 1.971$, $g_{\parallel} = 1.968$ and on the surface: $g_{\perp} = 1.943$, $g_{\parallel} = 1.922$) was reliably detected for the first time at 300 K in TiO_2 . We note that in the samples which were synthesized by the sol-gel method, such spin centers were detected in titania after vacuum treatment and only at 77 K (due to short relaxation times). The increase of spin-lattice relaxation time in this case is probably due to a change in the phonon spectrum of the samples. The illumination of the samples did not lead to the detection of new spin centers and their re-chargings. This indicates that the energy levels of Ti^{3+} centers are located near the bottom of the conduction band, and these centers are practically ionized at room temperature (i.e, they are paramagnetic).

An increase of the specific surface area (a decrease if nanocrystal size), at first glance, should lead to the increase in the concentration of near-surface defects. However, the ESR spectra of the samples under investigation show a reverse trend (Fig. 1). We note a sharp decrease in the amplitude of the Ti^{3+} related EPR signal. But we can observe the EPR signal, which corresponds to O_2^- radicals ($g_1 = 2.019$, $g_2 = 2.009$, $g_3 = 2.003$) [4]. We note that illumination of the samples led to an increase in the amplitude of the EPR signal from these centers, which can be explained by the capture of photoexcited electrons with adsorbed oxygen molecules and their conversion to O_2^- spin centers. These variations in the EPR spectrum with an increase in the specific surface area of the samples can be explained by the interaction of the oxygen molecules from the ambient air with the Ti^{3+} centers on the TiO_2 surface, which leads to a passivation of the last.

The obtained results are important for practical application. The work was supported by the Russian Foundation for Basic Research (No. 16-32-00800 mol_a).

1. Asahi R., Morikawa T., Ohwaki T., Aoki K., Taga Y.: *Science* **294**, 269 – 271 (2001)
2. Livraghi S., Votta A., Paganini M.C., Giamello E.: *Chem. Comm.* 498–500 (2005)
3. Hald P., Becker J., Bremholm M. *et al.*: *Journal of Solid State Chemistry* **179**, 2674–2680 (2006)
4. Kokorin A.I., Bahnemann D.W.: *Chemical Physics of Nanostructured Semiconductors*, Chapter 8. Electron Spin Resonance of Nanostructured Oxide Semiconductor. VSP 2003.

The Coherence of the Exciting Radiation and Amplitude of Oscillations of Echo Intensity vs External dc Magnetic Field

V. N. Lisin¹, A. M. Shegeda¹, and V. V. Samartsev^{1,2}

¹ Zavoisky Physical-Technical Institute, Kazan 420029, Russian Federation
valerylisin@gmail.com

² Kazan Federal University, Kazan 420008, Russian Federation

In works [1–4] we have been proposed a method of spectroscopy, ultrahigh resolution in the time domain, which uses the oscillation of the intensity and modulation of the shape of the photon echo response in the presence of pulse disturbance that splits the frequency of transitions of ions on two groups. It is necessary to mark that the first minimum at the echo intensity in $\text{LiLuF}_4:\text{Er}^{3+}$ (transition ${}^4I_{15/2} \rightarrow {}^4F_{9/2}$) was observed in the pulsed magnetic field which amplitude was ~ 2 G and duration 30 ns. Zeeman splitting in this field is ≈ 10 MHz, that is much less than the laser spectral width $0.2 \text{ cm}^{-1} \approx 6$ GHz. The physical reasons, allowing to observe the splitting of the optical line by several orders of magnitude smaller than the spectral width of the laser pulse weren't considered and aren't clear. For the solution of these questions, the amplitude of the oscillations in the first minimum of the photon echo intensity induced by the pulsed magnetic field h is studied vs the dc magnetic field H_{dc} values in systems of $\text{LiYF}_4:\text{Er}^{3+}$ and $\text{LiLuF}_4:\text{Er}^{3+}$.

In Fig. 1 you can see relative intensity of the two-pulse photon echo versus the magnetic pulse (MP) amplitude h in $\text{LiLuF}_4:\text{Er}^{3+}$ for different values of dc magnetic field $H = 5, 82, 200$ Oe. Here h is the average values of pulse magnetic field over the optically excited volume, I and I_0 are the photon echo intensity when MP on and off accordingly. MP duration is n . The value of rela-

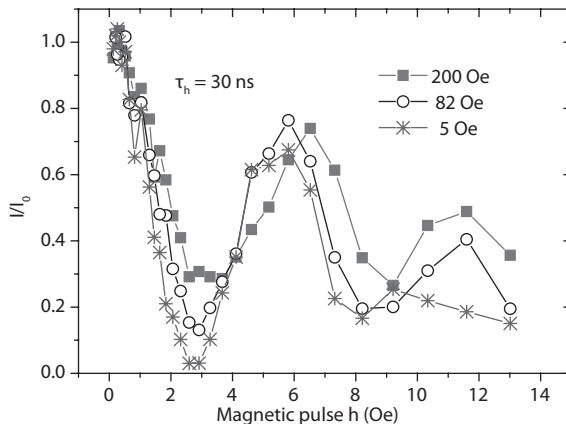


Fig. 1.

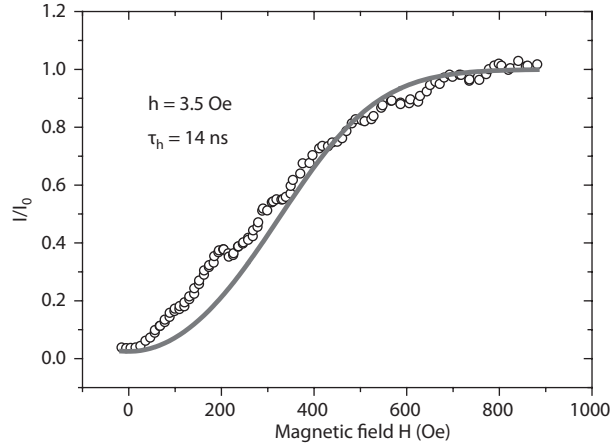


Fig. 2.

tive intensity I/I_0 in the point of the first minimum vs a constant magnetic field is shown in Fig. 2 use circles.

We get that I/I_0 does not depend on H for coherent excitation of the echo.

The technique of Morita [5] was used for the description of the experiment. In this theory, the electric field of the laser is described by complex random function. Time of correlation of Gaussian stationary process was considered equal to the reverse spectral half-width of the laser. We received the following expression for relative intensity of an echo in a point of the first minimum vs dc magnetic field:

$$\frac{I}{I_0} = \tanh \frac{H^2}{8H_\sigma^2}, \quad (1)$$

$$H_\sigma = \frac{\hbar\sigma}{(g_e - g_g)\beta}. \quad (2)$$

Here g_e and g_g are the g -factors of excited ($^4F_{9/2}$) and ground ($^4I_{15/2}$) states of erbium ion, β is the Bohr magneton, \hbar is the Planck constant, σ (rad/sec) is the parameter, describing distribution of frequencies of optical transitions ω_{eg} ,

$$f(\omega_{eg} - \omega) = \exp\left(-\frac{(\omega_{eg} - \omega)^2}{2\sigma^2}\right) / \sqrt{2\pi\sigma^2}. \quad (3)$$

In Fig. 2 the solid line represents the theoretical dependence (Eq. (1)) at $H_\sigma = 170$ Oe. Using this value and Eq. (2), we obtain that $\sigma/(2\pi) = 1.549$ GHz. The full line width at half maximum (see Eq. (3)) is equal $\text{FWHM} = 2.3548 \cdot \sigma/(2\pi) = 3.65$ GHz = 0.12 cm^{-1} . We simulated the distribution of ions in frequency using a single Gaussian. However Macfarlane [6] have observed a doublet structure on the f - f absorption lines of Er^{3+} in YLiF_4 (with natural

abundances of lithium isotopes) with splitting of 1.4 GHz and linewidths of 600 MHz. In our report we will experimentally get a distribution function instead of Eq. (3) and a comparison of the theoretical dependence with the experimental (as in Fig. 2) will be performed.

The financial support of the Foundation for Basic Research (grant 17-02-00701a) and RAS program “Fundamental optical spectroscopy and its applications” is gratefully acknowledged.

1. Lisin V., Shegeda A., Gerasimov K: JETP Letters **95**, 61 (2012)
2. Lisin V., Shegeda A.: JETP Letters **96**, 328 (2012)
3. Lisin V.N., Shegeda A.M., Samartsev V.V.: Laser Phys. Lett. **12**, 025701(2015)
4. Lisin V.N., Shegeda A.M., Samartsev V.V.: Laser Phys. Lett. **13**, 075202 (2016)
5. Morita N., Yajima T.: Phys. Rev. A **30**, 2525 (1984)
6. Macfarlane R.M., Cassanho A., Meltzer R.S.: Phys. Rev. Lett. **69**, 542(1992)

ESR Study of CuEr Dilute Alloys

S. Lvov and **E. Kukovitsky**

Lab of Physics of Carbon Nanostructures and Composite Systems,
Zavoisky Physical-Technical Institute 420029, Russia, lvov@kfti.knc.ru

The paramagnetic resonance spectrum of Er^{3+} in bulk metallic copper was investigated at 9.8 GHz over the temperature range of 1.7 to 4.2 K. The spectrum corresponds to a field of cubic symmetry with $g = 6.805 \pm 0.01$ and this value is in good agreement with the predicted value for Γ_7 doublet. The quality of the host gave us relatively narrow lines yielding a precise value of g -factor and thermal broadening. The residual ESR line width ($T = 0$ K) for even erbium isotopes in dilute alloys was only 4–5 Oe. The temperature and concentration variations of the ESR line width in CuEr alloy with negligible solubility have been investigated. Hyperfine structure for the isotope ^{167}Er was identified and hyperfine coupling constant $A = 74.25 \pm 0.1$ Oe was found to fit the individual line positions to within experimental accuracy (± 1.5 Oe). Improved-accuracy measurements of the hyperfine splitting of Er^{3+} ions in copper host reveal the weak hyperfine-structure exchange narrowing in alloys with higher erbium concentrations.

Peculiarities of the linewidth behavior indicate to the presence of RKKY interaction between erbium ions. The role of the RKKY interaction in connection with ESR in dilute alloys, prone to impurity segregation, has been emphasized and experimental results have been explained in terms of extended Bloch-Hasegawa theory.

DFT Calculations of the ^{14}N NQR Spectra of Some Heterocycles

S. Mamadazizov¹, M. Shelyapina², and G. Kupriyanova¹

¹ Institute of Physics and Mathematics, Immanuel Kant Baltic Federal University, Kaliningrad 236016, Russian Federation, sultonazar.mamadazizov@mail.ru

² Saint-Petersburg State University, St. Petersburg 199034, Russian Federation

Nuclear Quadrupole Resonance is a well-known technique for solid samples investigation. The main physical parameter that can be determined from the NQR spectra is the tensor of quadrupole interactions, which are interactions between the nuclear quadrupole moment and intercrystalline electric field gradients (EFG). In recent years, considerable interest has been shown in the study of different nitrogenous heterocycles, which are used in pharmaceuticals. Usually they are used as an isosteric substitutes for various functional groups that leads to creation of novel biologically active substances. NQR techniques, being sensitive to the local environment of ^{14}N nuclei, provide great opportunities to study these new substances.

NQR lines detection in new compounds could be a hard task, if there are no hints in literature, because one needs to scan a whole range of frequency with a small step (several tens of kHz) and even it could be harder to make correct assignment of obtained NQR spectra. In this case Density Functional Theory is a great help for solving named issues. Modern packages, such as Gaussian, make it easy to handle quantum mechanical calculations of NQR spectra, which helps in assignment of experimental lines.

In presented research, ^{14}N NQR spectra of several heterocycles: 5-amino-tetrazole, 5-aminotetrazole monohydrate, tetrazole, imidazole and benzotriazole were calculated. Nitrogen has spin $I = 1$. Thus, according to NQR theory nitrogen has three energy levels in inhomogeneous electric field. In ^{14}N NQR, all

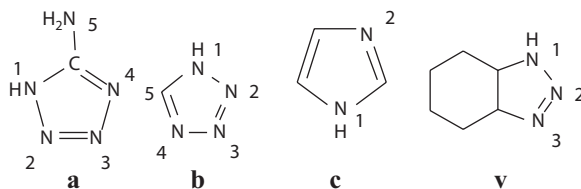


Fig. 1. Molecular structure of calculated objects: **a** 5-aminotetrazole, **b** tetrazole, **c** imidazole, **v** benzotriazole.

Table 1. Calculated quadrupole coupling constants Q_{cc} and anisotropy parameters η .

Nuclei	TZ		ATZH		Imidazole		Benzotriazole	
	Q_{cc} (MHz)	η	Q_{cc} (MHz)	η	Q_{cc} (MHz)	η	Q_{cc} (MHz)	η
N(1)	2.833	0.52	2.904	0.97	1.996	0.41	3.592	0.40
N(2)	4.403	0.64	4.183	0.81	4.104	0.06	4.751	0.82
N(3)	4.849	0.24	4.682	0.32	–	–	4.094	0.44
N(4)	4.533	0.28	3.519	0.92	–	–	–	–
N(5)	–	–	3.903	0.65	–	–	–	–

three transitions can be excited by radio-frequency field at the corresponding resonant frequencies:

$$v_{\pm} = (Q_{cc}/4)(3 \pm \eta); \quad v_0 = -(Q_{cc}/2)\eta$$

where η is anisotropy parameter and Q_{cc} is quadrupole coupling constant. These NQR parameters are determined as follow:

$$Q_{cc} = eQq_{zz}/\hbar; \quad \eta = (q_{yy} - q_{xx})/q_{zz}$$

q_{xx} , q_{yy} , q_{zz} are components of EFG tensor, \hbar – Planck constant, e – electron charge. Thus, using DFT one can calculate EFG tensor and all NQR parameters of quadrupolar nuclei. Calculated molecules structure provided in the Fig. 1. Tetrazole derivatives are highly nitrogenous, which makes difficult the process of ^{14}N NQR lines assignment. Also, NQR lines are quite close for some nitrogen. In case of 5-aminotetrazole monohydrate structure (a) in the Fig. 1 surrounded by 4 water molecules.

To calculate the ^{14}N NQR parameters in tetrazole derivatives a density functional theory (DFT) method with B3LYP hydride exchange-correlational functional has been used. This functional has confirmed itself as appropriate for providing trustworthy results for various properties of tetrazole derivatives, such as geometry, optical and electronic properties, thermal decomposition [1]. Results of DFT B3LYP calculations of ^{14}N NQR spectral parameters (quadrupole coupling constant Q_{cc} and the asymmetry parameter of the electric field gradient η) for named compounds are given in the Table 1.

Obtained theoretical results are in a good agreement with experimental data. In case of aminotetrazole correlation between calculated and experimental values is up to 97%. Furthermore, calculations can be helpful in studies of hydrogen bonds dynamics in samples in order to explain temperature effects and other dependent phenomena.

^{14}N NQR with Frank Sequence Excitation

I. Mershiev¹ and B. Blümich²

¹ Institute of Physics, Mathematics and Information Technology, Immanuel Kant Baltic Federal University, Kaliningrad 236016, Russian Federation, IMershiev@kantiana.ru

² Institute of Technical and Macromolecular Chemistry, RWTH Aachen University, Aachen D-52056, Germany

Nuclear quadrupolar resonance is a solid-state resonance spectroscopy method that allows the detection of substances that contains quadrupolar nuclei. One of the usages of this method is the detection of explosives and illicit substances, which contains the abundant ^{14}N isotope with nuclear spin $I = 1$. However, low frequency range, low sensitivity and high excitation power requirements limit the use of NQR spectroscopy for substance detection.

Stochastic excitation is an experimental method for NMR that allows reducing the radiofrequency excitation power up to several orders of magnitude [1]. Pseudo-random encoding allows using the coherent averaging for the FID data, which is sampled between the pulses. In this work, we propose a theoretical and experimental analysis of using the stochastic excitation in application to ^{14}N NQR spectroscopy. As the phase modulation source, Frank sequences was used [2]. In comparison with the binary M-sequence, it has a uniform power spectrum and does not cause artifacts in the reconstructed autocorrelation spectra. Stochastic excitation in NQR may have an advantage with the use of low power and battery-powered equipment, as well as for detection of substances with long T_1 relaxation times.

The financial support of the Ministry of Education and Science and DAAD foundation (grant 1.735.2016/2.2) is gratefully acknowledged.

1. Ernst R.R.: J. Magn. Reson. **3**, 10 (1970)
2. Blümich B., Gong Q., Byrne E., Greferath M.: J. Magn. Reson. **199**, 18 (2009)

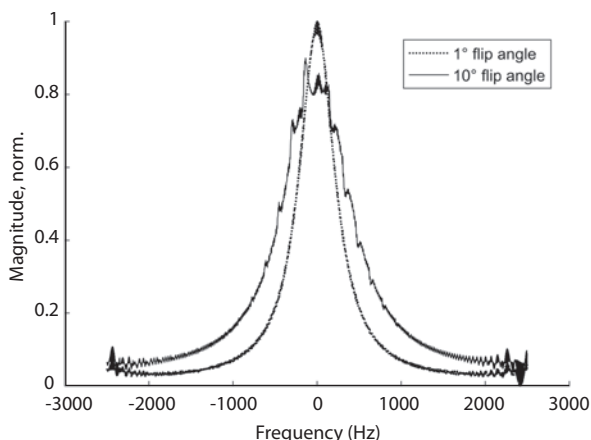


Fig. 1. Simulated NQR spectra for linear and nonlinear stochastic excitation modes.

EPR of $\{\text{Dy}^{\text{III}}\text{-Me}^{\text{III}}_2\text{-Dy}^{\text{III}}\}$ Clusters, $\text{Me}^{\text{III}} = \text{Cr}^{\text{III}}, \text{Mn}^{\text{III}}$

L. V. Mingalieva¹, Y. Peng², V. K. Voronkova¹, and A. K. Powell²

¹ Zavoisky Physical-Technical Institute, Russian Academy of Sciences, Kazan 420029, Russian Federation, ljudmila.vjacheslavovna@gmail.com

² Institute of Inorganic Chemistry, Karlsruhe Institute of Technology, Karlsruhe 76131, Germany

Clusters with rare-earth ions are being intensively studied as perspective for the design of single-molecule magnets SMM [1, 2]. The investigation of the influence of the dipole-dipole and exchange interactions on the SMM properties of 3d-4f clusters is an important aspect of the problem of creating promising clusters. Previously we explored the magnetic properties of the compound $[\text{DyFe}^{\text{III}}_2\text{Dy}(\mu_3\text{-OH})_2(\text{pmide})_2(\text{p-CH}_3\text{-PhCO}_2)_6]$ [3], is built of hetero nuclear clusters Fe_2Dy_2 .

In this work we present the results of the investigation of two new clusters $\{\text{Dy}^{\text{III}}\text{-Cr}^{\text{III}}_2\text{-Dy}^{\text{III}}\}$ and $\{\text{Dy}^{\text{III}}\text{-Mn}^{\text{III}}_2\text{-Dy}^{\text{III}}\}$ which are isostructural to Fe_2Dy_2 .

EPR investigations were carried out in a wide temperature range at the X- and Q-bands. Exchange interactions between 3d ions and Dy^{III} ions and the dependence of the magnetic properties of hetero nuclear $\{\text{Dy}^{\text{III}}\text{-Me}^{\text{III}}_2\text{-Dy}^{\text{III}}\}$ clusters on the Me-ion are discussed.

1. Mereacre V., Ako A. M., Filoti G., Bartolome J., Anson C.E., Powell A.K.: *Polyhedron* **29**, 244–247 (2010)
2. Kostakis G.E., Hewitt I.J., Ako A.M., Mereacre V., Powell A. K.: *Philos. Trans.* **368**, 1509–1536 (2010)
3. Baniodeh A., Lan Ya., Novitchi Gh., Mereacre V., Sukhanov A., Ferbinteanu M., Voronkova V., Ansona Ch.E., Powell A.K.: *Dalton Trans.* **42**, 8926 (2013)

Investigation of Charge Accumulation Processes in TiO₂-Based Nanoheterostructures

A. A. Minnekhanov^{1,2}, E. V. Vakhrina¹, and E. A. Konstantinova^{1,2}

¹ Faculty of Physics, Lomonosov Moscow State University, Moscow 119991, Russian Federation, minnekhanov@physics.msu.ru

² National Research Center Kurchatov Institute, Moscow 123182, Russian Federation

Titanium dioxide, TiO₂, invariably draws researchers' attention due to its unique physical and chemical properties and one of the most promising application areas of TiO₂ is photocatalysis. It was shown before [1] that the combination of redox-active oxides (such as MoO₃ or V₂O₅) weakly active during illumination with a high-photoactive semiconductors (TiO₂) makes it possible to create a photocatalytic systems with a function of accumulation of the photoexcited charge carriers [2]. The use of nanocrystalline titanium dioxide as the photo-generation component of the photo-accumulating systems allows the production of photocatalysts, which ensures the generation, separation, and accumulation of photoexcited charge carriers. The aim of this work is study of interaction of photoexcited charge carriers with defects (the most part of that is paramagnetic) in TiO₂/MoO₃ nanoheterostructures.

All details of the sample preparation were published in [2]. The EPR spectra were measured using an X-band Bruker ELEXSYS-500 spectrometer (9.5 GHz, sensitivity of $5 \cdot 10^{10}$ spin/G) in the temperature range of 10–300 K. illumination by the BRUKER ELEXSYS ER 202 UV lamp (50 W). The spin-Hamiltonian parameters were calculated by a computer simulation of the experimental EPR spectra using the EasySpin MATLAB toolbox.

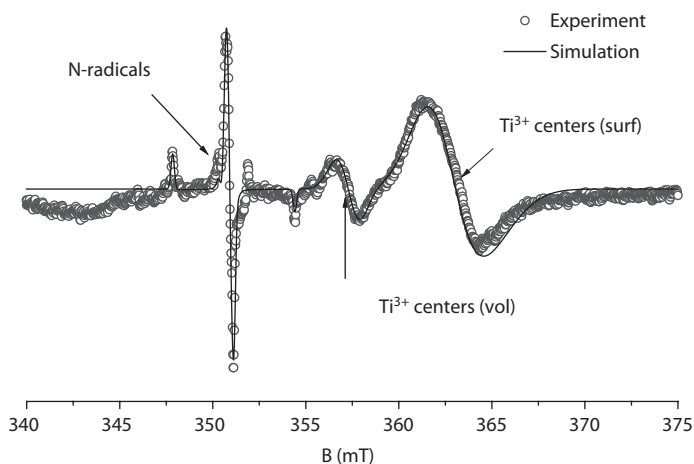


Fig. 1. Experimental and simulated EPR spectra of TiO₂/MoO₃ samples. $T = 300$ K.

The experimental EPR spectrum of $\text{TiO}_2/\text{MoO}_3$ sample obtained at 300 K and its computer simulation are shown in Fig. 1. According to the spin-Hamiltonian parameters extracted from the computer simulation and literature data [3] we can conclude that in the samples under investigation are present (from left to right in the EPR spectrum, Fig. 1) N-radicals ($g_1 = 2.007$, $g_2 = 2.0057$, $g_3 = 2.0043$, $A_1 = 0.13$ mT, $A_2 = 0.36$ mT, $A_3 = 3.29$ mT), Ti^{3+} volume centers ($g_{\perp} = 1.971$, $g_{\parallel} = 1.968$) and Ti^{3+} surface centers ($g_{\perp} = 1.942$, $g_{\parallel} = 1.928$).

The intensities of EPR-lines (I_{EPR}) change under illumination: I_{EPR} of N-radicals decreases and I_{EPR} of Ti^{3+} surface centers increases during illumination which indicates the recharge processes of defects in the samples. Since the effect of illumination was reversible we can describe it using the following equations: $\text{N}^{\bullet} - e^- \rightarrow \text{N}^+$ or $\text{N}^{\bullet} + e^- \rightarrow \text{N}^-$ (for N^{\bullet}) и $\text{Ti}^{4+} + e^- \rightarrow \text{Ti}^{3+}$ (for Ti^{3+}). Notice that defects keep the charging state very long time after the light is off. It can be caused by the fact that the photoexcited electron from TiO_2 is injected in MoO_3 while the hole remained in TiO_2 . Thus, the recombination of the photoexcited electrons and holes will be suppressed owing to their spatial separation. Therefore the photoexcited charge carriers can “live” a long time in the samples and can be trapped by defects. Thus, the $\text{TiO}_2/\text{MoO}_3$ samples possess function of charge accumulation that is very important for practical applications in the field of a photocatalysis as photocatalytic action of such samples can “last” for a long time after light switching off.

We are very grateful to Prof. Sviridov D.V. for sample preparation and Prof. Kokorin A.I. for helpful discussion. The work was supported by the Russian Foundation for Basic Research (No. 16-32-00800 mol_a).

1. Mendoza-Sanche B., Brousse T., Ramirez-Castro C., Nicolosi V., Grant P.: *Electrochimica Acta* **91**, 253–260 (2013)
2. Sviridova T.V., Sadovskaya L.Yu., Shchukina E.M., Logvinovich A.S., Shchukin D.G., Sviridov D.V.: *J. Photochem. Photobiol. A: Chem.* **327**, 44–50 (2016)
3. Kokorin A.I.: *Chemical Physics of Nanostructured Semiconductors* (Kokorin A.I., Bahnemann D.W., eds.), 203 p. Utrecht, Boston: VSP-Brill Academic Publishers 2003.

Nitrogen ^{14}N NMR Detection of Liquids

**G. V. Mozzhukhin¹, G. S. Kupriyanova², A. Maraşlı¹,
and B. Z. Rameev^{1,3}**

¹ Gebze Technical University, Gebze/Kocaeli 41400, Turkey, mgeorge@yandex.ru

² Baltic Federal University by Immanuel Kant, Kaliningrad 236041, Russian Federation

³ Zavoisky Physical-Technical Institute, Russian Academy of Sciences, Kazan 420029, Russian Federation

The first works on application of NMR method for detection of dangerous liquids have been published by Dr. L. J. Burnett group (see e.g. [1]). There is a huge number of various beverages (such as Pepsi, Coca-Cola, etc.), juices, dairy, alcohol drinks, etc. In total, there are hundreds (even thousands) of liquids around the world. It has been shown that for reliable discrimination in a large group of benign and threat liquids a number of NMR parameters (relaxation times T_1 and T_2 , as well as diffusion constant D) should be scanned [2–4]. On the other hand, for practical application in security it is very important to develop methods for *fast* detection. Therefore, NMR approaches to make measurements during several seconds (but not minutes or hours as in classical NMR) are highly desirable. For that reason, an approach [5], which relies on the detection of ^{14}N NMR signal of energetic substances as a secondary parameter for more reliable detection of dangerous liquids, looks very prospective.

It is well known that most of solid energetic and explosives materials includes the nitrogen nuclei of ^{14}N . The NMR nitrogen detection of energetic substances are characterized by the following features: i) the relative sensitivity of ^{14}N NMR is near 0.018 of NMR of ^1H ; ii) a number of nitrogen-based liquid explosives contains NO_2 group in their structure; iii) a total number of illicit and explosive liquids containing nitrogen in their structure is rather limited. In many cases, the bare fact of detection of ^{14}N NMR signal indicate threat.

In this work, a possibility to use ^{14}N NMR detection in practical applications has been studied. A special setup for ^{14}N NMR measurements has been assembled. ^{14}N NMR signal has been successfully detected in 12 nitrogen liquids, included in the test set. The CPMG and inversion recovery sequences have been used for measurements of T_2 and T_1 , respectively. The substances, containing NO_2 group in their structure (sodium nitrate, nitromethane, nitroethane, nitrobenzene), and toxic substances (acetonitrile, dimethylformamide and dimethylacetamide) have been measured.

^{14}N NMR signals of various nitrogen-based substances have been successfully detected and the relaxation parameters of the ^{14}N signals have been obtained. It has been shown that due to large chemical shift values of ^{14}N NMR signal, it is possible to observe splitting of FT NMR spectra of nitrogen-based compounds even by low field NMR device. The time of measurements is small, because values of T_1 – T_2 are typically short for ^{14}N nuclei. Thus, the feasibility of ^{14}N

NMR applications for detection of various energetic and illicit liquids has been demonstrated.

The work was supported by NATO Science for Peace and Security Programme (NATO SPS grant No. 985005 [G5005]) and TUBITAK grant under the Programme 2221 for Visiting Scientist (G. S. Kupriyanova). Authors also acknowledge a partial support by East Marmara Development Agency (MARKA, project No. TR42/16/ÜRETİM/0013) and by Research Fund of Gebze Technical University (grants Nos. BAP 2015-A-19 and BAP 2017-A-105-44).

1. Burnett L.J.: Liquid explosives detection. *Proc. SPIE* **2092**, 208–216 (1993)
2. Gradišek A., Apih T.: *Appl. Magn. Reson.* **38**, 485–493 (2010)
3. Rameev B., Mozzhukhin G.V., Khusnutdinov R., Aktas B., Konov A., Krylatyh N.A., Fattakhov Ya.V., Gabidullin D.D., Salikhov K.M.: *Proc. SPIE* 8357, Detection and Sensing of Mines, Explosive Objects, and Obscured Targets XVII, 83570Z (2012)
4. Konov A.B., Salikhov K.M., Vavilova E.L., Rameev B.Z.: Multiparameter NMR Identification of Liquid Substances, in NATO book: “Magnetic Resonance Detection of Explosives and Illicit Materials”, NATO Science for Peace and Security, Series B: Physics and Biophysics (T. Apih, B. Rameev, G. Mozzhukhin, J. Barras, eds.), pp. 111–122. Springer 2013.
5. Prado P.: Detecting Hazardous materials in containers utilizing nuclear magnetic resonance based measurements. Patent US 2014/0225614 A1, Aug. 14, 2014.

Determination of Aggregation Stability and MRI Contrast Efficiency of Magnetic Nanoparticles by NMR-Relaxometry

**A. V. Nikitina¹, Yu. V. Bogachev¹, A. A. Kostina¹, V. A. Sabitova¹,
Ya. Yu. Marchenko², and B. P. Nikolaev²**

¹ Department of Physics, Saint-Petersburg Electrotechnical University "LETI",
Saint-Petersburg 197376, Russian Federation, nastya_nikitina1996@mail.ru

² State Research Institute of Highly Pure Biopreparations,
Saint-Petersburg 197110, Russian Federation, 046_slava@mail.ru

At present, multifunctional magnetic nanoparticles (MNPs) are finding increasing applications in medicine for theranostics [1]. For this purpose, they must have certain magnetic characteristics, to be stable (have a low aggregation capacity), biocompatible, nontoxic, flexible and have a high magnetic resonance (MR) relaxation efficiency.

The aim of this work is the analysis and summarizing our experimental results of MR studies of composite MNPs to determine their aggregation stability and relaxation efficiency in aqueous solutions.

NMR measurements in a magnetic field of 7.1 T were performed on the NMR spectrometer CXP-300 (Bruker, Germany) for the resonant frequency of protons of 300 MHz. NMR measurements in a magnetic field of 0.33 T were performed on the NMR relaxometer (Spin Track, Russia) for the resonant frequency of protons of 14 MHz.

NMR measurements of T_1 and T_2 relaxation times were carried out for the following samples of magnetic nanoparticles:

1) superparamagnetic iron oxide nanoparticles in model media: in distilled water, in 2% agar-agar gel, in an aqueous solution of albumin (50 g/l);

2) magnetic nanoparticles based on iron oxide in the shell of dextran conjugated with some proteins (EGF – Epidermal Growth Factor and HSP70 – Heat Shock Protein);

3) standard sample of MNPs fluid MAG-DX 4104 (Chemicell, Germany).

For most samples studied graphic dependences of longitudinal R_1 and transverse R_2 , R' NMR relaxation rates of water protons on the concentration of magnetic nanoparticles $R_i(C)$ are linear and are described by the functions $R_i = r_i \cdot C + R_{0i}$, where C is the concentration of MNPs, R_{0i} is the constant determined by the relaxation rate of water protons in the absence of MNPs, r_i is the relaxation efficiency. For such samples the relaxation efficiency is defined as the tangent of the slope of the straight line $R_i(C)$ and has a constant value r_{st} .

The values of static relaxation efficiency for some investigated samples are shown in Table 1.

Higher values of the static relaxation efficiency correspond to a stronger negative MRI contrast abilities of this agent.

For some samples of MNPs the concentration dependence of the transverse relaxation rate of water protons $R_2(C)$ is non-linear. The analysis of this dependence shows a decrease in the relaxation efficiency with increasing MNPs

Table 1. Static relaxation efficiency.

Sample	MNP	MNP-FluidMAG-DX	MNP-EGF	MNP-Hsp70
r_{s1}, L (mMol · c)	1.55	0.87	0.33	1.27
r_{s2}, L (mMol · c)	301	260	216	211

concentration. The observed phenomenon was attributed to instability of these MNPs in aqueous solution and their ability to form clusters or aggregates when the MNPs concentration in the solution increases. This effect of MNPs aggregation was observed visually for some samples and increased with increasing residence time of the sample in the magnetic field of the NMR relaxometer. Similar results were obtained earlier in the NMR relaxation study of protons in aqueous solutions of iron oxide MNPs with Si-C shell [2].

In the case of nonlinear dependence $R_2(C)$ to determine the aggregation ability of the magnetic nanoparticles, rational to introduce the concept of dynamic relaxation efficiency, which can be found as the first derivative of a function at a given point of the curve $R_2(C)$, i.e. $r_{d2} = \partial R_2 / \partial C$. The dependence of the dynamic relaxation efficiency of the concentration is non-linear and allows to evaluate the aggregation stability of these magnetic nanoparticles.

The aggregation of the nanoparticles affects the outer-sphere proton relaxation processes and as well as the diffusion of protons in the vicinity of magnetic centers, resulting in lower relaxation rates as compared to single magnetic nanoparticles.

Acknowledgements: part of this work was supported by Ministry of Education and Science of the Russian Federation (project 3.6522.2017).

1. Shao H., Issadore D., Min C., Liong M., Chung J., Weissleder R., Lee H.: *Theranostics* **2**(1), 55 (2012)
2. Bogachev Yu.V., Chernenko Ju.S., Gareev K.G., Kononova I.E., Matyushkin L.B., Moshnikov V.A., Nalimova S.S.: *Appl. Magn. Reson.* **45**, 329 (2014)

Towards Determination of Distances between Nanoparticles and Grafted Paramagnetic Ions by NMR Relaxation

A. M. Panich¹ and N. A. Sergeev²

¹ Department of Physics, Ben-Gurion University of the Negev,
Be'er Sheva 8410501, Israel, pan@bgu.ac.il

² Department of Mathematics and Physics, Institute of Physics,
University of Szczecin, Szczecin 70-451, Poland, mykola.serheiev@usz.edu.pl

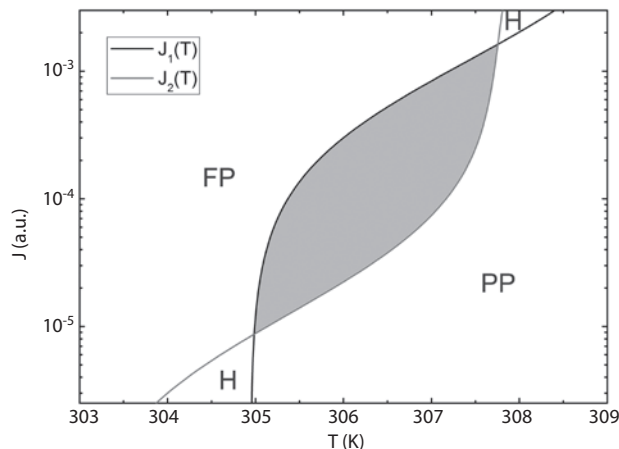
We developed an approach for determining distances between carbon nanoparticles and grafted paramagnetic ions and molecules by means of nuclear spin-lattice relaxation data. The approach was applied to copper-, cobalt- and gadolinium-grafted nanodiamonds, iron-grafted graphenes, manganese-grafted graphene oxide and activated carbon fibers that adsorb paramagnetic oxygen molecules. Our findings show that the aforementioned distances vary in the range of 2.7–5.4 Å and that the fixation of paramagnetic ions to nanoparticles is most likely implemented by means of the surface functional groups. The NMR data are compared with the results of EPR measurements and DFT calculations.

Multifunctional Properties of Ferromagnetics in Conditions of Photoexcitation

D. Pavlov and **R. Mamin**

Zavoisky Physical-Technical Institute, Russian Academy of Sciences, Kazan 420029,
Russian Federation, Dmitry.p.pavlov@gmail.co)

The results of a theoretical investigation of the dynamics of states in ferromagnetics arising due to illumination in the vicinity of phase transitions are presented. In the compounds of some ferromagnetics, in the vicinity of photostimulated phase transition, regions of phase coexistence arise, and also the emergence of unstable states. We investigated the appearance of a dynamic regime in ferromagnetics the phase transition under illumination conditions. To this end, a system of differential equations describing the change in the order parameter and the change in the number of electrons in the vicinity of the sticking zone is analyzed. It is shown that in the area of a phase transition under the conditions of a illumination, it is possible to exist of three stationary points on the phase plane corresponding to the equilibrium states of the system. The corresponding values of the pairs of the order parameter and the concentration of charge carriers on the defects are obtained. The equations of motion of the system are written. The regions of the appearance of the dynamic regime in the material near the phase transition are obtained for a nontrivial case of the order parameter, called the hysteresis region. The intensity and temperature in the hysteresis region are estimated. The dynamics of the system in the phase coordinates of the order parameter and the carrier density at the defects in the region of the phase transition are considered. A phase diagram of the various states of the system in the region of the phase transition in the coordinates of light intensity and temperature is obtained.



A Classical Vector Model for Magnetization of Two-Spin System with Dipole-Dipole Interaction

S. N. Polulyakh

¹ Physical-Technical Institute of CFU, Simferopol 295007, Russian Federation,
sergey.polulyakh@cfuv.ru

The system of isolated pair of identical spin $I = 1/2$ particles coupled by dipole interaction is considered in external magnetic field. Magnetization M of such system for the pulse experiment can be derived with the density matrix operator ρ :

$$\begin{aligned}
 M_+(t) = \sum & \left(\langle \Psi_{n1} | e^{-iHt} | \Psi_{n1} \rangle \langle \Psi_{n1} | \Phi_{n2}^j \rangle \langle \Phi_{n2}^j | e^{-iR_j \tau_j} | \Phi_{n2}^j \rangle \langle \Phi_{n2}^j | \dots \times \right. \\
 & \times \dots | \Phi_{n3}^1 \rangle \langle \Phi_{n3}^1 | e^{-iR_1 \tau_1} | \Phi_{n3}^1 \rangle \langle \Phi_{n3}^1 | I_z | \Phi_{n4}^1 \rangle \langle \Phi_{n4}^1 | e^{R_1 \tau_1} | \Phi_{n4}^1 \rangle \langle \Phi_{n4}^1 | \dots \times \\
 & \left. \times \dots | \Phi_{n5}^j \rangle \langle \Phi_{n5}^j | e^{iR_j \tau_j} | \Phi_{n5}^j \rangle \langle \Phi_{n5}^j | \Psi_{n6} \rangle \langle \Psi_{n6} | e^{iHt} | \Psi_{n6} \rangle \langle \Psi_{n6} | I_+ | \Psi_{n1} \rangle \right). \quad (1)
 \end{aligned}$$

Here operator R_j describes j -th exiting pulse of duration τ_j ; H is the Hamiltonian, which includes Zeeman and dipole interactions; ψ and ϕ are eigenfunctions for the corresponding operator. The right part of expression (1) contains a great number of elements that is the main problem for calculations. Therefore isochromatic spin groups of detuning $\Delta\omega = 0$ and finite $\pi/2$ or π pulses are considered as a rule.

Using the object-oriented programming tools of C# we developed specialized symbolic processor to compute magnetization (1) for arbitrary pulses and for any detuning $\Delta\omega$. We found also that the result of computation can be presented in compact form using classical magnetization vector and rotation matrices in 10D space. First three dimensions give traditional physical space where magnetic field determines the x_3 axis. Magnetization vector is observable in this 3D space only. Other dimensions are auxiliary mathematical variables. However we can interpret dimensions x_4 and x_5 , together with x_3 , as dipole space. Magnetization precession around x_3 axis with angular velocity given by dipole interactions takes place in this space. The rest five dimensions have a sense of multi-quantum space. Magnetization moves around x_{10} axis with the angular velocity $2\Delta\omega$. Frequency $2\Delta\omega$ corresponds to the change in magnetic quantum number $\Delta m = 2$. Precession with frequency $\Delta\omega$ corresponds to the single-quantum transition $\Delta m = 1$ and takes place in first 3D space.

The First Decade After Zavoisky's Discovery: the EPR Technique in USSR

V. Ptushenko^{1,2}

¹ A. N. Belozersky Institute of Physico-Chemical Biology, Moscow State University, Moscow 199234, Russian Federation, ptush@belozersky.msu.ru

² N. M. Emanuel Institute of Biochemical Physics of Russian Academy of Sciences, Moscow 199334, Russian Federation

Despite of the opinion that EPR discovery was impossible without radar technology, the first setup of E. K. Zavoisky worked in the radio frequency range and used the principles and details of classical radio technique. Nevertheless, the frequencies shifted towards decimeter waves and magnetrons and klystrons soon appeared as the microwave sources in the later works of Kazan scientific school, which contributed substantially to the development of EPR technique during the next years. Another forceful stream in the development of EPR spectroscopy techniques began later (near 1953) in Moscow, in the laboratory of oscillations of the P. N. Lebedev Physical Institute – although not completely independently, but with the arrival of A. A. Manenkov, a PhD student of S. A. Altshuler. The third and seemingly independent branch of the development of the EPR technique was associated with the N.N. Semenov's Institute of Chemical Physics (and namely with L. A. Blumenfeld, V. V. Voevodsky, and A. G. Semenov) and led to the first Soviet industrial EPR-spectrometer RE-1301 in 1961, i.e. decade and a half after Zavoisky's discovery.

Field-Induced Long-Range Magnetic Order in A_2MnTeO_6 ($A = Na, Li, Ag, Tl$)

**G. V. Raganyan¹, E. A. Zvereva¹, V. B. Nalbandyan²,
M. A. Evstigneeva², and A. N. Vasiliev¹**

¹ Faculty of Physics, Moscow State University, Moscow 119991, Russian Federation,
zvereva@mig.phys.msu.ru

² Chemistry Faculty, Southern Federal University, Rostov-on-Don 344090, Russian Federation

We report on the basic static and dynamic magnetic properties of new family triangular lattice 2D magnets A_2MnTeO_6 ($A = Na, Li, Ag, Tl$). All samples demonstrate the similar behavior and don't show a magnetic ordering at ambient conditions down to 2 K. The temperature dependence of magnetic susceptibility nicely follows the Curie-Weiss law in the high temperature range, but implies the wide range of the short-range magnetic correlations and relatively large negative Weiss temperature, which suggests a predominance of antiferromagnetic exchange interactions and a noticeable spin frustration since all compounds don't order up to lowest temperature used.

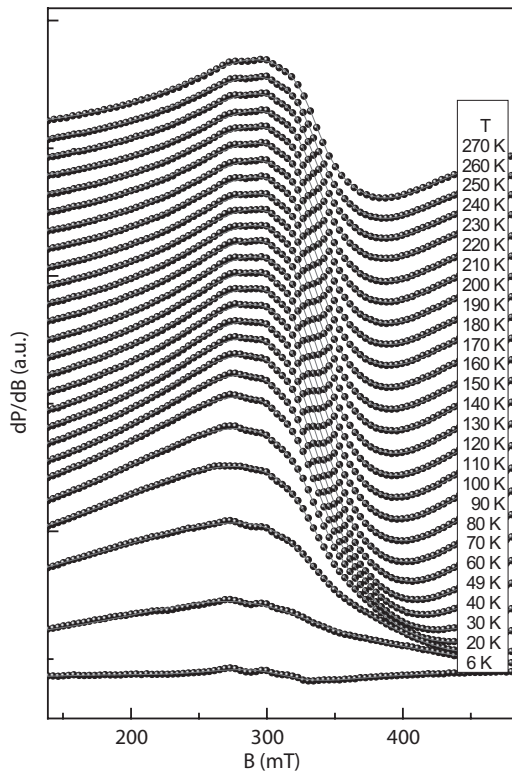


Fig. 1. Evolution of ESR spectra for Na_2MnTeO_6 with temperature.

Nevertheless, in applied magnetic fields the temperature dependence of the magnetic susceptibility is remarkably changed and one can observe a characteristic maximum, which most probably indicates antiferromagnetic ordering. Additional confirmation of the magnetic field effect has been obtained from the ESR data, which clearly show the degradation and disappearance of the resonance signal at helium temperature (Fig. 1). Such a signal fading implies opening of the energy gap for resonance excitations upon approaching the magnetically ordered state. The behavior of ESR linewidth has been analyzed and discussed in terms of critical broadening.

NMR Study a Fragmented Haldane Like Spin-Chains

**T. Salikhov¹, V. Kataev², M. Gunter³, H.-H. Klauss³, E. Zvereva⁴,
V. Nalbandyan⁵, and E. Vavilova¹**

¹ Zavoisky Physical-Technical Institute, 420029, Russia, tmsalikhov@gmail.com

² Leibniz Institute for Solid State and Materials Research IFW Dresden, D-01171, Germany

³ Institute for Solid State Physics, TU Dresden, D-01069, Germany

⁴ Faculty of Physics, Moscow State University, 119991, Russian Federation

⁵ Chemistry Faculty, Southern Federal University, 344090, Russian Federation

Quantum magnetic phenomena in spin networks with reduced spatial dimensions of magnetic interactions is one of the most actual problems in condensed matter physics. The systems where magnetic ions are arranged in 1D structure called spin-chains. One of the important classes of spin chains is the Haldane chain. This is a one-dimensional Heisenberg chain with integer spins and antiferromagnetic (AFM) nearest-neighbor coupling. Here we present the study of 2 samples with different realization of Haldane like chains. First one is $\text{NiCl}_3\text{C}_6\text{H}_5\text{CH}_2\text{CH}_2\text{NH}_3$ with spin-1 and AFM nearest-neighbor interaction. Second one is $\text{Li}_3\text{Cu}_2\text{SbO}_6$ with spins $S = 1/2$ but alternating AFM-FM coupling. If FM coupling stronger than AFM coupling, at some temperature, such system can be consider as a Haldane chains. Because two FM coupling spins with spins $S = 1/2$ behaves like one spin with $S = 1$. In both cases the defects in the chains create the finite size fragments and lead to complex interplay of Haldane like behavior and short range magnetic order.

Magnetic Properties of Mixed-Valent System $\text{LiMn}_2\text{TeO}_6$

**T. Salikhov¹, E. Zvereva², V. Nalbandyan³, R. Sarkar⁴,
H.-H. Klauss⁴, and E. Vavilova¹**

¹ Zavoisky Physical-Technical Institute, 420029, Russia, tmsalikhov@gmail.com

² Faculty of Physics, Moscow State University, Moscow 119991, Russian Federation

³ Chemistry Faculty, Southern Federal University, 344090, Russian Federation

⁴ Institute for Solid State Physics, TU Dresden, D-01069, Germany

The oxides containing manganese in the mixed valence state attract a special interest of scientists [1, 2]. Along with promising practical applications, the manganites are very interesting from the fundamental point of view because they are the prototypes of strongly correlated systems.

Here we present ^7Li NMR study a mixed-valent compound $\text{LiMn}_2\text{TeO}_6$. NMR measurements were done in different magnetic fields from 0.6 T to 6.6 T. Preliminary magnetic measurements indicate the establishment of the anti-ferromagnetic ordering. From NMR spectrums, we assume the internal fields revealing about magnetic structure for this sample.

1. Prodi A., Gilioli E., Gauzzi A., Licci F., Marezio M., Bolzoni F., Huang Q., Santoro A., Lynn J.W.: *Nature Materials* **3**, 48 (2004)
2. Coey M.: *Nature* **430**, 155 (2004)

Magnetic Resonance Investigation in the Polycrystalline Pr_{0.8}Sr_{0.2}MnO₃ Films: Features of the Magnetic States above Curie Temperature

**Yu. Samoshkina¹, M. Rautskii¹, D. Velikanov¹, M. Volochaev²,
A. Sokolov¹, N. Andreev³, and V. Chichkov³**

¹Kirensky Institute of Physics, Federal Research Center KSC SB RAS, Krasnoyarsk 660036,
Russian Federation, uliag@iph.krasn.ru

²Federal Research Center KSC SB RAS, Krasnoyarsk 660036, Russian Federation

³National University of Science and Technology "MISiS", Moscow 119049, Russian Federation

The doped manganites attract the attention associated with the phenomenon of colossal magnetoresistance (CMR) characteristic for these materials [1]. The CMR nature still causes heated discussions, but it is assumed that the magnetic inhomogeneity in the region of phase transition (T_C) play an important role in the CMR formation [2, 3].

In this work, we investigated the polycrystalline films Pr_{0.8}Sr_{0.2}MnO₃ ($d = 20\text{--}150$ nm) in the temperature interval 100–350 K using electron magnetic resonance (EMR) method. The samples were prepared by dc magnetron sputtering with the “facing-target” scheme that allows transferring elements from a target to a substrate without changes in the composition. Single-crystal zirconium oxide stabilized by yttrium (YSZ) was used as the substrate, which has a large mismatch of the crystal lattice with the manganite. The temperature dependences of the magnetic susceptibility and magnetic circular dichroism (MCD) were investigated additionally for Pr_{0.8}Sr_{0.2}MnO₃/YSZ.

The data of the inverse magnetic susceptibility ($1/\chi$) of the samples indicate a low temperature of phase transition ($T_C \sim 115$ K) in contrast to single crystals of the same composition. Above T_C the dependence $1/\chi(T)$ deviates from the Curie Weiss law and the calculated effective magnetic moment is overestimated, that indicates the ferromagnetic inclusions in the paramagnetic region of the samples.

Temperature dependences of the parameters of the observed EMR line (effective g -value, the linewidth, the intensity line, the angular variation of the resonance fields) were investigated separately for the YSZ substrate and for all Pr_{0.8}Sr_{0.2}MnO₃/YSZ samples. The experimental observation in the ranges of $T_C < T < 145$ K is discussed within the framework of the Griffiths theory that predicts the existence of the ferromagnetic correlations short-range order above T_C [4]. It is determine that the strain between the Pr_{0.8}Sr_{0.2}MnO₃ crystallites causes phase separation in the films, thereby understating T_C and extending the boundaries of Griffiths-like phase. The presence of internal phase separation in the films is not excluded, but the dominant role of external phase separation is emphasized that explains the weak dependence of T_C and the borders of the Griffiths-like phase on the thickness of the films.

The samples in the system “film + substrate” above the Griffiths temperature (145 K) also exhibit anomalous paramagnetic behavior, in particular a step

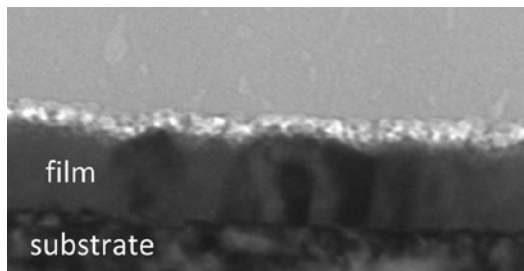


Fig. 1. Electron microscopic image of a cross-section of the $\text{Pr}_{0.8}\text{Sr}_{0.2}\text{MnO}_3/\text{YSZ}$ sample ($d = 30$ nm).

change of the resonance linewidth is observed. The low-field resonance line appears in the EMR spectra additionally. At that, the interface at the boundary film-substrate, estimated earlier, is not observed (Fig. 1). The angular dependences of the resonance field of the EMR lines taken at high temperatures indicate the presence of the magnetic anisotropy in the YSZ substrate.

The characteristic features of the dependence $1/\chi(T)$ and the presence MCD signal at high temperatures suggest the existence of a charge ordering in the films. The possibility of formation of a charge ordering in the samples and nature of the additional EMR line are discussed.

The work was supported by the Russian Foundation for Basic Researches, Grant No. 16-32-00209 mol_a and the Grant of the President of the Russian Federation No. NSh- 7559.2016.2. The reported study was funded by Krasnoyarsk Region Science and Technology Support Fund in the framework of participation in the event: “Modern Development of Magnetic Resonance 2017”.

1. Coey M.D., Viret M., von Molnar S.: *Advances in Physics* **48**, 167 (1999)
2. Salamon M.B., Lin P., Chun S.H.: *Phys. Rev. Lett.* **88**, 197203 (2002)
3. Dagotto E.: *New J. Phys.* **7**, 67 (2005)
4. Griffiths R.B.: *Phys. Rev. Lett.* **23**, 17 (1969)

NMR and Water Molecules Diffusion in Nanochannels of Natrolite

A. V. Sapiga¹ and N. A. Sergeev²

¹ Physical-Technical Institute, V. I. Vernadsky Crimean Federal University, Simferopol 295007, Russian Federation, sapiga_av@mail.ru

² Department of Mathematics and Physics, Institute of Physics, University of Szczecin, Poland, mykola.serheiev@usz.edu.pl

The mobility of water molecules in natrolite ($\text{Na}_{16}\text{Al}_{16}\text{Si}_{24}\text{O}_8 \cdot 16\text{H}_2\text{O}$) has been investigated by a method of the analyses of the NMR spectra shape in a range of temperatures 200–570 K. The mineral natrolite is the typical zeolite with the narrow nanochannels and it is a good model crystal for study of water molecules diffusion by NMR techniques. The analysis of the PMR spectrum shape of ^1H nuclei modification allows to conclude that the process of averaging of PMR spectrum passes in two stages (Fig. 1). In a range of temperatures from 320 K to 350 K in PMR spectrum the averages between doublets 1 and 2, and also doublets 3 and 4 are observed (Fig. 1). In specific case of natrolite when a water molecule jumps between two positions the average value of the intramolecular local magnetic field $b_m = (b_1 + b_2)/2$. Here b_1 and b_2 are the where is intermolecular contribution to the second moment NMR for the first and second positions of water molecule in rigid crystal lattice.

Using the PMR and structural data the possible pathways of water molecules in natrolite channels have been determined. From our results it follows that in natrolite there is the diffusion of water molecules along the Schottky defects and the process diffusion of water molecules is a collective process, participants in whom there are a framework of natrolite, sodium ions and water molecules.

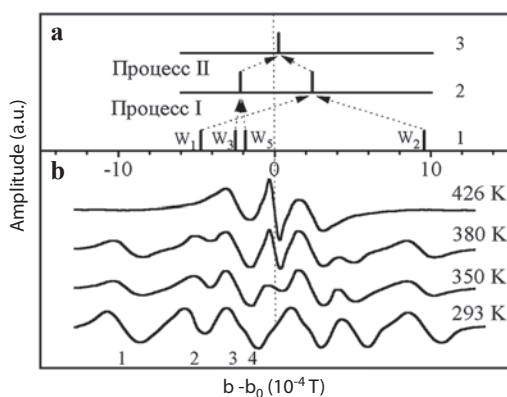


Fig. 1. The temperature modification of PMR spectrum for case when \mathbf{B}_0 has the angle 40° with the c -axis and lie in $[110]$ plane. **a** The diagram of local field averaging. **b** The spectrum shapes for different temperatures. W_1 – W_6 is local field for different position of water molecules. Process I – diffusion along c -axis. Process II – diffusion along $[110]$ direction.

Alignment of Anisotropic Particles by Magnetic Field as Seen by NMR

N. A. Sergeev¹, A. M. Panich², and S. D. Goren²

¹ Department of Mathematics and Physics, Institute of Physics, University of Szczecin, Szczecin 70-451, Poland, mykola.serheiev@usz.edu.pl

² Department of Physics, Ben-Gurion University of the Negev, Be'er Sheva 8410501, Israel, pan@bgu.ac.il

We applied ^{13}C and ^{205}Tl NMR for studying alignment of particles of graphene and high temperature superconductor $(\text{Tl}_{0.5}\text{Pb}_{0.5})(\text{Ba}_{0.2}\text{Sr}_{0.8})_2\text{Ca}_2\text{Cu}_3\text{O}_y$ caused by magnetic field. We found that the field of 8 T causes minor alignment of powder graphene and somewhat better alignment of fluffy graphene particles. Herewith the effect of alignment is well pronounced in ^{205}Tl spectra of the superconducting particles fixed in epoxy in the field of 8 T. This effect is reflected in the ^{205}Tl line shape measured in a magnetic field of 1.17 T and becomes much more pronounced in measurements made in high magnetic field of 8 T. Spectra simulations allow determining the degree of the particles' alignment.

Wide-Band EPR Spectroscopy of the Black Garnets

**G. S. Shakurov¹, V. A. Vazhenin², A. P. Potapov², V. A. Isaev³,
A. V. Lebedev³, and S. A. Migachev¹**

¹Zavoisky Physical-Technical Institute, Russian Academy of Sciences, Kazan 420029,
Russian Federation, shakurov@kfti.knc.ru

²Ural Federal University, Ekaterinburg 620000, Russian Federation

³Kuban State University, Krasnodar 350040, Russian Federation

The crystals of yttrium-aluminum-garnets (YAG) doped with the chromium ions acquire black color under certain conditions of growth. The optical properties of such crystals are usually attributed to tetravalent state of the chromium in the tetrahedral environment. One of the important applications of black garnets is a passive Q-switch in the laser physics. Although this material has been used in practice for more than 20 years, the EPR spectrum of the Cr⁴⁺ ions in tetrahedral environment is still not registered. There is only one work which studied the Cr⁴⁺ ion in the octahedron by using acoustic paramagnetic resonance [1]. We undertook study of YAG doped with Cr by high-frequency (37–850 GHz) tunable EPR spectroscopy method at the liquid helium temperature. The measurements on the X-band EMX Plus Bruker EPR spectrometer at room temperature were also carried out. Two crystals of “black” garnet were investigated. The first sample (N1) was grown in NII Polyus (Moscow) and had chromium concentration 0.5%, the second crystal (N2) with 0.15% chromium and 0.5% neodymium was grown in Kuban State University (Krasnodar).

In both crystals, EPR signals belonging to the Cr³⁺ ions in the octahedral positions were registered. The line widths of Cr³⁺ in the N2 crystal were more narrow than in N1 one. The weak lines from Fe³⁺ ions (N1, N2) in the X-band and EPR spectrum from Nd³⁺ (N2) were also observed. Besides, using tunable EPR spectrometer, we found signals that belong to the non-Kramers ions. These EPR lines are caused by transitions between ground and exciting levels with zero-field-splittings values within frequency region 40–60 GHz. The number of centers and their intensity in crystals N1 and N2 were different. The angular diagrams, field frequency dependencies and possible origin of non-Kramers ions are discussed in the report.

1. Akhmadullin I.Sh. *et al.*: *Fizika Tverdogo Tela* **33**, 2546 (1991)

The Study of the Receptor Properties of Decasubstituted Pillar[5]arenes to Fluorescein dye by Methods of the High Resolution NMR Spectroscopy

**P. Skvortsova^{1,2}, D. Shurpik², I. Stoikov², Y. Zuev¹,
and B. Khairutdinov^{1,2}**

¹ Kazan Institute of Biochemistry and Biophysics, Kazan 420111, Russian Federation, skvpolina@gmail.com

² Kazan Federal University, Kazan 420008, Russian Federation, public.mail@kpfu.ru

Dyes has found a variety of applications in science and technology. In our studies, we used a fluorescein (**A**) dye from the triarylmethane group. Fluorescein has found wide application in the textile industry, it is used to study the pathways of groundwater. Fluorescein is widely used in biochemistry and molecular biology as biological paints for the determination of antigens and antibodies. Thus, the development of a universal system that allows the reversible binding of fluorescein will open the way for the creation of controlled fluorescent containers of targeted drug delivery. This will, in turn, allow visualization of the pathways of drug agent penetration into the cell.

Pillar[5]arenes are a new class of paracyclophanes, that they are able to bind both low-molecular and high-molecular substrates, including dyes, mainly due to electrostatic and hydrogen interactions, forming various associates.

In the work the decasubstituted pillar[5]arenes **1** and **2**, containing amide and ammonium fragments, was studied by high resolution NMR spectroscopy. The NMR spectra of the compounds were completely assigned using homo- and heteronuclear correlation experiments: ¹H-¹H COSY, ¹H-¹H NOESY, ¹H-¹³C HSQC, ¹H-¹³C HMBC. The formation of the pillar[5]arene complex with the fluorescein was shown by NMR diffusometry and two-dimensional NOESY spectroscopy. The stoichiometry of the resulting complex was confirmed by UV spectroscopy.

The work was supported by the Russian Foundation for Basic Research No. 17-03-00858a.

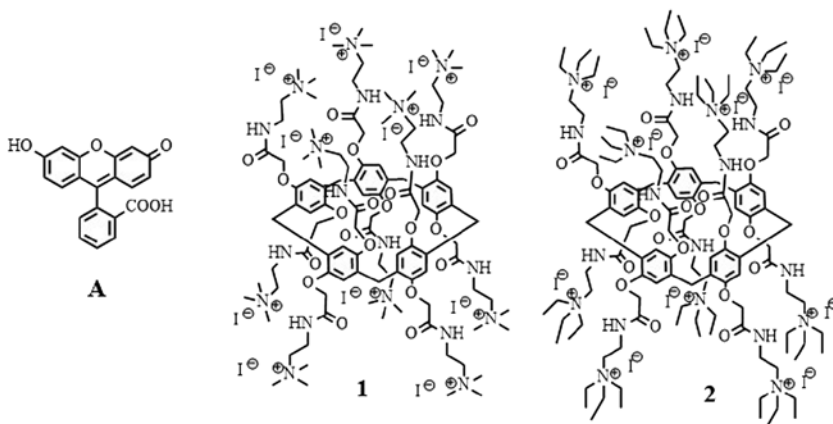


Fig. 1. Structure of the investigated pillararenes.

Photo-Induced States of Copper Complexes of Coproporphyrin I: from Monomer to Dimer Systems

A. A. Sukhanov¹, Y. E. Kandrashkin¹, L. I. Savostina^{1,2},
V. K. Voronkova¹, and V. S. Tyurin³

¹Zavoisky Physical-Technical Institute, Russian Academy of Sciences, Kazan 420029, Russian Federation, vio@kfti.knc.ru

²Kazan Federal University, Kazan 420008, Russian Federation, lusavostina@gmail.com

³A. N. Frumkin Institute of Physical Chemistry and Electrochemistry RAS, Moscow 119071, Russian Federation

Natural metalloporphyrins are very important types of compounds being key fragments of enzymes, hemoglobin, photosynthetic center. Synthetic derivatives of natural metalloporphyrins found wide applications in many fields of science and technology, and especially important in medicine. Metal complexes of coproporphyrin I (CPP-I) possessing four carboxyl groups are of particular interest due to their increased hydrophilicity providing solubility in aqueous solutions which is beneficial for their applications as sensitizers in medicine [1]. In addition, carboxyl groups can interact with each other forming supramolecular ensembles, consequently CCP-I complexes are remarkable supramolecular building blocks.

Multiporphyrin systems have new properties compared with their monomeric fragments. At the same time, there is practically no data on electron spin polarization (ESP) in such systems. This is especially true for metalloporphyrins with paramagnetic ions. We previously studied the supramolecular compounds based on 5-(4'-(aza-15-crown-5)-phenyl) copper porphyrin (CuP), that are capable for dimerization [2]. As far as we know, this is the only example of observation of photo-induced states of the copperporphyrin dimer.

In this work we present the study of copper (II) complex of CCP-I (CuCCP-1) which has the ability to form dimers in certain solvents. The CW EPR spectra of the CuCPP-1 complex unambiguously show the presence of only monomeric

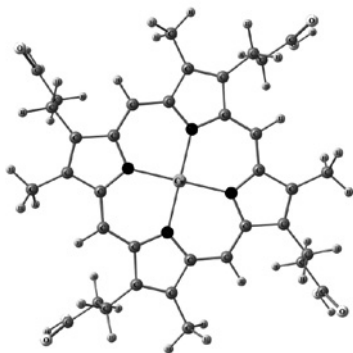


Fig. 1. Molecular structure of CuCCP-1 monomer complex calculated using DFT method.

complexes in *o*-terphenyl and monomeric and dimeric complexes in solutions of mixture of chloroform and isopropanol. It was established that between copper ions in the dimer an antiferromagnetic exchange interaction is realized whose value is not less than 1 cm^{-1} .

The experimental spectra of CuCCP-1 after photoexcitation in different solutions were fitting with calculated ones and their time dependences and electron spin polarization were analyzed.

This work was supported by the Russian Foundation for Basic Research (project No. 16-03-00586)

1. Tyurin V.S., Erzina D.R., Zamilatskov I.A., Chernyadiev A.Yu., Ponomarev G.V., Yashunskiy D.V., Maksimova A.V., Krasnovskiy A.A., Tsivadze A.Yu.: *Macroheterocycles* **8**, no. 4, 376–383 (2015)
2. Kandrashkin Yu.E., Iyudin V.S., Voronkova V.K., Mikhailitsyna E.A., Tyurin V.S.: *Appl Magn Reson.* **44**, 967–981(2013)

Distance between Separated Charges in the Ion-Radical Pair $P_{700}^+A_1^-$ of the Photosystem I Reaction Center Complex Incorporated into Trehalose Matrix at Different Dehydration Levels Measured Using Out-of-Phase ESEEM

A. A. Sukhanov¹, M. D. Mamedov², A. Yu. Semenov²,
and K. M. Salikhov¹

¹ Zavoiskey Physical-Technical Institute, Russian Academy of Sciences, Kazan 420029, Russian Federation, ansukhanov@mail.ru

² A. N. Belozersky Institute of Physical-Chemical Biology, Moscow State University, Moscow 119992, Russian Federation

Disaccharide trehalose is known as an outstanding protector of the proteins against denaturation induced by freezing, heating, and drying. The extreme stabilization of proteins incorporated into trehalose glasses stems from the dramatic hindering of internal protein dynamics, which prevents loss of the native structure [1]. Recently, the coupling between light-induced electron transfer and protein-solvent dynamics in photosystem I (PS I) was studied at room temperature by incorporating this large protein complex into trehalose glasses at different hydration levels [2].

In the present work, we have tested the distance between the photooxidized PS I primary donor P_{700}^+ and the phylloquinone acceptor A_1^- incorporated into dry trehalose matrices (trehalose/PS I molar ratio – 40.000:1) by measuring the EPR signals in the Q-band using ELEXSYS E580 spectrometer (Bruker). Rehydration of the sample was performed at room temperature and was achieved by exposing matrices to saturated LiCl and $MgCl_2$ aqueous solutions in order to equilibrate them at humidity $r = 11\%$ and $r = 33\%$, respectively [2]. Equilibration of the samples was completed in 14 days. Light excitation was achieved by a Nd:YAG laser (Quantel), with energy 3 mJ per pulse. The distance between separated charges in $P_{700}^+A_1^-$ radical pair was measured using the out-of-phase ESEEM technique at room temperature [3]. The results obtained show that the distances between separated charges at relative humidity $r = 11\%$ and $r = 33\%$ humidity is different.

We are grateful to the Russian Foundation for Basic Research (project No. 15-43-02538) for partial financial support. We are thankful to Prof. K. Moebius for helpful advises.

1. Cordone L. *et al.*: *Curr. Org. Chem.* **19**, 1684–1706 (2015)
2. Malferrari *et al.*: *Biochim Biophys Acta* **1857**, 1440–1464(2016)
3. Salikhov K.M., Kandrashkin Yu.E., Salikhov A.K.: *Appl. Magn. Reson.* **3**, 199 (1992)

EPR Study of Al₂Er₂ Molecular Cluster

A. A. Sukhanov¹, Y. Peng², V. K. Voronkova¹, and A. K. Powell²

¹ Zavoisky Physical-Technical Institute, Russian Academy of Sciences, Kazan 420029, Russian Federation, ansukhanov@mail.ru

² Institute of Inorganic Chemistry, Karlsruhe Institute of Technology, Karlsruhe 76131, Germany

The study of single molecule-magnets (SMMs) have attracted widespread attention in the past decades because each individual molecule of SMMs can act as a single-domain nanomagnet at a certain blocking temperature in the absence of an external magnetic field, retaining its magnetization once magnetized [1]. Most known SMM are molecular clusters and the time of conservation of the magnetization depends both on the isotropic and on the anisotropic spin-spin interactions between the paramagnetic centers in the cluster. Now, the chemistry of coordination clusters is aimed at developing of design a new clusters with a view towards the synthesis and investigation of the SMM based on 3d- and 4f-ions [2].

Previously, we investigated tetranuclear Fe₂Dy₂ clusters that exhibit SMM property [3] in this work we represent investigation of new 3d-4f cluster Al₂Er₂ by electron paramagnetic resonance (EPR) spectroscopy. The EPR measurements of polycrystalline samples were made in X, Q, W-band in the 60–5 K temperature range. The free Er³⁺ ion has a 4f¹¹ configuration with a ⁴I_{15/2} ground state. In a crystal field of low symmetry, the ground state ⁴I_{15/2} splits into eight Kramers doublets. Since only the lowest doublet is populated at liquid helium temperature, the ground spin state of Er³⁺ ion can be described by a effective spin $S = 1/2$. The low-temperature spectra of Al₂Er₂ cluster were described in the model taking into account the spin-spin interaction between two Er³⁺ ions isotropic part of which results in the singlet ($S = 0$) and triplet ($S = 1$) multiplets. This model is well described EPR spectra in X-band but for Q- and W-bands this model isn't correct. We suppose that that forbidden transitions between triplet and singlet multiplets in the EPR spectrum are observed in Q- and W- bands. This is possible in the model taking into account the spin-spin interaction between two Er³⁺ ions and hyperfine interaction. Observation of the forbidden transitions in the EPR spectrum is possible when the spin-spin and hyperfine interactions are of the same value. Erbium has five even isotopes ¹⁶²Er, ¹⁶⁴Er, ¹⁶⁶Er, ¹⁶⁸Er, and ¹⁷⁰Er, with nuclear spin $I = 0$ and a total natural abundance of 77.05%, and one isotope, ¹⁶⁷Er, with nuclear spin $I = 7/2$ (natural abundance 22.95%). The ratios of the values of the exchange interaction and the hyperfine interaction will be established from the simulation of the EPR spectra.

We are grateful to the Program of the Presidium of RAS No. 1.26 for partial financial support.

1. Gatteschi D., Sessoli R., Villain J.: Molecular nanomagnets, Vol. 5. Oxford University Press on Demand 2006.
2. Tang J., Zhang P.: Lanthanide single molecule magnets. Springer 2015.
3. Baniodeh A., Lan Y., Novitchi G., Mereacre V., Sukhanov A., Ferbinteanu M., Voronkova V., Anson C.E., Powell A.K.: Dalton Transactions **42**, 8926–8938 (2013)

Triplet State Delocalization in Zincporphyrin Dimer Probed by TR EPR

A. A. Sukhanov¹, V. K. Voronkova¹, and V. S. Tyurin²

¹ Zavoisky Physical-Technical Institute, Russian Academy of Sciences, Kazan 420029, Russian Federation, vio@kfti.knc.ru

² A. N. Frumkin Institute of Physical chemistry and Electrochemistry RAS, Moscow 119071, Russian Federation

Synthetic derivatives of natural metalloporphyrins found wide applications in many fields of science and technology, and especially important in medicine [1]. The study of the spin processes in photoexcited conjugated metalloporphyrins may be crucial for search for new classes of the light-controlling magnetic molecular systems. In this work we present the results of time-resolved EPR (TR EPR) study of zinc (II) complex of CCP-I aimed at determining the possible delocalization of triplet states and the transfer of photoexcitation in these systems. Information on extent of triplet state delocalization was obtained from the zero-field splitting (ZFS). The TR EPR measurements were carried out on an X-band EPR Eleksys E-580 spectrometer (Bruker). Light excitation of the samples was achieved by a Nd:YAG laser (Brilliant B Quantel), with energy 10 mJ per pulse to the sample and repetition rate 10 Hz. Samples for EPR experiments were prepared by dissolving ZnCPP-1 complex in *o*-terphenyl and in mixture of chloroform and isopropanol. In the first case, only monomer complexes are expected to form, in the latter case monomer and dimer complexes are expected. This is confirmed by TR EPR data. A significant decrease of the ZFS parameters and change of polarization sign in the dimer complex is established.

This work was supported by the Russian Foundation for Basic Research (project No. 16-03-00586)

1. Smith K.M.: Porphyrins and Metalloporphyrins. Amsterdam: Elsevier 1972; The Porphyrin Handbook (K. M. Kadish, K. M. Smith, R. Guilard, eds.). New York: Academic Press 2000.

EPR Study of Ribosomal Translational Complexes

**I. Timofeev^{1,4}, O. Krumkacheva^{1,4}, A. Kuzhelev^{1,3,4}, A. Malygin^{2,4},
D. Graifer^{2,4}, M. Meschaninova², A. Ven'yaminova², M. Fedin^{1,4},
G. Karpova^{2,4}, and E. Bagryanskaya^{3,4}**

¹ International Tomography Center SB RAS, Novosibirsk 630090, Russian Federation,
ivan.timofeev@tomo.nsc.ru

² Institute of Chemical Biology and Fundamental Medicine SB RAS, Novosibirsk 630090,
Russian Federation

³ N. N. Vorozhtsov Novosibirsk Institute of Organic Chemistry SB RAS, Novosibirsk 630090,
Russian Federation

⁴ Novosibirsk State University, Novosibirsk 630090, Russian Federation

mRNA provides genetic information in the course of translation – process of protein synthesis handled by supramolecular ribosomal complexes. As far as conformational changes are highly involved in regulation of the protein synthesis, the studying of structural dynamics of ribosome and its ligands is of importance for understanding of the process. Recently, DEER/PELDOR was employed for determining structural changes of mRNA analog being part of ribosomal complexes and for evaluating dynamic properties of ribosomal ligands [1].

In this work, to model a structured mRNA, we used a doubly spin-labeled 11-mer RNA UGUGUUCGACA, which bore nitroxide spin labels at the C5 atom of the 5'-terminal uridine and at the C8 atom of the 3'-terminal adenosine. Applying DEER/PELDOR we studied complexes of a human 80S ribosome with participation of the mRNA, which formed codon-anticodon interactions with tRNAs fixed at ribosomal E, P, A sites.

The measurement of intramolecular distances in the mRNA allowed establishing the fundamental differences between the conformations of the mRNA fixed at ribosomal mRNA-binding site by codon-anticodon interaction with P site-bound tRNA and the mRNA associated with the ribosome in the absence of tRNA. We revealed that the A and E site-bound tRNAs contribute to the stability of the ribosomal complexes. Obtained data allowed making conclusion concerning the absence of codon-anticodon interaction at the E site.

The work was supported by Russian Science Foundation (No. 14-14-00922).

EPR Study of Light-Induced Metastable States in Two-Spin $\text{Cu}(\text{hfac})_2\text{L}^{\text{R}}$ Compounds

**S. Tumanov^{1,2}, M. Fedin^{1,2}, S. Veber^{1,2}, S. Tolstikov¹, N. Artiukhova¹,
and V. Ovcharenko¹**

¹ International Tomography Center SB RAS, Novosibirsk 630090, Russian Federation

² Novosibirsk State University, Novosibirsk 630090, Russian Federation

Molecular magnets $\text{Cu}(\text{hfac})_2\text{L}^{\text{R}}$, where hfac is hexafluoroacetylacetonate and L^{R} is nitronyl-nitroxide radical, undergo thermo- and light-induced phase transitions. Within the transition, the magnetic moment changes, along with the geometry and character of exchange interaction in spin clusters. Similarity of magnetic effects in $\text{Cu}(\text{hfac})_2\text{L}^{\text{R}}$ to classical spin-crossover caused a significant scientific interest to these systems. Namely, some of them experience LIESST effect at cryogenic temperatures. Previously mostly $\text{Cu}(\text{hfac})_2\text{L}^{\text{R}}$ with three-spin exchange clusters were studied. In 2015 we obtained first results proving photo-switching in polymeric compounds containing two-spin exchange clusters [1]. Therefore, the purpose of the present work was to establish relationships between structures of two- and three-spin compounds and their magnetic properties.

Method of Continuous Wave Electron Paramagnetic Resonance spectroscopy was used due to high sensitivity to the magneto-structural transitions in $\text{Cu}(\text{hfac})_2\text{L}^{\text{R}}$. We studied two different two-spin systems with different structure and magnetic moment behavior and one three-spin system for comparison. We found significant difference in relaxation parameters of two-spin systems from self-decelerating relaxation of three-spin systems [1]. Namely, two-spin compounds feature extremely high stability of photoinduced states in the temperature range 5–20 K, with relaxation rate up to 200 hours. We showed that the origin of long relaxation is not the cooperativity effect, but high energy barrier between light-induced and ground states. In its turn, high energy barrier is caused by stronger structural distortion of two-spin exchange cluster. Namely, difference in Cu-O distance within exchange spin cluster between light-induced and ground states is greater for two-spin systems than for the three-spin analogues. This work has been supported by FASO Russia (project 0333-2016-0001), RFBR (No. 15-03-07640 and 17-33-80025) and the RF President's Grant (MK-3597.2017.3)

1. Veber S. *et al.*: Inorganic Chemistry **54**, no. 7, 3446–3455 (2015)

2. Fedin M. *et al.*: Inorganic Chemistry **51**, no. 1, 709–717 (2012)

Electrically Detected FMR of Permalloy Microstrip via Spin Rectification Effect

M. Vafadar¹ and **B. Rameev^{1,2}**

¹ Physics Department, Gebze Technical University, Gebze, Kocaeli 41400, Turkey, mortezavafadar@gmail.com

² Zavoisky Physical-Technical Institute, Russian Academy of Sciences, Kazan 420029, Russian Federation

Ferromagnetic microstrip of Permalloy (Py) under externally-applied magnetic field, shows anisotropic magnetoresistance (AMR) – a type of electric resistance, which depends on the direction of magnetization with respect to the current direction. Ferromagnetic resonance (FMR) of a sample excited by a microwave field will lead to an oscillating resistance, which can couple nonlinearly to an oscillating current and produce a rectified dc voltage. This so-called spin rectification effect provides a novel technique for the study of magnetization dynamics by electrical detection.

New generation of FMR spectroscopy technique uses the microwave fields produced by a coplanar waveguide (CPW) located near the micro- or nano-patterned magnetic sample. Lock-in technique is usually used to measure the spin rectified dc voltage. Electrical detection by spin rectification serves as a powerful tool to investigate spin dynamics in monolayer nano-structured samples since this technique: 1) can provide a high microwave field density due to small distance between the CPW and sample, 2) has a voltage signal, which is independent of sample volume, but depends on sample resistance and can be tailored by careful device fabrication, and 3) uses the highly sensitive measurements of lock-in amplification which can detect voltages down to the several nV scale [1].

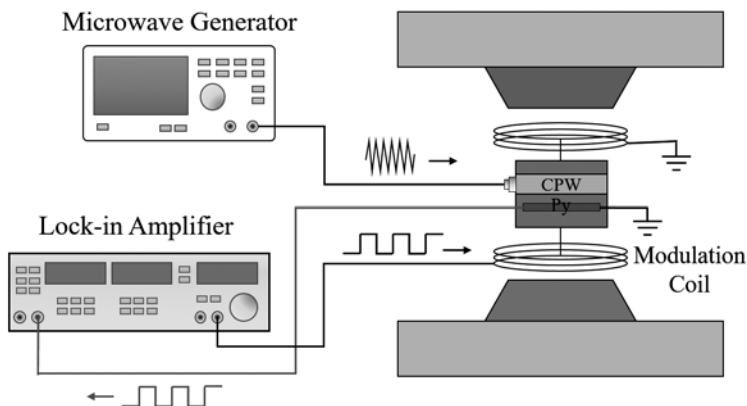


Fig. 1.

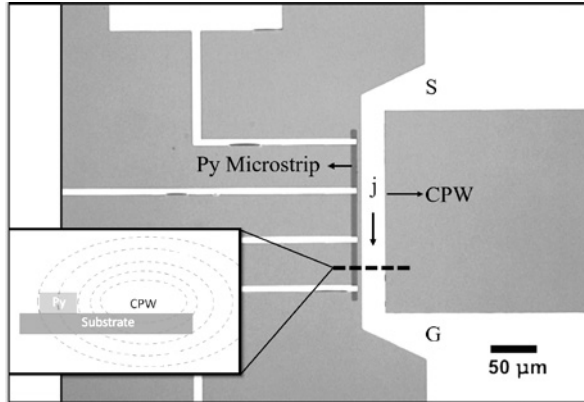


Fig. 2.

The schematic of measurement setup is shown in Fig. 1. A modulation coil, around the sample, is connected to reference output of lock-in amplifier. The reference signal modulates the induced dc current, which then can be detected by lock-in with high accuracy.

The dynamic magnetization, which leads to oscillating resistance, is driven by a time dependent magnetic field, $h_0 \cos(\omega t + \varphi)$, where φ is the relative phase between microwave electric and magnetic fields. Relative phase φ determines a lineshape of the electrically detected FMR signal. To properly analyze the FMR lineshape, φ has to be determined for each frequency independently [2]. In this study, different experimental configurations namely various Py strip lengths and distances from CPW were tested at various frequencies. In fabrication process of the device (Fig. 2) magnetron sputtering and photolithography technique were used.

Spin rectification effect can play significant role in novel technologies like *microwave sensing*, imaging, and wireless energy harvesting (converting microwave frequency fields into a dc power source). Thanks to high phase sensitivity of discussed FMR technique it can be used as spintronic phase *sensing* devices [3]. In one example, the slight shifts of a microwave source phase were used to obtain near-field microwave imaging of the dielectric grating with the channels containing a mixture of water and isopropyl alcohol [4].

This work was supported by NATO Science for Peace and Security Programme, NATO SPS project No. 985005 (G5005).

1. Harder M., Gui Y., Hu C.-M.: Phys. Rep. May 2016.
2. Harder M., Cao Z.X., Gui Y.S., Fan X.L., Hu C. M.: Phys. Rev. B – Condens. Matter Mater. Phys. **84**, no. 5, 1–12 (2011)
3. Zhu X.F., Harder M., Wirthmann A., Zhang B., Lu W., Gui Y.S., Hu C.-M.: Proc. SPIE – Int. Soc. Opt. Eng. **7995**, 1–6 (2011)
4. Wirthmann A., Fan X., Gui Y.S., Martens K., Williams G., Dietrich J., Bridges G.E, Hu C.M., Phys. Rev. Lett. **105**, no. 1, pp. 1–4 (2010)

Spin Properties of [Fe(Salten)Cl] Complex Solutions Studied by NMR and EPR

**M. Volkov, O. Turanova, E. Milordova, E. Frolova,
I. Ovchinnikov, and A. Turanov**

Zavoisky Physical-Technical Institute, Russian Academy of Sciences, Kazan 420029,
Russian Federation, mihael-volkov@yandex.ru

Interest in the [Fe(Salten)Cl] complex is caused by its active use as a precursor for synthesis of both mono and polynuclear complexes with a spin state variation: high-spin (HS) $S = 5/2$, low spin (LS) $S = 1/2$ and spin crossover (HS \leftrightarrow LS) properties. As a result of measurements carried out by EPR and magnetic susceptibility, it was noted that the investigated compound exists only in the HS state in solid state in a wide temperature range of 5–300 K.

The spin properties of this compound in solutions have not been studied, although during the preparation of the solution a visual change in the color of the solution from purple to violet is observed.

EPR measurements of vitrified precursor solutions in acetonitrile and in a mixture of chloroform/toluene solvents (1:1) allowed us to detect the coexistence of HS and LS states of Fe(III) centers in the temperature range of 5–200 K. At the same time a significant solvent effect on the amount of LS fraction was found. It turned out, that in a strongly polar acetonitrile the number of LS complexes substantially exceeds that in the chloroform/toluene mixture. The EPR spectral lines of liquid precursor solutions are considerably broadened, that makes it impossible to accurately determine the ratio of HS and LS fractions.

For measuring the volume magnetic susceptibility of the tested samples in solutions the method of “stationary coaxial ampoule” was used [1]. The value of the magnetic susceptibility of the tested substance is linearly related to the splitting of the signal from the standard caused by the form factor. In this paper an acetone was used as a standard substance. NMR spectra were recorded on ^{13}C nuclei. It was found that at $T = 235$ K the paramagnetic contribution from the precursor dissolved at a concentration of 3 mmol/l in acetonitrile is almost half of that in the chloroform/toluene mixture. It confirms the fact that there is an approximately equal amount of the HS and LS fractions in the first case and there is the predominance of the HS state in the second case.

1. Vul'fson S.G.: Molecular Magnetochemistry, 261 p. Moscow: Nauka 1991.

Nanoscale Magnetic Resonance Imaging of Intracellular Proteins

**P. Wang, S. Chen, M. Guo, S. Peng, M. Wang, F. Shi,
X. Rong, J. Su, and J. Du**

CAS Key Laboratory of Microscale Magnetic Resonance and Department of Modern Physics,
University of Science and Technology of China, Hefei 230026, China
Hefei National Laboratory for Physical Sciences at the Microscale, University of Science and
Technology of China, Hefei 230026, China
Synergetic Innovation Center of Quantum Information and Quantum Physics, University of Science
and Technology of China, Hefei 230026, China
wpf@ustc.edu.cn

In past decades, magnetic resonance imaging (MRI) has made a great success with noninvasive spatial evaluation of tissues and organs in life science. However, the conventional MRI has a resolution of much worse than a single cell even with the state-of-the-art technology [1, 2] and hence is unable to resolve the intracellular molecules or analyze their structure in the nanoscale. We demonstrate MRI of in-situ ferritin proteins inside a human liver cancer cell (HepG2) by using a single electron spin of nitrogen vacancy centre in diamond as a probe under ambient conditions with ~ 10 nanometer resolution. We fix the cells by high pressure freezing and substituting the water by resin and therefore keep the in-situ structure and distribution of proteins. The single spin probe scans over the cross section of the the ferric ions in the ferritin. The ferritins are found to assemble to the clusters in the cytoplasm, which is further verified by imaging their ion cores under the transmission electron microscope. The progress on MRI enables a new capability for imaging the biomolecular distribution and analyzing structures in situ and the 3-dimensional MRI tomography of a single cell under ambient conditions with several molecular resolution.

1. Aguayo J.B. *et al.*: Nature **322**, 190 (1986)
2. Paul G., Sir Peter M.: Rep. Prog. Phys. **65**, 1489 (2002)

Diluted Iron Oxide in $K_2O-Al_2O_3-B_2O_3$ Studied Method EPR

I. V. Yatsyk^{1,2}, R. M. Eremina^{1,2}, P. S. Shirshnev³, and F. G. Vagizov²

¹ Zavoisky Physical-Technical Institute, Russian Academy of Sciences, Kazan 420029, Russian Federation, i.yatsyk@gmail.com

² Kazan Federal University, Kazan 420008, Russian Federation

³ Saint Petersburg National Research University of Information Technologies, Mechanics and Optics (ITMO University), St. Petersburg 197101, Russian Federation

Great interest in borate glasses and crystals is due to attractive physical properties. In particular, the borate compounds, un-doped and doped with rare-earth and transition elements, are very promising materials for nonlinear optics, quantum electronics and laser technology [1, 2], scintillators and thermoluminescent dosimeters [3], detectors and transformers of the ionizing radiation [4]. We investigated the $K_2O-Al_2O_3-B_2O_3$ (KAB) glasses. The first sample was doped

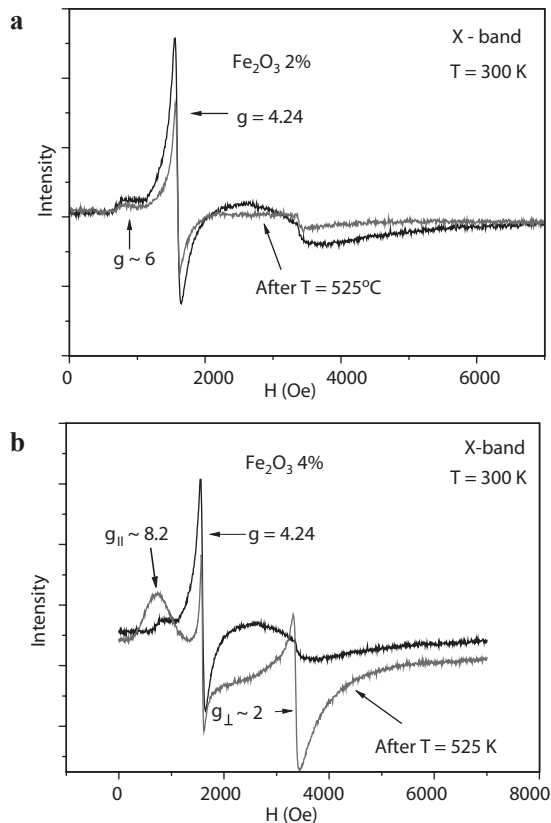


Fig. 1. The ESR spectra in KAB glasses with Fe_2O_3 : **a** 2% and **b** 4%, before and after annealing.

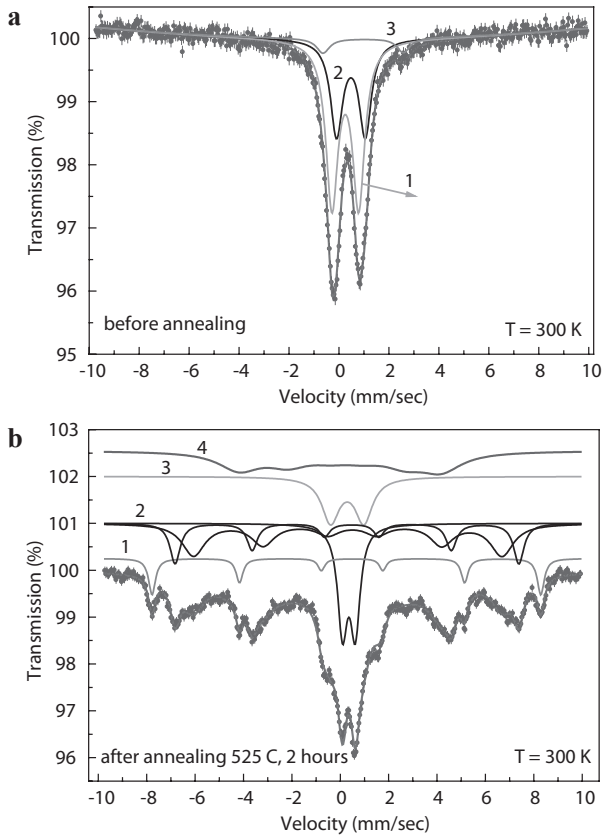


Fig. 2. Mössbauer spectra in KAB: **a** before and **b** after annealing.

by 2% and second sample has 4% Fe_2O_3 iron oxide, the third sample KAB + 4% Fe_2O_3 was annealed 2 hours at 525 °C.

The continuous wave (CW) EPR spectra of iron oxides 2% and 4% before and after annealing were recorded on a Bruker EMX+ spectrometer at the frequency of 9.4 GHz. Three group of signals were observed in magnetic resonance spectra (see Fig. 1). The first line has $g \sim 4.2$. Detailed description of the features of the spin Hamiltonian for the observation of this line are given in the paper [5]. The magnetic resonance lines of complex shapes near $g_{\parallel} \sim 6$ and $g_{\perp} \sim 2$ and with weak intensity were observed in spectra samples before annealing. The line with $g_{\parallel} \sim 6$ was described by transition between level of doublet $|\pm 1/2\rangle$ for Fe^{3+} in octahedron position where term of ground state is ${}^6\text{S}_{5/2}$. The intensity of magnetic resonance signals with $g_{\perp} \sim 2$ and $g_{\parallel} \sim 8.2$ were increased in samples after annealing process. These lines can be connected with ferromagnetic clusters $\alpha\text{-Fe}_2\text{O}_3$ of large size with strong magnetic anisotropy.

A Mössbauer spectra obtained with the Mössbauer spectrometer MS-1104EM at 300 K (see Fig. 2). The Mössbauer spectrum the sample KAB + 4% Fe_2O_3 before annealing at room temperature, is a set of 3 main doublets.

Probably the doublet the No. 1 relates to the atoms of Fe^{3+} in tetrahedral positions. The doublet No. 2 can be attributed to atoms Fe^{3+} in octahedron positions. Probably Fe^{2+} ions were occupied tetrahedral positions for a doublet number 3. After annealing, the Mössbauer spectrum has changed dramatically. The sextets were formed in third sample after annealing. We believe that ferromagnetic clusters ($\alpha\text{-Fe}_2\text{O}_3$) with different size were formed in third sample.

1. Kindrata I.I., Padyaka B.V., Drzewieckia A.: *Journal of Luminescence* **187**, 546 (2017)
2. Babkina A.N., Khodasevicha M.A., Shirshnev P.S.: *Optics and Spectros.* **122**, 214 (2017)
3. Radiat U.A.: *Phys. Chem.* **85**, 23 (2013)
4. Adawy A.E., Khaled N.E., El-Sersy A.R., Hussein A., Donya H.: *Appl. Radiat. Isot.* **68**, 1132 (2010)
5. Kliava J.: *Phys. Stat. Sol. (b)* **134**, 411 (1986)

Temperature Dependence of Resonance Field of EMR Signals in Biological Tissues

S. Yurtaeva¹ and V. Efimov²

¹ Zavoisky Physical-Technical Institute, Russian Academy of Sciences, Kazan 420029, Russian Federation, s.yurtaeva@kfti.knc.ru

² IFMB, KFU, Kazan 420008, Russian Federation, vefimov.51@mail.ru

Presently there are many experimental data about the observation of electron magnetic resonance (EMR) signals in the samples of biological tissues which depend on the orientation of magnetic field. Magnetic resonance characteristics of such signals, ferromagnetic in nature, differ essentially from the other EPR signals, in particular paramagnetic signals connected with Fe ions in proteins. The nature and the source of the signals are still of the interest, as they are the subject of discussion on the origin of spontaneous magnetization in biological tissues. Determination of the source may be useful for bio-medical application as such signals are detected in a number of different biological objects: brain tissues, tumors, pathological and healthy rat tissues, DNA samples, in organs of navigation and magnetoreception in insects, birds and others. Previously in the course of our research such signals were observed in cancer tumors [1], pathological rat tissues [2] and in heart and brain of snail. Such signals accompany the intensive processes of iron accumulation in tissues.

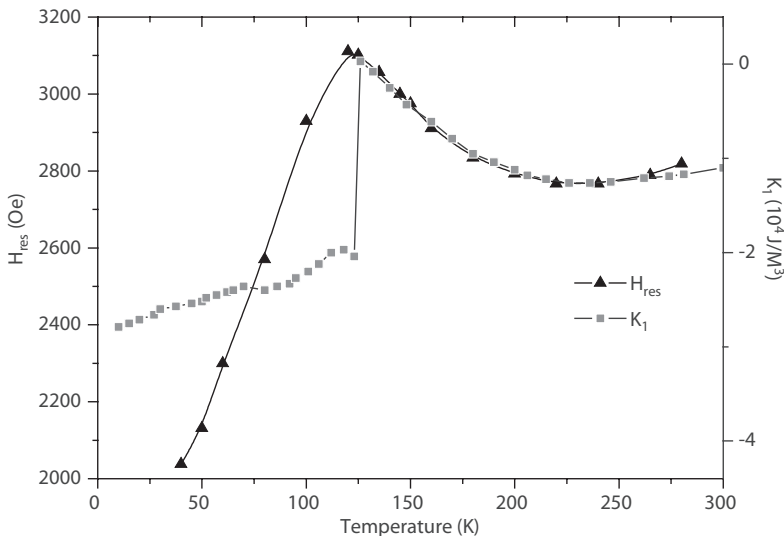


Fig. 1. Typical temperature dependence of resonance field (triangles) and parameter of magneto-crystalline anisotropy of bulk magnetite (squares).

The one of the most important characteristics of the signals is non-monotonic temperature behavior of resonance field (H_{res}) (Fig. 1). When decreasing the temperature from room temperature to helium one H_{res} reaches its maximum value within the interval 100–125 K and further is substantially decreasing.

In the present study the analysis of temperature dependence of resonance field H_{res} was done. Two temperature intervals with the phase transition (PT) at their boundary were found. It was determined that H_{res} anomaly in the vicinity of 100–125 K is due to Verwey PT, character to magnetite crystals. At the temperatures above Verwey PT the high correlation between the temperature dependence of the H_{res} (T) and temperature dependence of magnetite magnetocrystalline constant $|K_1|$ [3], was detected. Correlation coefficient was $\sim 0.95 \div 0.98$.

The peculiarity of magnetite structure at room temperature is the existence of hopping electrons on iron cations. The shape of temperature dependence above Verwey PT is due to hopping mechanism between Fe^{2+} and Fe^{3+} cations. In the temperature interval below Verwey PT, when decreasing the temperature, there is the fixation of electrons in definite position, as a result the crystal structure of magnetite is transformed from cubic to monoclinic and magnetic moment is falling. In EPR spectroscopy this is manifested in decreasing the integral intensity of signal and displacement of the signal to the lower fields. But H_{res} displacement with temperature is not so sharp as magnetocrystalline anisotropy of bulk magnetite (Fig. 1). This may be explained in a following way. Biogenic magnetite is growing in tissues in a form of nanocrystals of a few to hundreds nm size. In decreasing of nanocrystal size Verwey PT temperature may go down. As a consequence, Verwey PT for the particles of different size happens at different temperatures from 124 K (bulk magnetite) to 80 K, as it is known for magnetotactic bacteria. Hence Verwey PT manifestation in temperature dependence H_{res} (T) may be smeared. So despite of the parameter K_1 in bulk-magnetite shows first order Verwey PT, H_{res} demonstrates second order PT. Second order PT for H_{res} (T) may be also connected with non-stoichiometry of crystal structure (the presence of vacancies) an also simultaneous coexistence of two crystal phases high temperature and low temperature phases.

The analysis of the literature showed that the character of temperature dependence H_{res} (T) coincides with the similar temperature dependence for magnetite powder with the particle size from a hundred to more [4]. This fact confirms that EMR signals with temperature dependence H_{res} (T) in Fig. 1. belong to nanocrystalline magnetite. There was also observed the transformation of lineshape from asymmetric Dyson-like shape, confirming hopping conduction higher Verwey PT to symmetric Lorentz one confirming the loss of mobility by electrons.

1. Yurtaeva S.V., Efimov V.N., Silkin N.I. *et al.*: Appl. Magn. Res. **42**, 299–311 (2012)
2. Yurtaeva S.V., Efimov V.N. *et al.*: Appl. Magn. Res. **47**, 555–565 (2016)
3. R. Řezníček, V. Chlan, H. Štěpánková, P. Novák, M. Maryško. J. Phys.: Condens. Matter **24**, 055501 (7pp) (2012)
4. Hagiwara M., Nagata K., Nagata K.: J. Phys. Soc. of Japan **67**, no. 10, 3590–3600 (1998)

^{31}P NMR Spectrum of Rat Blood in Conditions of Spinal Cord Injury

**S. Yurtaeva¹, M. Volkov¹, G. Yafarova^{1,2}, D. Silantieva²,
and E. Yamalitdinova²**

¹ Zavoisky Physical-Technical Institute, Russian Academy of Sciences, Kazan 420029,
Russian Federation, s.yurtaeva@kfti.knc.ru

² Kazan Federal University, Kazan 420008, Russian Federation, gusadila@mail.ru

The secondary damage of tissues in conditions of Spinal Cord Injury (SCI) is an extremely actual problem. Despite of this fact there are not any effective methods of treatment of SCI in acute period. And one of the reasons for this is a multifactor nature of molecular mechanisms of it. Searching for new approaches for SCI treatment motivates investigators for deeper and more detailed study of molecular processes in SCI by using the different new methods, which could give the molecular information about injury processes inaccessible for traditional methods. One of the new approaches to study of SCI mechanisms may become the ^{31}P Nuclear Magnetic Resonance Spectroscopy (NMR) of blood. ^{31}P NMR spectroscopy is a direct non-invasive technique, which allows to characterize phosphorus organic and inorganic substances in blood such as 2,3-diphosphoglycerates, inorganic phosphates, phospholipids, ATP and some others. Phosphorus compounds may reflect the general state of the organism after SCI and so ^{31}P NMR spectroscopy possess prognostic potential.

NMR experiments were performed on an “Avance 400” Bruker NMR spectrometer at the temperature 20 °C. The carrier frequency for ^{31}P nuclei was 162 MHz. The duration of 90° pulses for ^{31}P nuclei was 14 μs . ^{31}P NMR spectrum was obtained within 40 min using 1024 acquisitions. 85% H_3PO_4 signal was used as the chemical shift reference for ^{31}P .

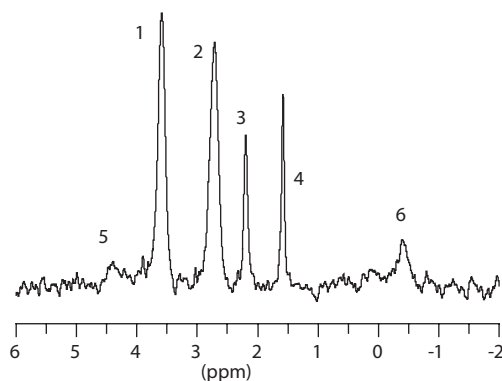


Fig. 1. Typical ^{31}P NMR spectrum of blood of injured rat.

The blood samples of two groups of experimental animals (intact rats and rats after experimental model of spinal cord contusion) were investigated. It is known, that the main signals in ^{31}P NMR whole blood spectra are the signals of 2,3-diphosphoglycerates, inorganic phosphates, phospholipids, ATP and some others [1–3]. In this study in ^{31}P NMR spectra of blood we detected the following intensive signals (Fig. 1): the signals of 2,3-diphosphoglycerates (1, 2 signals), the signals of inorganic phosphates (3, 4 signals) and in some cases weak signals of adenosine monophosphate (AMP) – signal 5, and phospholipids (PL) – signal 6. In the field of negative chemical shifts there were also weak α , β , γ ATP signals, but too weak for quantitative estimation. It is known that the molecules of 2,3-diphosphoglycerates may be used to monitor hypoxia in organism. Increasing in the amount of inorganic phosphates after SCI is regarded as a decrease in the enzymatic activity of 2,3-diphosphoglycerates.

The analysis and comparison of ^{31}P NMR signals of blood of injured and intact rats showed the following results. In the blood of injured rats the increasing of intensities of 2,3-diphosphoglycerate and inorganic phosphate signals were observed, that means the hypoxia in condition of SCI is growing. The relative separation of the 2,3-DPG resonances was about 0.9 ppm and the average relative separation of intra and extracellular inorganic phosphates resonances was about 0.6 ppm. These parameters are connected with the acidity of media. Additionally, in ^{31}P NMR blood spectra of injured rats the remarkable displacement of the most intensive lines 1, 2, 3, 4 to the direction of lower chemical shift values was observed, that indicates the change in acidity of the environment with the reduction of pH. The change of chemical shift varied from 0.1 to 0.4. Such variation of chemical shift corresponded to variation of pH for 0.1÷0.2. ^{31}P NMR spectroscopy allows to estimate the intracellular pH in erythrocytes according to [4]. In control rats it was about 7.2 and in SCI rats about 7.1.

In whole blood samples of injured rats the phospholipids resonances at about $-0.3\div-0.4$ ppm were observed which were usually absent in control rats blood. Additionally in some cases after SCI a weak line of adenosine monophosphate, a product of disruption of ATP, was observed.

Thus, in the acute phase of SCI, the decreasing of energy stability of erythrocytes and the disturbance of the glycolysis process in them were observed. The method of NMR spectroscopy of blood after SCI makes possible to observe the injury processes in dynamics and allows to change tactics of treatment operatively.

The present research was partially supported by Scientific Program of Presidium of RAS 1.26P.

1. Horn M., Neubauer S., Bomhard M. *et al.*: *MAGMA* **1**, 55–60 (1993)
2. Horn M., Kadgien M., Schnackerz K. *et al.*: *J. Cardiovascular Magn. Reson.* **2**, 143 (2000)
3. Lam Y.F., Lin A.K., Ho C.: *Blood* **54**, 196–209 (1979)
4. Moon R.B., Richards J.H.: *J. Biol. Chem.* **248**(20), 7276 (1973)
5. Kim S.W., Charter R.A., Chai C.J., Kim S.K., Kim E.S.: *Paraplegia* **28**, 441 (1990)

Peculiarities of the Application of a Multi-Pulse Sequence for Spin Coherence Control

**R. Zaripov¹, E. Vavilova¹, I. Khairuzhdinov¹, E. Anisimova^{1,2},
T. Salikhov¹, V. Voronkova¹, K. Salikhov¹, M. Abdulmalic³, F. Meva⁴,
S. Weheabby³, T. Ruffer³, B. Büchner^{5,6}, and V. Kataev⁵**

¹ Zavoiisky Physical-Technical Institute, Russian Academy of Sciences, Kazan 420029, Russian Federation, zaripov@kfti.knc.ru

² Kazan Federal University, Kazan 420008, Russian Federation

³ Technical University of Chemnitz, Chemnitz D-09107, Germany

⁴ Department of Pharmaceutical Sciences, University of Douala, BP 2701, Cameroon

⁵ Institute of Solid State Research IFW Dresden, Dresden D-01171, Germany

⁶ Institut für Festkörperphysik, Technische Universität Dresden D-01062 Dresden, Germany

The control of spin coherence is one of the main tasks in the development of quantum computing. The pulse protocols proposed to date for the realization of logical quantum operations imply the use of multi-pulse protocols [1, 2]. Moreover, multi-pulse protocols have recently been actively used in magnetic resonance in dynamic decoupling schemes [3] and as a consequence of a substantial enhancement of the observable in the pulse electron spin resonance (ESR) protocols [4, 5].

In our works, we also used multi-pulse sequences, in particular, the Carr-Purcell-Meiboom-Gill sequence (CPMG) to study spin decoherence mechanisms [6, 7]. One of the main mechanisms of the electron spin decoherence in solids is the spectral diffusion caused by random modulation of the hyperfine interaction with nuclear spins. It was shown [6, 7] that a contribution of the spectral diffusion to the spin decoherence is depending on CPMG sequence parameters. This observation opens a way to the controlled changing of a spin decoherence time, from one side, and it provides a method of recognizing of the spectral diffusion mechanism contribution to the spin decoherence.

However, the application of multi-pulse protocols in solid state NMR and ESR is associated with some difficulties due to the appearance of additional echo signals which complicate the observed signals. The contributions of unwanted echoes and ways to eliminate them are discussed in this work.

This work was supported by the Deutsche Forschungsgemeinschaft through the Focused Research Unit FOR1154 and by the Program of the Presidium of RAS No. 1.26.

1. Cory D.G., Price M.D., Maas W. *et al.*: Phys. Rev. Lett. **81**, 2152 (1998)
2. Volkov M. Yu., Salikhov K.M.: Appl. Magn. Reson. **41**, 145 (2011)
3. Ali Ahmed M.A., Alvarez G.A., Suter D.: Phys. Rev. A **87**, 042309 (2013)
4. Mentink-Vigier F., Collauto A., Feintuch A. *et al.*: J. Magn. Reson. **236**, 117 (2013)
5. Mitrikas G.; Prokopiou G.: J. Magn. Reson. **254**, 75 (2015)
6. Zaripov R.; Vavilova E.; Miluykov B. *et al.*: Phys. Rev. B **88**, 094418 (2013)
7. Zaripov R., Vavilova E., Khairuzhdinov I. *et al.*: Beilstein J. Nanotechnol. **8**, 943 (2017)

Determination of HFI Constants of Cu Oxamato-Complex by ENDOR and ED NMR Techniques

R. Zaripov¹, E. Vavilova¹, I. Khairuzhdinov¹, K. Salikhov¹,
V. Voronkova¹, M. A. Abdulmalic², F. E. Meva³, S. Weheabby²,
T. Ruffer², B. Büchner^{4,5}, and V. Kataev⁴

¹ Zavoisky Physical-Technical Institute, Russian Academy of Sciences, Kazan 420029, Russian Federation

² Technische Universität Chemnitz, Fakultät für Naturwissenschaften, Institut für Chemie, Chemnitz D-09111, Germany

³ Department of Pharmaceutical Sciences, Faculty of Medicine and Pharmaceutical Sciences, University of Douala, BP 2701, Cameroon

⁴ Leibniz Institute for SolidState and Materials Research IFW Dresden, Dresden D-01171, Germany

⁵ Institut für Festkörperphysik, Technische Universität Dresden, Dresden D-01062, Germany

Cu(II)-(bis)oxamato and Cu(II)-(bis)oxamidato complexes have attracted in the recent past substantial attention as precursor materials for the synthesis of the corresponding polynuclear complexes which in their turn have been investigated with regard to the magnetic superexchange interactions between the Cu spins mediated by the O and N ligands [1]. In this context, the transfer of the spin density from the central metal ion to the ligands and next via the oxamato or oxamidato unit bridging two neighbored paramagnetic transition metal ions is important for the maintaining of the superexchange interaction. This transfer also gives rise to the hyperfine (HF) coupling between the Cu electron spin $S = 1/2$ and ^{14}N nuclear spins $I = 1$ which has been studied with ESR techniques in some detail [2].

We have applied the pulse ELDOR detected NMR (EDNMR) and ENDOR techniques to determine the tensors of the transferred Cu ($S = 1/2$) – ^{14}N ($I = 1$) hyperfine interaction (HFI) in single crystal with anionic complex fragments $[\text{Cu}(\text{opba})]^{2-}$ (Fig. 1). We performed simulations of EDNMR and ENDOR data to analyze values of HFI tensors and their relative orientations in the system. We have treated a model electron-nuclear system of the coupled $S = 1/2$ and $I = 1$ spins using the spin density matrix formalism.

1. Abdulmalic M.A., Aliabadi A., Petr A., Krupskaya Y., Kataev V., Büchner B., Hahn T., Kortus J., Ruffer T.: Dalton Trans. **41**, no. 48, 14657–14670 (2012)
2. Zaripov R., Vavilova E., Khairuzhdinov I., Salikhov K., Voronkova V., Abdulmalic M.A., Meva F.E., Ruffer T., Büchner B., Kataev V.: Beilstein J. Nanotechnol. **8**, 943–955 (2017)

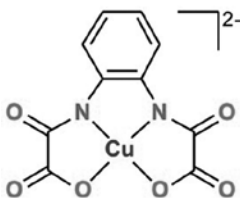


Fig. 1. Chemical structures of the anionic complex fragments $[\text{Cu}(\text{opba})]^{2-}$.

Topological Zero Modes in Few-Layer Nanographenes: EPR, CESR and Magnetic Susceptibility Studies

A. M. Ziatdinov

Institute of Chemistry, Far-Eastern Branch of the Russian Academy of Sciences.
Vladivostok 690022, Russian Federation, ziatdinov@ich.dvo.ru

According to the data of theoretical and experimental [1–5] studies, near zigzag edges of honeycomb carbon structures the π -electronic states with zero energy (topological zero modes) stabilize and the density of edge π -electronic states $D(E)$ at the Fermi level E_F dozens of times exceeds the value of corresponding parameter for macroscopic ordered graphite although the energy of the $D(E)$ maximum is ~ 30 meV less than the E_F [6]. Mentioned modes substantially change known properties of nanosized carbon structures [1–6], but also may initiate essentially new phenomena such as edge magnetism [7] and edge superconductivity [8]. The zigzag edges of single- or few-layer graphene are perfect one-dimensional conductors owing to a set of gapless states that are topologically protected against backscattering and demonstrate atomic limit edge-mode quantum electrical conduction via spin-polarized edge states [9]. Near armchair edges of honeycomb carbon structures similar electronic states do not exist [1–6].

In recent years a new field of research in the technology of nanoscale carbon structures has been developed, which is aimed at fine adjustment of their properties with changing chemical state of peripheral atoms. For instance, the emergence of topological zero modes has been established recently at etching graphenic *armchair* edges by hydrogen [10]. However, with appreciating the significance of those works, up to now the problem of influence of adsorbed molecules (adsorbate) on the edge π -electronic band and, thereby, on the properties of nanosized carbon structures, was not treated properly. At the same time, evidently, this information is important for establishing the reasons and mechanisms of changing the properties of carbon nanostructures under the influence of different reagents, for ranking the factors determining their structural organization, electronic structure and chemical reactivity, as well as for solving problems of practical application.

In this work the results of investigations by EPR, CESR and magnetic susceptibility methods of electronic and magnetic structure of few-layer nanographenes (nanographites) and their changes under the influence of adsorbed molecules and edge covalent bonds are presented. In electronically decoupled nanographenes the presence of specific edge π -electronic states with zero energy (topological zero modes) and reversible decrease of $D(E_F)$ at their interaction with adsorbed molecules of oxygen, chlorine and water have been established. The explanation of discovered effect has been proposed in the terms of model of spin splitting of edge π -electronic states, initiated by transferring small portion of electronic density from nanographites to adsorbed molecules. It has been shown that change in sign of the temperature coefficient of current carrier spin relaxation rate at

presence of adsorbate may be accounted for by their interactions with edge spin-split (magnetically ordered) states. Saturation of free (dangling) σ -orbitals of the edge carbon atoms with chlorine 3p-electrons neither eliminates edge π -electronic states with zero energy nor initiates their spin splitting. However, formation of such covalent bonds changes some characteristics of the current carriers.

This work was supported by the Russian Federal Agency for Scientific Organizations (project No. 0265-2015-0002) and Russian Academy of Sciences (project “Far East”, No. 15-I-3-007).

1. Fujita M., Wakabayashi K., Nakada K., Kusakabe K.: *J. Phys. Soc. Jpn.* **65**, 1920 (1996)
2. Kobayashi Y., Fukui K., Enoki T., Kusakabe K.: *Phys. Rev. B* **71**, 193406 (2005)
3. Ziatdinov M., Fujii S., Kusakabe K., Mori T., Enoki T.: *Phys. Rev. B* **87**, 115427 (2013)
4. Enoki T., Ando T.: *Physics and Chemistry of Graphene: Graphene to Nanographene*, 476 pp. Singapore: Pan Stanford Publishing Pte Ltd., 2013.
5. Ziatdinov A.M.: *Russian Chemical Bulletin* **64**, 1 (2015)
6. Niimi Y., Matsui T., Tagami K., Tsukada M., Fukuyama H.: *Appl. Surf. Sci.* **241**, 43 (2005)
7. Son Y.-W., Cohen M.L., Louie S.G.: *Nature* **444**, 347 (2006)
8. Sasaki K., Jiang J., Saito R., Onari S., Tanaka Y.: *J. Phys. Soc. Jpn.* **76**, 033702 (2007)
9. Kinikar A., Sai T.P., Bhattacharyya S., Agarwala A., Biswas T., Sarker S.K., Krishnamurthy H.R., Jain M., Shenoy V.B., Ghosh A.: *Nature Nanotechnology*, doi:10.1038/nnano.2017.24 (2017)
10. Ziatdinov M., Lim H., Fujii S., Kusakabe K., Kiguchi M., Enoki T., Kim Y.: *Phys. Chem. Chem. Phys.* **19**, 5145 (2017)

AUTHOR INDEX

Abdulmalic, M. A.	198, 199
Abramov, N. N.	26
Adonin, N.	146
Afanasyeva, E. F.	80
Akhmedzhanov, R. A.	48
Akhmetov, M. M.	114
Alakshin, E. M.	41
Aleksandrov, A.	140
Alekseev, A. V.	138
Alfonsov, A.	62
Aliyev, M. N.	111
Andreev, N.	174
Andreev, N. K.	115
Andrianov, V. V.	130
Anikin, A.	71, 140
Anishchik, S. V.	64
Anisimov, N. V.	69
Anisimova, E.	117, 198
Anson, C. E.	53
Archipov, R.	140
Artiukhova, N.	186
Bagryanskaya, E.	9, 185
Baibekov, E. I.	49
Bakirov, M. M.	118, 119, 132, 138
Bakirova, D. R.	148
Balaev, D. A.	42
Baniodeh, A.	53
Batulin, R. G.	127
Bayazitov, A. A.	71
Bennati, M.	105
Berzhansky, V. N.	134
Bittl, R.	12
Bizyaev, D.	103
Blümich, B.	158
Bochkin, G. A.	47
Bogach, A. V.	61
Bogachev, Yu. V.	164
Bogomyakov, A. S.	122

Bolginov, V. V.	26
Bowman, M. K.	17
Bragin, A.	140
Brendler, E.	82
Büchner, B.	62, 198, 199
Bukharaev, A.	103
Bukhtiyarova, G. A.	42
Bunkov, Yu. M.	94
Cemortan, V.	53
Chankina, O. V.	64
Chen, H.	17
Chen, S.	190
Chernyaev, A. P.	69
Chervonova, U. V.	122
Chibotaru, L. F.	53
Chichkov, V.	26, 174
Chirkov, V. V.	119
Chushnikov, A. I.	139
Demishev, S. V.	61, 63
Denisov, G. S.	23, 99
Dolgorukov, G. A.	41
Dolphin, D. H.	44
Domracheva, N. E.	120, 122
Du, J.	190
Dvinskikh, S. V.	56
Dzheparov, F. S.	20
Dzuba, S. A.	80
Efimov, V.	194
Efimova, A. A.	23
Eichhoff, U.	68
Elgabarty, H.	99
Enkin, N.	105
Eremina, R. M.	100, 191
Esin, R. G.	139
Esmaili, A.	111
Evstigneeva, M. A.	32, 170
Fakhrutdinov, A.	71, 140
Falin, M. L.	123, 124
Farhutdinov, A. R.	94
Fattakhov, Ya. V.	71, 140
Fedin, M.	21, 81, 146, 149, 185, 186
Fel'dman, E. B.	47
Filipov, V. B.	61, 63
Fine, B. V.	22
Fowler, B. R.	17
Fraerman, A. A.	28
Frolova, E.	125, 129, 189

Gabbasov, B. F.	111, 127
Gafiyatullin, L.	129
Gafurov, M. R.	83
Gainutdinov, Kh. L.	130
Galeev, R. T.	118
Galukhin, A. V.	83
Garifyanov, N.	102
Gavrilova, T. P.	100
Gemming, S.	82
Gervits, L. L.	69
Gilmanov, M. I.	61, 63
Gilmutdinov, I. F.	127, 142
Gilyazov, L.	140
Gippius, A. A.	134
Glushkov, V. V.	61, 63
Gnezdilov, O.	140
Goenko, I. A.	132
Golovchanskiy, I. A.	26
Golubev, A.	140
Gorbovanov, A. I.	134
Goren, S. D.	177
Gorev, R. V.	36
Gorshenin, M.	140
Gorshenin, S.	140
Goryunov, Yu. V.	136
Gotovko, S. K.	30
Gracheva, I. N.	83
Grafe, H.-J.	62
Graifer, D.	185
Gruzdev, M. S.	120, 122
Gulyaev, M. V.	69
Gumarov, G. G.	114, 119, 132, 138
Gumarov, A. I.	111
Gunter, M.	172
Guo, M.	190
Gusev, N. S.	28
Gushchin, L. A.	48
Hälg, M.	7
Hara, S.	6
Hirao, R.	46
Höger, S.	79
Hosseini, E.	46
Huber, M.	10
Iakovleva, M.	62
Ibragimova, M. I.	139

Idiyatullin, B. Z.	148
Imaev, A.	140
Isaev, V. A.	178
Ivanov, A.	140
Ivanov, D.	140
Ivanov, K.	46, 64
Ivanov, M.	146
Ivanova, T.	125, 142
Iversen, B. B.	150
Iyudin, V. S.	130
Kandrashkin, Y. E.	180
Kanzaki, Y.	44
Karashtin, E. A.	28
Kardash, M. E.	80
Karpova, G.	185
Kataev, V.	60, 62, 172, 198, 199
Kawashima, C.	44
Khabibrakhmanov, I. I.	130
Khabipov, R. Sh.	71, 140
Khaibullina, D. K.	139
Khairutdinov, B.	179
Khairuzhdinov, I.	117, 198, 199
Khalilov, L.	24
Khaliulin, B. M.	111
Khaliullin, G.	11
Khanipov, T.	103
Khasanov, R.	102
Khaymovich, I. M.	27
Khundiryakov, V. E.	71
Kiiamov, A. G.	127
Kinjyo, S.	44
Klauss, H.-H.	172, 173
Klochkov, A. V.	41
Köhler, T.	82
Kokorin, A. I.	88
Kolbanev, I. V.	88
Kolker, A. M.	122
Kolmychek, I. A.	28
Kondratyeva, E. I.	41
Konvalov, D.	140
Konov, K.	100
Konstantinova, E. A.	150, 160
Konygin, G. N.	114, 132
Kopasov, A.	27
Korableva, S. L.	123

Kostina, A. A.	164
Krasnorussky, V. N.	61
Krumkacheva, O.	185
Kuchugura, M. A.	32
Kukovitsky, E.	102, 155
Kupriyanova, G. S.	144, 156, 162
Kurbakov, A. I.	32
Kurganskii, I.	146
Kusova, A. M.	148
Kutovoi, S. A.	100
Kuzhelev, A.	185
Kuzmin, V. V.	41
Kuzmina, D.	149
Latypov, V. A.	123, 124
Le, N. T.	150
Lebedev, A. V.	178
Leushin, A. M.	124
Likhtenshtein, G. I.	86
Lin, W. C.	44
Liou, S.-H.	105
Lis, O. N.	138
Lisin, V. N.	152
Lorenz, W. E. A.	7
Lvov, D. V.	20
Lvov, S.	155
Malygin, A.	185
Mamadazizov, S.	156
Mamedov, M. D.	182
Mamin, G. V.	83
Mamin, R.	167
Mannig, A.	38
Maraşlı, A.	144, 162
Marchenko, Ya. Yu.	164
Martyanov, O. N.	42
Maryasov, A. G.	17, 21
Matsuoka, H.	44, 79
McDowell, C. A.	44
Mel'nikov, A. S.	27
Melnikova, D.	140
Mereacre, V.	53
Meschaninova, M.	185
Meva, F. E.	198, 199
Meyer, D. C.	82
Migachev, S. A.	178
Milordova, E.	129, 189
Mingalieva, L. V.	125, 142, 159
Minnekhanov, A. A.	160

Mironov, V. L.	36
Molin, Yu. N.	64
Mori, N.	44
Mozzhukhin, G. V.	57, 144, 162
Mumdzhi, I.	140
Murzakaev, V.	140
Murzina, T. V.	28
Nakagawa, T.	44
Nakazawa, S.	46
Nalbandyan, V. B.	32, 170, 172, 173
Nateprov, A. N.	136
Nath, R.	62
Neese, F.	79
Nentwich, M.	82
Nikitin, N. P.	111
Nikitin, S.	127, 140
Nikitina, A. V.	164
Nikolaev, B. P.	164
Nishio, T.	44
Nizov, N. A.	48
Nizov, V. A.	48
Nurgazizov, N.	103
Nuzhina, D. S.	41
Ohmichi, E.	6
Ohta, H.	6
Okubo, S.	6
Orlando, T.	105
Orlinskii, S. B.	83
Ovcharenko, V. I.	122, 186
Ovchinnikov, I.	125, 129, 142, 189
Panich, A. M.	40, 166, 177
Pavlov, D.	167
Pekola, J. P.	27
Peng, Y.	159, 183
Peng, S.	190
Petrova, M.	125
Petukhov, V. Yu.	114, 119, 132, 138, 139
Pirogov, Yu. A.	69
Polshakov, V. I.	90
Polulyakh, S. N.	134, 168
Poryvaev, A.	149
Potapov, A. P.	178
Povarov, K. Yu.	7, 38
Powell, A. K.	53, 159, 183
Prihod'ko, S.	146
Ptushenko, V.	169
Pylaeva, S. A.	99

-
- Raganyan, G. V. 32, 170
Rameev, B. Z. 57, 144, 162, 187
Rautskii, M. 174
Retegen, M. 79
Rodionov, A. A. 83
Rong, X. 190
Rüffer, T. 117, 198, 199
Ryazanov, V. V. 26
Rybin, D. S. 114, 132
Sabitova, V. A. 164
Sadikov, A. 140
Safin, T. R. 94
Safiullin, G. M. 124
Safiullin, K. R. 41
Sakhin, V. 102
Sakurai, T. 6
Salikhov, T. 172, 173, 198
Salikhov, K. M. 15, 108, 117, 118, 182, 198, 199
Samarin, A. N. 61, 63
Samarin, N. A. 61
Samartsev, V. V. 152
Samoshkina, Yu. 174
Sapiga, A. V. 176
Sarkar, R. 173
Sato, K. 44, 46
Savostina, L. I. 180
Sayakhov, A. 140
Schiemann, O. 79
Schmitt, L. 79
Sebastiani, D. 99
Semenov, A. V. 61, 63
Semenov, A. Yu. 182
Sergeev, N. A. 166, 176, 177
Shagalov, V. A. 71, 140
Shakurov, G. S. 178
Shegeda, A. M. 152
Shelyapina, M. 156
Shereshevskii, I. A. 27
Shestakov, A. V. 100
Sheveleva, A. 81, 149
Shi, F. 52, 190
Shiomi, D. 44, 46
Shirshnev, P. S. 191
Shitsevalova, N. Yu. 61, 63
Shurpik, D. 179
Silachev, D. N. 69
Silantieva, D. 196

Sinicin, A. M.	109
Sitdikov, I. R.	71
Sitnitsky, A. E.	148
Skirda, V.	140
Skorohodov, E. V.	36
Skourski, Y.	62
Skvortsova, P.	179
Sladkov, K. D.	28
Sluchanko, N. E.	61, 63
Smirnov, A. I.	7, 38
Sobgayda, D. A.	48
Sokolov, A.	174
Soldatov, T. A.	7, 30, 38
Stanislavovas, A. A.	41
Stoikov, I.	179
Streltsov, S. V.	32
Sugisaki, K.	44
Su, J.	190
Sukhanov, A. A.	53, 180, 182, 183, 184
Sungatullina, M. I.	130
Sviridov, D. V.	88
Sviridova, T. V.	88
Svistov, L. E.	30
Syryamina, V. N.	80
Tadokoro, M.	44
Tagirov, L. R.	111
Tagirov, M. S.	14, 41, 94
Takahashi, H.	6
Takui, T.	2, 44, 46
Talanov, Yu.	102
Tanimoto, K.	46
Tarasov, V. F.	16, 100
Teitel'baum, G.	102
Timofeev, I.	185
Tkach, I.	105
Tolstikov, S.	186
Tolstoy, P. M.	23, 99
Toyota, K.	44, 46
Tseytlin, M.	78
Tumanov, S.	186
Tupikina, E. Yu.	23, 99
Turanov, A.	189
Turanova, O.	125, 129, 142, 189
Tyurin, V. S.	180, 184
Ulanov, V. A.	109
Ungur, L.	53

Vafadar, M.	187
Vagizov, F. G.	191
Vakhitov, I. R.	111
Vakhrina, E. V.	160
Vasil'ev, S. G.	47
Vasiliev, A. N.	32, 170
Vavilova, E.	62, 82, 117, 172, 173, 198, 199
Vazhenin, V. A.	178
Vdovicheva, N.	27
Veber, S. L.	21, 81, 186
Velikanov, D.	174
Ven'yaminova, A.	185
Vieru, V.	53
Vins, V. G.	64
Volkov, V. I.	47, 96
Volkov, D. V.	69
Volkov, M.	189, 196
Volochaev, M.	174
Volodin, A. P.	36
Vorobeva, V. E.	120, 122
Voronkova, V. K.	53, 159, 180, 183, 184, 198, 199
Vyalikh, A.	82
Wang, M.	190
Wang, P.	190
Weheabby, S.	198, 199
Weigel, T.	82
Wulf, E.	38
Yafarova, G.	196
Yafarova, G. G.	130
Yakushkin, S. S.	42
Yamalitdinova, E.	196
Yamamoto, S.	46
Yamane, T.	44
Yanilkin, I. V.	111
Yatsyk, I. V.	139, 191
Yokokura, N.	44
Yokoyama, S.	44
Yurtaeva, S.	194, 196
Yusupov, R. V.	111, 127
Zagumennyi, A. I.	100
Zainullin, R. R.	109
Zaripov, R. B.	82, 117, 132, 198, 199
Zavartsev, Yu. D.	100
Zefirov, T. L.	130
Zelensky, I. V.	48
Zheludev, A.	7, 38
Zhou, H. D.	30

Zhukov, I. V.	64
Ziatdinov, A. M.	34, 200
Ziatdinova, N. I.	130
Zick, K.	74
Zschornak, M.	82
Zuev, Yu. F.	148, 179
Zueva, E.	122, 125, 129
Zverev, D.	127, 140
Zvereva, E. A.	32, 170, 172, 173

© Федеральное государственное бюджетное учреждение науки
Казанский физико-технический институт имени Е. К. Завойского
Казанского научного центра Российской академии наук, 2017

Ответственный редактор: В. К. Воронкова; редакторы С. М. Ахмин, Л. В. Мосина; технический редактор
О. Б. Яндуганова. Издательство КФТИ КазНЦ РАН,
420029, Казань, Сибирский тракт, 10/7, лицензия № 0325 от 07.12.2000.

Отпечатано с оригиналов заказчика

АО «Информационно-издательский центр» · Казань, ул. Чехова 28, телефон +7 (843) 236 94 26

